The role of cellular development in multicellular antiphage defense of *Streptomyces*

Inaugural Dissertation

for the attainment of the title of doctor in the Faculty of Mathematics and Natural Sciences at the Heinrich-Heine-University Düsseldorf

presented by

Tom Luthe

from Witten

Düsseldorf, December 2023

The thesis has been conducted at the Institute of Bio- and Geosciences, IBG-1: Biotechnology, Forschungszentrum Jülich GmbH, from May 2020 until December 2023 under the supervision of Prof. Dr. Julia Frunzke.

Published by permission of the Faculty of Mathematics and Natural Sciences at Heinrich-Heine-University Düsseldorf.

Supervisor:

Prof. Dr. Julia Frunzke

Institute of Bio- and Geosciences, IBG-1: Biotechnology

Forschungszentrum Jülich GmbH, Jülich

Mentor:

Prof. Dr. Nick Wierckx

Institute of Bio- and Geosciences, IBG-1: Biotechnology

Forschungszentrum Jülich GmbH, Jülich

Date of oral examination: Monday, 22 April 2024

It’s not a question of can or can’t. There are some things in life you just do.

- Lightning (Final Fantasy XIII)

The research presented in this doctoral thesis has been published in the following articles:

Sharma, V., Hardy, A., **Luthe, T.,** & Frunzke, J. (2021). Phylogenetic Distribution of WhiB- and Lsr2-Type Regulators in Actinobacteriophage Genomes. *Microbiology Spectrum*. *9*(3), e0072721. https://doi.org/10.1128/Spectrum.00727-21

Luthe, T., Kever, L., Hänsch, S., Hardy, A., Tschowri, N., Weidtkamp-Peters, S., & Frunzke, J. (2023a). Streptomyces development is involved in the efficient containment of viral infections. *MicroLife*, *4*. https://doi.org/10.1093/femsml/uqad002

Luthe, T., Kever, L., Thormann, K., & Frunzke, J. (2023b). Bacterial multicellular behavior in antiviral defense. *Current Opinion in Microbiology*, *74*, 102314. https://doi.org/10.1016/j.mib.2023.102314

To be submitted:

Luthe, T. & Frunzke, J. (2023). Investigation on *Streptomyces* Phage-encoded WhiB-like Transcriptional Regulators.

Further published contributions not discussed in this doctoral thesis:

Kever, L., Hardy, A., **Luthe, T.,** Hünnefeld, M., Gätgens, C., Milke, L., Wiechert, J., Wittmann, J., Moraru, C., Marienhagen, J., & Frunzke, J. (2022). Aminoglycoside Antibiotics Inhibit Phage Infection by Blocking an Early Step of the Infection Cycle. *MBio*, *13*(3). https://doi.org/10.1128/mbio.00783-22

Sharma, V., Hünnefeld, M., **Luthe, T.,** & Frunzke, J. (2023). Systematic analysis of prophage elements in actinobacterial genomes reveals a remarkable phylogenetic diversity. *Scientific Reports*, *13*(1), 4410. https://doi.org/10.1038/s41598-023-30829-z

Abbreviations

a.u.	Arbitrary units
aa	Amino acids
ATP	Adenosine triphosphate
BGC	Biosynthetic gene cluster
bp	Base pairs
c-di-GMP	Cyclic di-guanosine monophosphate
Cas	CRISPR-associated
ChIP	Chromatin immunoprecipitation
CRISPR	Clustered regularly interspaced short palindromic repeats
DGC	Diguanylate cyclase
DNA	Deoxyribonucleic acid
dsDNA	Double-stranded DNA
dsRNA	Double-stranded RNA
e.g.	*exempli gratia*
et al.	*et alii*
GlcNAc	N-actetylglucosamine
i.e.	*id est*
PDE	Phosphodiesterase
PFU	Plaque-forming units
R-M	Restriction-modification
RNA	Ribonucleic acid
RNAP	RNA polymerase
ssDNA	Single-stranded DNA
ssRNA	Single-stranded RNA
TPM	Transcripts per million
Wbl	WhiB-like
WT	Wild type

Further abbreviations not included in this section are used according to international standards, as for example listed in the author guidelines of the Journal of Cell Biology (https://rupress.org/jcb/pages/standard-abbreviations).

Table of contents

1. Summary

Bacteriophages, the viruses of bacteria, are ubiquitously found and represent the most abundant biological entities on the planet. Phage predation poses a constant threat to bacterial communities and results in an ongoing arms race characterized by continuous adaptation and counter-adaptation. In order to promote their survival and distribution, soil bacteria like *Streptomyces* developed diverse strategies including key features of filamentous, multicellular growth and a multifaceted secondary metabolite production.

This doctoral thesis focused on the impact of cellular development on phage infection during the multicellular life cycle of *Streptomyces*. We observed enhanced differentiation of interface mycelium directly surrounding the lysis zones of diverse phage-host pairs. Interestingly, this differentiation was accompanied by development-dependent growing and shrinking dynamics, which revealed the emergence of transiently resistant mycelial structures crucial for the containment of viral infections. This transient resistance is provided by the developmental cell surface changes that render the cells less susceptible to phage infection and enable regrowth into the lysis zone. This was additionally shown by a reduced adsorption of phage particles to older mycelium and non-growing spores. Transcriptome analysis revealed that phage infection triggers an upregulation of chloramphenicol biosynthesis genes, which could have a role in communicating ongoing infection to neighboring cells. Direct antiphage effects were not observed for the phages tested in this study. Moreover, during early infection, these data showed downregulation of *chaplin* and *rodlin* genes as well as almost all *whi* genes involved in sporulation. This could facilitate phage propagation and may be actively induced by the phage.

Bioinformatic analysis of phage genomes revealed the Actinobacteria-specific family of WhiB-like proteins as most abundant transcriptional regulators in actinobacteriophages. In the *Streptomyces* host, WhiB-like proteins are involved in differentiation, sporulation and antibiotic resistance. While we found WhiB-like regulators to be encoded by 32% of all analyzed *Streptomyces* phages, almost 90% of these phages were categorized as virulent. In addition to WhiB, especially FtsK and ParB-like proteins relevant to sporulation processes are encoded by smaller subsets of bacteriophages infecting *Streptomyces*. The diverse WhiB-like regulators encoded by *Streptomyces* phages both share conserved features of their host counterparts and have modified domains, which potentially mediate distinct functionalities. To further elucidate the role of these regulators, we used complementation and overexpression assays with a set of diverse phage-encoded WhiB-like proteins in *S. venezuelae*. Intriguingly, none of the phage genes restored the sporulation phenotype in a host *whiB* deletion strain. However, constitutive expression of phage *whiB* genes in the wild-type strain revealed multiple changes in cellular development. Chymera-encoded WhiB resulted in accelerated sporulation, whereas unbranched hyphal elongation and a delay of differentiation was caused by expression of *whiB* originating from Alderaan and Coruscant. These changes also influence efficacy of phage propagation.

Taken together, the results of this thesis emphasize multicellular development as a key feature in phage-host interactions in *Streptomyces*. The work presented highlights the importance of transient phage resistance as an essential layer of *Streptomyces* antiviral immunity. It further implies the potential engagement of phage proteins in interfering with the regulatory network governing cellular development, thereby improving phage propagation.

2. Scientific context and key results

2.1 *Streptomyces*

2.1.1 General characteristics and secondary metabolism

Streptomyces is a genus of Gram-positive Actinobacteria that expresses unique characteristics and plays a key role in various ecological niches. It is highly adapted to and widespread in terrestrial and aquatic as well as host-associated environments. With 718 validly published names and 742 available genomes spanning 213 species (https://www.bacterio.net/genus/streptomyces, Nikolaidis et al., 2023), *Streptomyces* is a vast group of important environmental bacteria playing a crucial role by establishing unique relationships and engaging in cross-kingdom communication with other organisms, such as fungi and plants (Barka et al., 2016; Krespach et al., 2023). These interactions often lead to the exchange of signaling molecules and nutrient sharing. Furthermore, *Streptomyces* spp. contribute to essential biogeochemical processes by decomposing and recycling of organic matter due to an extensive set of extracellular hydrolytic enzymes (Chater et al., 2010).

One of the fundamental features of *Streptomyces* is its ability to produce a wide range of bioactive secondary metabolites. These natural products are organic compounds that are not directly involved in the growth, development, or reproduction of the bacteria but play a vital role in their survival and interactions with the environment (Seyedsayamdost, 2019). *Streptomyces* spp. produce a significant proportion of natural products used as pharmaceuticals, in agriculture and biotechnology including antibiotics, antifungals, antivirals, antitumor agents, immunosuppressants, protein inhibitors and others (Alam et al., 2022; Barka et al., 2016; Demain, 1999). This rich source of valuable compounds has revolutionized medicine and agriculture by providing effective treatments for various human diseases and protecting plants and animals from pathogens. Prominent examples of antibiotics produced by *Streptomyces* include aminoglycosides, of which streptomycin was the first antibiotic successfully used to treat tuberculosis (Schatz & Waksman, 1944), the broad-spectrum-acting tetracyclines (Petković et al., 2017) and chloramphenicol (Fernández-Martínez et al., 2014).

The metabolic potential of *Streptomyces* for secondary metabolite production can be attributed to its unique genetic makeup and complex regulatory networks. Compared to other bacteria, their linear genomes are considerably large, ranging from 5.7 to 12.1 Mb with high GC contents of averaging 71.7% (Nikolaidis et al., 2023). Due to their linear chromosomes, *Streptomyces* genomes are organized in a core region spanning 50% of the genome surrounding the center and origin of replication and the two arms encompassing 25% each on the left and right of this core. While most genes in the core

region are stable and conserved across the genus and within species, the arms express especially high fluctuations and rearrangements due to horizontal gene transfer, recombination, duplication or deletion events impacting as much as 1 Mb of the whole genome (Bentley et al., 2002; Nikolaidis et al., 2023; Z. Zhang et al., 2022). Interestingly, biosynthetic gene clusters (BGCs) encoding enzymes responsible for the biosynthesis of secondary metabolites are found to be overrepresented on the arms of the chromosomes where the high plasticity contributes to a division of labor and effective production of natural products (Nikolaidis et al., 2023; Z. Zhang et al., 2020, 2022). Recent comparative analyses of *Streptomyces* genomes revealed an average of 31 BGCs encoded per genome with some harboring up to over 50, each potentially producing a distinct compound (Nikolaidis et al., 2023; Otani et al., 2022). However, the production of many secondary metabolites is highly regulated and often occurs only under specific environmental conditions or during different stages of growth and development, remaining cryptic or silent under standard laboratory conditions (Z. Liu et al., 2021). This again highlights the genetic diversity and flexibility of *Streptomyces* to adapt to different environmental conditions and the complex interplay between secondary metabolism and cellular development.

2.1.2 Multicellular development

Unlike many other bacteria, *Streptomyces* exhibit a complex multicellular lifestyle characterized by filamentous growth, the formation of a dense vegetative mycelium and the production of spores, formed on specialized reproductive structures called aerial hyphae (**Figure 1**) (Flärdh & Buttner, 2009). Transition through the different stages of this multicellular development is orchestrated by a repertoire of genes that operate in a highly coordinated manner. Key elements of the underlying regulatory network include *bld* and *whi* genes, which regulate processes leading to profound morphological and physiological changes such as germination, tip extension, septation, aerial mycelium formation, coordinated cell death and cell division during sporulation. Additionally, antibiotic synthesis is also coupled to this network (Flärdh & Buttner, 2009; McCormick & Flärdh, 2012). Major influences modulating differentiation are extracellular as well as intracellular signaling molecules such as γ-butyrolactones or cyclic di-guanosine monophosphate (c-di-GMP) driven by environmental cues ranging from nutrient availability, pH and temperature to osmolarity or small molecules secreted by other cells (Bush et al., 2015).

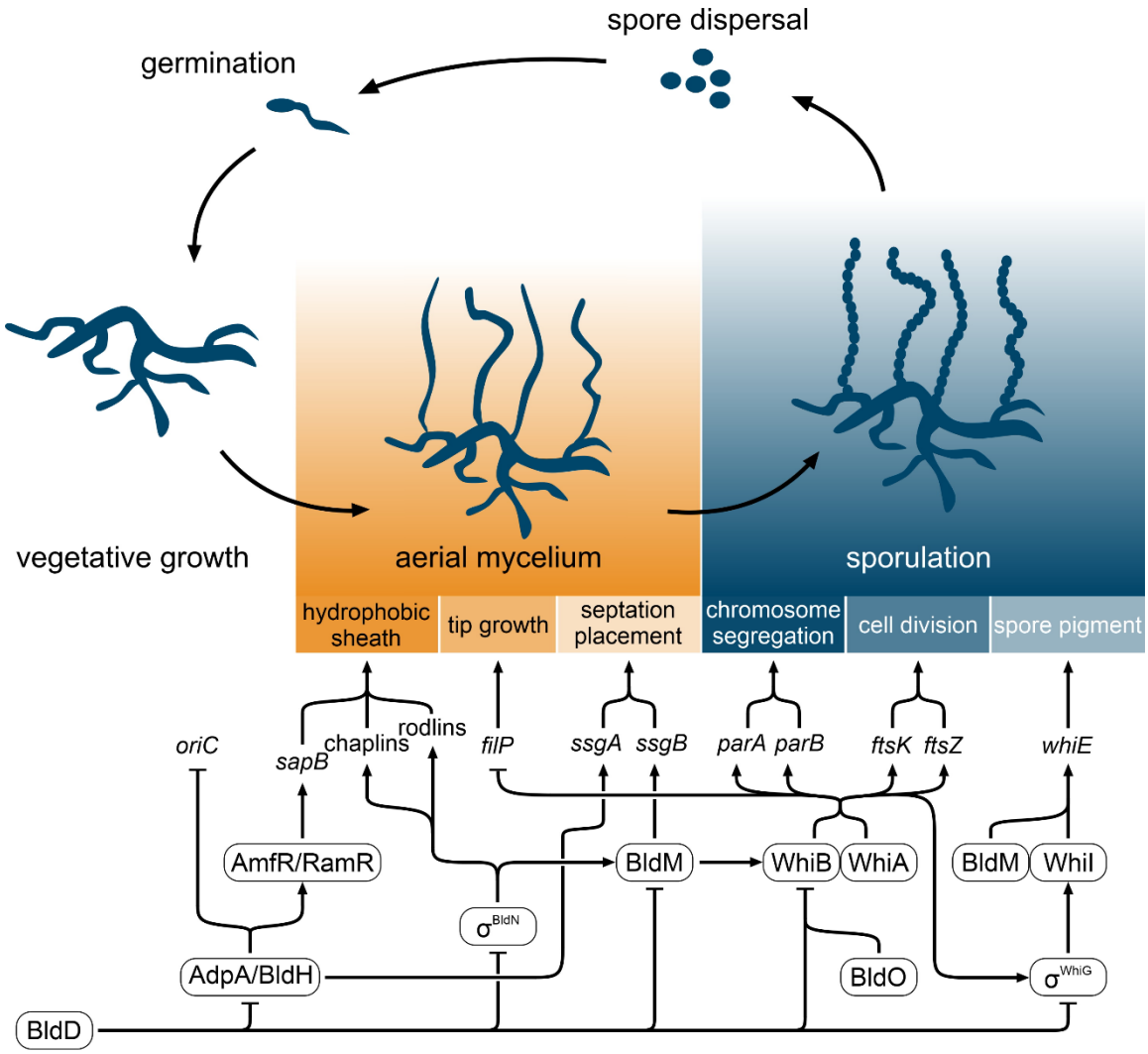

Figure 1: Simplified *Streptomyces* multicellular development and its regulatory network. The *Streptomyces* life cycle starts with a single spore germinating and growing by tip extension into a branched vegetative mycelium. Upon stress or nutrient depletion, the mycelium starts growing unbranched, hydrophobic aerial hyphae. The transition from aerial hyphae to spores is called sporulation and consists of cessation of tip growth, initiation of chromosome segregation and cell division, as well as spore maturation. The underlying regulatory network is controlled by the master regulator BldD, repressing expression of key regulatory genes encoding Bld proteins important for aerial hyphae formation and Whi proteins responsible for sporulation. In order to erect aerial hyphae, first genome replication is blocked by AdpA/BldH, which also activates AmfR/RamR expressing *sapB*, a component of the hydrophobic sheath. Sigma factor σ^{BldN} induces expression of the *chaplin* and *rodlin* genes essential for aerial hyphae formation. Additionally, *bldM* expression is activated by σ^{BldN}. BldM regulates the expression of *ssgB,* which, together with *ssgA* expression activated by AdpA/BldH, is necessary for the correct placement of future septation sites in the aerial hyphae. Key regulators of sporulation are WhiA and WhiB controlling their regulon together. WhiA is constitutively produced. Production of WhiB is transcriptionally controlled by inhibition through BldD and BldO as well as BldM mediated activation. Targets of WhiAB are *filP*, thereby stopping tip growth, *parA* and *parB* responsible for chromosome segregation, *ftsK* and *ftsZ* performing cell division and *whiG* encoding the sigma factor σ^{WhiG} activating *whiI* expression. WhiI forms a heterodimer with BldM regulating formation of the spore pigment by activating expression of *whiE*, which is an essential part of spore maturation. It has to be noted that the regulatory network shown here is not complete but shows only a few key regulators and downstream targets important and best studied so far. Arrows with pointy ends indicate activation, blunt ends indicate inhibition of expression. The figure is inspired by and partly based on Bush et al., 2015.

Starting the cycle, a typically dormant spore germinates upon favorable conditions (i.e. sufficient nutrients and moisture) by growing one or two germ tubes, elongating and forming a dense vegetative mycelium by tip extension and continuous branching (Bobek et al., 2017). This polar form of growth is directed by the polarisome (or tip-organizing center), composed of the essential protein DivIVA recruiting the cell wall biosynthesis machinery, along with co-localized Scy and FilP (Flärdh, 2010; Fröjd & Flärdh, 2019). This vegetative growth undergoes irregular cross-wall formation and results in multigenomic compartments that are distinct from cell division septation (Bush et al., 2022; McCormick et al., 1994). Unfavorable conditions, such as nutrient depletion and stress, induce the switch from vegetative mycelial growth to the formation of aerial hyphae. This is a key cell fate milestone tightly controlled by several *bld* genes, named after the bald colony phenotype observed in deletion mutants lacking the fuzzy aerial hyphae. The so-called master regulator BldD controls a regulon of more than 160 targets, acting as a repressor on regulators and downstream genes typically activated by these regulators (den Hengst et al., 2010). When dimerized by a tetrameric form of c-di-GMP, inhibition by BldD maintains an active growth state of the mycelium. The dissociation of the BldD dimer from the DNA then starts the cascade of developmental differentiation (Bush et al., 2015; Tschowri et al., 2014). Aerial hyphae formation begins with the inhibition of DNA replication by AdpA/BldH binding to the *oriC* (Wolański et al., 2012). It involves the formation of a hydrophobic sheath consisting of rodlins, chaplins and SapB facilitated by the sigma factor σ^{BldN}, thereby enabling erection of the hyphae into the air (Bibb et al., 2012; Claessen et al., 2003, 2004). The process ends with the placement of division sites known to be regulated by activation of *ssgA* and *ssgB* expression through AdpA/BldH and a homodimer of BldM, respectively (Willemse et al., 2011).

Importantly, preceding the formation of aerial hyphae are the processes of secondary metabolite production and programmed cell death-like mechanisms (Rigali et al., 2008; Tenconi et al., 2018). To ensure sufficient carbon and nitrogen resources available for aerial hyphae formation, parts of the old vegetative mycelium undergo a coordinated cell death, releasing nutrients into the surrounding area ready for uptake and use (Manteca et al., 2006, 2007; Miguélez et al., 1999). The production of secondary metabolites is hypothesized to be coordinated with this drastic step to protect these resources from other soil-living competitors (Rigali et al., 2008). Some key developmental regulators, like AdpA/BldH or parts of important protein families such as WhiB-like (Wbl) proteins WblA and WblC, therefore have (dual) functions connecting both multicellular differentiation and secondary metabolite production and resistance (Bush, 2018; Płachetka et al., 2021).

The process of sporulation, the transition from aerial hyphae to spores, is under the control of several *whi* genes, named after their white appearance of aerial hyphae lacking formation of the colored spore pigment. Most important during early sporulation are WhiA and WhiB, which act cooperatively on their regulon by recruiting the RNA polymerase initiation complex (Lilic et al., 2023). Interestingly, WhiA is an exception among the developmental regulators in *Streptomyces*. Besides activating its own expression, its gene is constitutively expressed and not known to be repressed by any other protein (Bush et al., 2013). Opposingly, the production of WhiB is strongly regulated by the repression of BldD and BldO, as well as activation by BldM (Al-Bassam et al., 2014; Bush et al., 2017; den Hengst et al., 2010). Targets of their regulon are essential genes for tip growth, where they inhibit expression of *filP*, and initiation of sporulation, septation and chromosome segregation, by activating *ftsZ*, *ftsK*, *parA,* and *parB* (Bush et al., 2013, 2016). Additionally, in controlling further spore maturation by the sigma factor σ^{WhiG} and its targets WhiH and WhiI, which are responsible for cell wall changes and pigment production, WhiA and WhiB act as gatekeepers of successful spore formation (Flärdh & Buttner, 2009).

2.2 Bacteriophages

2.2.1 Definition, diversity and life styles

Viruses of bacteria, known as bacteriophages or phages, are ubiquitously found. With an estimated 10^{31} total particles and 10^{24} infections per second shaping bacterial communities in every environment, they are the most abundant biological entities on the planet (Clokie et al., 2011; Cobián Güemes et al., 2016; Mushegian, 2020; Williamson et al., 2017).

Discovered by Frederick Twort and Felix d'Hérelle in 1915 and 1917 these "ultra-microscopic viruses" or "invisible microbes" (D'Hérelle, 1917; Twort, 1915) were readily recognized for their ability of killing bacteria and their potential in treating diseases caused by bacterial pathogens (Sulakvelidze et al., 2001). Due to the double-sided characteristic of phages in host specificity and the lack of consistent, reliable success, as well as fundamental understanding of phage biology, the advent of more broadly active and easy-to-use chemical antibiotics, such as penicillin, discovered in 1928, replaced bacteriophages in this regard (Hutchings et al., 2019; Sulakvelidze et al., 2001). Therefore, the focus of bacteriophage research shifted from clinical use to basic research, resulting in fundamental breakthroughs in the understanding of biology and chemistry, accompanied by discoveries leading to the development and application of tools and techniques used in modern biotechnology and molecular biology today (Salmond & Fineran, 2015).

Making phages visible by using the electron microscope started the detailed description of phages as virus particles of huge diversity (Luria et al., 1943; Ruska, 1940). While the majority of phage particles known to date can be assigned to one of the three morphotypes - myo-, sipho- and podovirus - of tailed bacteriophages (*Caudoviricetes*), many further structures have been described, including polyhedral, pleomorphic or filamentous with some having a lipid membrane (**Figure 2**) (Ackermann, 2007; Dion et al., 2020). However, phage diversity is not only apparent in terms of morphology but also in genome type and genetic equipment (Dion et al., 2020; Krupovic et al., 2011). Among the isolated and characterized phages, dsDNA phages are most abundant. This is in part due to enrichment and isolation biases introduced by the choice of hosts and methods used in classic isolation procedures (Gill & Hyman, 2010). However, current isolation-independent metagenomic and transcriptomic analyses have revealed even greater diversity than expected, adding many more ssDNA- and RNA-containing phage sequences (Creasy et al., 2018; Neri et al., 2022). These recent advances in genomics have led to a reclassification effort establishing a genome-based megataxonomy of viruses, grouping bacteriophages with their related eukaryote-infecting counterparts based on sequence

data rather than host range and morphotypes (**Figure 2**) (Koonin et al., 2020; Turner et al., 2021).

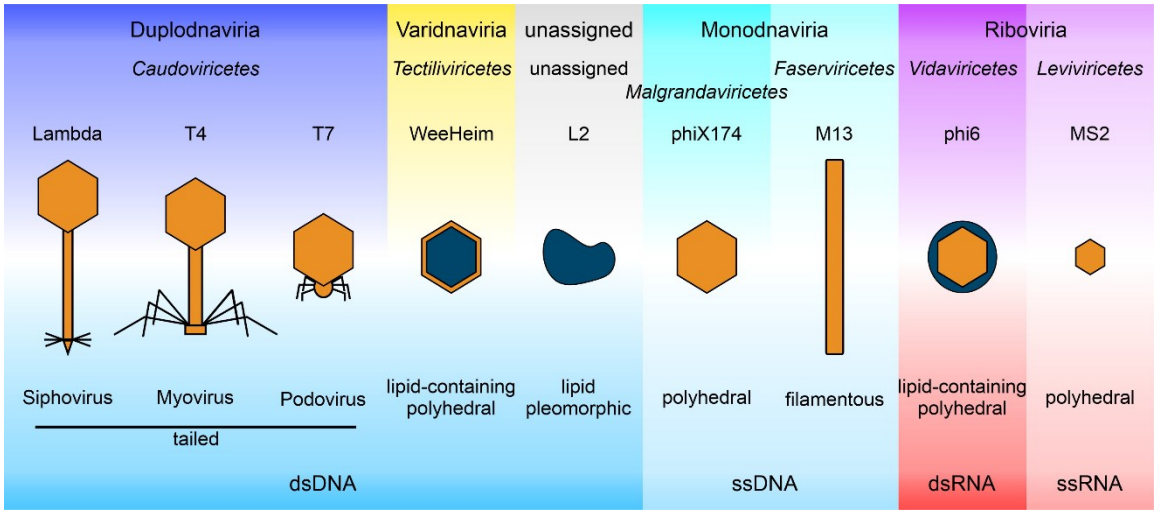

Figure 2: Bacteriophage morphologies, genomes, and classification. Bacteriophage genomes can consist of dsDNA, ssDNA, dsRNA, or ssRNA. The dsDNA phages are assigned to the two viral realms of Duplodnaviria and Varidnaviria and can also be found in the group of unassigned viruses. In the Duplodnaviria, the tailed phages in the class *Caudoviricetes* can have sipho-, myo-, and podovirus morphologies. For example Lambda has a long, flexible but non-contractile tail, T4 has a medium, contractile tail, and T7 has a very short tail, respectively. WeeHeim is an example for a polyhedral particle containing a lipid membrane inside of the protein capsid, belonging to the *Tectiliviricetes* class of Varidnaviria. L2 is an unassigned pleomorphic lipid particle. ssDNA phages belong to the Monodnaviria realm and classes *Malgrandaviricetes* (polyhedral protein capsid, e.g. phiX174) as well as *Faserviricetes* (filamentous protein tubes, e.g. M13). In the realm of Riboviria, both double stranded and single stranded RNA-containing bacteriophages are located. *Vidaviricetes*, like phi6, have dsRNA genomes and a polyhedral protein capsid surrounded by a lipid envelope. The smallest phage particles contain ssRNA, are polyhedral and belong to phages in the class *Leviviricetes* (e.g. MS2). The figure is inspired by Hyman & Abedon, 2012 and based on the newest taxonomy information of the International Committee on Taxonomy of Viruses (ICTV, 2022 release).

Bacteriophages, like other viruses, depend on a metabolically active host cell to replicate and release progeny in a productive infection. In an effort to propagate in a bacterial population, different phages follow different life styles (**Figure 3**) (Hobbs & Abedon, 2016). Regardless of the type of infection, all phages must first attach to the cell surface of a suitable bacterial host during adsorption by recognizing specific receptors and irreversibly bind to these before the genome is injected (Bertozzi Silva et al., 2016). While virulent phages immediately take over the host cell and produce virions in a lytic cycle, temperate phages establish more or less stable associations with their host, termed lysogeny. The decision-making of temperate phages regarding whether to follow the lysogenic or lytic cycle depends on several parameters including host fitness, or cell and phage densities. To decide on integration and excision, several *Bacillus* phages use the so-called arbitrium system, communicating via phage-encoded small peptides, whereas phages of *Vibrio* use host-encoded quorum sensing molecules to measure host density (Erez et al., 2017; Silpe & Bassler, 2019). By integrating into the bacterial genome at specific attachment sites or

residing in an episomal, plasmid state, the now called prophage is tightly regulated, replicated, and dispersed in vertical transmission during cell division (Brady et al., 2021; Oppenheim et al., 2005; Shao et al., 2019). This can be beneficial for the host due to an increased fitness by the lysogenic expression of virulence factors, toxins, or auxiliary metabolic enzymes (Howard-Varona et al., 2017; Waldor & Mekalanos, 1996). Nevertheless, upon prophage induction the lytic cycle can be initiated. Then, both virulent and temperate phages use host enzymes as well as phage-encoded proteins to replicate the phage genome, produce virion proteins, assemble the phage particles, and finally be released from the host cell by the production of holins and lysins, leading to membrane disruption (Young, 1992). Some bacteriophages, especially filamentous phages of the class *Faserviricetes*, are not released by lysis but by extrusion or budding, leaving the host cell intact. This lifestyle is termed chronic infection (Hobbs & Abedon, 2016).

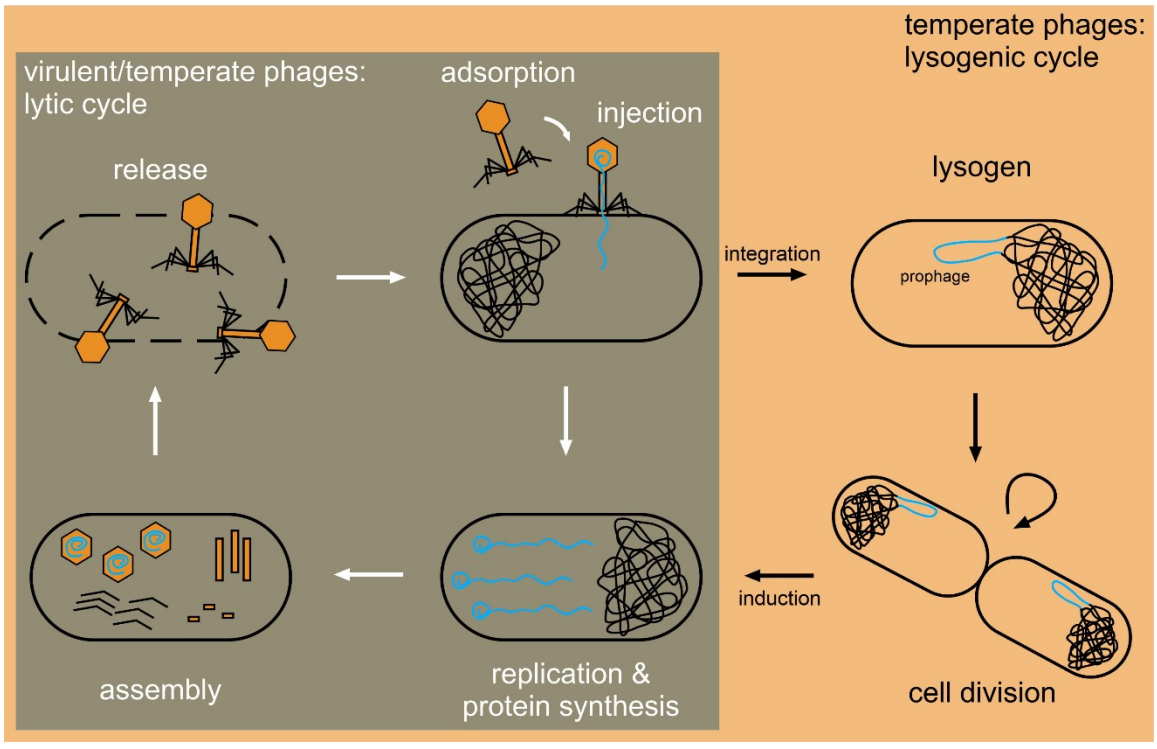

Figure 3: Virulent and temperate bacteriophage life styles. The bacteriophage infection begins with recognizing the bacterial host and adsorption to specific receptors, irreversibly binding the host cell. After the injection of the phage genome into the cell, temperate phages can follow the lysogenic cycle. As a so-called prophage, they integrate into the bacterial chromosome, or reside extrachormosomally as an episome (not shown). The prophage is replicated via host genome replication and cell division. DNA damage or other stress conditions can trigger induction of the prophage, resulting in excision from the host genome. Like virulent phages, induced prophages follow the lytic cycle using the host machinery for genome replication and protein biosynthesis. Phage particles are assembled and packed with a single genome each eventually leaving the host cell by disruption of the host cell wall (lysis). The figure is inspired by Doss et al., 2017.

2.2.2 Actinobacteriophages and viral dark matter

Historically, in an attempt to make results comparable and facilitate discovery, fundamental bacteriophage research focused on a relatively small set of phages (mostly T phages) infecting the Gram-negative *Escherichia coli* under standardized conditions, making it the model system it is today. This approach, called the “phage treaty”, was rewarded by fast and reliable outcomes that led to numerous breakthroughs in understanding biological principles and laid the basis for Nobel Prize-winning discoveries (Salmond & Fineran, 2015). Undoubtedly, the identification of DNA as the genetic material (Hershey & Chase, 1952), insights into the nature of mutation (Luria & Delbrück, 1943), the discovery and application of restriction-modification enzymes (Luria & Human, 1952), or the T7 polymerase expression system (Tabor & Richardson, 1985), to name a few, significantly contributed to our understanding of the molecular basis of life in general. However, phenomena such as the formation of a phage pseudonucleus in *Pseudomonas* (Chaikeeratisak et al., 2017), phages using communication-based decision-making (Erez et al., 2017) or the recent explosion in new antiphage defense systems, including CRISPR-Cas (Barrangou et al., 2007; Georjon & Bernheim, 2023), were only made possible by studying non-model phages and a broad variety of bacterial hosts.

Actinobacteriophages are viruses that infect bacteria belonging to the Gram-positive phylum Actinobacteria. There have been an enormous effort to isolate, sequence and characterize these phages across all associated host genera. This effort has expanded the number of phages infecting, for example, *Mycobacterium* alone from 70 to over 2000 fully sequenced genomes in one decade (Hatfull, 2020). Out of a total of 24,083 isolated phages, there are 4,557 finished genomes of phages infecting the *Actinobacteria* genera, including *Actinoplanes* (1)*, Arthrobacter* (450)*, Brevibacterium* (2)*, Corynebacterium* (25)*, Gordonia* (724)*, Microbacterium* (607)*, Mycobacterium* (2276)*, Propionibacterium* (55)*, Rhodococcus* (67)*, Rothia* (1)*, Streptomyces* (346)*, Tetrasphaera* (1), and *Tsukumurella* (2) currently curated at The Actinobacteriophage Database (phagesdb.org, November 2023). Additionally, there are probably more phages not publicly available isolated and stored in laboratories around the world, which are not directly participating in the isolation programs PHIRE (Phage Hunters Integrating Research and Education) or SEA-PHAGES (Science Education Alliance-Phage Hunters Advancing Genomics and Evolutionary Science) integrating high school and undergraduate students in actual research (Hatfull, 2015b).

Despite the significant bias towards phages infecting one single genus (i.e. *Mycobacterium*), the wealth of actinobacteriophage genomic data across all genera is astonishing. Remarkably, despite these huge numbers, almost all actinobacteriophages

belong to the dsDNA-carrying *Caudoviricetes*, where the majority displays a siphovirus morphology (Hatfull, 2020). Such an abundance of genomic data also clearly highlights how little is known about the diversity and function of phage-encoded proteins. For the majority of actinobacteriophages, only around 30% of the genes have assigned functions and are related to already known genes (Hatfull, 2015a, 2020). In fact, there is not a single bacteriophage genome with every single one of its genes being completely and functionally annotated. This is independent of genome size, the duration of knowing, or the intensity of studying it. One of the smallest phages, ssDNA phage Mini, has only four predicted genes and one of them encodes for a hypothetical protein of unknown function (Zhan & Chen, 2019). Additionally, phages T4 and Lambda, despite being heavily studied for decades already, still have 38% and 9.5% of their encoding proteins annotated as hypothetical, respectively (GenBank, November 2023). Similarly, metagenomic analyses show that, depending on the sample, between 40% and 90% of the sequences of viral origin cannot be aligned to any existing reference sequence (Gregory et al., 2019; Krishnamurthy & Wang, 2017). This is in line with many newly isolated actinobacteriophages not fitting into one of the 156 established actinobacteriophage clusters of related phages, hence forming singletons sharing less than 35% of their genes with other already known actinobacteriophages (Hatfull, 2020). Both of these phenomena are referred to as genomic or viral dark matter, presenting an enormous potential for future discoveries studying this growing diversity (Dion et al., 2020; Payne et al., 2021). Initial studies on the broader actinobacteriophage genomic landscape have already identified unique characteristics regarding transcriptional regulation, prophage distribution, and the distinct antiphage defense systems of their hosts (Dedrick et al., 2017; Georjon et al., 2023; Sharma et al., 2021, 2023).

2.2.3 Antiphage defense systems

Bacteriophage predation of bacteria is a perfect example of the Red Queen hypothesis, representing an ongoing arms race resulting in the continuous adaptation and counter-adaptation of bacterial defense strategies and phage-encoded antidefense mechanisms (Stern & Sorek, 2011; van Valen, 1973). Antiphage defense can act on every step during the infection cycle including adsorption interference, blocking genome injection, targeting of phage nucleic acids by restriction-modification or CRISPR-Cas immunity, as well as abortive infection, and toxin-antitoxin systems (**Figure 4**). The most commonly observed resistance mechanism of bacteria under laboratory and clinically conditions is interference with initial adsorption of the phage (Gordillo Altamirano & Barr, 2021). This interference can be achieved through mutation, post-translational glycosylation, complete loss,

changes in abundance and distribution, or shielding of the typical protein and lipopolysaccharide receptors. It may also involve the forming or adjusting of a capsule, and using competitive inhibitors, binding and blocking either the receptor or the phage itself (Destoumieux-Garzón et al., 2005; Harvey et al., 2018; Hesse et al., 2020; Labrie et al., 2010). Classical antiphage defense mechanisms provided through prophages are superinfection exclusion mechanisms that inhibit secondary infections. This is achieved by blocking entry of the phage genome with mostly membrane anchored proteins or by employing immunity repressor proteins that block expression of the lytic genes of intruder phages (Labrie et al., 2010; Mavrich & Hatfull, 2019). Additionally, prophages also influence phage receptor availability and intracellular mechanisms (Bondy-Denomy et al., 2016).

If phage genetic material has entered the bacterial cell, two well-described defense systems are commonly found in the majority of bacterial species. Restriction-modification (R-M) and CRISPR-Cas (Clustered Regularly Interspaced Palindromic Repeats – CRISPR-associated protein) systems both target viral nucleic acids and cleave them. A particularly important characteristic of immune systems, in order to confer effective resistance, is the ability to detect and distinguish between foreign and host DNA. As an innate immune system, for R-M systems, modification of host DNA (typically methylation) readily protects specific recognition sequences targeted by restriction endonucleases resulting in digestion of only foreign, non-modified DNA (Bickle & Krüger, 1993). On the other hand, the CRISPR-Cas system is an adaptive immune system, memorizing previous infections by integrating short sequences of foreign nucleic acid, known as spacers, in CRISPR arrays divided by repeat regions. These spacers are then expressed as small guide RNAs for further detection and targeting of similar invading DNA or RNA, which is then cleaved by the associated Cas protein (Hille & Charpentier, 2016). Interestingly, certain CRISPR-Cas systems can also be host-directed cleaving phage and host transcripts alike upon phage detection. But acting together with a restriction-modification system, phage infection can be cleared more effectively and brings back bacterial cells from dormancy (Williams et al., 2023).

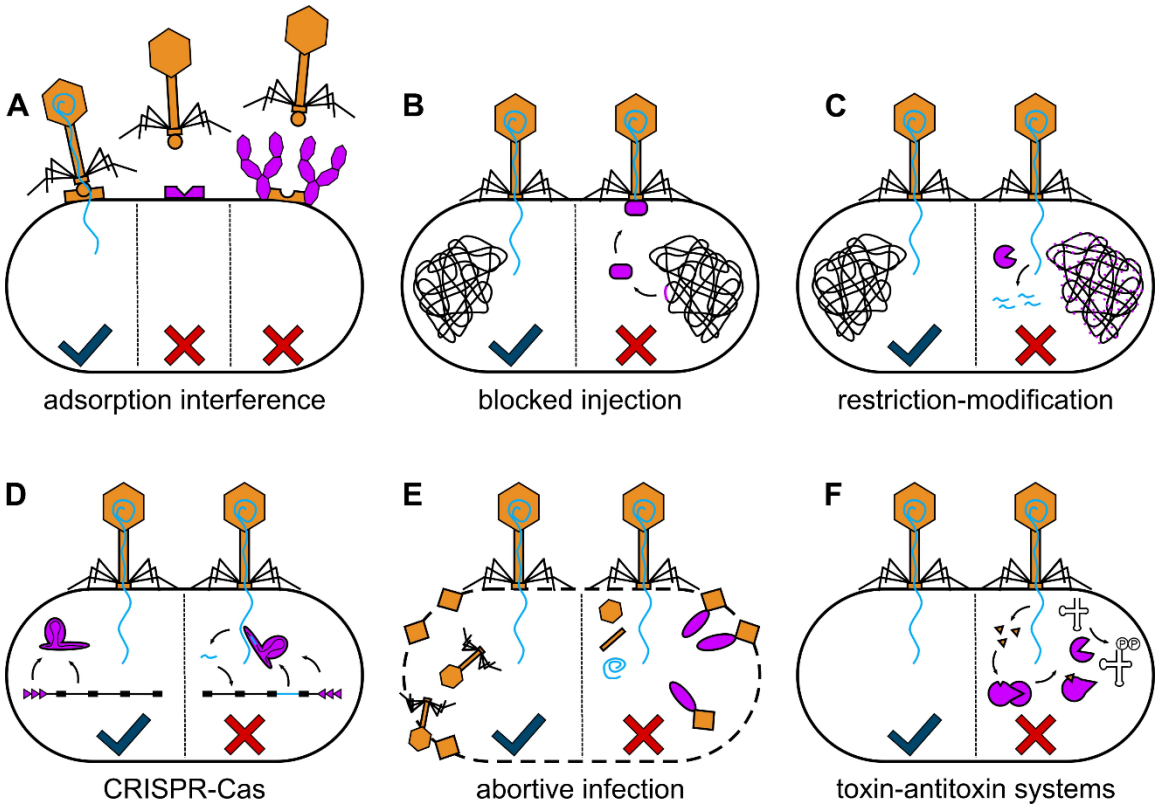

Figure 4: Antiphage defense systems in bacteria. The main strategies in antiphage defense systems are schematically and exemplarily presented. (**A**) Adsorption interference acts prior to phage attachment, blocking the particle from host recognition and binding. For example through adapting or shielding the receptor. (**B**) Blocking of injection of the bacteriophage genome is often mediated through (pro-)phage-encoded proteins, conferring superinfection exclusion. (**C**) Modification of the host genome by e.g. methylation, allows cleavage of foreign, unmodified DNA recognized by specific restriction sites through restriction enzymes. (**D**) CRISPR-Cas adaptive immunity relies on survival of prior infections, memorizing short phage sequences that guide cleavage of similar infecting DNA or RNA. Upon sensing phage infection, (**E**) abortive infection mechanisms lead to cell death prior to completion of the phage life cycle thereby blocking further spread of infection to neighboring cells. (**F**) Toxin-antitoxin systems also work on recognizing ongoing infection, releasing the antitoxin module from its toxin counterpart. This results in detrimental effects for both phage and host, often leading to cell death. The blue tick represents productive phage infection, while the red cross indicates active antiphage defense resulting in failed phage propagation. Phage proteins are represented in orange, host defense in purple, phage DNA in blue and host DNA in black. The figure is inspired and partly based on Georjon & Bernheim, 2023 as well as Labrie et al., 2010.

As a last resort defense strategy, bacteria have developed systems that lead to cell death, stopping the propagation of infectious phage particles. This broader concept of multiple and diverse mechanisms is typically termed abortive infection and is triggered by sensing the ongoing infection through, for example, phage proteins or altered expression profiles (Lopatina et al., 2020). Cell death can be achieved by different measures, including the use of phage-encoded lysins and holins to induce premature lysis, ion disbalance leading to depolarization of the cytoplasmic membrane, or phosphorylation of tRNAs inhibiting protein biosynthesis (Durmaz & Klaenhammer, 2007; Parma et al., 1992; T. Zhang et al., 2022). Many of these strategies involve toxin-antitoxin systems that are activated by the presence of phage proteins or RNA. Additionally, cyclic oligonucleotide-based antiphage

signaling systems, known as CBASS, play a role in these defense mechanisms, too (Banh et al., 2023; Kelly et al., 2023).

As shown by recent studies, the antiphage defense arsenal of bacteria is expanding rapidly and in some cases is assumed to provide the evolutionary origin of eukaryote and human immune systems (Bernheim & Sorek, 2020; Tesson et al., 2022; Wein & Sorek, 2022). With over 100 systems, some of which are not yet fully understood but classified into known defense mechanisms, the diversity of antiphage defense is vast and presented in the most recent update on antiphage defense systems of bacteria (Georjon & Bernheim, 2023). Most genomes encode multiple, different systems, adding up lines of defense and some systems can be ubiquitously found in even distantly related bacteria. What is particular interesting to note is, that especially Actinobacteria encode a unique repertoire of, in part, newly recognized types of defense systems which are distinct from other phyla (Georjon et al., 2023). Especially *Streptomyces* makes use of its signature traits and exploits for example anthracyclines and aminoglycosides, or cellular development to protect itself against phage infection (Kever et al., 2022; Luthe et al., 2023a).

2.3 Phage-host interactions in the context of multicellular development

2.3.1 Multicellular antiphage defense

Most prominent antiphage defense systems described so far are active on a single cell level, mostly intracellularly. While an effective defense in single bacterial cells protects the entire population by stopping the reproduction of phages, there are several additional strategies employed by bacteria in a community setting. Regardless whether this setting is multicellular in terms of filamentous growth, as seen in cyanobacteria and *Streptomyces*, or microbial assemblies of biofilms and swarms, most bacterial species are known to be structured and organized by some kind of multicellularity under certain environmental conditions (Lyons & Kolter, 2015; Shapiro, 1988). Besides being essential for reproduction and survival, multicellularity not only improves nutrient availability, resistance to physical stress, antimicrobial agents or competitors but also protection from predators such as bacteriophages. These multicellular antiphage defense strategies of bacteria comprise the use of i) membrane vesicles and ii) quorum sensing molecules, iii) biofilm formation and iv) production of small molecules acting as antiphage defense, as well as v) cellular development (**Figure 5**) and are the focus of our recent review article (Luthe et al., 2023b).

One of the main concepts of multicellularity is the intercellular communication. For bacteria this concept is termed quorum sensing in which the production and recognition of small molecules, called autoinducers, modulate virulence, biofilm formation, horizontal gene transfer, and bioluminescence dependent on, for example, cell density (Duddy & Bassler, 2021). It was shown that quorum sensing is also used to shape the defense of bacteria against phage infection by triggering specific intracellular defense systems. In this context, quorum sensing is activating the *cas* gene expression in *Pseudomonas* and *Serratia* species to increase CRISPR-Cas immunity or triggers abortive infection in *E. coli* (Hazan & Engelberg-Kulka, 2004; Høyland-Kroghsbo et al., 2016; Patterson et al., 2016). To stop further phage spread in *Vibrio* and *E. coli* populations, some autoinducers lead to a downregulation of the respective phage receptor genes in neighboring cells (Høyland-Kroghsbo et al., 2013; Tan et al., 2015). As part of this communication, membrane vesicles, important in intercellular interactions of DNA transfer or metabolite export, can be used to improve the communication via quorum sensing and other signaling molecules, fostering a more robust defense reaction (Toyofuku et al., 2017). However, membrane vesicles were also described to have a more direct role in protecting the community from viral infection acting as decoys to which phages adsorb. This results in less productive infections (Beerens et al., 2021; Reyes-Robles et al., 2018).

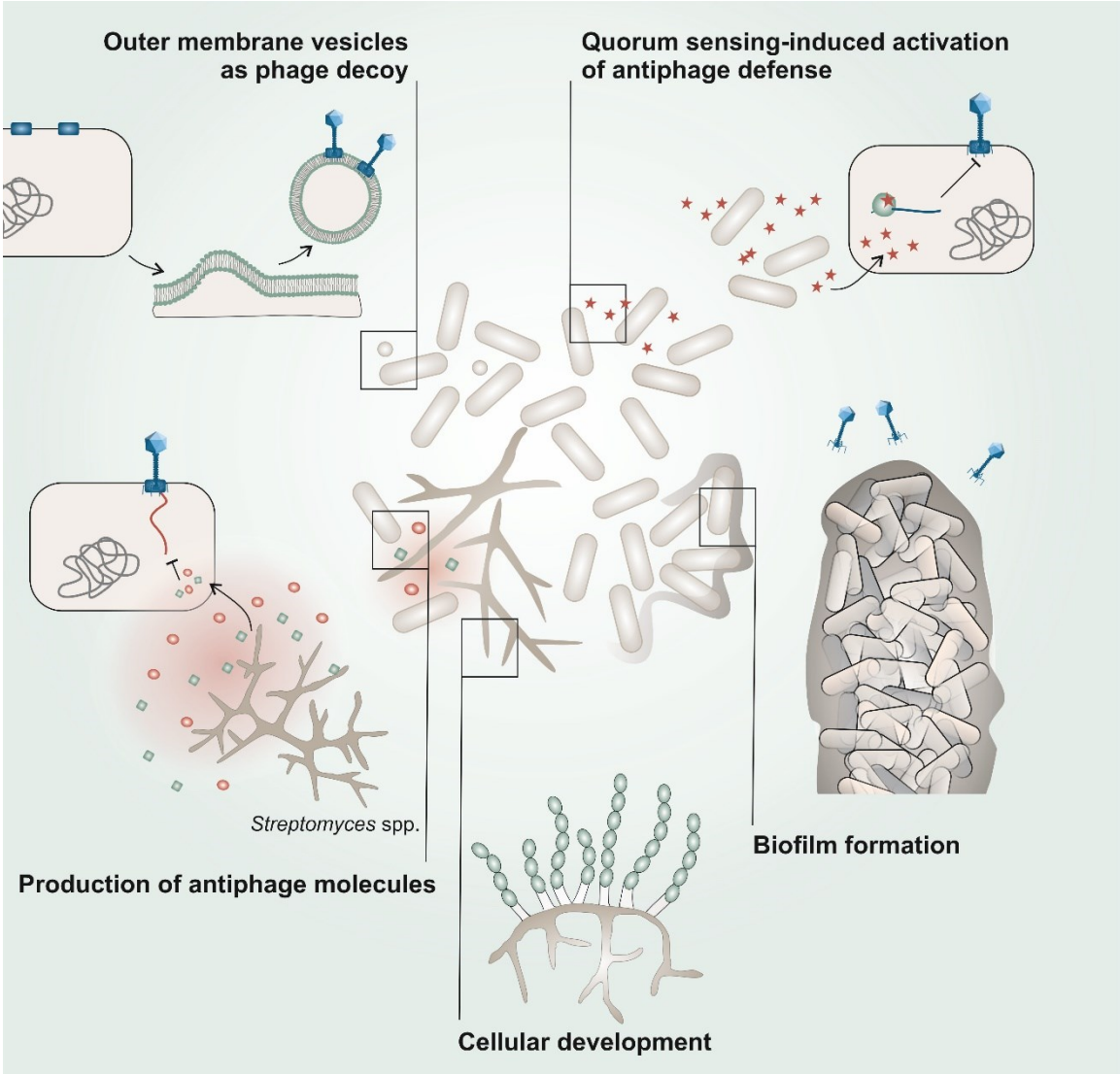

Figure 5: Bacterial multicellular strategies in antiviral defense. Protection against phages on a multicellular level can be mediated by i) extrusion of outer membrane vesicles sequestering phages, which prevents attachment to susceptible cells. ii) Quorum sensing-mediated antiphage defense systems rely on autoinducers (red stars) for transcriptional activation of RM-, CRISPR-, abortive infection, and other systems. iii) Biofilm formation and trapping of phages via interaction with components of the extracellular matrix reduces diffusivity of phage particles and propagation upon infection. iv) Secretion of antiphage molecules (e.g. anthracyclines or aminoglycosides) confers a chemical defense by inhibiting an early step in the infection cycle. v) Cellular development allows for the emergence of transient phage resistance due to reduced susceptibility of distinct developmental stages (from Luthe et al., 2023b).

Both quorum sensing and membrane vesicles play crucial roles when it comes to biofilm formation of bacteria. Biofilms themselves are one of the major forms of multicellular bacterial associations in many environments and therefore play a crucial role in phage-host interactions as well (Flemming & Wuertz, 2019; Lyons & Kolter, 2015). Although the accumulation and immobilization of many prey bacteria in one place seems to be a disadvantage, there are inherent biofilm properties that are of notice when it comes to phage predation. Increased co-infections per cell can lead to a reduced phage propagation per particle. Additionally, nutrient as well as oxygen gradients in the biofilm

affect the metabolic activity of many associated cells resulting in the accumulation of slow growing, dormant or dead cells, which are not suitable for propagation of most phages. Nonetheless, like membrane vesicles, they can still lead to phage adsorption and result in a reduction of infectious particles in the extracellular environment (Ciofu et al., 2022; Łoś et al., 2007; Simmons et al., 2020). Further, with biofilms producing an extracellular matrix, bacteria are densely packed and embedded in exopolysaccharides, proteins, lipids and other molecules reducing the diffusion of the non-motile bacteriophages drastically, thereby slowing spread and blocking access to susceptible hosts (Flemming et al., 2023; González et al., 2018). Parts of this protective matrix of *E. coli*, proteins called curli fibers, were also shown to trap phages in an active state and by that conferring additional protection not only against direct infection but also towards bacterial competitors invading the biofilm (Bond et al., 2021; Vidakovic et al., 2018).

As already described previously and for *Streptomyces* in particular, bacteria produce and exchange many diverse small molecules. These may not only function as signaling and communication tools, but can also exhibit direct antiphage properties themselves. Two prominent examples of this chemical defense against phages recently described are the DNA intercalating anthracyclines and the bactericidal aminoglycoside antibiotics targeting the 16S rRNA of the 30S ribosomal subunit (Hardy et al., 2022; Kever et al., 2022; Kronheim et al., 2018). Both groups are active against several phages infecting *E. coli*, *Pseudomonas* and *Streptomyces* at an early step during infection on an intracellular level. The exact mechanisms of action are not yet discovered but, at least for aminoglycosides the antiphage and antibiotic functions were shown to be distinct (Kever et al., 2022). In order for this chemical defense to work in a community, it is necessary for the cells to be resistant to this canonical property. In nature, producer cells of these molecules typically express self-resistance mechanisms and can live with the accumulated compound in the environment reaching local concentrations high enough for creating an antiviral milieu (Hopwood, 2007; Kever et al., 2022; Tenconi & Rigali, 2018). This resistance prerequisite could be seen as a selective pressure for mutualistic communities between kin cells or different species applying a division of labor and thereby excluding competitors (Traxler & Rozen, 2022).

2.3.2 *Streptomyces* development as a transient phage resistance mechanism

Phage infection results in enhanced differentiation in *Streptomyces*

Despite increased efforts in phage isolation, *Streptomyces* phages are still mostly published solely by genome announcements or characterized on a very basal level (the two most recent examples being Cleary et al., 2023; Ongenae et al., 2023) and were rather investigated for the use as tools in genetic engineering of their hosts (Baltz, 2012; Kormanec et al., 2019). Just recently, interest in the unique genetic equipment and phage-host interactions started to rise and yielded first, more detailed insights into their unique properties and interactions (deCarvalho et al., 2023; Kever et al., 2022; Kronheim et al., 2018). Important for these investigations is the appreciation of the natural soil environment of *Streptomyces* and its corresponding phages as a spatially structured and densely populated habitat of high microbial diversity (Fierer, 2017; Williamson et al., 2017). With sometimes extreme local gradients and close contacts between competitors and predators, survival strategies of soil-living bacteria are as specialized as diverse and interactions are impacted differently compared to aqueous habitats (Srinivasiah et al., 2008). These circumstances have to be taken into account when it comes to investigation in the laboratory. Therefore, infection on solid media closely resembles environmental conditions regarding phage distribution, *Streptomyces* complex multicellular development and the overall life cycle. Plaque formation represents the hallmark of phage infection, visualizing the lytic activity of replication. In our recent study, we shed light onto the importance of *Streptomyces* multicellular development during phage infection with a focus on growth on solid media (Luthe et al., 2023a).

When infecting three *Streptomyces* species, *S. venezuelae*, *S. coelicolor* and *S. griseus*, with a set of two different phages each, plaque formation showed distinct developmental patterns of enhanced aerial hyphae formation directly surrounding the infection interface (**Figure 6A**). Depending on the host, this phenomenon was altered in its spatiotemporal dynamics, but always resulted in a distinct ring of cellular differentiation surrounding the lysis zone. In order to follow this initial observation, investigation focused on one phage-host pair, namely Alderaan and *Streptomyces venezuelae*. *S. venezuelae* is the most important *Streptomyces* model species for the study of differentiation during multicellular development. In comparison to both other model strains *S. griseus* and *S. coelicolor*, it has the ability to complete its full life cycle including sporulation not only on solid media but also in liquid cultures (Glazebrook et al., 1990). This enabled the use of a great set of modern technologies including omics methods such as RNA- and ChIP-sequencing, RT-qPCR as well as fluorescence microscopy (Gomez-Escribano et al., 2021). With that, key insights into the regulatory network of development were gained and *S. venezuelae*

research is the basis for most of the knowledge reviewed in chapter 2.1.2 (Multicellular development). Alderaan, on the other hand, is a virulent phage in the temperate BC cluster of *S. venezuelae* infecting actinobacteriophages. This phage was chosen for further investigation as it was isolated and first described in our laboratory and formed reliable plaques of a decent size. It has a typical siphovirus morphology with a rather small genome of 34 kb having the same high GC-content as its host (72%) (Hardy et al., 2020).

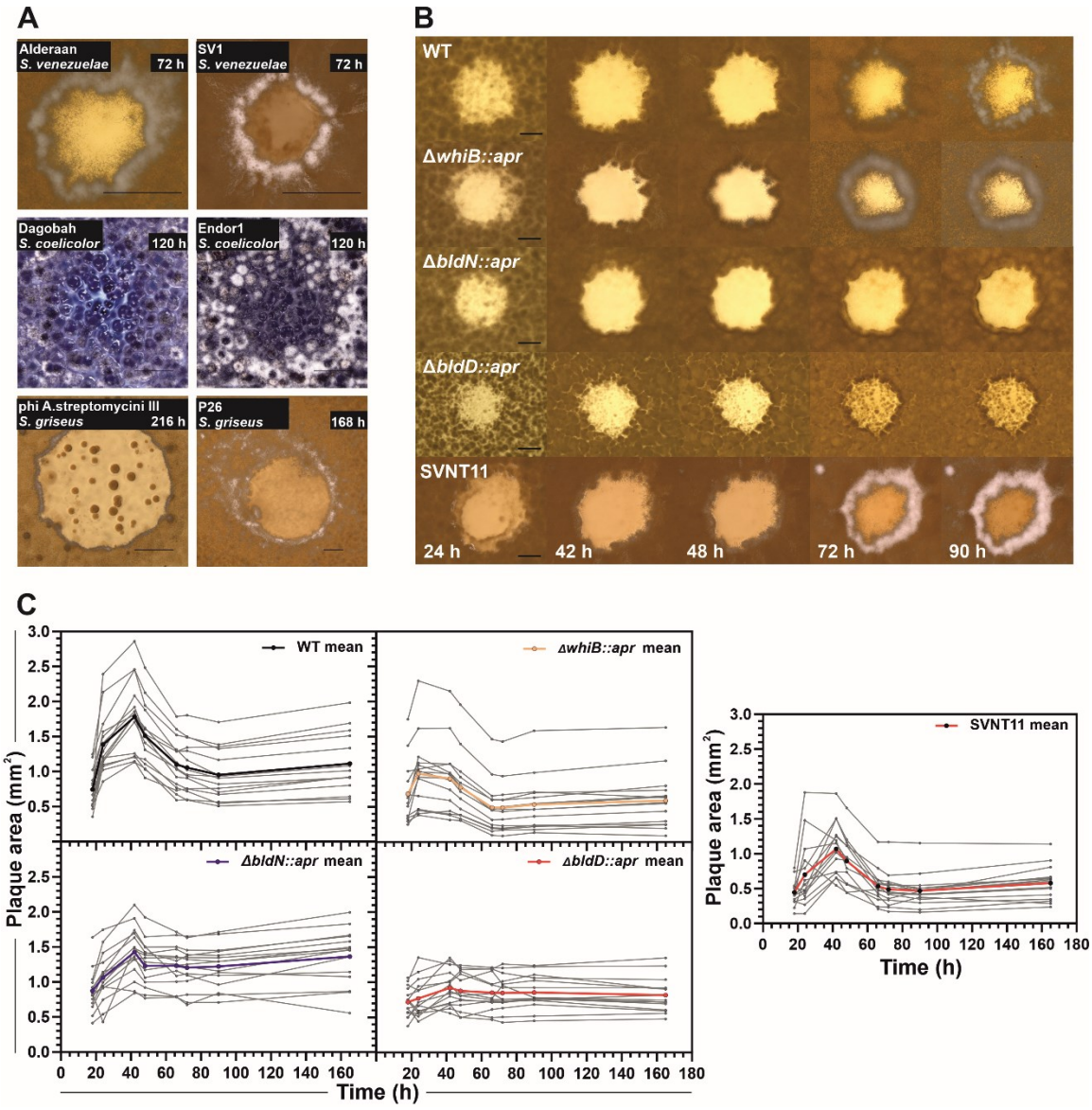

Figure 6: Phage infection in *Streptomyces* results in enhanced development and characteristic plaque dynamics. (**A**) Stereo microscopy of representative plaques of phages Alderaan and SV1 infecting *S. venezuelae*, Dagobah and Endor1 infecting *S. coelicolor* and phi A.streptomycini III and P26 infecting *S. griseus* at different time points. Scale bars represent 500 µm. (**B**) Time resolved stereo microscopy of *S. venezuelae* WT, Δ*whiB*, Δ*bldN*, Δ*bldD* and Δ*bldD* complementation (SVNT11) strains infected with Alderaan. Shown is the development of one representative single plaque per strain over time. Scale bars represent 200 µm. (**C**) Plaque area in mm^2 measured for 15 individual plaques of each strain over time with calculated means. The figure is adapted and modified from Luthe et al., 2023a.

Using a stereomicroscope for monitoring of plaque growth over time revealed growing and shrinking dynamics of the plaque formed by Alderaan on the *S. venezuelae* wild-type strain (**Figures 6B & 6C**). Maximum plaque size was reached around 42 h after infection followed by regrowing of the mycelium into the lysis zone and subsequent erecting visible aerial hyphae. This suggested regrowth of transiently phage-resistant mycelium due to developmental differentiation. Three *S. venezuelae* mutant strains, defective at different stages during development, were used for a comparative analysis of the influence of development on this phenotype. Strains used comprised the hypersporulating *S. venezuelae* strain Δ*bldD::apr* (Tschowri et al., 2014) and strain Δ*bldN::apr* restricted to vegetative growth (Bibb et al., 2012). Additionally, strain Δ*whiB::apr* was used, which is able to form aerial hyphae but is blocked in the formation of spores (Bush et al., 2016). Although initial phage infectivity was the same for all three developmental mutants and the wild-type strain, significant differences in plaque size and visible development were found. On the Δ*whiB* strain, infection resulted in smaller plaque sizes and faster differentiation but overall a less pronounced dynamics compared to the wild type. For Δ*bldN*, the infection interface is not differentiating into aerial mycelium. In line with our hypothesis, the plaques formed on this strain remain large and constant in size. On the other hand, Alderaan plaques formed on the hypersporulating strain Δ*bldD* stay significantly smaller throughout the experiment missing both initial enlargement and shrinkage as well as morphological differentiation. However, plaques on this strain got turbid at later time points, showing growth inside of the lysis zone due to the production of spores without formation of aerial hyphae. In addition, we could show that complementation of, for example, Δ*bldD* restored plaque size, visible development and a growing and shrinking phenotype comparable to the WT. Interestingly, further investigation of the regrowing interface mycelium of all strains showed that this apparent resistance to still viable phages in the lysis zone is lost after fresh inoculation when used for new infection with phage Alderaan. This highlights the transient nature of the observed regrowth provided by differentiation and indicates a critical role of development during phage infection.

Multicellular development changes phage susceptibility

Plaque dynamics, in general, are far more complex than being a simple matter of host metabolic state, when phages cannot replicate in bacteria entering the stationary phase (Abedon & Yin, 2009). Although some phages, especially T7-like podoviruses, are described to form larger and ever growing plaques even on mature and stationary phase bacterial lawns, the majority of plaques at some point cease in growth and stay at a constant size (Kawasaki et al., 2016; Yin, 1991). The resulting size and kinetics are unique

to the phage-host pair and environmental parameters as they are defined by phage properties such as adsorption rate, latent period, burst size as well as diffusivity. Diffusivity itself is defined by properties of the phage particle like size or hydrophobicity as well as the density of the bacterial lawn and agar (Gallet et al., 2011; Ghanem et al., 2019; You & Yin, 1999). In this regard, infection of developed and mature mycelium in our case additionally showed overall reduced plaque sizes on mature lawns (**Figure 7A**). This most likely can be attributed to a reduced diffusivity due to the formation of an already dense mycelium. Nonetheless, we also observed differences in timing of complete inhibition of plaque formation depending on the ability of the host to sporulate.

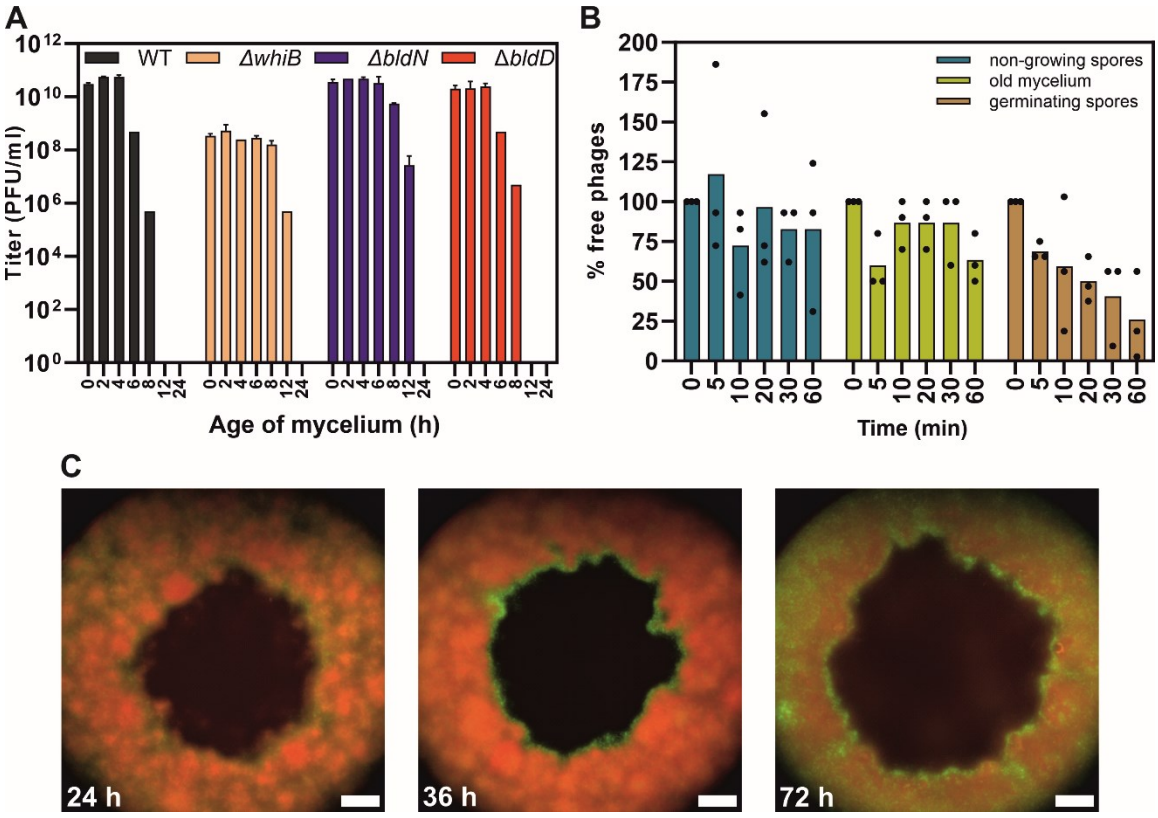

Figure 7: Effects of multicellular development on phage susceptibility. (**A**) Phage Alderaan infection of *S. venezuelae* WT and developmental mutant strains Δ*whiB*, Δ*bldN* and Δ*bldD*. Infection was performed on lawns of the respective strain after growing for the indicated time (n=2). (**B**) Adsorption of Alderaan as percentage of free phages in the medium. Spores incubated for 4 h in SM-buffer (turquois, non-growing) or GYM medium (brown, germinating) and a 24 h culture (yellow, old mycelium) were infected with Alderaan and the titer was measured over time (n=3). (**C**) Wide-field fluorescence microscopy of Alderaan infected *S. venezuelae* plaque interface mycelium stained with propidium iodide (red) and SYTO9 (green) 24, 36 and 72 h after infection shows distinct developmental patterns emerging over time. Representative plaques from three biological replicates are shown as merged images. Scale bars represent 200 µm. The figure is adapted and modified from Luthe et al., 2023a.

That said, spores are, by definition, metabolically inactive and thereby spore formation nicely resembles the previously mentioned defense strategy of dormancy seen for example in biofilms or upon CRISPR-Cas induction (Łoś et al., 2007; Williams et al., 2023). Furthermore, it reflects one of the mechanisms of antibiotic tolerance associated with the phenomenon of persister cells enduring antibiotic pressure via reduced metabolic activity (Fisher et al., 2017). For endospores of *Bacillus subtilis*, phage infection and lysis were shown to be halted until germination occurred, slowing down phage replication and lowering overall phage burden of the population (Gabiatti et al., 2018). In addition to this inactivity, *Streptomyces* spores have a thicker and altered cell surface providing further classical forms of antiphage defense. This includes adsorption interference through the changed availability of the phage receptor and reduced DNA injection due to the increased thickness of the envelope (Bradley & Ritzi, 1968; Sexton & Tocheva, 2020). The transient change in surface composition is not restricted to spores, but also includes prior formation of the hydrophobic sheath consisting of surface proteins SapB, chaplins and rodlins on the aerial hyphae being also a key feature of mature spores (Bobek et al., 2017; Claessen et al., 2004; Yang et al., 2017). We were able to observe reduced adsorption to mature mycelium and inactive spores compared to freshly germinating spores underlining the impact of differentiation on phage attachment for *Streptomyces* (**Figure 7B**). Additionally, fluorescence microscopy showed distinct developmental patterns emerging around the lysis zone visualized by propidium iodide and SYTO9 staining (**Figure 7C**). These patterns reveal changes in the cell wall which lead to the impermeability towards propidium iodide (Ladwig et al., 2015). Such changes can be seen as a similar strategy known in other, unicellular bacteria like *Staphylococcus aureus* shielding the phage receptor (Nordström & Forsgren, 1974) or for example *E. coli* producing capsules protecting from adsorption of T4 and T7 (Scholl et al., 2005; Soundararajan et al., 2019). Additionally, components of the cell wall can be changed in order to evade phage predation as seen with *Klebsiella* or *Salmonella* modifying capsule components or O-antigen length, respectively (Cota et al., 2015; Hesse et al., 2020). Furthermore, but rather on the opposite, *Streptomyces* spp., *E. coli*, *B. subtilis*, *Listeria monocytogenes* and *Enterococcus faecalis* were recently shown to reversibly shed their complete cell wall in osmoprotective environments rendering cells transiently resistant to phages (Fabijan et al., 2021; Ongenae et al., 2021, 2022; Wohlfarth et al., 2023).

How do *Streptomyces* sense phage infection?

Although the exact mechanism of active regrowth of *Streptomyces* into the lysis zone is not yet understood, cell surface changes in the course of multicellular development present a plausible explanation. This is in line with the report of plaque constriction in

Bacillus subtilis infected with phages SPP1 or Phi29. There, modifications of wall teichoic acids interfering with phage attachment were shown to be induced by the response of sigma factor SigX and led to regrowth into the plaque area (Tzipilevich et al., 2022). In both cases only local changes in cells directly neighboring active phage infected ones were triggered, indicating sensing of phages or ongoing infection (i.e. lysis) in close proximity prior to being infected. But the exact signaling cascade, whether this is specific or regulated under a more general stress response, remains unknown in both cases. Bacterial lysis leads to the release of many metabolites and cell components to the environment acting as possible signaling molecules being sensed by non-infected neighboring cells. For example, antibiotic induced lysis releases the so-called necrosignal AcrA, a periplasmic protein, in different Gram-negative and -positive species. In *E. coli*, this leads to increased antibiotic resistance upon recognition of the signal due to subsequent modulation of efflux, reactive oxygen species catabolism and membrane permeability (Bhattacharyya et al., 2020). Furthermore, extracellular ATP and DNA were shown to stimulate biofilm formation in *E. coli* and modulate antimicrobial resistance by phosphokinase activities in *Salmonella* (Johnson et al., 2013; Xi & Wu, 2010). Moreover, sensing of lysis and resulting upregulation of antibacterial pathways is reported in *Pseudomonas* (LeRoux et al., 2015). For eukaryotic systems it is known that parts of the bacterial peptidoglycan can be recognized, which triggers the innate immune responses (Crump et al., 2020). In fact, *Streptomyces* is able to sense and distinguish between the nitrogen and carbon source N-acetylglucosamine (GlcNAc) originating from chitin or its own peptidoglycan that impacts development and secondary metabolism (Rigali et al., 2008). This could be triggered by the phage induced lysis making GlcNAc from peptidoglycan available for the surrounding cells acting as a starvation signal. Similarly, increased availability of iron is important for aerial hyphae formation otherwise limiting expression of *bldN* and production of chaplins, rodlins as well as BldM (Traxler et al., 2012).

As for example shown for *S. venezuelae* in contact with *Saccharomyces cerevisiae*, under glucose depletion or at high pH, *Streptomyces* can switch to a noncanonical growth termed exploration forming fast growing, unbranched vegetative hyphae. This mode of growth can be induced in distant *Streptomyces* cells by transmission and sensing of the volatile organic compound trimethylamine (Jones et al., 2017). When infecting exploratory cells with Alderaan, we found *Streptomyces* switching back from exploration to the production of spores indicating two distinct signaling pathways (**Figure 8**). Additionally, there are several well-known signaling molecules described influencing the regulation of developmental differentiation which could also play a role in the sensing of phage infection. Notably, the quorum sensing molecule γ-butyrolactone is involved in the release

from inhibition of the *adpA/bldH* gene eventually being responsible for SapB-dependent aerial hyphae production and stopping of chromosome replication (Ohnishi et al., 2005; Płachetka et al., 2021). Most importantly, the second messenger c-di-GMP is essential for BldD and σ^{WhiG} activity influencing both early and late developmental processes (den Hengst et al., 2010; Gallagher et al., 2020; Tschowri et al., 2014). High c-di-GMP levels inside of the cell lead to the active repression of developmental processes whereas a decrease in c-di-GMP availability starts differentiation (Tschowri et al., 2014). Transient changes of the c-di-GMP level could be measured during phage infection by adapting a novel fluorescent biosensor, which was successfully tested in *Pseudomonas* and *Caulobacter* (Kaczmarczyk et al., 2022). The c-di-GMP pool is maintained through multiple diguanylate cyclases (DGC) and phosphodiesterases (PDE). *S. venezuelae* encodes a total of 7 DGCs and 4 PDEs. Among them, the membrane-associated ones harboring sensory domains can receive intra- and extracellular inputs of, for example, oxygen, light, antibiotics, quorum sensing molecules as well as other secondary metabolites released by *Streptomyces* or other bacteria (Al-Bassam et al., 2018; Hengge, 2009; Römling et al., 2013). Some of these c-di-GMP modulating enzymes, especially CdgC, were shown to have clear impacts on the development of *Streptomyces* probably being influenced by extracellular stimuli (Al-Bassam et al., 2018). Furthermore, this signaling could additionally be facilitated by the phage-triggered release of membrane vesicles as shown for T4 and T7 infections which could improve communicating ongoing infections to not-yet-infected neighbors (Mandal et al., 2021; Toyofuku et al., 2017).

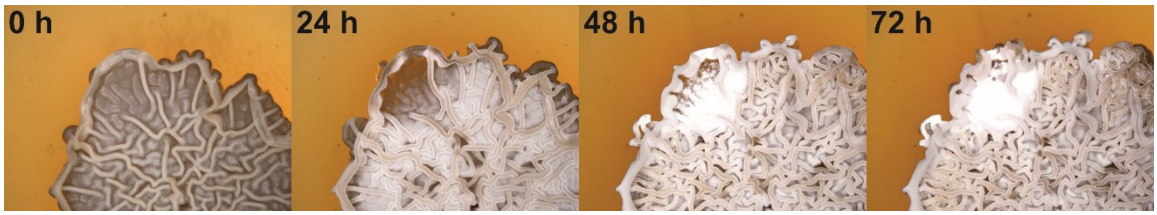

Figure 8: Explorer cells switch back to sporulation when infected with phage Alderaan. Time series stereo microscopy of *S. venezuelae* explorer cells infected with Alderaan after 6 days of initial exploratory growth. The figure is adapted and modified from Luthe et al., 2023a.

Transcriptomic modulation of the multicellular development upon phage infection

Interestingly, transcriptomic data showed a modulation of the developmental regulatory network and downstream genes in *S. venezuelae* during Alderaan infection compared to uninfected conditions (**Figure 9**). In plaque interface mycelium sampled at an early stage of plaque development, 24 h after infection, almost all *whi* genes (i.e. *whiA*, *whiB*, *whiD*, *whiE*, *whiH*, *whiI*), *bldM* and *bldO* as well as other downstream genes essential for aerial hyphae formation and sporulation like *ssgB*, *rdlAC* and *chpBCF* were downregulated while phage transcripts were high. At this time point the phage is replicating, development into

aerial hyphae has not been initiated and the plaque is growing. After 72 h post infection, a complete absence of Alderaan transcripts could be observed and downregulation of all genes except for *whiD* and *whiE* was relieved. Furthermore, genes *bldH*, *bldN*, *chpCE*, *filP*, *sapB* and *sigN*, which are essential for aerial mycelium formation were upregulated in the mycelium surrounding the lysis zone. At this later time point, we observed a completely contained infection, visible differentiation and a constriction of the plaque. While phages, following a typically parasitic behavior, are known to take over host transcription in order to facilitate propagation, infection can also lead to downregulation of cell division and biofilm genes (Finstrlová et al., 2022; Wahl & Sen, 2019). Beyond the transcriptional level, phage-induced inhibition of cell division was shown in *Bacillus subtilis* and *Escherichia coli* as a key step to avoid splitting up resources and phage components synthesized in different parts of the cell and thereby increasing the productivity of infection (C. R. Stewart et al., 2013; Kiro et al., 2013). Furthermore, phages infecting spore-forming *Bacillus* spp. are improving dispersal for example through spores and regulate sporulation as observed for phage SPβ (Abe et al., 2014; Gabiatti et al., 2018). This is additionally highlighted by phage-encoded sigma-factors, found to be ubiquitously distributed among bacteriophages infecting spore-forming hosts like *Bacillus*. These were already shown to have impact on the regulation of sporulation processes (Schuch & Fischetti, 2009; Schwartz et al., 2022).

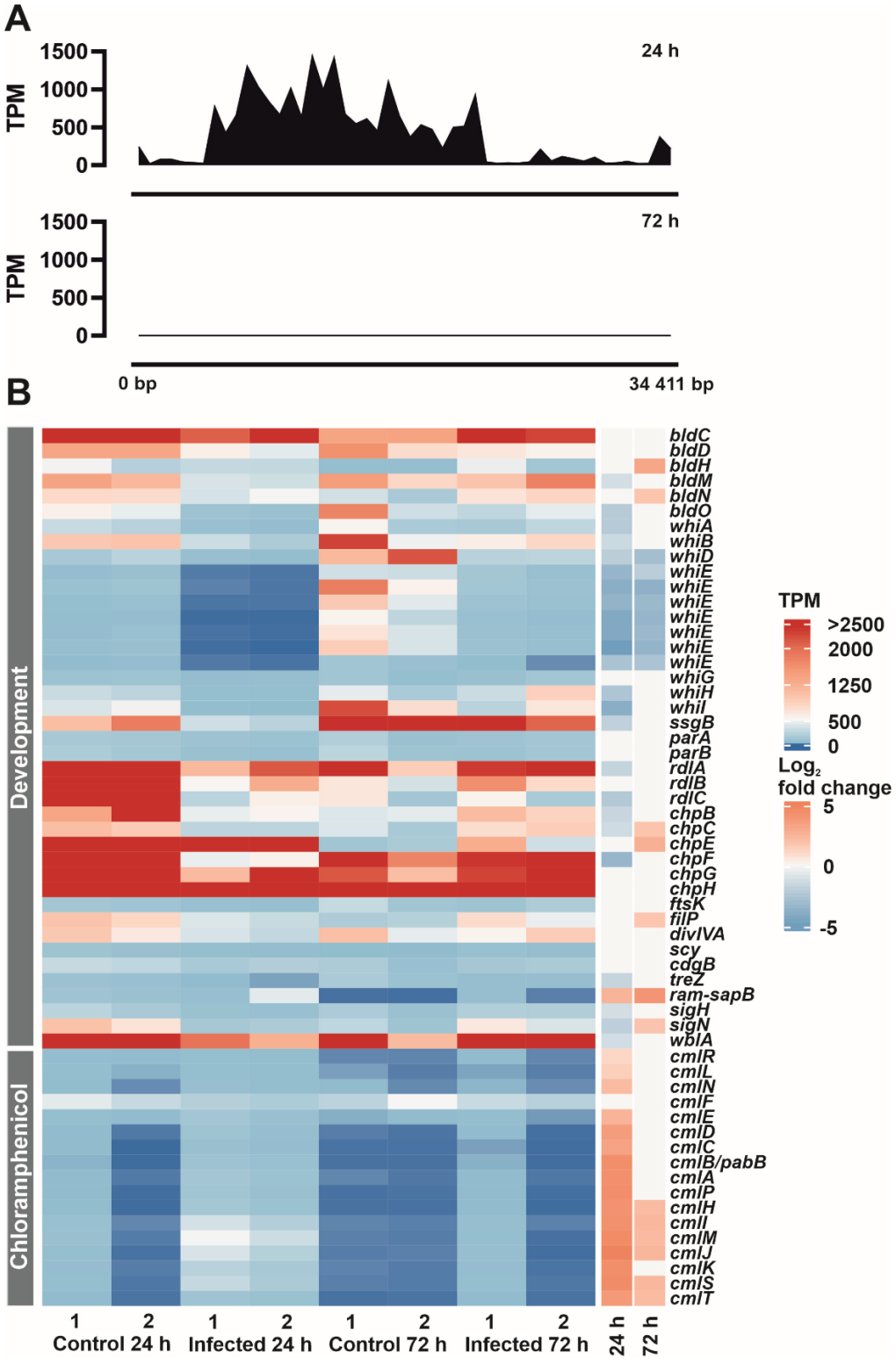

Figure 9: Transcriptome analysis of plaque interface mycelium. (**A**) Alderaan gene expression over the complete genome in transcripts per million (TPM) detected at an early (24 h) and late (72 h) time point. (**B**) Heat map of selected genes involved in *Streptomyces* multicellular development and the chloramphenicol biosynthesis gene cluster. The expression levels are shown in TPM for each sample as indicated by the legend. Two independent biological replicates are represented as control or infected at both 24 h and 72 h time points. The log_2 fold change calculated for infected vs control at the given time point is annotated on the right, color-coded according to the legend. Empty boxes represent samples where differential gene expression was not significant (FDR p-value > 0.05). The figure is adapted and modified from Luthe et al., 2023a.

Another interesting observation is the enhanced expression of the complete chloramphenicol biosynthetic gene cluster at the 24 h time point under infection conditions (**Figure 9B**). Although aminoglycosides produced by *Streptomyces* were shown to effectively inhibit phage infection (Kever et al., 2022), we did not observe a direct effect of chloramphenicol as another translation inhibiting antibiotic on Alderaan infection. However, antibiotics can have other, more subtle effects on the microbial community for example by interfering with antidefense or as a signaling molecule by which infection could be communicated (Aminov, 2009; Chevallereau et al., 2021; Pons et al., 2023; Spagnolo et al., 2021). One such example would be the polyketide antibiotic actinorhodin. Although it is not affecting phage infection, production of actinorhodin was triggered by infection (Hardy et al., 2020). Moreover, it was shown that secreted actinorhodin induces its own expression upon uptake in neighboring cells (Xu et al., 2012).

The integration of transcriptomic data, along with the transient resistance exhibited during *Streptomyces* cellular differentiation, underscores the pivotal role of multicellular development in phage-host interactions within *Streptomyces*. Interestingly, Alderaan encodes a WhiB-like transcriptional regulator. These regulators are known for their involvements in regulation of secondary metabolite production, sporulation and differentiation in *Streptomyces* (Bush, 2018). Accordingly, such a phage-encoded WhiB-like regulator could be implicated in active host manipulation, potentially providing antidefense measures. These might counteract the host cellular development as a multicellular defense strategy in order to keep surrounding cells in a susceptible stage for further propagation.

2.3.3 *Streptomyces* phages encode diverse developmental regulators

WhiB-like transcriptional regulators are most abundant in actinobacteriophages

From the initial set of five isolated *Streptomyces* phages in our lab, two were found to harbor a *whiB* gene encoding for a WhiB-like transcriptional regulator (Hardy et al., 2020). As it is known for many phages, to encode transcriptional factors similar to their host counterparts, we were interested in the identity and abundance in transcriptional regulators of actinobacteriophages (Sharma et al., 2021). A systematic search with known bacterial and phage transcriptional regulator domains in 2951 complete genomes of actinobacteriophages revealed a total of 13 distinct transcription factors to be present in as little as 0.4% to almost 24% of the phage genomes. Among these, WhiB-like transcriptional regulators are most abundant being found in almost one quarter of all analyzed genomes. Together with Cro/CI-like, MerR-like and Lsr2-like regulators, the

abundance of these four families of transcriptional regulators suggests major roles in transcriptional control in both virulent and temperate phages as well as for phages infecting a variety of associated Actinobacteria host genera. WhiB and Lsr2 type regulators are Actinobacteria-specific and phage-encoded, which show a negative correlation with Cro/CI and MerR type regulators. They were therefore investigated in more detail. As expected, the diversity of WhiB and Lsr2 over all actinobacteriophages is huge but appeared to be cluster-specific. Interestingly, especially 176 *Mycobacterium* phages harbor two copies of *whiB* genes, whereas most other actinobacteriophages have only one gene. Multiple gene copies of *lsr2* were predominantly found in *Mycobacterium* (34) and *Streptomyces* (32) infecting phages. Lsr2 is encoded by phages infecting five host genera (*Arthrobacter*; *Gordonia*, *Microbacterium*, *Mycobacterium*, *Streptomyces*) with the greatest abundance found in *Streptomyces*-infecting phages (35%) (**Figure 10A**). Similarly, WhiB is encoded by a high percentage of *Streptomyces* phages (31%) only surpassed by 38% of phages infecting *Corynebacterium*. With nine genera, the host spectrum of *whiB*-carrying phages is broader than that of Lsr2-encoding phages (*Arthrobacter*, *Corynebacterium*, *Gordonia*, *Microbacterium*, *Mycobacterium*, *Propionibacterium*, *Rhodococcus*, *Streptomyces* and *Tsukumurella*) (**Figure 10B**). Interestingly, phages harboring these genes are predominantly temperate (76%).

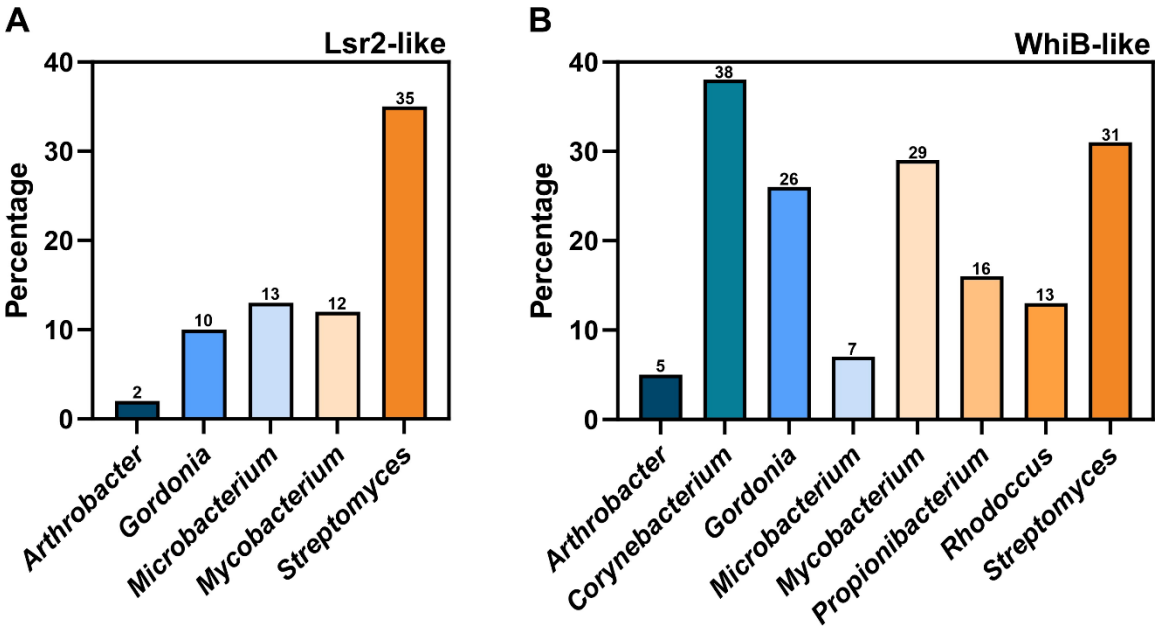

Figure 10: Abundance of WhiB-like and Lsr2-like transcriptional regulators in actinobacteriophages. Shown are the percentages of Lsr2-like (**A**) and WhiB-like (**B**) protein encoding bacteriophage genomes according to the known host genera. The figure is adapted and modified from Sharma et al., 2021.

While the extensively studied lysogenic cycle of *E. coli* infecting lambda phages showed that Cro/CI-like regulators are mainly responsible for lysis-lysogeny processes (Oppenheim et al., 2005; Shao et al., 2019), functions of WhiB-like and Lsr2-like

regulators in actinobacteriophages are not well understood. Neighboring gene content can be used to exploit the conserved gene synteny between multiple species as functional blocks to infer potential functions from this genomic context (Huynen et al., 2000). Accordingly, analysis of flanking regions 5 kb up- and downstream was performed to infer possible functions of phage-encoded WhiB-like and Lsr2-like regulators in our data set. As expected, the genomic context varies drastically between different genera and further between clusters of the same host genera infecting phages. Although most genes in these clusters are highly diverse and encode predominantly hypothetical proteins as well as domains of unknown function, at least for some clusters and phages, this analysis provided conserved synteny. These suggest potential functions for both WhiB and Lsr2 family regulators in the context of lysis-lysogeny decision-making and DNA metabolism. Especially interesting is the genome context of the *lsr2* gene in cluster A mycobacteriophages. Many phages in this cluster are lacking an integrase cassette and are maintained in an extrachromosomal state using the DNA partitioning system ParABS (Dedrick et al., 2016; Wetzel et al., 2020). Here, *lsr2* is found next to the *parABS* locus, a region of a low GC content, which is considered to be the *ori* region of these phages. Lsr2-like regulators of actinobacteriophages, like the xenogeneic silencer CgpS in *Corynebacterium glutamicum*, are already known to bind and silence especially AT-rich DNA regions and to be involved in regulating lysogeny (Pfeifer et al., 2016; Wiechert et al., 2020). Therefore, Lsr2 might allow prophage maintenance in *Mycobacterium* by silencing the *parABS* system. Additionally, host-encoded Lsr2 in *Mycobacterium* was shown to be essential for propagation of diverse mycobacteriophages as it is required for establishing a zone of phage replication inside of the cell. Interestingly, the phage-encoded version of Lsr2 of the same phages was not able to compensate for a loss of host Lsr2 nor was it as essential for infection (Dulberger et al., 2023).

Virulent *Streptomyces* phages encode diverse WhiB-like proteins

In an attempt to reduce the complexity from our analyses and to further focus on our previous findings highlighting the importance of multicellular development in phage-host interactions in *Streptomyces*, we continued the investigation of WhiB-like regulators in phages specifically infecting *Streptomyces*. In addition, we expanded this by looking for host development-associated proteins to be encoded by these phages (Luthe & Frunzke, to be submitted). A set of 337 complete and annotated *Streptomyces* phage genomes revealed the presence of genes encoding WhiB-like (Wbl) family transcriptional regulators as the most abundant development-associated genes found in one-third of genomes (32.3%). This is confirming our previous finding almost exactly, with now over 100 additional *Streptomyces* genomes added in the analysis. Furthermore, from the list of 57

development-associated gene products used, in addition to WhiB family proteins, FtsK-like, ParB-like, ParA-like and SsgA family proteins were found to be encoded in different combinations by *Streptomyces* phages which are mostly actinobacteriophage cluster specific (**Figure 11A**). Most commonly, Wbl proteins are encoded as the only developmental protein of a given phage (51) followed by the combination of WhiB-like, FtsK-like and ParB-like proteins (44) exclusively encoded by cluster BE phages. It is especially interesting that the vast majority (89.9%) of phages encoding a Wbl protein or any of the developmental proteins (86.0%) were predicted or described to be virulent (**Figure 11B**). This is significantly enriched compared to the rather equal distribution of virulent (49.0%) and temperate (47.7%) phages over all 337 analyzed genomes. Moreover, this is in stark contrast to the picture over all actinobacteriophages harboring *whiB* genes described earlier, thereby most probably excluding a distinct role of WhiB-like transcriptional regulators in lysis-lysogeny decision making for *Streptomyces* phages and underlining the functional diversity of these regulators.

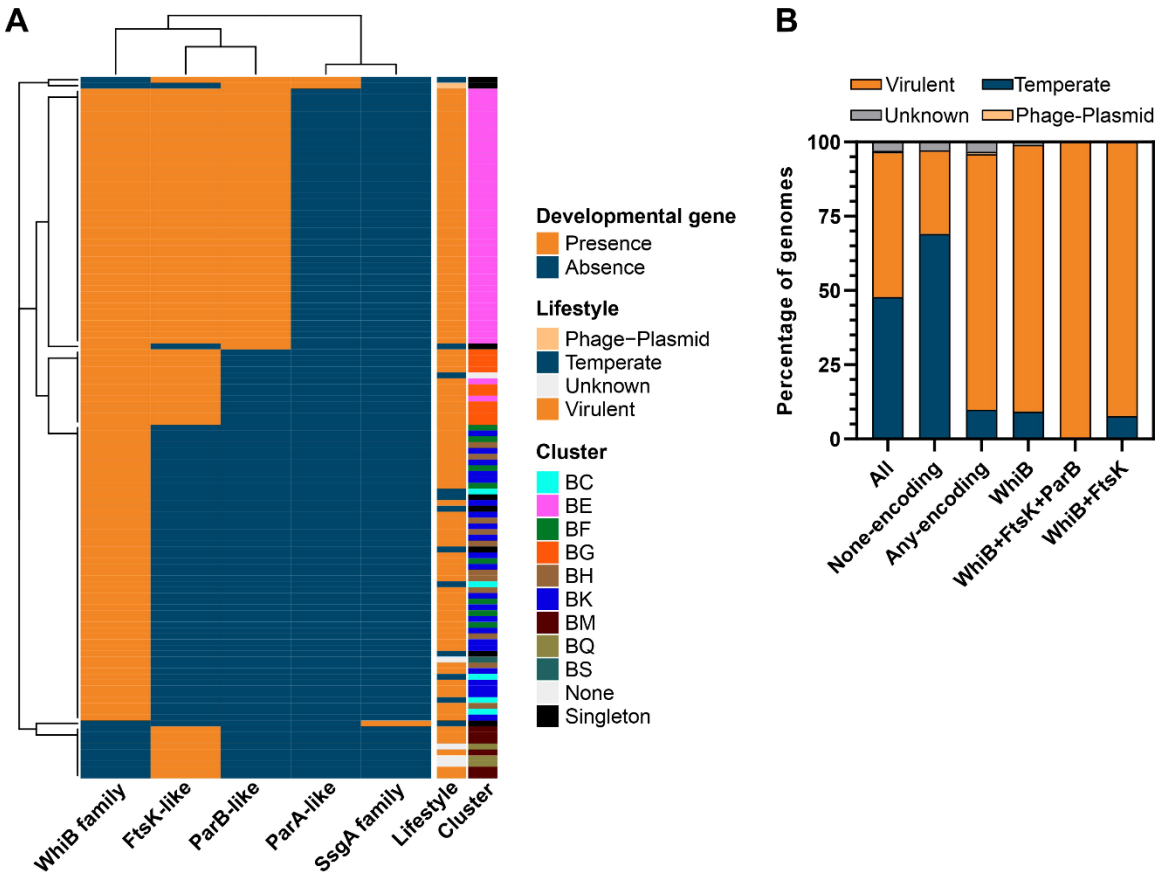

Figure 11: Phage-encoded developmental proteins found in *Streptomyces* phages. (**A**) The heat map represents the distribution of presence (orange) or absence (blue) of genes encoding a development-associated protein for each phage having at least one of these genes. Annotation of the predicted/described lifestyle and actinobacteriophage clusters of each phage is given as color-coded in the legend. Shown are only the hits of all 337 genomes investigated. (**B**) Percentage of phages belonging to the virulent, temperate, phage-plasmid or unknown lifestyles according to their respective genetic equipment. The figure is adapted and modified from Luthe & Frunzke, to be submitted.

The Actinobacteria-specific Wbl family of transcriptional regulators were found to have homologues in diverse bacterial genera including *Mycobacterium*, *Corynebacterium* and *Streptomyces* fulfilling different functions. These range from regulation of virulence, cell division and antibiotic resistance in *Mycobacterium* to cell division and response to heat and oxidative stress in *Corynebacterium*. In *Streptomyces venezuelae*, the 14 paralogues of Wbl proteins have roles in the regulatory network of cellular development as well as antibiotic production and resistance (Bush, 2018). Like the name-giving prototype in *Streptomyces*, WhiB, all members coordinate a [4Fe-4S] cluster using four conserved cysteines and feature a [G(V/I)WGG] motif facing this cluster, which was shown to be important for protein-protein interactions (Bush, 2018; Lilic et al., 2023; Soliveri et al., 2000). Indeed, for WhiB function in *Streptomyces*, it was recently shown, that an intact [4Fe-4S] cluster is essential for interacting with the sigma factor σ^A in order to recruit the RNA polymerase (RNAP) initiation complex to the promoter and enable transcription (Lilic et al., 2023). In that case, WhiB acts as a bridge between the RNAP bound sigma factor and WhiA. WhiA itself binds DNA with its C-terminal helix-turn-helix domain at the unique GACAC recognition motif in variable distances upstream of the -35 sequence (Bush et al., 2013; Kaiser & Stoddard, 2011; Lilic et al., 2023). By that, WhiA and WhiB co-regulate activation of sporulation genes shown exemplarily for *sepX* in *S. venezuelae* (Lilic et al., 2023). While Wbl proteins are also interacting with DNA, most of them bind to variable, not conserved DNA sequences. Their binding probably relies on other transcription factors like WhiA and sigma factors for specificity (Bush, 2018). An exception are the class V regulators like WhiB7 and WblC responsible for antibiotic resistance regulation in *Mycobacterium* and *Streptomyces*, respectively. These Wbl proteins have a unique AT-hook binding especially to AT-rich sequences directly upstream of the target promoter, thereby activating expression independent of a WhiA homolog (Burian et al., 2013; Lilic et al., 2021, 2023). Interestingly, while WhiAB co-regulate the majority of genes in *Streptomyces* with an activating effect, the expression of *filP* is notably subjected to negative regulation (Bush et al., 2013, 2016). However, the mechanism of repression compared to the recent insights into activation has not yet been investigated.

In our analyses, we compared all 110 *Streptomyces* phage-encoded WhiB-like transcriptional regulators with the 14 *S. venezuelae*-encoded ones (subset shown in **Figure 12A**). Here, we found the [4Fe-4S] cluster coordinating cysteines as a conserved key functional feature in all but two phage-encoded proteins. Especially these two proteins encoded by phages Jay2Jay and BRock are the shortest Wbl proteins among both phage and host versions (55 and 82 aa, respectively) missing each one cysteine residue. Therefore they probably fail to form the [4Fe-4S] cluster, potentially impairing complex formation with the sigma factor as previously shown for WhiB and WhiD (Lilic et al., 2023;

M. Y. Y. Stewart et al., 2020). Additionally, the glycine-rich, five residue motif (G[V/I]WGG) facing the [4Fe-4S] cluster is present in all phage Wbl proteins as well but subject to some variation in a subset of phages which appears to be cluster- rather than host-specific (**Figure 12A**, boxed residues 84-88). Especially, all five BC cluster phages replaced the tryptophan residue at position 86 with arginine. In contrast, Wbl proteins from all 11 BH and four of 22 BK cluster phages were characterized by an exchange of the valine/isoleucine residue 85 with threonine. Furthermore, all eight BF cluster phages substituted the first glycine residue 84 with threonine as well as the tryptophan at position 86 with arginine. None of these modifications was found in the host-encoded homologues. More precisely, unlike seen here in the *Streptomyces* phages this motif is highly conserved across Actinobacteria genera (Bush, 2018). Furthermore, for *Mycobacterium*-encoded Wbl proteins three residues directly next to this motif, which are mostly conserved among orthologues of the same class in different genera but not among paralogues within the same species, were shown to determine sigma factor binding specificity (Burian et al., 2013; Bush, 2018; Casonato et al., 2012). These adjacent amino acids are mostly conserved in phage-encoded Wbl family proteins with the respective changes in the (G[V/I]WGG) motif. Taken together, it is tempting to speculate that changes directly next to and in this motif likely affect the protein-protein interactions and probably modulate the affinity towards different sigma factors or other interaction partners.

Phylogenetic analysis of WhiB-like transcriptional regulators from seven *S. venezuelae* infecting phages with all 14 paralogues of the Wbl family in *S. venezuelae* supported grouping of the five cluster BC phage-encoded WhiB-like proteins of Alderaan, Papayasalad, Austintatious, Bioscum and Ididsumtinwong (**Figure 12B**). However, they only form a weakly-supported sister group with host-encoded WblM, the largest *S. venezuelae* Wbl protein with an unknown function and not associated with one of the five major classes (Bush, 2018). The WhiB-like protein of cluster BE phage Coruscant appears to be randomly placed on the tree with the lowest overall support value. Singleton phage Chymera on the other hand encodes a WhiB-like protein clustering as a well-supported sister group with host-encoded WhiB and WblH. Despite WblH being related closest to WhiB, like WblM it has an unknown function that probably is distinct from that of WhiB and therefore this is likely to be the case for the Wbl regulator of Chymera, too. Nonetheless, the well-supported distinction between WhiB family proteins from Chymera and BC phages is a first indicator of the different functions of these proteins between phages infecting the same host strain.

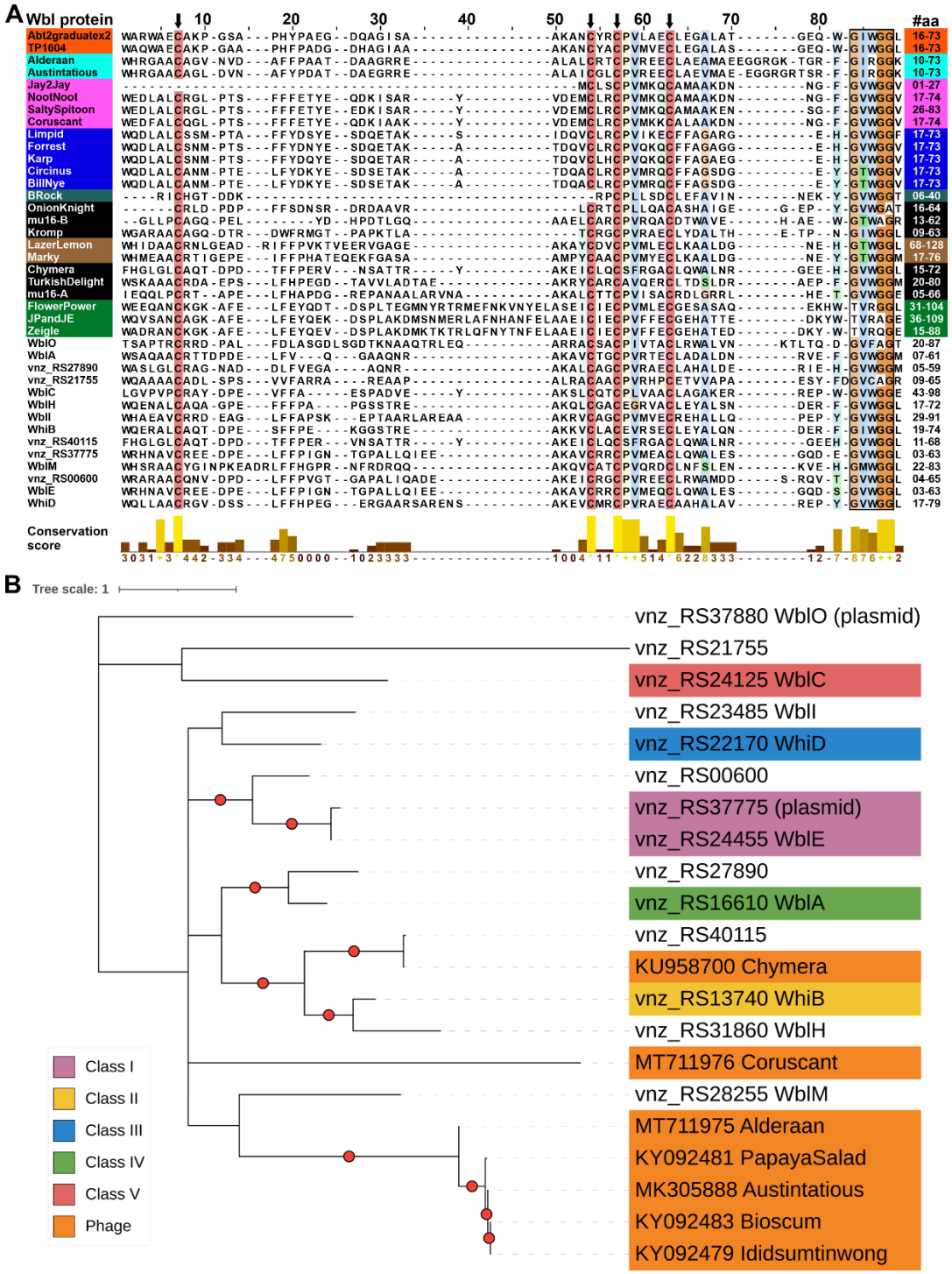

Figure 12: Amino acid sequence analysis of WhiB-like transcriptional regulators. (**A**) Multiple sequence alignment of the conserved middle region of a representative subset of 39 host- and phage-encoded WhiB-like transcriptional regulators. Labels of phage-encoded Wbl proteins are highlighted according to their actinobacteriophage cluster in red (BG), turquoise (BC), pink (BE), blue (BK), petrol (BS), brown (BH), green (BF) and black (singleton). *S. venezuelae* sequence labels are white. The alignment shows the four conserved cysteines (black arrows) and the (G[V/I]WGG) motif (box). For each position the conservation score is given based on physico-chemical similarity for all 124 Wbl proteins. (**B**) Phylogenetic tree of WhiB-like regulators from *S. venezuelae* and the phages infecting *S. venezuelae*. Full-length amino acid sequences were used for alignment with MUSCLE and tree drawing using the WAG+G+I+F model. From 500 bootstrap replicates, values over 50% are marked with a red dot. Labels are color-coded according to the five classes of paralogues and the origin of sequence as given in the legend. The figure is adapted and modified from Luthe & Frunzke, to be submitted.

Phage-encoded WhiB-like regulators influence cellular development

Using the Δ*whiB*::apr strain of *S. venezuelae* NRRL B-65442 which is unable to sporulate and to form the green spore pigment (Bush et al., 2016), we were able to perform complementation assays with different phage-encoded WhiB variants (**Figure 13A**). Here, the host and different phage *whiB* variants were expressed under the native host *whiB* promoter in the Δ*whiB* strain. Phage-encoded WhiB proteins being able to restore the wild-type phenotype probably fulfill a similar function as the host WhiB in *Streptomyces*. As expected for the host-encoded WhiB, the positive control, the wild-type phenotype could be fully restored. In contrast, expressing *whiB* genes of phages Alderaan, Coruscant and Chymera under the same *S. venezuelae* promoter failed to restore full sporulation. Hence, host WhiB function is clearly separated from that of the known *S. venezuelae* phage WhiB-like diversity. In a next step, phage-encoded Wbl proteins were produced constitutively in the *S. venezuelae* WT. This approach yielded morphological differences induced by the phage-encoded WhiB-like proteins (**Figure 13B**). The constitutive expression of *whiB* from singleton phage Chymera resembled the host *whiB* overexpression phenotype, sporulating earlier than the WT. In contrast, strains producing WhiB-like proteins from Alderaan and Coruscant showed elongated hyphae and delayed sporulation. Although morphological changes were also observed for basal expression of *whiB* of mycobacteriophage TM4 in *Mycobacterium smegmatis*, these led to a reduced susceptibility towards TM4 representing a superinfection exclusion mechanism (Rybniker et al., 2010). In contrast, infection with Alderaan and Coruscant showed no differences in initial susceptibility of the four strains expressing *whiB* from Alderaan, Coruscant, Chymera or *S. venezuelae* compared to infection of the WT despite exhibiting morphological changes (**Figure 13C**). However, plaque sizes of Alderaan infecting strains of increased sporulation were smaller than on the other strains (**Figure 13D**). This is nicely resembling the observations made when infecting the hypersporulating Δ*bldD* strain with Alderaan in our previous study (Luthe et al., 2023a). This once more underlines the crucial role of sporulation in the context of phage-host interaction. The fact, that active production of prophage-encoded WhiB is reducing efficient propagation of a second phage fits to the overall topic of diverse phage-phage competition mechanisms predominantly seen in prophages applying superinfection immunity (Ko & Hatfull, 2018; Owen et al., 2021; Patel & Maxwell, 2023).

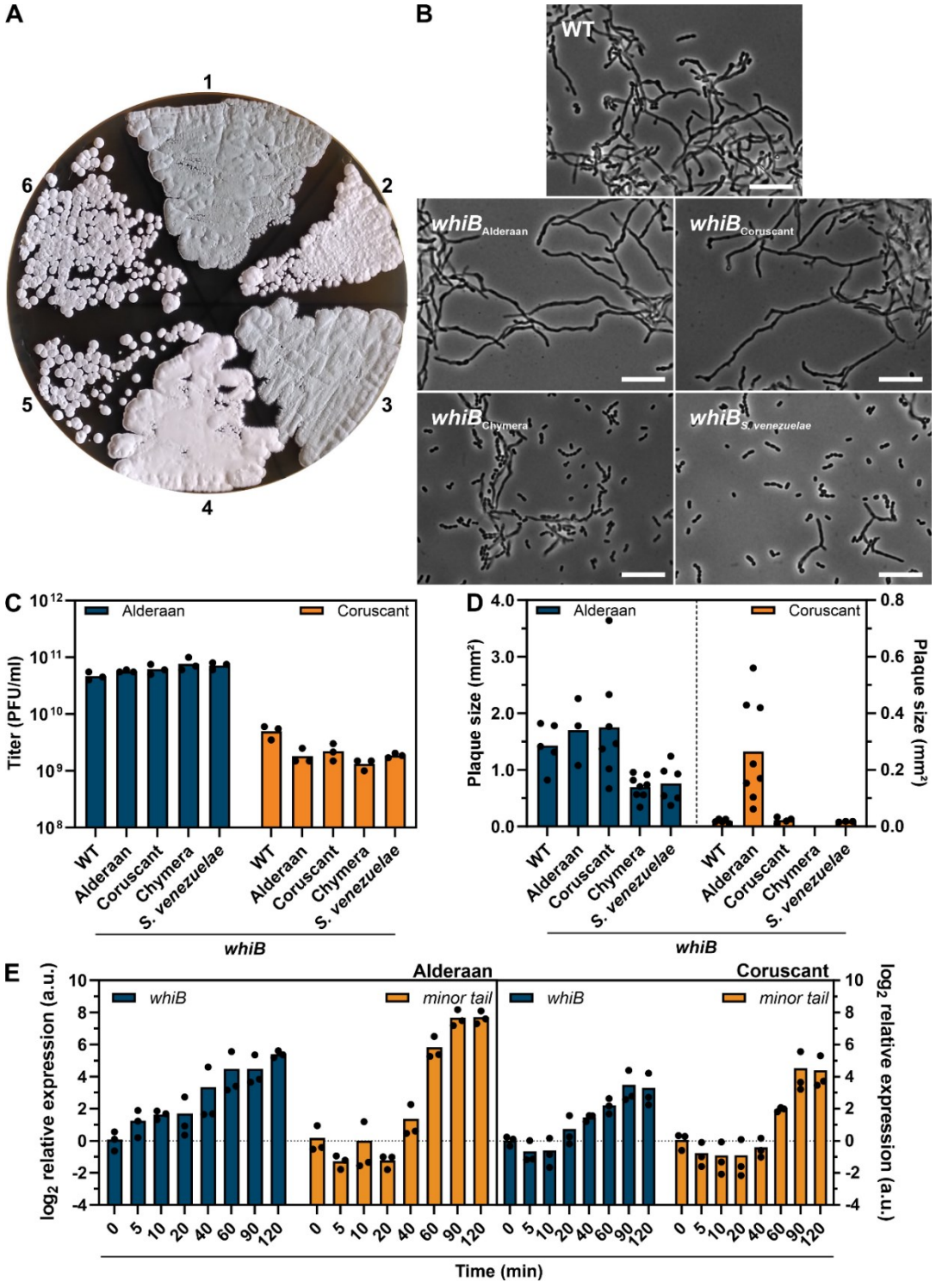

Figure 13: Phenotypic characterization of the effect of phage-encoded Wbl proteins. (**A**) The complementation assay compares the formation of the green spore pigment of the *S. venezuelae* WT (1) with the Δ*whiB* strain (2) and complementations with *whiB* from *S. venezuelae* (3), Alderaan (4), Coruscant (5) and Chymera (6) under the native host *whiB* promoter after 2 days grown on MYM agar. (**B**) *S. venezuelae* WT and wild-type strains constitutively expressing *whiB* from Alderaan, Coruscant, Chymera and *S. venezuelae* grown for 24 h in GYM medium examined under the microscope show morphological differences. Scale bars represent 10 µm. (**C**) Titer of Alderaan and Coruscant on strains expressing *whiB* of the indicated origins are comparable to titers achieved on the WT (n=3). (**D**) Plaque sizes of Alderaan and Coruscant differ on specific overexpressing strains. (**E**) Gene expression of Alderaan and Coruscant *whiB* and *minor tail* genes during liquid infection of *S. venezuelae* are shown as $\log_2$ fold relative expression from an RT-qPCR experiment (n=3). The figure is adapted and modified from Luthe & Frunzke, to be submitted.

Interestingly, the expression of *whiB* from Alderaan resulted in bigger plaque sizes for the infection with Coruscant, hinting towards a mechanism that is improving phage propagation as discussed below (**Figure 13D**). This indicates clear differences in the functions of Alderaan and Coruscant encoded Wbl proteins as expression of the gene from Coruscant has no impact on plaque sizes of Alderaan despite a similar phenotype in the host. Such phage-phage interactions and improvement of infection with proteins from different phages are also seen in other phage-host systems. This was observed for example with *Pseudomonas* phages producing anti-CRISPR proteins cooperatively improving other phages propagation by blocking the Cas3 and Cas9 activities (Borges et al., 2018) as well as so-called arming of phages with specific effector payload in order to improve for example phage therapy approaches in urinary tract infections with *E. coli* and *Klebsiella* (Du et al., 2023; Kilcher et al., 2018). Whether interaction with the *Streptomyces* multicellular development, as hypothesized previously, is responsible for the Alderaan WhiB-like protein effect on Coruscant propagation is not yet clear. In this regard, it will be essential to establish phage genome engineering techniques for our *Streptomyces* system which will enable deleting, silencing, tagging or manipulating the *whiB* genes of the bacteriophages and provide the basis for more in-depth investigations (Ghosh et al., 2023; Kilcher et al., 2018; Marinelli et al., 2008; Wetzel et al., 2021). Unfortunately, approaches in modifying both Alderaan and Coruscant genomes were not yet successful because *Streptomyces* genetic engineering exhibits unique hurdles due to its life cycle, high GC-content and comparatively limited readily available genetic tools.

We observed that phage-encoded WhiB-like transcriptional regulators can induce distinct morphological changes in the *Streptomyces* host and that they have impact on phage propagation. Therefore, we investigated if these genes are expressed under native infection conditions. By using RT-qPCR during liquid infections of *S. venezuelae* WT with Alderaan or Coruscant, expression for both *whiB* genes was proven (**Figure 13E**). For Coruscant, expression of *whiB* could be measured earliest 20 min after infection, for Alderaan, *whiB* was expressed already 5 min after infection. In both cases, the expression started significantly earlier but was also less pronounced compared to the respective minor tail gene measured as control. This characterizes the phage *whiB* genes as active, early genes of moderate expression. Usually, expression of early genes is important for controlling and directing host metabolism and for the directly following expression of middle and late phage genes (Datta & Mandal, 1998; Godinho et al., 2018; McAllister & Barrett, 1977; Son et al., 2022). Hence, for phage-encoded WhiB-like regulators being produced early, the two main hypotheses regarding their function would be i) interaction with the host regulatory network in order to manipulate for example differentiation and development or ii) involvement in its own phage gene expression. In multiple phage-host

pairs such strategies are already known and could explain how both functions are achieved. The RNA polymerase initiation complex could be actively recruited to specific promoters of either host or phage development genes (Mallory et al., 1990; Muñoz-Espín et al., 2010), RNAP complex binding site of specific host promoters could be blocked (Jiang et al., 2023) or the phage-encoded proteins could enforce direct competition with host-encoded regulators for binding the host sigma factors or additional factors like WhiA, depleting these pools and thereby inhibiting host transcription (B. Liu et al., 2014; Wahl & Sen, 2019). A key next step regarding these open questions would be the illumination of the regulons of phage-encoded WhiB-like proteins by applying chromatin immuno-precipitation (ChIP) – sequencing. This was already used routinely for bacterial regulators and could be combined with the identification of protein interaction partners exemplified in recent studies on *Streptomyces* WhiB (Bush et al., 2016; Lilic et al., 2023).

2.4 Conclusion and future perspectives

The ever-growing wealth of phage genomes sequenced, genes predicted and antiphage defense systems discovered in recent years demands for an increase in our efforts to investigate the identity and function of a broader diversity of phages and their unique genetic equipment. The majority of isolated and sequenced phages is yet far away from being fully characterized or understood. Especially, phage-host systems with unusual traits for bacteria, as for example the filamentous growth and multicellular development presented by *Streptomyces* spp., are understudied in their phage-host interactions regarding these remarkable features. To this end, like the historical “phage treaty” focused on a fixed set of phages, which were shared between researchers, systematic phage collections are of immense value to the research community when openly providing and sharing information and samples.

This doctoral thesis addresses multicellular development at the center of phage-host interactions in the environmentally and biotechnologically relevant *Streptomyces* bacteria. It highlights host differentiation providing transient resistance against bacteriophages as an important multicellular strategy in antiviral defense of bacteria. Susceptibility to phage infection is affected by the developmental state of the surrounding cells. So far, the formation of a dense mycelium, transition to aerial hyphae and following sporulation, *Streptomyces* development as a defense strategy best resembles a combination of both biofilm-associated dormancy and diffusivity aspects, as well as interference with adsorption and injection due to the alteration of the cell envelope. However, the suggested necessity of signaling and sensing ongoing infection in neighboring cells is a feature known and extensively investigated in eukaryotic systems. Damage-associated molecular patterns in animals and plants initiate innate immune responses triggered by signals such as extracellular ATP released upon cell damage (Khakh & Burnstock, 2009; Tanaka et al., 2014). Furthermore, protection of kin cells by differentiation and shielding susceptible parts of the mycelium described in this thesis corresponds to a division of labor comparable to lung epithelial barrier cells. These cells can be less susceptible to infection, provide a physical barrier and trigger inflammation upon pathogen recognition (de Waal et al., 2022; Hammad & Lambrecht, 2015). Nevertheless, key insights into the exact mechanism of antiphage defense provided by *Streptomyces* differentiation is still missing. This is in part due to the lack of knowledge about *Streptomyces* phage receptors, which could give vital indications in further studies on how development confers its resistance.

While host multicellular development appears to be a key feature of antiphage defense in *Streptomyces*, the presented work additionally highlights the WhiB-like family of proteins to be the most abundant transcriptional regulators in *Streptomyces* phages. This group of

phage-encoded regulators is highly diversified and probably expands the known functions of their host-encoded homologues. Although phage-encoded Wbl proteins are highly associated to virulent phages, we found a prophage-encoded version that resulted in distinct morphological changes opposing those of virulent phages. All three of the investigated regulators influenced the development of the host. Chymera-encoded WhiB induced hypersporulation, which reduced plaque formation of Alderaan, whereas Alderaan encoded WhiB led to unbranched, elongated hyphae that improved plaque size of Coruscant. The *whiB* from Coruscant in turn had no impact on Alderaan infections. Whether these distinctive morphological changes and effects are direct results of the encoded WhiB-like proteins or the work of additional gene products is yet unclear. Questions remain open to which degree phages actively manipulate developmental processes during infection and which role WhiB-like proteins have in that.

By discovering the role of cellular development mediated antiphage defense and the diversity and abundance of phage-encoded WhiB-like transcriptional regulators, this thesis expanded the knowledge on intricate microbial interactions in nature. The foundations laid here, provide opportunities for further in-depth investigations on the exact mechanisms of the complex interdependencies between cellular development, secondary metabolite production and phage predation. Illuminating the signaling and sensing during infection and the role of phage-encoded WhiB will reveal even greater complexity and holds the potential for tailored use in molecular biology and biotechnological applications.

2.5 References

Abe, K., Kawano, Y., Iwamoto, K., Arai, K., Maruyama, Y., Eichenberger, P., & Sato, T. (2014). Developmentally-regulated excision of the SPβ prophage reconstitutes a gene required for spore envelope maturation in *Bacillus subtilis*. *PLoS Genetics*, *10*(10), e1004636. https://doi.org/10.1371/journal.pgen.1004636

Abedon, S. T., & Yin, J. (2009). Bacteriophage plaques: theory and analysis. In *Methods in molecular biology (Clifton, N.J.)* (Vol. 501, pp. 161–174). https://doi.org/10.1007/978-1-60327-164-6_17

Ackermann, H.-W. (2007). 5500 Phages examined in the electron microscope. *Archives of Virology*, *152*(2), 227–243. https://doi.org/10.1007/s00705-006-0849-1

Al-Bassam, M. M., Bibb, M. J., Bush, M. J., Chandra, G., & Buttner, M. J. (2014). Response regulator heterodimer formation controls a key stage in *Streptomyces* development. *PLoS Genetics*, *10*(8), e1004554. https://doi.org/10.1371/journal.pgen.1004554

Al-Bassam, M. M., Haist, J., Neumann, S. A., Lindenberg, S., & Tschowri, N. (2018). Expression Patterns, Genomic Conservation and Input Into Developmental Regulation of the GGDEF/EAL/HD-GYP Domain Proteins in *Streptomyces*. In *Frontiers in Microbiology* (Vol. 9). https://www.frontiersin.org/articles/10.3389/fmicb.2018.02524

Alam, K., Mazumder, A., Sikdar, S., Zhao, Y.-M., Hao, J., Song, C., Wang, Y., Sarkar, R., Islam, S., Zhang, Y., & Li, A. (2022). *Streptomyces*: The biofactory of secondary metabolites. *Frontiers in Microbiology*, *13*, 968053. https://doi.org/10.3389/fmicb.2022.968053

Aminov, R. I. (2009). The role of antibiotics and antibiotic resistance in nature. *Environmental Microbiology*, *11*(12), 2970–2988. https://doi.org/https://doi.org/10.1111/j.1462-2920.2009.01972.x

Baltz, R. H. (2012). *Streptomyces* temperate bacteriophage integration systems for stable genetic engineering of actinomycetes (and other organisms). *Journal of Industrial Microbiology & Biotechnology*, *39*(5), 661–672. https://doi.org/10.1007/s10295-011-1069-6

Banh, D. V, Roberts, C. G., Morales-Amador, A., Berryhill, B. A., Chaudhry, W., Levin, B. R., Brady, S. F., & Marraffini, L. A. (2023). Bacterial cGAS senses a viral RNA to initiate immunity. *Nature*. https://doi.org/10.1038/s41586-023-06743-9

Barka, E. A., Vatsa, P., Sanchez, L., Gaveau-Vaillant, N., Jacquard, C., Meier-Kolthoff, J. P., Klenk, H.-P., Clément, C., Ouhdouch, Y., & van Wezel, G. P. (2016). Taxonomy, Physiology, and Natural Products of Actinobacteria. *Microbiology and Molecular Biology Reviews : MMBR*, *80*(1), 1–43. https://doi.org/10.1128/MMBR.00019-15

Barrangou, R., Fremaux, C., Deveau, H., Richards, M., Boyaval, P., Moineau, S., Romero, D. A., & Horvath, P. (2007). CRISPR Provides Acquired Resistance Against Viruses in Prokaryotes. *Science*, *315*(5819), 1709–1712. https://doi.org/10.1126/science.1138140

Beerens, D., Franch-Arroyo, S., Sullivan, T. J., Goosmann, C., Brinkmann, V., & Charpentier, E. (2021). Survival Strategies of *Streptococcus pyogenes* in Response to Phage Infection. In *Viruses* (Vol. 13, Issue 4). https://doi.org/10.3390/v13040612

Bentley, S. D., Chater, K. F., Cerdeño-Tárraga, A.-M., Challis, G. L., Thomson, N. R., James, K. D., Harris, D. E., Quail, M. A., Kieser, H., Harper, D., Bateman, A., Brown, S., Chandra, G., Chen, C. W., Collins, M., Cronin, A., Fraser, A., Goble, A., Hidalgo, J., … Hopwood, D. A. (2002). Complete genome sequence of the model

actinomycete *Streptomyces coelicolor* A3(2). *Nature*, *417*(6885), 141–147. https://doi.org/10.1038/417141a

Bernheim, A., & Sorek, R. (2020). The pan-immune system of bacteria: antiviral defence as a community resource. *Nature Reviews Microbiology*, *18*(2), 113–119. https://doi.org/10.1038/s41579-019-0278-2

Bertozzi Silva, J., Storms, Z., & Sauvageau, D. (2016). Host receptors for bacteriophage adsorption. *FEMS Microbiology Letters*, *363*(4). https://doi.org/10.1093/femsle/fnw002

Bhattacharyya, S., Walker, D. M., & Harshey, R. M. (2020). Dead cells release a 'necrosignal' that activates antibiotic survival pathways in bacterial swarms. *Nature Communications*, *11*(1), 4157. https://doi.org/10.1038/s41467-020-17709-0

Bibb, M. J., Domonkos, A., Chandra, G., & Buttner, M. J. (2012). Expression of the chaplin and rodlin hydrophobic sheath proteins in *Streptomyces venezuelae* is controlled by σ(BldN) and a cognate anti-sigma factor, RsbN. *Molecular Microbiology*, *84*(6), 1033–1049. https://doi.org/10.1111/j.1365-2958.2012.08070.x

Bickle, T. A., & Krüger, D. H. (1993). Biology of DNA restriction. *Microbiological Reviews*, *57*(2), 434–450. https://doi.org/10.1128/mr.57.2.434-450.1993

Bobek, J., Šmídová, K., & Čihák, M. (2017). A Waking Review: Old and Novel Insights into the Spore Germination in *Streptomyces*. *Frontiers in Microbiology*, *8*, 2205. https://doi.org/10.3389/fmicb.2017.02205

Bond, M. C., Vidakovic, L., Singh, P. K., Drescher, K., & Nadell, C. D. (2021). Matrix-trapped viruses can prevent invasion of bacterial biofilms by colonizing cells. *ELife*, *10*. https://doi.org/10.7554/eLife.65355

Bondy-Denomy, J., Qian, J., Westra, E. R., Buckling, A., Guttman, D. S., Davidson, A. R., & Maxwell, K. L. (2016). Prophages mediate defense against phage infection through diverse mechanisms. *The ISME Journal*, *10*(12), 2854–2866. https://doi.org/10.1038/ismej.2016.79

Borges, A. L., Zhang, J. Y., Rollins, M. F., Osuna, B. A., Wiedenheft, B., & Bondy-Denomy, J. (2018). Bacteriophage Cooperation Suppresses CRISPR-Cas3 and Cas9 Immunity. *Cell*, *174*(4), 917-925.e10. https://doi.org/10.1016/j.cell.2018.06.013

Bradley, S. G., & Ritzi, D. (1968). Composition and ultrastructure of *Streptomyces venezuelae*. *Journal of Bacteriology*, *95*(6), 2358–2364. https://doi.org/10.1128/jb.95.6.2358-2364.1968

Brady, A., Felipe-Ruiz, A., Gallego del Sol, F., Marina, A., Quiles-Puchalt, N., & Penadés, J. R. (2021). Molecular Basis of Lysis–Lysogeny Decisions in Gram-Positive Phages. *Annual Review of Microbiology*, *75*(1), 563–581. https://doi.org/10.1146/annurev-micro-033121-020757

Burian, J., Yim, G., Hsing, M., Axerio-Cilies, P., Cherkasov, A., Spiegelman, G. B., & Thompson, C. J. (2013). The mycobacterial antibiotic resistance determinant WhiB7 acts as a transcriptional activator by binding the primary sigma factor SigA (RpoV). *Nucleic Acids Research*, *41*(22), 10062–10076. https://doi.org/10.1093/nar/gkt751

Bush, M. J. (2018). The actinobacterial WhiB-like (Wbl) family of transcription factors. *Molecular Microbiology*, *110*(5), 663–676. https://doi.org/10.1111/mmi.14117

Bush, M. J., Bibb, M. J., Chandra, G., Findlay, K. C., & Buttner, M. J. (2013). Genes required for aerial growth, cell division, and chromosome segregation are targets of WhiA before sporulation in *Streptomyces venezuelae*. *MBio*, *4*(5), e00684-13. https://doi.org/10.1128/mBio.00684-13

Bush, M. J., Chandra, G., Bibb, M. J., Findlay, K. C., & Buttner, M. J. (2016). Genome-Wide Chromatin Immunoprecipitation Sequencing Analysis Shows that WhiB Is a Transcription Factor That Cocontrols Its Regulon with WhiA To Initiate Developmental Cell Division in *Streptomyces*. *MBio*, *7*(2), e00523-16. https://doi.org/10.1128/mBio.00523-16

Bush, M. J., Chandra, G., Findlay, K. C., & Buttner, M. J. (2017). Multi-layered inhibition of *Streptomyces* development: BldO is a dedicated repressor of whiB. *Molecular Microbiology*, *104*(5), 700–711. https://doi.org/10.1111/mmi.13663

Bush, M. J., Gallagher, K. A., Chandra, G., Findlay, K. C., & Schlimpert, S. (2022). Hyphal compartmentalization and sporulation in *Streptomyces* require the conserved cell division protein SepX. *Nature Communications*, *13*(1). https://doi.org/10.1038/s41467-021-27638-1

Bush, M. J., Tschowri, N., Schlimpert, S., Flärdh, K., & Buttner, M. J. (2015). c-di-GMP signalling and the regulation of developmental transitions in streptomycetes. *Nature Reviews. Microbiology*, *13*(12), 749–760. https://doi.org/10.1038/nrmicro3546

Casonato, S., Cervantes Sánchez, A., Haruki, H., Rengifo González, M., Provvedi, R., Dainese, E., Jaouen, T., Gola, S., Bini, E., Vicente, M., Johnsson, K., Ghisotti, D., Palù, G., Hernández-Pando, R., & Manganelli, R. (2012). WhiB5, a transcriptional regulator that contributes to *Mycobacterium tuberculosis* virulence and reactivation. *Infection and Immunity*, *80*(9), 3132–3144. https://doi.org/10.1128/IAI.06328-11

Chaikeeratisak, V., Nguyen, K., Khanna, K., Brilot, A. F., Erb, M. L., Coker, J. K. C., Vavilina, A., Newton, G. L., Buschauer, R., Pogliano, K., Villa, E., Agard, D. A., & Pogliano, J. (2017). Assembly of a nucleus-like structure during viral replication in bacteria. *Science*, *355*(6321), 194–197. https://doi.org/10.1126/science.aal2130

Chater, K. F., Biró, S., Lee, K. J., Palmer, T., & Schrempf, H. (2010). The complex extracellular biology of *Streptomyces*. *FEMS Microbiology Reviews*, *34*(2), 171–198. https://doi.org/10.1111/j.1574-6976.2009.00206.x

Chevallereau, A., Pons, B. J., van Houte, S., & Westra, E. R. (2021). Interactions between bacterial and phage communities in natural environments. *Nature Reviews. Microbiology*. https://doi.org/10.1038/s41579-021-00602-y

Ciofu, O., Moser, C., Jensen, P. Ø., & Høiby, N. (2022). Tolerance and resistance of microbial biofilms. *Nature Reviews Microbiology*, *20*(10), 621–635. https://doi.org/10.1038/s41579-022-00682-4

Claessen, D., Rink, R., de Jong, W., Siebring, J., de Vreugd, P., Boersma, F. G. H., Dijkhuizen, L., & Wosten, H. A. B. (2003). A novel class of secreted hydrophobic proteins is involved in aerial hyphae formation in *Streptomyces coelicolor* by forming amyloid-like fibrils. *Genes & Development*, *17*(14), 1714–1726. https://doi.org/10.1101/gad.264303

Claessen, D., Stokroos, I., Deelstra, H. J., Penninga, N. A., Bormann, C., Salas, J. A., Dijkhuizen, L., & Wösten, H. A. B. (2004). The formation of the rodlet layer of streptomycetes is the result of the interplay between rodlins and chaplins. *Molecular Microbiology*, *53*(2), 433–443. https://doi.org/10.1111/j.1365-2958.2004.04143.x

Cleary, K. E., Pelagalli, C., Cassford, M., Berry, N., Aguas, E., Kim, B., DeCarvalho, T., Jacobs-Sera, D., Caruso, S. M., & Cornely, K. (2023). Genome sequence of *Streptomyces* BM cluster phage Frankenweenie. *Microbiology Resource Announcements*, *12*(11), e00592-23. https://doi.org/10.1128/MRA.00592-23

Clokie, M. R., Millard, A. D., Letarov, A. V, & Heaphy, S. (2011). Phages in nature. *Bacteriophage*, *1*(1), 31–45. https://doi.org/10.4161/bact.1.1.14942

Cobián Güemes, A. G., Youle, M., Cantú, V. A., Felts, B., Nulton, J., & Rohwer, F. (2016). Viruses as Winners in the Game of Life. *Annual Review of Virology*, *3*(1), 197–214. https://doi.org/10.1146/annurev-virology-100114-054952

Cota, I., Sánchez-Romero, M. A., Hernández, S. B., Pucciarelli, M. G., García-Del Portillo, F., & Casadesús, J. (2015). Epigenetic Control of *Salmonella enterica* O-Antigen Chain Length: A Tradeoff between Virulence and Bacteriophage Resistance. *PLoS Genetics*, *11*(11), e1005667. https://doi.org/10.1371/journal.pgen.1005667

Creasy, A., Rosario, K., Leigh, B. A., Dishaw, L. J., & Breitbart, M. (2018). Unprecedented Diversity of ssDNA Phages from the Family *Microviridae* Detected within the Gut of a Protochordate Model Organism (*Ciona robusta*). In *Viruses* (Vol. 10, Issue 8). https://doi.org/10.3390/v10080404

Crump, G. M., Zhou, J., Mashayekh, S., & Grimes, C. L. (2020). Revisiting peptidoglycan sensing: interactions with host immunity and beyond. *Chemical Communications (Cambridge, England)*, *56*(87), 13313–13322. https://doi.org/10.1039/d0cc02605k

D'Hérelle, F. H. (1917). Sur un microbe invisible antagoniste des bacilles dysentériques. *C.R. Acad. Sci.*, *165*, 373–375.

Datta, H. J., & Mandal, N. C. (1998). Identification of an early positive regulatory gene of mycobacteriophage L1. *The Journal of General Virology*, *79 (Pt 1)*, 205–210. https://doi.org/10.1099/0022-1317-79-1-205

de Waal, A. M., Hiemstra, P. S., Ottenhoff, T. H. M., Joosten, S. A., & van der Does, A. M. (2022). Lung epithelial cells interact with immune cells and bacteria to shape the microenvironment in tuberculosis. *Thorax*, *77*(4), 408 LP – 416. https://doi.org/10.1136/thoraxjnl-2021-217997

deCarvalho, T., Mascolo, E., Caruso, S. M., López-Pérez, J., Weston-Hafer, K., Shaffer, C., & Erill, I. (2023). Simultaneous entry as an adaptation to virulence in a novel satellite-helper system infecting *Streptomyces* species. *The ISME Journal*. https://doi.org/10.1038/s41396-023-01548-0

Dedrick, R. M., Jacobs-Sera, D., Bustamante, C. A. G., Garlena, R. A., Mavrich, T. N., Pope, W. H., Reyes, J. C. C., Russell, D. A., Adair, T., Alvey, R., Bonilla, J. A., Bricker, J. S., Brown, B. R., Byrnes, D., Cresawn, S. G., Davis, W. B., Dickson, L. A., Edgington, N. P., Findley, A. M., … Hatfull, G. F. (2017). Prophage-mediated defence against viral attack and viral counter-defence. *Nature Microbiology*, *2*, 16251. https://doi.org/10.1038/nmicrobiol.2016.251

Dedrick, R. M., Mavrich, T. N., Ng, W. L., Cervantes Reyes, J. C., Olm, M. R., Rush, R. E., Jacobs-Sera, D., Russell, D. A., & Hatfull, G. F. (2016). Function, expression, specificity, diversity and incompatibility of actinobacteriophage *parABS* systems. *Molecular Microbiology*, *101*(4), 625–644. https://doi.org/10.1111/mmi.13414

Demain, A. L. (1999). Pharmaceutically active secondary metabolites of microorganisms. *Applied Microbiology and Biotechnology*, *52*(4), 455–463. https://doi.org/10.1007/s002530051546

den Hengst, C. D., Tran, N. T., Bibb, M. J., Chandra, G., Leskiw, B. K., & Buttner, M. J. (2010). Genes essential for morphological development and antibiotic production in *Streptomyces coelicolor* are targets of BldD during vegetative growth. *Molecular Microbiology*, *78*(2), 361–379. https://doi.org/10.1111/j.1365-2958.2010.07338.x

Destoumieux-Garzón, D., Duquesne, S., Peduzzi, J., Goulard, C., Desmadril, M., Letellier, L., Rebuffat, S., & Boulanger, P. (2005). The iron–siderophore transporter FhuA is the receptor for the antimicrobial peptide microcin J25: role of the microcin Val11–Pro16 β-hairpin region in the recognition mechanism. *Biochemical Journal*,

389(3), 869–876. https://doi.org/10.1042/BJ20042107

Dion, M. B., Oechslin, F., & Moineau, S. (2020). Phage diversity, genomics and phylogeny. *Nature Reviews. Microbiology*, *18*(3), 125–138. https://doi.org/10.1038/s41579-019-0311-5

Doss, J., Culbertson, K., Hahn, D., Camacho, J., & Barekzi, N. (2017). A Review of Phage Therapy against Bacterial Pathogens of Aquatic and Terrestrial Organisms. In *Viruses* (Vol. 9, Issue 3). https://doi.org/10.3390/v9030050

Du, J., Meile, S., Baggenstos, J., Jäggi, T., Piffaretti, P., Hunold, L., Matter, C. I., Leitner, L., Kessler, T. M., Loessner, M. J., Kilcher, S., & Dunne, M. (2023). Enhancing bacteriophage therapeutics through in situ production and release of heterologous antimicrobial effectors. *Nature Communications*, *14*(1), 4337. https://doi.org/10.1038/s41467-023-39612-0

Duddy, O. P., & Bassler, B. L. (2021). Quorum sensing across bacterial and viral domains. *PLOS Pathogens*, *17*(1), e1009074. https://doi.org/10.1371/journal.ppat.1009074

Dulberger, C. L., Guerrero-Bustamante, C. A., Owen, S. V, Wilson, S., Wuo, M. G., Garlena, R. A., Serpa, L. A., Russell, D. A., Zhu, J., Braunecker, B. J., Squyres, G. R., Baym, M., Kiessling, L. L., Garner, E. C., Rubin, E. J., & Hatfull, G. F. (2023). Mycobacterial nucleoid-associated protein Lsr2 is required for productive mycobacteriophage infection. *Nature Microbiology*. https://doi.org/10.1038/s41564-023-01333-x

Durmaz, E., & Klaenhammer, T. R. (2007). Abortive Phage Resistance Mechanism AbiZ Speeds the Lysis Clock To Cause Premature Lysis of Phage-Infected *Lactococcus lactis*. *Journal of Bacteriology*, *189*(4), 1417–1425. https://doi.org/10.1128/jb.00904-06

Erez, Z., Steinberger-Levy, I., Shamir, M., Doron, S., Stokar-Avihail, A., Peleg, Y., Melamed, S., Leavitt, A., Savidor, A., Albeck, S., Amitai, G., & Sorek, R. (2017). Communication between viruses guides lysis-lysogeny decisions. *Nature*, *541*(7638), 488–493. https://doi.org/10.1038/nature21049

Fabijan, A. P., Kamruzzaman, M., Martinez-Martin, D., Venturini, C., Mickiewicz, K., Flores-Rodriguez, N., Errington, J., & Iredell, J. R. (2021). L-form switching confers antibiotic, phage and stress tolerance in pathogenic *Escherichia coli*. *BioRxiv*. https://doi.org/10.1101/2021.06.21.449206

Fernández-Martínez, L. T., Borsetto, C., Gomez-Escribano, J. P., Bibb, M. J., Al-Bassam, M. M., Chandra, G., & Bibb, M. J. (2014). New Insights into Chloramphenicol Biosynthesis in *Streptomyces venezuelae* ATCC 10712. *Antimicrobial Agents and Chemotherapy*, *58*(12), 7441–7450. https://doi.org/10.1128/aac.04272-14

Fierer, N. (2017). Embracing the unknown: disentangling the complexities of the soil microbiome. *Nature Reviews. Microbiology*, *15*(10), 579–590. https://doi.org/10.1038/nrmicro.2017.87

Finstrlová, A., Mašlaňová, I., Blasdel Reuter, B. G., Jiří, D., Götz, F., & Pantůček, R. (2022). Global Transcriptomic Analysis of Bacteriophage-Host Interactions between a Kayvirus Therapeutic Phage and *Staphylococcus aureus*. *Microbiology Spectrum*, *10*(3), e00123-22. https://doi.org/10.1128/spectrum.00123-22

Fisher, R. A., Gollan, B., & Helaine, S. (2017). Persistent bacterial infections and persister cells. *Nature Reviews Microbiology*, *15*(8), 453–464. https://doi.org/10.1038/nrmicro.2017.42

Flärdh, K. (2010). Cell polarity and the control of apical growth in *Streptomyces*. *Current*

Opinion in Microbiology, *13*(6), 758–765. https://doi.org/10.1016/j.mib.2010.10.002

Flärdh, K., & Buttner, M. J. (2009). *Streptomyces* morphogenetics: dissecting differentiation in a filamentous bacterium. *Nature Reviews. Microbiology*, *7*(1), 36–49. https://doi.org/10.1038/nrmicro1968

Flemming, H.-C., van Hullebusch, E. D., Neu, T. R., Nielsen, P. H., Seviour, T., Stoodley, P., Wingender, J., & Wuertz, S. (2023). The biofilm matrix: multitasking in a shared space. *Nature Reviews Microbiology*, *21*(2), 70–86. https://doi.org/10.1038/s41579-022-00791-0

Flemming, H.-C., & Wuertz, S. (2019). Bacteria and archaea on Earth and their abundance in biofilms. *Nature Reviews Microbiology*, *17*(4), 247–260. https://doi.org/10.1038/s41579-019-0158-9

Fröjd, M. J., & Flärdh, K. (2019). Apical assemblies of intermediate filament-like protein FilP are highly dynamic and affect polar growth determinant DivIVA in *Streptomyces venezuelae*. *Molecular Microbiology*, *112*(1), 47–61. https://doi.org/10.1111/mmi.14253

Gabiatti, N., Yu, P., Mathieu, J., Lu, G. W., Wang, X., Zhang, H., Soares, H. M., & Alvarez, P. J. J. (2018). Bacterial Endospores as Phage Genome Carriers and Protective Shells. *Applied and Environmental Microbiology*, *84*(18). https://doi.org/10.1128/AEM.01186-18

Gallagher, K. A., Schumacher, M. A., Bush, M. J., Bibb, M. J., Chandra, G., Holmes, N. A., Zeng, W., Henderson, M., Zhang, H., Findlay, K. C., Brennan, R. G., & Buttner, M. J. (2020). c-di-GMP Arms an Anti-σ to Control Progression of Multicellular Differentiation in *Streptomyces*. *Molecular Cell*, *77*(3), 586-599.e6. https://doi.org/10.1016/j.molcel.2019.11.006

Gallet, R., Kannoly, S., & Wang, I.-N. (2011). Effects of bacteriophage traits on plaque formation. *BMC Microbiology*, *11*, 181. https://doi.org/10.1186/1471-2180-11-181

Georjon, H., & Bernheim, A. (2023). The highly diverse antiphage defence systems of bacteria. *Nature Reviews Microbiology*. https://doi.org/10.1038/s41579-023-00934-x

Georjon, H., Tesson, F., Shomar, H., & Bernheim, A. (2023). Genomic characterization of the antiviral arsenal of Actinobacteria. *Microbiology (Reading, England)*, *169*(8). https://doi.org/10.1099/mic.0.001374

Ghanem, N., Stanley, C. E., Harms, H., Chatzinotas, A., & Wick, L. Y. (2019). Mycelial Effects on Phage Retention during Transport in a Microfluidic Platform. *Environmental Science & Technology*, *53*(20), 11755–11763. https://doi.org/10.1021/acs.est.9b03502

Ghosh, C., Popella, L., Dhamodharan, V., Jung, J., Barquist, L., Höbartner, C., & Vogel, J. (2023). A side-by-side comparison of peptide-delivered antisense antibiotics employing different nucleotide mimics. *BioRxiv*, 2023.07.11.548539. https://doi.org/10.1101/2023.07.11.548539

Gill, J. J., & Hyman, P. (2010). Phage choice, isolation, and preparation for phage therapy. *Current Pharmaceutical Biotechnology*, *11*(1), 2–14. https://doi.org/10.2174/138920110790725311

Glazebrook, M. A., Doull, J. L., Stuttard, C., & Vining, L. C. (1990). Sporulation of *Streptomyces venezuelae* in submerged cultures. *Journal of General Microbiology*, *136*(3), 581–588. https://doi.org/10.1099/00221287-136-3-581

Godinho, L. M., El Sadek Fadel, M., Monniot, C., Jakutyte, L., Auzat, I., Labarde, A., Djacem, K., Oliveira, L., Carballido-Lopez, R., Ayora, S., & Tavares, P. (2018). The Revisited Genome of *Bacillus subtilis* Bacteriophage SPP1. In *Viruses* (Vol. 10,

Issue 12). https://doi.org/10.3390/v10120705

Gomez-Escribano, J. P., Holmes, N. A., Schlimpert, S., Bibb, M. J., Chandra, G., Wilkinson, B., Buttner, M. J., & Bibb, M. J. (2021). *Streptomyces venezuelae* NRRL B-65442: genome sequence of a model strain used to study morphological differentiation in filamentous actinobacteria. *Journal of Industrial Microbiology & Biotechnology*. https://doi.org/10.1093/jimb/kuab035

González, S., Fernández, L., Gutiérrez, D., Campelo, A. B., Rodríguez, A., & García, P. (2018). Analysis of Different Parameters Affecting Diffusion, Propagation and Survival of Staphylophages in Bacterial Biofilms. *Frontiers in Microbiology*, *9*, 2348. https://doi.org/10.3389/fmicb.2018.02348

Gordillo Altamirano, F. L., & Barr, J. J. (2021). Unlocking the next generation of phage therapy: the key is in the receptors. *Current Opinion in Biotechnology*, *68*, 115–123. https://doi.org/https://doi.org/10.1016/j.copbio.2020.10.002

Gregory, A. C., Zayed, A. A., Conceição-Neto, N., Temperton, B., Bolduc, B., Alberti, A., Ardyna, M., Arkhipova, K., Carmichael, M., Cruaud, C., Dimier, C., Domínguez-Huerta, G., Ferland, J., Kandels, S., Liu, Y., Marec, C., Pesant, S., Picheral, M., Pisarev, S., … Sullivan, M. B. (2019). Marine DNA Viral Macro- and Microdiversity from Pole to Pole. *Cell*, *177*(5), 1109-1123.e14. https://doi.org/10.1016/j.cell.2019.03.040

Hammad, H., & Lambrecht, B. N. (2015). Barrier Epithelial Cells and the Control of Type 2 Immunity. *Immunity*, *43*(1), 29–40. https://doi.org/10.1016/j.immuni.2015.07.007

Hardy, A., Kever, L., & Frunzke, J. (2022). Antiphage small molecules produced by bacteria - beyond protein-mediated defenses. *Trends in Microbiology*. https://doi.org/10.1016/j.tim.2022.08.001

Hardy, A., Sharma, V., Kever, L., & Frunzke, J. (2020). Genome Sequence and Characterization of Five Bacteriophages Infecting *Streptomyces coelicolor* and *Streptomyces venezuelae*: Alderaan, Coruscant, Dagobah, Endor1 and Endor2. *Viruses*, *12*(10), 1065. https://doi.org/10.3390/v12101065

Harvey, H., Bondy-Denomy, J., Marquis, H., Sztanko, K. M., Davidson, A. R., & Burrows, L. L. (2018). *Pseudomonas aeruginosa* defends against phages through type IV pilus glycosylation. *Nature Microbiology*, *3*(1), 47–52. https://doi.org/10.1038/s41564-017-0061-y

Hatfull, G. F. (2015a). Dark Matter of the Biosphere: the Amazing World of Bacteriophage Diversity. *Journal of Virology*, *89*(16), 8107–8110. https://doi.org/10.1128/jvi.01340-15

Hatfull, G. F. (2015b). Innovations in Undergraduate Science Education: Going Viral. *Journal of Virology*, *89*(16), 8111–8113. https://doi.org/10.1128/jvi.03003-14

Hatfull, G. F. (2020). Actinobacteriophages: Genomics, Dynamics, and Applications. *Annual Review of Virology*, *7*(1), 37–61. https://doi.org/10.1146/annurev-virology-122019-070009

Hazan, R., & Engelberg-Kulka, H. (2004). *Escherichia coli mazEF*-mediated cell death as a defense mechanism that inhibits the spread of phage P1. *Molecular Genetics and Genomics*, *272*(2), 227–234. https://doi.org/10.1007/s00438-004-1048-y

Hengge, R. (2009). Principles of c-di-GMP signalling in bacteria. *Nature Reviews Microbiology*, *7*(4), 263–273. https://doi.org/10.1038/nrmicro2109

Hershey, A. D., & Chase, M. (1952). INDEPENDENT FUNCTIONS OF VIRAL PROTEIN AND NUCLEIC ACID IN GROWTH OF BACTERIOPHAGE. *Journal of General Physiology*, *36*(1), 39–56. https://doi.org/10.1085/jgp.36.1.39

Hesse, S., Rajaure, M., Wall, E., Johnson, J., Bliskovsky, V., Gottesman, S., & Adhya, S. (2020). Phage Resistance in Multidrug-Resistant *Klebsiella pneumoniae* ST258 Evolves via Diverse Mutations That Culminate in Impaired Adsorption. *MBio*, *11*(1). https://doi.org/10.1128/mBio.02530-19

Hille, F., & Charpentier, E. (2016). CRISPR-Cas: biology, mechanisms and relevance. *Philosophical Transactions of the Royal Society B: Biological Sciences*, *371*(1707), 20150496. https://doi.org/10.1098/rstb.2015.0496

Hobbs, Z., & Abedon, S. T. (2016). Diversity of phage infection types and associated terminology: the problem with “Lytic or lysogenic”. *FEMS Microbiology Letters*, *363*(7). https://doi.org/10.1093/femsle/fnw047

Hopwood, D. A. (2007). How do antibiotic-producing bacteria ensure their self-resistance before antibiotic biosynthesis incapacitates them? *Molecular Microbiology*, *63*(4), 937–940. https://doi.org/https://doi.org/10.1111/j.1365-2958.2006.05584.x

Howard-Varona, C., Hargreaves, K. R., Abedon, S. T., & Sullivan, M. B. (2017). Lysogeny in nature: mechanisms, impact and ecology of temperate phages. *The ISME Journal*, *11*(7), 1511–1520. https://doi.org/10.1038/ismej.2017.16

Høyland-Kroghsbo, N. M., Mærkedahl, R. B., & Svenningsen, S. Lo. (2013). A Quorum-Sensing-Induced Bacteriophage Defense Mechanism. *MBio*, *4*(1), e00362-12. https://doi.org/10.1128/mBio.00362-12

Høyland-Kroghsbo, N. M., Paczkowski, J., Mukherjee, S., Broniewski, J., Westra, E., Bondy-Denomy, J., & Bassler, B. L. (2016). Quorum sensing controls the *Pseudomonas aeruginosa* CRISPR-Cas adaptive immune system. *Proceedings of the National Academy of Sciences*, *114*(1), 131–135. https://doi.org/10.1073/pnas.1617415113

Hutchings, M. I., Truman, A. W., & Wilkinson, B. (2019). Antibiotics: past, present and future. *Current Opinion in Microbiology*, *51*, 72–80. https://doi.org/https://doi.org/10.1016/j.mib.2019.10.008

Huynen, M., Snel, B., Lathe, W. 3rd, & Bork, P. (2000). Predicting protein function by genomic context: quantitative evaluation and qualitative inferences. *Genome Research*, *10*(8), 1204–1210. https://doi.org/10.1101/gr.10.8.1204

Hyman, P., & Abedon, S. T. (2012). Smaller fleas: viruses of microorganisms. *Scientifica*, *2012*, 734023. https://doi.org/10.6064/2012/734023

Jiang, M., Li, Y., Sun, B., Xu, S., Pan, T., & Li, Y. (2023). Phage transcription activator RinA regulates *Staphylococcus aureus* virulence by governing *sarA* expression. *Genes & Genomics*, *45*(2), 191–202. https://doi.org/10.1007/s13258-022-01352-8

Johnson, L., Horsman, S. R., Charron-Mazenod, L., Turnbull, A. L., Mulcahy, H., Surette, M. G., & Lewenza, S. (2013). Extracellular DNA-induced antimicrobial peptide resistance in *Salmonella enterica* serovar Typhimurium. *BMC Microbiology*, *13*(1), 115. https://doi.org/10.1186/1471-2180-13-115

Jones, S. E., Ho, L., Rees, C. A., Hill, J. E., Nodwell, J. R., & Elliot, M. A. (2017). *Streptomyces* exploration is triggered by fungal interactions and volatile signals. *ELife*, *6*. https://doi.org/10.7554/eLife.21738

Kaczmarczyk, A., Vliet, S. van, Jakob, R. P., Reinders, A., Klotz, A., Maier, T., & Jenal, U. (2022). A Novel Biosensor Reveals Dynamic Changes of C-di-GMP in Differentiating Cells with Ultra-High Temporal Resolution. *BioRxiv*, 2022.10.18.512705. https://doi.org/10.1101/2022.10.18.512705

Kaiser, B. K., & Stoddard, B. L. (2011). DNA recognition and transcriptional regulation by the WhiA sporulation factor. *Scientific Reports*, *1*(1), 156.

https://doi.org/10.1038/srep00156

Kawasaki, T., Narulita, E., Matsunami, M., Ishikawa, H., Shimizu, M., Fujie, M., Bhunchoth, A., Phironrit, N., Chatchawankanphanich, O., & Yamada, T. (2016). Genomic diversity of large-plaque-forming podoviruses infecting the phytopathogen *Ralstonia solanacearum*. *Virology*, *492*, 73–81. https://doi.org/https://doi.org/10.1016/j.virol.2016.02.011

Kelly, A., Arrowsmith, T. J., Went, S. C., & Blower, T. R. (2023). Toxin–antitoxin systems as mediators of phage defence and the implications for abortive infection. *Current Opinion in Microbiology*, *73*, 102293. https://doi.org/https://doi.org/10.1016/j.mib.2023.102293

Kever, L., Hardy, A., Luthe, T., Hünnefeld, M., Gätgens, C., Milke, L., Wiechert, J., Wittmann, J., Moraru, C., Marienhagen, J., & Frunzke, J. (2022). Aminoglycoside Antibiotics Inhibit Phage Infection by Blocking an Early Step of the Infection Cycle. *MBio*, *13*(3), e0078322. https://doi.org/10.1128/mbio.00783-22

Khakh, B. S., & Burnstock, G. (2009). The Double Life of ATP in Humans. *Scientific American Magazine*, *301*(6). https://doi.org/10.1038/scientificamerican1209-84

Kilcher, S., Studer, P., Muessner, C., Klumpp, J., Loessner, M. J., & Adhya, S. (2018). Cross-genus rebooting of custom-made, synthetic bacteriophage genomes in L-form bacteria. *Proceedings of the National Academy of Sciences of the United States of America*, *115*(3), 567–572. https://doi.org/10.1073/pnas.1714658115

Kiro, R., Molshanski-Mor, S., Yosef, I., Milam, S. L., Erickson, H. P., & Qimron, U. (2013). Gene product 0.4 increases bacteriophage T7 competitiveness by inhibiting host cell division. *Proceedings of the National Academy of Sciences*, *110*(48), 19549–19554. https://doi.org/10.1073/pnas.1314096110

Ko, C.-C., & Hatfull, G. F. (2018). Mycobacteriophage Fruitloop gp52 inactivates Wag31 (DivIVA) to prevent heterotypic superinfection. *Molecular Microbiology*, *108*(4), 443–460. https://doi.org/https://doi.org/10.1111/mmi.13946

Koonin, E. V, Dolja, V. V, Krupovic, M., Varsani, A., Wolf, Y. I., Yutin, N., Zerbini, F. M., & Kuhn, J. H. (2020). Global Organization and Proposed Megataxonomy of the Virus World. *Microbiology and Molecular Biology Reviews : MMBR*, *84*(2). https://doi.org/10.1128/MMBR.00061-19

Kormanec, J., Rezuchova, B., Homerova, D., Csolleiova, D., Sevcikova, B., Novakova, R., & Feckova, L. (2019). Recent achievements in the generation of stable genome alterations/mutations in species of the genus *Streptomyces*. *Applied Microbiology and Biotechnology*, *103*(14), 5463–5482. https://doi.org/10.1007/s00253-019-09901-0

Krespach, M. K. C., Stroe, M. C., Netzker, T., Rosin, M., Zehner, L. M., Komor, A. J., Beilmann, J. M., Krüger, T., Scherlach, K., Kniemeyer, O., Schroeckh, V., Hertweck, C., & Brakhage, A. A. (2023). *Streptomyces* polyketides mediate bacteria–fungi interactions across soil environments. *Nature Microbiology*, *8*(7), 1348–1361. https://doi.org/10.1038/s41564-023-01382-2

Krishnamurthy, S. R., & Wang, D. (2017). Origins and challenges of viral dark matter. *Virus Research*, *239*, 136–142. https://doi.org/https://doi.org/10.1016/j.virusres.2017.02.002

Kronheim, S., Daniel-Ivad, M., Duan, Z., Hwang, S., Wong, A. I., Mantel, I., Nodwell, J. R., & Maxwell, K. L. (2018). A chemical defence against phage infection. *Nature*, *564*(7735), 283–286. https://doi.org/10.1038/s41586-018-0767-x

Krupovic, M., Prangishvili, D., Hendrix, R. W., & Bamford, D. H. (2011). Genomics of bacterial and archaeal viruses: dynamics within the prokaryotic virosphere.

Microbiology and Molecular Biology Reviews : MMBR, *75*(4), 610–635. https://doi.org/10.1128/MMBR.00011-11

Labrie, S. J., Samson, J. E., & Moineau, S. (2010). Bacteriophage resistance mechanisms. *Nature Reviews Microbiology*, *8*(5), 317–327. https://doi.org/10.1038/nrmicro2315

Ladwig, N., Franz-Wachtel, M., Hezel, F., Soufi, B., Macek, B., Wohlleben, W., & Muth, G. (2015). Control of Morphological Differentiation of *Streptomyces coelicolor* A3(2) by Phosphorylation of MreC and PBP2. *PloS One*, *10*(4), e0125425. https://doi.org/10.1371/journal.pone.0125425

LeRoux, M., Kirkpatrick, R. L., Montauti, E. I., Tran, B. Q., Peterson, S. B., Harding, B. N., Whitney, J. C., Russell, A. B., Traxler, B., Goo, Y. A., Goodlett, D. R., Wiggins, P. A., & Mougous, J. D. (2015). Kin cell lysis is a danger signal that activates antibacterial pathways of *Pseudomonas aeruginosa*. *ELife*, *4*, e05701. https://doi.org/10.7554/eLife.05701

Lilic, M., Darst, S. A., & Campbell, E. A. (2021). Structural basis of transcriptional activation by the *Mycobacterium tuberculosis* intrinsic antibiotic-resistance transcription factor WhiB7. *Molecular Cell*, *81*(14), 2875-2886.e5. https://doi.org/10.1016/j.molcel.2021.05.017

Lilic, M., Holmes, N. A., Bush, M. J., Marti, A. K., Widdick, D. A., Findlay, K. C., Choi, Y. J., Froom, R., Koh, S., Buttner, M. J., & Campbell, E. A. (2023). Structural basis of dual activation of cell division by the actinobacterial transcription factors WhiA and WhiB. *Proceedings of the National Academy of Sciences*, *120*(11). https://doi.org/10.1073/pnas.2220785120

Liu, B., Shadrin, A., Sheppard, C., Mekler, V., Xu, Y., Severinov, K., Matthews, S., & Wigneshweraraj, S. (2014). A bacteriophage transcription regulator inhibits bacterial transcription initiation by σ-factor displacement. *Nucleic Acids Research*, *42*(7), 4294–4305. https://doi.org/10.1093/nar/gku080

Liu, Z., Zhao, Y., Huang, C., & Luo, Y. (2021). Recent Advances in Silent Gene Cluster Activation in *Streptomyces*. *Frontiers in Bioengineering and Biotechnology*, *9*, 632230. https://doi.org/10.3389/fbioe.2021.632230

Lopatina, A., Tal, N., & Sorek, R. (2020). Abortive Infection: Bacterial Suicide as an Antiviral Immune Strategy. *Annual Review of Virology*, *7*(1), 371–384. https://doi.org/10.1146/annurev-virology-011620-040628

Łoś, M., Golec, P., Łoś, J. M., Węglewska-Jurkiewicz, A., Czyż, A., Węgrzyn, A., Węgrzyn, G., & Neubauer, P. (2007). Effective inhibition of lytic development of bacteriophages λ, P1 and T4 by starvation of their host, *Escherichia coli*. *BMC Biotechnology*, *7*(1), 13. https://doi.org/10.1186/1472-6750-7-13

Luria, S. E., & Delbrück, M. (1943). MUTATIONS OF BACTERIA FROM VIRUS SENSITIVITY TO VIRUS RESISTANCE. *Genetics*, *28*(6), 491–511. https://doi.org/10.1093/genetics/28.6.491

Luria, S. E., Delbrück, M., & Anderson, T. F. (1943). Electron Microscope Studies of Bacterial Viruses. *Journal of Bacteriology*, *46*(1), 57–77. https://doi.org/10.1128/JB.46.1.57-77.1943

Luria, S. E., & Human, M. L. (1952). A NONHEREDITARY, HOST-INDUCED VARIATION OF BACTERIAL VIRUSES. *Journal of Bacteriology*, *64*(4), 557–569. https://doi.org/10.1128/jb.64.4.557-569.1952

Luthe, T., & Frunzke, J. (2023). Investigation on *Streptomyces* Phage-encoded WhiB-like Transcriptional Regulators. *To Be Submitted*.

Luthe, T., Kever, L., Hänsch, S., Hardy, A., Tschowri, N., Weidtkamp-Peters, S., &

Frunzke, J. (2023a). *Streptomyces* development is involved in the efficient containment of viral infections. *MicroLife*, *4*. https://doi.org/10.1093/femsml/uqad002

Luthe, T., Kever, L., Thormann, K., & Frunzke, J. (2023b). Bacterial multicellular behavior in antiviral defense. *Current Opinion in Microbiology*, *74*, 102314. https://doi.org/https://doi.org/10.1016/j.mib.2023.102314

Lyons, N. A., & Kolter, R. (2015). On the evolution of bacterial multicellularity. *Current Opinion in Microbiology*, *24*, 21–28. https://doi.org/10.1016/j.mib.2014.12.007

Mallory, J. B., Alfano, C., & McMacken, R. (1990). Host virus interactions in the initiation of bacteriophage lambda DNA replication. Recruitment of *Escherichia coli* DnaB helicase by lambda P replication protein. *The Journal of Biological Chemistry*, *265*(22), 13297–13307.

Mandal, P. K., Ballerin, G., Nolan, L. M., Petty, N. K., & Whitchurch, C. B. (2021). Bacteriophage infection of *Escherichia coli* leads to the formation of membrane vesicles via both explosive cell lysis and membrane blebbing. *Microbiology*, *167*(4), 001021. https://doi.org/10.1099/mic.0.001021

Manteca, A., Claessen, D., Lopez-Iglesias, C., & Sanchez, J. (2007). Aerial hyphae in surface cultures of *Streptomyces lividans* and *Streptomyces coelicolor* originate from viable segments surviving an early programmed cell death event. *FEMS Microbiology Letters*, *274*(1), 118–125. https://doi.org/10.1111/j.1574-6968.2007.00825.x

Manteca, A., Fernandez, M., & Sanchez, J. (2006). Cytological and biochemical evidence for an early cell dismantling event in surface cultures of *Streptomyces antibioticus*. *Research in Microbiology*, *157*(2), 143–152. https://doi.org/10.1016/j.resmic.2005.07.003

Marinelli, L. J., Piuri, M., Swigonová, Z., Balachandran, A., Oldfield, L. M., van Kessel, J. C., & Hatfull, G. F. (2008). BRED: a simple and powerful tool for constructing mutant and recombinant bacteriophage genomes. *PloS One*, *3*(12), e3957. https://doi.org/10.1371/journal.pone.0003957

Mavrich, T. N., & Hatfull, G. F. (2019). Evolution of Superinfection Immunity in Cluster A Mycobacteriophages. *MBio*, *10*(3). https://doi.org/10.1128/mBio.00971-19

McAllister, W. T., & Barrett, C. L. (1977). Roles of the early genes of bacteriophage T7 in shutoff of host macromolecular synthesis. *Journal of Virology*, *23*(3), 543–553. https://doi.org/10.1128/JVI.23.3.543-553.1977

McCormick, J. R., & Flärdh, K. (2012). Signals and regulators that govern *Streptomyces* development. *FEMS Microbiology Reviews*, *36*(1), 206–231. https://doi.org/10.1111/j.1574-6976.2011.00317.x

McCormick, J. R., Su, E. P., Driks, A., & Losick, R. (1994). Growth and viability of *Streptomyces coelicolor* mutant for the cell division gene *ftsZ*. *Molecular Microbiology*, *14*(2), 243–254. https://doi.org/10.1111/j.1365-2958.1994.tb01285.x

Miguélez, E. M., Hardisson, C., & Manzanal, M. B. (1999). Hyphal death during colony development in *Streptomyces antibioticus*: morphological evidence for the existence of a process of cell deletion in a multicellular prokaryote. *The Journal of Cell Biology*, *145*(3), 515–525. https://doi.org/10.1083/jcb.145.3.515

Muñoz-Espín, D., Holguera, I., Ballesteros-Plaza, D., Carballido-López, R., & Salas, M. (2010). Viral terminal protein directs early organization of phage DNA replication at the bacterial nucleoid. *Proceedings of the National Academy of Sciences*, *107*(38), 16548–16553. https://doi.org/10.1073/pnas.1010530107

Mushegian, A. R. (2020). Are There 1031 Virus Particles on Earth, or More, or Fewer?

Journal of Bacteriology, *202*(9), 10.1128/jb.00052-20. https://doi.org/10.1128/jb.00052-20

Neri, U., Wolf, Y. I., Roux, S., Camargo, A. P., Lee, B., Kazlauskas, D., Chen, I. M., Ivanova, N., Zeigler Allen, L., Paez-Espino, D., Bryant, D. A., Bhaya, D., Krupovic, M., Dolja, V. V, Kyrpides, N. C., Koonin, E. V, & Gophna, U. (2022). Expansion of the global RNA virome reveals diverse clades of bacteriophages. *Cell*, *185*(21), 4023-4037.e18. https://doi.org/10.1016/j.cell.2022.08.023

Nikolaidis, M., Hesketh, A., Frangou, N., Mossialos, D., Van de Peer, Y., Oliver, S. G., & Amoutzias, G. D. (2023). A panoramic view of the genomic landscape of the genus *Streptomyces*. *Microbial Genomics*, *9*(6). https://doi.org/10.1099/mgen.0.001028

Nordström, K., & Forsgren, A. (1974). Effect of Protein A on Adsorption of Bacteriophages to *Staphylococcus aureus*. *Journal of Virology*, *14*(2), 198–202. https://doi.org/10.1128/jvi.14.2.198-202.1974

Ohnishi, Y., Yamazaki, H., Kato, J., Tomono, A., & Horinouchi, S. (2005). AdpA, a Central Transcriptional Regulator in the A-Factor Regulatory Cascade That Leads to Morphological Development and Secondary Metabolism in *Streptomyces griseus*. *Bioscience, Biotechnology, and Biochemistry*, *69*(3), 431–439. https://doi.org/10.1271/bbb.69.431

Ongenae, V., Briegel, A., & Claessen, D. (2021). Cell wall deficiency as an escape mechanism from phage infection. *Open Biology*, *11*(9), 210199. https://doi.org/10.1098/rsob.210199

Ongenae, V., Kempff, A., van Neer, V., Shomar, H., Tesson, F., Rozen, D., Briegel, A., & Claessen, D. (2023). Genome sequence and characterization of *Streptomyces* phages Vanseggelen and Verabelle, representing two new species within the genus Camvirus. *Scientific Reports*, *13*(1), 20153. https://doi.org/10.1038/s41598-023-47634-3

Ongenae, V., Mabrouk, A. S., Crooijmans, M., Rozen, D., Briegel, A., & Claessen, D. (2022). Reversible bacteriophage resistance by shedding the bacterial cell wall. *Open Biology*, *12*(6), 210379. https://doi.org/10.1098/rsob.210379

Oppenheim, A. B., Kobiler, O., Stavans, J., Court, D. L., & Adhya, S. (2005). Switches in bacteriophage lambda development. *Annual Review of Genetics*, *39*, 409–429. https://doi.org/10.1146/annurev.genet.39.073003.113656

Otani, H., Udwary, D. W., & Mouncey, N. J. (2022). Comparative and pangenomic analysis of the genus *Streptomyces*. *Scientific Reports*, *12*(1), 18909. https://doi.org/10.1038/s41598-022-21731-1

Owen, S. V, Wenner, N., Dulberger, C. L., Rodwell, E. V, Bowers-Barnard, A., Quinones-Olvera, N., Rigden, D. J., Rubin, E. J., Garner, E. C., Baym, M., & Hinton, J. C. D. (2021). Prophages encode phage-defense systems with cognate self-immunity. *Cell Host & Microbe*, *29*(11), 1620-1633.e8. https://doi.org/10.1016/j.chom.2021.09.002

Parma, D. H., Snyder, M., Sobolevski, S., Nawroz, M., Brody, E., & Gold, L. (1992). The Rex system of bacteriophage lambda: tolerance and altruistic cell death. *Genes & Development*, *6*(3), 497–510. https://doi.org/10.1101/gad.6.3.497

Patel, P. H., & Maxwell, K. L. (2023). Prophages provide a rich source of antiphage defense systems. *Current Opinion in Microbiology*, *73*, 102321. https://doi.org/https://doi.org/10.1016/j.mib.2023.102321

Patterson, A. G., Jackson, S. A., Taylor, C., Evans, G. B., Salmond, G. P. C., Przybilski, R., Staals, R. H. J., & Fineran, P. C. (2016). Quorum Sensing Controls Adaptive Immunity through the Regulation of Multiple CRISPR-Cas Systems. *Molecular Cell*,

64(6), 1102–1108. https://doi.org/10.1016/j.molcel.2016.11.012

Payne, L. J., Todeschini, T. C., Wu, Y., Perry, B. J., Ronson, C. W., Fineran, P. C., Nobrega, F. L., & Jackson, S. A. (2021). Identification and classification of antiviral defence systems in bacteria and archaea with PADLOC reveals new system types. *Nucleic Acids Research*, *49*(19), 10868–10878. https://doi.org/10.1093/nar/gkab883

Petković, H., Lukežič, T., & Šušković, J. (2017). Biosynthesis of Oxytetracycline by *Streptomyces rimosus*: Past, Present and Future Directions in the Development of Tetracycline Antibiotics. *Food Technology and Biotechnology*, *55*(1), 3–13. https://doi.org/10.17113/ftb.55.01.17.4617

Pfeifer, E., Hünnefeld, M., Popa, O., Polen, T., Kohlheyer, D., Baumgart, M., & Frunzke, J. (2016). Silencing of cryptic prophages in *Corynebacterium glutamicum*. *Nucleic Acids Research*, *44*(21), 10117–10131. https://doi.org/10.1093/nar/gkw692

Płachetka, M., Krawiec, M., Zakrzewska-Czerwińska, J., & Wolański, M. (2021). AdpA Positively Regulates Morphological Differentiation and Chloramphenicol Biosynthesis in *Streptomyces venezuelae*. *Microbiology Spectrum*, *9*(3), e0198121. https://doi.org/10.1128/Spectrum.01981-21

Pons, B. J., Dimitriu, T., Westra, E. R., & van Houte, S. (2023). Antibiotics that affect translation can antagonize phage infectivity by interfering with the deployment of counter-defenses. *Proceedings of the National Academy of Sciences*, *120*(4), e2216084120. https://doi.org/10.1073/pnas.2216084120

Reyes-Robles, T., Dillard, R. S., Cairns, L. S., Silva-Valenzuela, C. A., Housman, M., Ali, A., Wright, E. R., & Camilli, A. (2018). *Vibrio cholerae* Outer Membrane Vesicles Inhibit Bacteriophage Infection. *Journal of Bacteriology*, *200*(15), e00792-17. https://doi.org/10.1128/JB.00792-17

Rigali, S., Titgemeyer, F., Barends, S., Mulder, S., Thomae, A. W., Hopwood, D. A., & van Wezel, G. P. (2008). Feast or famine: the global regulator DasR links nutrient stress to antibiotic production by *Streptomyces*. *EMBO Reports*, *9*(7), 670–675. https://doi.org/10.1038/embor.2008.83

Römling, U., Galperin, M. Y., & Gomelsky, M. (2013). Cyclic di-GMP: the first 25 years of a universal bacterial second messenger. *Microbiology and Molecular Biology Reviews : MMBR*, *77*(1), 1–52. https://doi.org/10.1128/MMBR.00043-12

Ruska, H. (1940). Die Sichtbarmachung der bakteriophagen Lyse im Übermikroskop. *Naturwissenschaften*, *28*(3), 45–46. https://doi.org/10.1007/BF01486931

Rybniker, J., Nowag, A., van Gumpel, E., Nissen, N., Robinson, N., Plum, G., & Hartmann, P. (2010). Insights into the function of the WhiB-like protein of mycobacteriophage TM4--a transcriptional inhibitor of WhiB2. *Molecular Microbiology*, *77*(3), 642–657. https://doi.org/10.1111/j.1365-2958.2010.07235.x

Salmond, G. P. C., & Fineran, P. C. (2015). A century of the phage: past, present and future. In *Nature reviews. Microbiology* (Vol. 13, Issue 12, pp. 777–786). https://doi.org/10.1038/nrmicro3564

Schatz, A., & Waksman, S. A. (1944). Effect of Streptomycin and Other Antibiotic Substances upon *Mycobacterium tuberculosis* and Related Organisms.,. *Proceedings of the Society for Experimental Biology and Medicine*, *57*(2), 244–248. https://doi.org/10.3181/00379727-57-14769

Scholl, D., Adhya, S., & Merril, C. (2005). *Escherichia coli* K1's Capsule Is a Barrier to Bacteriophage T7. *Applied and Environmental Microbiology*, *71*(8), 4872–4874. https://doi.org/10.1128/AEM.71.8.4872-4874.2005

Schuch, R., & Fischetti, V. A. (2009). The Secret Life of the Anthrax Agent *Bacillus*

anthracis: Bacteriophage-Mediated Ecological Adaptations. *PLOS ONE*, *4*(8), e6532. https://doi.org/10.1371/journal.pone.0006532

Schwartz, D. A., Lehmkuhl, B. K., & Lennon, J. T. (2022). Phage-Encoded Sigma Factors Alter Bacterial Dormancy. *MSphere*, e0029722. https://doi.org/10.1128/msphere.00297-22

Sexton, D. L., & Tocheva, E. I. (2020). Ultrastructure of Exospore Formation in *Streptomyces* Revealed by Cryo-Electron Tomography. *Frontiers in Microbiology*, *11*, 581135. https://doi.org/10.3389/fmicb.2020.581135

Seyedsayamdost, M. R. (2019). Toward a global picture of bacterial secondary metabolism. *Journal of Industrial Microbiology and Biotechnology*, *46*(3–4), 301–311. https://doi.org/10.1007/s10295-019-02136-y

Shao, Q., Trinh, J. T., & Zeng, L. (2019). High-resolution studies of lysis-lysogeny decision-making in bacteriophage lambda. *The Journal of Biological Chemistry*, *294*(10), 3343–3349. https://doi.org/10.1074/jbc.TM118.003209

Shapiro, J. A. (1988). Bacteria as Multicellular Organisms. *Scientific American Magazine*, *258*(6), 82. https://doi.org/10.1038/scientificamerican0688-82

Sharma, V., Hardy, A., Luthe, T., & Frunzke, J. (2021). Phylogenetic Distribution of WhiB- and Lsr2-Type Regulators in Actinobacteriophage Genomes. *Microbiology Spectrum*, *9*(3), e0072721. https://doi.org/10.1128/Spectrum.00727-21

Sharma, V., Hünnefeld, M., Luthe, T., & Frunzke, J. (2023). Systematic analysis of prophage elements in actinobacterial genomes reveals a remarkable phylogenetic diversity. *Scientific Reports*, *13*(1), 4410. https://doi.org/10.1038/s41598-023-30829-z

Silpe, J. E., & Bassler, B. L. (2019). A Host-Produced Quorum-Sensing Autoinducer Controls a Phage Lysis-Lysogeny Decision. *Cell*, *176*(1–2), 268-280.e13. https://doi.org/10.1016/j.cell.2018.10.059

Simmons, E. L., Bond, M. C., Koskella, B., Drescher, K., Bucci, V., & Nadell, C. D. (2020). Biofilm Structure Promotes Coexistence of Phage-Resistant and Phage-Susceptible Bacteria. *MSystems*, *5*(3), 10.1128/msystems.00877-19. https://doi.org/10.1128/msystems.00877-19

Soliveri, J. A., Gomez, J., Bishai, W. R., & Chater, K. F. (2000). Multiple paralogous genes related to the *Streptomyces coelicolor* developmental regulatory gene *whiB* are present in *Streptomyces* and other actinomycetes. *Microbiology (Reading, England)*, *146 (Pt 2*, 333–343. https://doi.org/10.1099/00221287-146-2-333

Son, B., Patterson-West, J., Thompson, C. O., Iben, J. R., & Hinton, D. M. (2022). Setting Up a Better Infection: Overexpression of the Early Bacteriophage T4 Gene *motB* During Infection Results in a More Favorable tRNA Pool for the Phage. *PHAGE (New Rochelle, N.Y.)*, *3*(3), 141–152. https://doi.org/10.1089/phage.2022.0023

Soundararajan, M., von Bünau, R., & Oelschlaeger, T. A. (2019). K5 Capsule and Lipopolysaccharide Are Important in Resistance to T4 Phage Attack in Probiotic *E. coli* Strain Nissle 1917. *Frontiers in Microbiology*, *10*, 2783. https://doi.org/10.3389/fmicb.2019.02783

Spagnolo, F., Trujillo, M., & Dennehy, J. J. (2021). Why Do Antibiotics Exist? *MBio*, *12*(6), e01966-21. https://doi.org/10.1128/mBio.01966-21

Srinivasiah, S., Bhavsar, J., Thapar, K., Liles, M., Schoenfeld, T., & Wommack, K. E. (2008). Phages across the biosphere: contrasts of viruses in soil and aquatic environments. *Research in Microbiology*, *159*(5), 349–357. https://doi.org/10.1016/j.resmic.2008.04.010

Stern, A., & Sorek, R. (2011). The phage-host arms race: Shaping the evolution of microbes. *BioEssays*, *33*(1), 43–51. https://doi.org/https://doi.org/10.1002/bies.201000071

Stewart, C. R., Deery, W. J., Egan, E. S. K., Myles, B., & Petti, A. A. (2013). The product of SPO1 gene *56* inhibits host cell division during infection of *Bacillus subtilis* by bacteriophage SPO1. *Virology*, *447*(1), 249–253. https://doi.org/https://doi.org/10.1016/j.virol.2013.09.005

Stewart, M. Y. Y., Bush, M. J., Crack, J. C., Buttner, M. J., & Le Brun, N. E. (2020). Interaction of the *Streptomyces* Wbl protein WhiD with the principal sigma factor σ(HrdB) depends on the WhiD [4Fe-4S] cluster. *The Journal of Biological Chemistry*, *295*(28), 9752–9765. https://doi.org/10.1074/jbc.RA120.012708

Sulakvelidze, A., Alavidze, Z., & Morris Jr, J. G. (2001). Bacteriophage Therapy. *Antimicrobial Agents and Chemotherapy*, *45*(3), 649–659. https://doi.org/10.1128/aac.45.3.649-659.2001

Tabor, S., & Richardson, C. C. (1985). A bacteriophage T7 RNA polymerase/promoter system for controlled exclusive expression of specific genes. *Proceedings of the National Academy of Sciences*, *82*(4), 1074–1078. https://doi.org/10.1073/pnas.82.4.1074

Tan, D., Svenningsen, S. Lo, & Middelboe, M. (2015). Quorum Sensing Determines the Choice of Antiphage Defense Strategy in *Vibrio anguillarum*. *MBio*, *6*(3), e00627-15. https://doi.org/10.1128/mBio.00627-15

Tanaka, K., Choi, J., Cao, Y., & Stacey, G. (2014). Extracellular ATP acts as a damage-associated molecular pattern (DAMP) signal in plants. In *Frontiers in Plant Science* (Vol. 5). https://www.frontiersin.org/articles/10.3389/fpls.2014.00446

Tenconi, E., & Rigali, S. (2018). Self-resistance mechanisms to DNA-damaging antitumor antibiotics in actinobacteria. *Current Opinion in Microbiology*, *45*, 100–108. https://doi.org/https://doi.org/10.1016/j.mib.2018.03.003

Tenconi, E., Traxler, M. F., Hoebreck, C., van Wezel, G. P., & Rigali, S. (2018). Production of Prodiginines Is Part of a Programmed Cell Death Process in *Streptomyces coelicolor*. *Frontiers in Microbiology*, *9*, 1742. https://doi.org/10.3389/fmicb.2018.01742

Tesson, F., Hervé, A., Mordret, E., Touchon, M., D'Humières, C., Cury, J., & Bernheim, A. (2022). Systematic and quantitative view of the antiviral arsenal of prokaryotes. *Nature Communications*, *13*(1), 2561. https://doi.org/10.1038/s41467-022-30269-9

Toyofuku, M., Morinaga, K., Hashimoto, Y., Uhl, J., Shimamura, H., Inaba, H., Schmitt-Kopplin, P., Eberl, L., & Nomura, N. (2017). Membrane vesicle-mediated bacterial communication. *The ISME Journal*, *11*(6), 1504–1509. https://doi.org/10.1038/ismej.2017.13

Traxler, M. F., & Rozen, D. E. (2022). Ecological drivers of division of labour in *Streptomyces*. *Current Opinion in Microbiology*, *67*, 102148. https://doi.org/https://doi.org/10.1016/j.mib.2022.102148

Traxler, M. F., Seyedsayamdost, M. R., Clardy, J., & Kolter, R. (2012). Interspecies modulation of bacterial development through iron competition and siderophore piracy. *Molecular Microbiology*, *86*(3), 628–644. https://doi.org/https://doi.org/10.1111/mmi.12008

Tschowri, N., Schumacher, M. A., Schlimpert, S., Chinnam, N. B., Findlay, K. C., Brennan, R. G., & Buttner, M. J. (2014). Tetrameric c-di-GMP mediates effective transcription factor dimerization to control *Streptomyces* development. *Cell*, *158*(5), 1136–1147. https://doi.org/10.1016/j.cell.2014.07.022

Turner, D., Kropinski, A. M., & Adriaenssens, E. M. (2021). A Roadmap for Genome-Based Phage Taxonomy. In *Viruses* (Vol. 13, Issue 3). https://doi.org/10.3390/v13030506

Twort, F. W. (1915). AN INVESTIGATION ON THE NATURE OF ULTRA-MICROSCOPIC VIRUSES. *The Lancet*, *186*(4814), 1241–1243. https://doi.org/https://doi.org/10.1016/S0140-6736(01)20383-3

Tzipilevich, E., Pollak-Fiyaksel, O., Shraiteh, B., & Ben-Yehuda, S. (2022). Bacteria elicit a phage tolerance response subsequent to infection of their neighbors. *The EMBO Journal*, *41*(3), e109247. https://doi.org/10.15252/embj.2021109247

van Valen, L. (1973). A New Evolutionary Law. *Evol. Theory*, *1*, 1–30.

Vidakovic, L., Singh, P. K., Hartmann, R., Nadell, C. D., & Drescher, K. (2018). Dynamic biofilm architecture confers individual and collective mechanisms of viral protection. *Nature Microbiology*, *3*(1), 26–31. https://doi.org/10.1038/s41564-017-0050-1

Wahl, M. C., & Sen, R. (2019). Exploiting phage strategies to modulate bacterial transcription. *Transcription*, *10*(4–5), 222–230. https://doi.org/10.1080/21541264.2019.1684137

Waldor, M. K., & Mekalanos, J. J. (1996). Lysogenic Conversion by a Filamentous Phage Encoding Cholera Toxin. *Science*, *272*(5270), 1910–1914. https://doi.org/10.1126/science.272.5270.1910

Wein, T., & Sorek, R. (2022). Bacterial origins of human cell-autonomous innate immune mechanisms. *Nature Reviews. Immunology*. https://doi.org/10.1038/s41577-022-00705-4

Wetzel, K. S., Aull, H. G., Zack, K. M., Garlena, R. A., & Hatfull, G. F. (2020). Protein-Mediated and RNA-Based Origins of Replication of Extrachromosomal Mycobacterial Prophages. *MBio*, *11*(2). https://doi.org/10.1128/mBio.00385-20

Wetzel, K. S., Guerrero-Bustamante, C. A., Dedrick, R. M., Ko, C.-C., Freeman, K. G., Aull, H. G., Divens, A. M., Rock, J. M., Zack, K. M., & Hatfull, G. F. (2021). CRISPY-BRED and CRISPY-BRIP: efficient bacteriophage engineering. *Scientific Reports*, *11*(1), 6796. https://doi.org/10.1038/s41598-021-86112-6

Wiechert, J., Filipchyk, A., Hünnefeld, M., Gätgens, C., Brehm, J., Heermann, R., & Frunzke, J. (2020). Deciphering the Rules Underlying Xenogeneic Silencing and Counter-Silencing of Lsr2-like Proteins Using CgpS of *Corynebacterium glutamicum* as a Model. *MBio*, *11*(1), 10.1128/mbio.02273-19. https://doi.org/10.1128/mbio.02273-19

Willemse, J., Borst, J. W., de Waal, E., Bisseling, T., & van Wezel, G. P. (2011). Positive control of cell division: FtsZ is recruited by SsgB during sporulation of *Streptomyces*. *Genes & Development*, *25*(1), 89–99. https://doi.org/10.1101/gad.600211

Williams, M. C., Reker, A. E., Margolis, S. R., Liao, J., Wiedmann, M., Rojas, E. R., & Meeske, A. J. (2023). Restriction endonuclease cleavage of phage DNA enables resuscitation from Cas13-induced bacterial dormancy. *Nature Microbiology*, *8*(3), 400–409. https://doi.org/10.1038/s41564-022-01318-2

Williamson, K. E., Fuhrmann, J. J., Wommack, K. E., & Radosevich, M. (2017). Viruses in Soil Ecosystems: An Unknown Quantity Within an Unexplored Territory. *Annual Review of Virology*, *4*(1), 201–219. https://doi.org/10.1146/annurev-virology-101416-041639

Wohlfarth, J. C., Feldmüller, M., Schneller, A., Kilcher, S., Burkolter, M., Meile, S., Pilhofer, M., Schuppler, M., & Loessner, M. J. (2023). L-form conversion in Gram-positive bacteria enables escape from phage infection. *Nature Microbiology*, *8*(3),

387–399. https://doi.org/10.1038/s41564-022-01317-3

Wolański, M., Jakimowicz, D., & Zakrzewska-Czerwińska, J. (2012). AdpA, key regulator for morphological differentiation regulates bacterial chromosome replication. *Open Biology*, *2*(7), 120097. https://doi.org/10.1098/rsob.120097

Xi, C., & Wu, J. (2010). dATP/ATP, a Multifunctional Nucleotide, Stimulates Bacterial Cell Lysis, Extracellular DNA Release and Biofilm Development. *PLOS ONE*, *5*(10), e13355. https://doi.org/10.1371/journal.pone.0013355

Xu, Y., Willems, A., Au-yeung, C., Tahlan, K., & Nodwell, J. R. (2012). A Two-Step Mechanism for the Activation of Actinorhodin Export and Resistance in *Streptomyces coelicolor*. *MBio*, *3*(5), 10.1128/mbio.00191-12. https://doi.org/10.1128/mbio.00191-12

Yang, W., Willemse, J., Sawyer, E. B., Lou, F., Gong, W., Zhang, H., Gras, S. L., Claessen, D., & Perrett, S. (2017). The propensity of the bacterial rodlin protein RdlB to form amyloid fibrils determines its function in *Streptomyces coelicolor*. *Scientific Reports*, *7*, 42867. https://doi.org/10.1038/srep42867

Yin, J. (1991). A quantifiable phenotype of viral propagation. *Biochemical and Biophysical Research Communications*, *174*(2), 1009–1014. https://doi.org/10.1016/0006-291x(91)91519-i

You, L., & Yin, J. (1999). Amplification and spread of viruses in a growing plaque. *Journal of Theoretical Biology*, *200*(4), 365–373. https://doi.org/10.1006/jtbi.1999.1001

Young, R. (1992). Bacteriophage lysis: mechanism and regulation. *Microbiological Reviews*, *56*(3), 430–481. https://doi.org/10.1128/mr.56.3.430-481.1992

Zhan, Y., & Chen, F. (2019). The smallest ssDNA phage infecting a marine bacterium. *Environmental Microbiology*, *21*(6), 1916–1928. https://doi.org/10.1111/1462-2920.14394

Zhang, T., Tamman, H., Coppieters ’t Wallant, K., Kurata, T., LeRoux, M., Srikant, S., Brodiazhenko, T., Cepauskas, A., Talavera, A., Martens, C., Atkinson, G. C., Hauryliuk, V., Garcia-Pino, A., & Laub, M. T. (2022). Direct activation of a bacterial innate immune system by a viral capsid protein. *Nature*, *612*(7938), 132–140. https://doi.org/10.1038/s41586-022-05444-z

Zhang, Z., Du, C., de Barsy, F., Liem, M., Liakopoulos, A., van Wezel, G. P., Choi, Y. H., Claessen, D., & Rozen, D. E. (2020). Antibiotic production in *Streptomyces* is organized by a division of labor through terminal genomic differentiation. *Science Advances*, *6*(3), eaay5781. https://doi.org/10.1126/sciadv.aay5781

Zhang, Z., Shitut, S., Claushuis, B., Claessen, D., & Rozen, D. E. (2022). Mutational meltdown of putative microbial altruists in *Streptomyces coelicolor* colonies. *Nature Communications*, *13*(1), 2266. https://doi.org/10.1038/s41467-022-29924-y

3. Publications and manuscripts

Author contributions to the articles and manuscripts of this dissertation were assigned according to the “Contributor Roles Taxonomy (CRediT)” (https://credit.niso.org/).

Role	Definition
Conceptualization	Ideas; formulation or evolution of overarching research goals and aims
Data curation	Management activities to annotate (produce metadata), scrub data and maintain research data (including software code, where it is necessary for interpreting the data itself) for initial use and later re-use
Formal analysis	Application of statistical, mathematical, computational, or other formal techniques to analyze or synthesize study data
Funding acquisition	Acquisition of the financial support for the project leading to this publication
Investigation	Conducting a research and investigation process, specifically performing the experiments, or data/evidence collection
Methodology	Development or design of methodology; creation of models
Project administration	Management and coordination responsibility for the research activity planning and execution
Resources	Provision of study materials, reagents, materials, patients, laboratory samples, animals, instrumentation, computing resources, or other analysis tools
Software	Programming, software development; designing computer programs; implementation of the computer code and supporting algorithms; testing of existing code components
Supervision	Oversight and leadership responsibility for the research activity planning and execution, including mentorship external to the core team
Validation	Verification, whether as a part of the activity or separate, of the overall replication/reproducibility of results/experiments and other research outputs
Visualization	Preparation, creation and/or presentation of the published work, specifically visualization/data presentation
Writing – original draft	Preparation, creation and/or presentation of the published work, specifically writing the initial draft (including substantive translation)
Writing – review and editing	Preparation, creation and/or presentation of the published work by those from the original research group, specifically critical review, commentary or revision – including pre- or post-publication stages.

3.1 Bacterial multicellular behavior in antiviral defense

Luthe, T., Kever, L., Thormann, K., & Frunzke, J.

Published in *Current Opinion in Microbiology*, 2023

Role	Definition
Conceptualization	JF (40%), TL (32.5%), LK (27.5%)
Data curation	-
Formal analysis	-
Funding acquisition	JF (75%), KT (25%)
Investigation	-
Methodology	-
Project administration	JF (40%), TL (32.5%), LK (27.5%)
Resources	-
Software	-
Supervision	JF (100%)
Validation	-
Visualization	LK (60%), TL (30%), JF (10%)
Writing – original draft	TL (35%), JF (35%), LK (15%), KT (15%)
Writing – review and editing	TL (40%), JF (40%), LK (10%), KT (10%)

Overall contribution: 35%

Available online at www.sciencedirect.com

ScienceDirect

Current Opinion in Microbiology

Bacterial multicellular behavior in antiviral defense

Tom Luthe[1], Larissa Kever[1], Kai Thormann[2] and Julia Frunzke[1]

Multicellular behavior benefits seemingly simple organisms such as bacteria, by improving nutrient uptake, resistance to stresses, or by providing advantages in predatory interactions. Several recent studies have shown that this also extends to the defense against bacteriophages, which are omnipresent in almost all habitats. In this review, we summarize strategies conferring protection against phage infection at the multicellular level, covering secretion of small antiphage molecules or membrane vesicles, the role of quorum sensing in phage defense, the development of transient phage resistance, and the impact of biofilm components and architecture. Recent studies focusing on these topics push the boundaries of our understanding of the bacterial immune system and set the ground for an appreciation of bacterial multicellular behavior in antiviral defense.

Addresses
[1] Institute of Bio- und Geosciences, IBG-1: Biotechnology, Forschungszentrum Jülich, 52425 Jülich, Germany
[2] Institute of Microbiology and Molecular Biology, Justus-Liebig University Gießen, 35392 Gießen, Germany

Corresponding author: Frunzke, Julia (j.frunzke@fz-juelich.de)

Current Opinion in Microbiology 2023, **74**:102314

This review comes from a themed issue on **Evolution of anti-viral defense**

Edited by **Philip Kranzusch**

Available online xxxx

https://doi.org/10.1016/j.mib.2023.102314

Introduction

"*All for one and one for all, united we stand divided we fall.*"
Alexandre Dumas, The Three Musketeers

Viruses infecting bacteria, so-called bacteriophages, represent the most abundant predator on this planet, shaping life in almost all ecosystems. The ongoing 'arms race' between phages and bacteria has led to the evolution of diverse antiphage strategies collectively referred to as the bacterial 'immune system' [1,2]. Classical examples are restriction modification (RM), Clustered Regularly Interspaced Short Palindromic Repeats with CRISPR-associated proteins (CRISPR–Cas), and abortive infection (Abi) encoded by a large fraction of bacterial genomes. Currently, we are experiencing an unprecedented expansion of our understanding of bacterial antiviral immunity driven by the identification of numerous new antiphage systems — several of which are hinting toward a prokaryotic origin of human cell-autonomous innate immune mechanisms [3,4]. These groundbreaking discoveries were made possible by the finding that antiviral systems often colocalize in so-called 'defense islands' in prokaryotic genomes and by intensive screenings based on functional selection [5–8].

Effective antiviral defense of a single bacterial cell also protects the entire population, as it stops the spread of infection and prevents the release of new phages. Most of the systems described recently function at the intracellular level by targeting phage nucleic acids or by triggering death of the infected cell. However, several studies reported on bacterial antiphage strategies, which are shared by cells in a community and therefore can potentially be considered as antiviral public goods (Figure 1).

In natural environments, microbial communities typically show a high order of organization and emergent properties of bacterial multicellularity. The advantages of multicellular behavior are numerous and include the improved acquisition of nutrients, resistance to physical stresses or antimicrobial molecules, and the protection from predators [9]. In this short review, we will move toward the appreciation of bacterial multicellular behavior in antiviral defense. These mechanisms include the production and secretion of antiphage small molecules, membrane vesicles (MVs), quorum sensing (QS)-based activation of defense systems, the development of transient phage resistance, and the impact of biofilm architecture.

Quorum sensing

The concept of QS is at the heart of bacterial multicellularity as it defines the ability of bacterial populations to make group decisions. This communication between cells is mediated via the production and recognition of small molecules, so-called autoinducers, which can affect bacterial behavior associated with virulence, biofilm formation, horizontal gene transfer, and bioluminescence [10,11]. Several studies clearly show that QS also has an effect on the susceptibility of bacteria toward phage infection and on the coordination of phage defense strategies.

In the presence of the autoinducers AHL, CAI-1, or AI-2, phage adsorption was shown to be reduced for

Figure 1

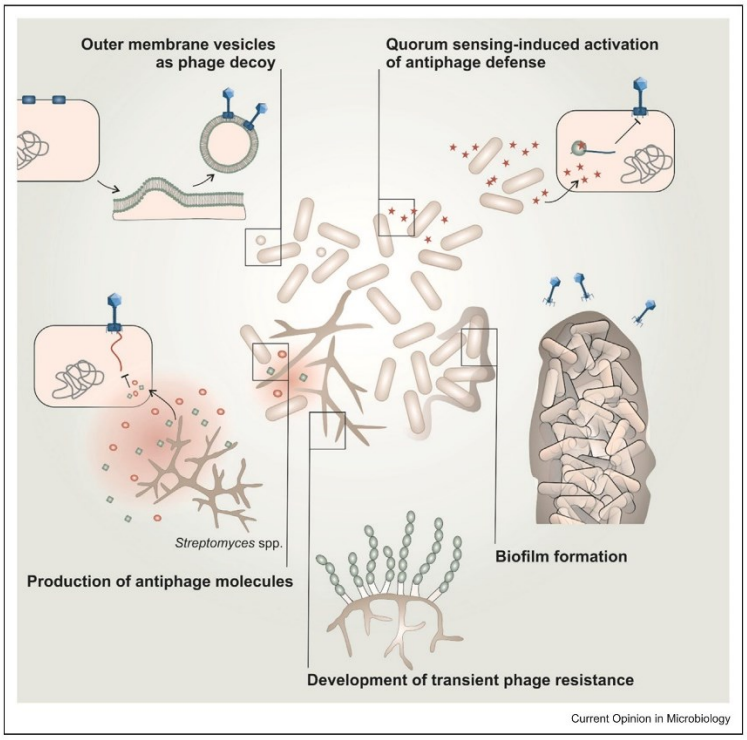

Bacterial multicellular strategies in antiviral defense. Protection against phages on a multicellular level can be mediated by i) extrusion of outer MVs sequestering phages, which prevents attachment to susceptible cells. ii) Quorum sensing-mediated antiphage defense systems rely on autoinducers (red stars) for transcriptional activation of RM-, CRISPR-, Abi-, and other systems. iii) Biofilm formation and trapping of phages via interaction with components of the extracellular matrix reduces diffusivity of phage particles and propagation upon infection. iv) Secretion of antiphage molecules (e.g. anthracyclines or aminoglycosides) confers a chemical defense by inhibiting an early step in the infection cycle. v) Cellular development allows for the emergence of transient phage resistance due to reduced susceptibility of distinct developmental stages.

Escherichia coli phages λ and χ, as well as different *Vibrio* phages by downregulation of the respective receptor genes [12–14]. Communication via QS also led to the inactivation of phages via the production of hemagglutinin protease in *Vibrio cholerae* [12]. QS was further shown to affect the adaptive immunity of CRISPR–Cas by activating *cas* gene expression in *Pseudomonas aeruginosa* and *Serratia* [15,16]. Moreover, QS peptides triggered abortive infection in *E. coli* through the *mazEF* toxin–antitoxin module, which was shown to inhibit the spread of phage P1 [17]. Besides this direct impact on phage defense, the influence of QS on phage susceptibility can also be indirect via the downregulation of metabolic activity affecting phage infection [18,19].

Considering the diverse effects of QS on bacterial antiviral defense, it is not surprising that phages also eavesdrop on the communication of their host to optimize their infection strategy. These antidefense mechanisms include, for example, receptors binding the host autoinducer and thereby derepressing lysis genes [11,20,21]. Further, *Pseudomonas* phage DMS3 was shown to directly inhibit LasR, the master regulator of QS, by expressing a small antiactivator protein as counterdefense strategy [22].

Chemical defense

Besides the exchange of information, small molecules produced and secreted by bacteria can also have themselves antiphage properties as recently described for compounds belonging to the classes of anthracyclines and aminoglycosides. Environmental bacteria, especially members of the genus of *Streptomyces*, are prolific producers of bioactive compounds, which are known to provide important fitness advantages in competitive, cooperative, as well as predatory interactions [23]. Inhibition of phage infection by bacterial small molecules received first attention in the 1950s and 1960s with a

special emphasis on the identification of antiphage molecules applicable in agricultural and medical sectors as summarized in a recent review article [24]. It is, however, striking that their potential role as part of the antiviral immune system of bacteria remained a major blind spot.

Recently, DNA-intercalating molecules belonging to the class of anthracyclines were shown to inhibit infection of several dsDNA phages infecting *Streptomyces coelicolor*, *E. coli*, or *Pseudomonas aeruginosa* [25]. Anthracyclines are naturally produced by *Streptomyces* and are among the most efficient anticancer agents used in clinics [26]. Mechanistically, these compounds were proposed to interfere with phage infection at an early step of the phage life cycle, namely between DNA injection and replication. However, a direct *in vivo* interaction between the compounds and phage DNA was not shown, yet [25].

A second class of antibiotics, which recently gained interest in the context of phage defense, are aminoglycosides [27]. Like anthracyclines, aminoglycosides are mainly produced by *Streptomyces*. These bactericidal, polycationic antibiotics act by targeting the 16S rRNA of the 30S ribosomal subunit, thereby interfering with bacterial protein translation [28]. Inhibition of phages by these compounds was observed for disparate dsDNA phages infecting Gram-positive and Gram-negative bacterial hosts.

It is striking that several — if not most — of the previously described antiphage compounds produced by bacteria have antibacterial properties, too. In nature, producers of antimicrobial molecules typically express a sophisticated set of self-resistance mechanisms [29,30]. This needs to be considered to allow the appreciation of potential antiviral effects of the respective molecule. First insights gained for aminoglycosides suggest that the molecular targets for inhibition of bacteria and phages are distinct. Acetylation of the aminoglycoside antibiotic apramycin abolished the antibacterial activity of the compound, but did not affect its antiphage properties [27].

The ecological relevance of chemically mediated antiphage defense by small molecules is supported by the inhibitory effect of culture supernatants of natural producer strains secreting the molecules [25,27]. Accordingly, with their excretion into the environment and their broad-spectrum activity, these secondary metabolites — dependent on locally achieved concentrations — could provide a chemical defense against phages at the community level by creating an antiviral milieu. However, resistance to the antibacterial effect of the molecule(s) is prerequisite to be able to benefit from the antiviral properties of the respective molecule. This could select for mutualistic communities thriving by a division of labor between kin cells or even different species and would exclude random competitors without the respective resistance [31].

Apart from a direct interference of bacterial small molecules with phage infection, bacteriostatic protein translation inhibitors can also provide protection against phage infection by increasing the efficiency of CRISPR–Cas immunity. This can be achieved either by decelerating phage reproduction, which extends the time for the acquisition of adaptive CRISPR immunity [32], or by interfering with the production of phage-encoded antidefense proteins [33].

Development of transiently resistant phenotypes

Recent studies revealed the development of transient resistance as an important factor involved in the containment of phage infection, especially in structured environments. For *Bacillus subtilis*, it was shown that neighboring cells respond to phage infection by D-alanylation of their cell wall-teichoic acids, thereby rendering their peptidoglycan layer resistant to phage attachment enabling active growth and constriction of plaque size [34]. Also, in *Streptomyces*, cellular development of transiently phage-resistant mycelium was shown to be important for the containment of viral infections. *S. venezuelae* mutants restricted to vegetative growth showed larger plaques and no constriction of plaque size [35]. These studies highlight the importance of cell envelope modifications and cellular development to counteract phage spread. Remarkably, it was now shown for several species that complete cell wall shedding represents a ubiquitous strategy to endure phage attack in osmoprotective environments [36,37].

Considering the role of cellular development for the containment of infections, it is likely to assume that phages fight back by manipulating cellular development for their own purposes. At early stages of phage Alderaan infection, transcriptome analysis of *Streptomyces* cells at the plaque interface revealed a downregulation of genes involved in cell development [35]. Further, the excision of *B. subtilis* prophage SPβ was shown to reconstitute the polysaccharide synthesis gene *spsM*, thereby contributing to spore dispersal [38].

Membrane vesicles

Another protective shield has been shown to be provided by the secretion of MVs, which are generated by all living cells. As ubiquitous components of the extracellular space and integral parts of biofilms, MVs affect intercellular interaction in manifold ways, including DNA transfer, metabolite export, virulence, and cell–cell communication. Although the most extensively studied

MVs are derived from the outer membrane of Gram-negative bacteria, there are different routes and triggers of membrane vesicle formation in both Gram-negative and -positive cells [39,40].

Several recent studies revealed that MVs may protect from viral predation by acting as phage decoys leading to adsorption of phages and resulting in less productive phage infections of the population [41–45]. Phage-induced lysis of bacterial cells is supposed to contribute extensively to the formation of MVs in nature [46]. This raises the possibility that MVs may serve as a defense mechanism by transporting signaling molecules such as QS molecules in a concentrated manner, as has been suggested for *Paracoccus denitrificans* [47,48]. This could help bacteria communicate and coordinate their defense against phages more effectively. Further research is needed to understand the exact role of MVs in bacterial antiviral defense.

Biofilms

Among the huge body of studies that have addressed the interaction of phages with their hosts, most of the data — in particular studies on molecular mechanisms underlying the phage–host tug-of-war — stems from planktonic cultures, where diffusing phages have more or less free access to their prey cells. However, in most environments, the majority of bacteria exists in biofilms, where the bacteria are physically associated with each other in a self-produced matrix engulfing the community [49–51]. This results in a number of inherent properties of the biofilm community that drastically increases the tolerance of the bacterial populations against all kinds of environmental stresses. It has been observed that, most times, the inherent recalcitrance of cells in biofilms also extends to phage predation.

Intuitively, a local accumulation of potential prey cells may seem beneficial for phage predation, however, the prey clustering is likely to result in increased coinfections causing a drop in phage propagation per particle [52]. In addition, all biofilm communities are characterized by a pronounced metabolic stratification due to different access to metabolites including oxygen. Thus, many cells within the community exhibit a reduced metabolic activity up to the point of dormancy [53]. Although there are some phages that are able to infect and lyse dormant cells, many if not most phages do not proliferate efficiently at low metabolic activity of the host cells [54–57]. Such dormant, dead, or phage-resistant cells may still efficiently bind phage particles and thus serve as potent phage absorbers or a shield that protects their susceptible counterparts [58–64].

Another important factor that governs phage–biofilm interactions is the biofilm matrix, which is encasing the bacterial cells and commonly consists of various polymeric substances such as exopolysaccharides, various proteins, nucleic acids, and lipids [50]. Intuitively and as predicted by a biofilm simulation network [65], the interaction of phages and bacteria depends on the ability of the rather large phage particles to diffuse through the biofilm and, thus, to a significant part on the interaction of phages with the matrix. Correspondingly, several studies demonstrate that the biofilm matrix limits phage diffusion and viral predation of the cells [66–70]. An exopolysaccharide named stewartan showed concentration-dependent limiting of phage diffusion, unless the phages were decorated with corresponding depolymerases to counteract this defense [71]. Another study showed that active phages are captured by extracellular proteinaceous assemblages referred to as curli. Notably, the tight binding of phages by these structures implicates that matrix components may have evolved to efficiently absorb specific intruding phages [72]. Phages can thus be efficiently retained in the biofilm, and it has been shown that this not only prevents the embedded cells from phage contact and infection but may also turn the captured phages into a protective barrier against other susceptible invading or evading bacteria [72–74].

Taken together, cells in biofilms are generally more recalcitrant toward phage assaults. This can mainly be attributed to the biofilm structure and the resulting spatial and metabolic stratification, which in concert limits access to the prey cells and successful phage proliferation. The studies implicate that, as a whole, a biofilm community is a reservoir of a multitude of phage–host interactions, which we are only beginning to understand [75,76].

Conclusions and future perspectives

The recent discovery of numerous new systems impressively demonstrates the gaps in our understanding of the bacterial immune system [1,3]. In this short review, we summarize strategies conferring protection at the multicellular level by the secretion of small molecules, MVs, or via components of the biofilm matrix. In the past, antiviral defense has been mainly studied at the level of isolated systems. It is, however, the interaction between different lines of defense, which ultimately shapes the immune system — a notion that is well accepted for antiviral immunity in eukaryotes, but still very underdeveloped for the prokaryotic world. Technological advances now enable the spatiotemporal analysis of the interaction and complementation of different antiviral mechanisms providing unprecedented insights into their interaction and interdependencies within bacterial species [77,78].

The majority of microbial interactions take place in spatially structured environments. Consequently, several factors, such as the physiological status of neighboring

cells and the structure and individual components of the biofilm, have important implications for the range of microbial interactions. Several recent studies reveal the predominance of short-range interactions in densely packed bacterial communities and the impact of system architecture and cell permeability on spatial scales [79,80]. Consequently, these factors likely also shape the dimensions of antiviral defense provided through the secretion of small molecules or MVs. The spatiotemporal analysis of antiviral defense at the multicellular level will also allow to study the response of bacterial populations to viral infection and represents a powerful approach for the identification of new multicellular strategies involved in the communication between cells and the establishment of complex interaction networks through genetic and/or phenotypic diversification [81,82].

These recent examples provide first insights into the multiple dimensions of bacterial multicellular behavior and its relevance for antiviral defense. Combining molecular mechanistic, evolutionary, and ecological approaches is now essential for a comprehensive understanding of the ecological relevance of these systems in the context of microbial interaction.

Data Availability

No data were used for the research described in the article.

Declaration of Competing Interest

The authors declare that they have no known competing financial interests or personal relationships that could have appeared to influence the work reported in this paper.

Acknowledgements

Research in the Frunzke Lab is supported by the European Research Council (ERC Starting Grant 757563) and the Deutsche Forschungsgemeinschaft (SPP 2330, project 464434020 and CRC 1535 , project 458090666 / CRC1535/1). The Thormann Lab is supported by the Deutsche Forschungsgemeinschaft (SPP 2330, TH831/10-1).

References and recommended reading

Papers of particular interest, published within the period of review, have been highlighted as:

- • of special interest
- •• of outstanding interest

1. Bernheim A, Sorek R: **The pan-immune system of bacteria: antiviral defence as a community resource**. *Nat Rev Microbiol* 2020, **18**:113-119.
2. Hampton HG, Watson BNJ, Fineran PC: **The arms race between bacteria and their phage foes**. *Nature* 2020, **577**:327-336.
3. Tal N, Sorek R: **SnapShot: bacterial immunity**. *Cell* 2022, **185**:578-578.e571.
4. Wein T, Sorek R: **Bacterial origins of human cell-autonomous innate immune mechanisms**. *Nat Rev Immunol* 2022, **22**:629-638.
5. Doron S, Melamed S, Ofir G, Leavitt A, Lopatina A, Keren M, Amitai G, Sorek R: **Systematic discovery of antiphage defense systems in the microbial pangenome**. *Science* (6379) 2018, **359**:eaar4120.
6. Gao L, Altae-Tran H, Böhning F, Makarova KS, Segel M, Schmid-Burgk JL, Koob J, Wolf YI, Koonin EV, Zhang F: **Diverse enzymatic activities mediate antiviral immunity in prokaryotes**. *Science* 2020, **369**:1077-1084.
7. Vassallo CN, Doering CR, Littlehale ML, Teodoro GIC, Laub MT: **A functional selection reveals previously undetected anti-phage defence systems in the *E. coli* pangenome**. *Nat Microbiol* 2022, **7**:1568-1579.
8. Millman A, Melamed S, Leavitt A, Doron S, Bernheim A, Hör J, Garb J, Bechon N, Brandis A, Lopatina A, *et al.*: **An expanded arsenal of immune systems that protect bacteria from phages**. *Cell Host Microbe* 2022,1556-1569.
9. Lyons NA, Kolter R: **On the evolution of bacterial multicellularity**. *Curr Opin Microbiol* 2015, **24**:21-28.
10. Abisado RG, Benomar S, Klaus JR, Dandekar AA, Chandler JR: **Bacterial quorum sensing and microbial community interactions**. *mBio* 2018, **9**:e02331-17.
11. Duddy OP, Bassler BL: **Quorum sensing across bacterial and viral domains**. *PLoS Pathog* 2021, **17**:e1009074.
12. Hoque MM, Naser IB, Bari SM, Zhu J, Mekalanos JJ, Faruque SM: **Quorum regulated resistance of *Vibrio cholerae* against environmental bacteriophages**. *Sci Rep* 2016, **6**:37956.
13. Høyland-Kroghsbo NM, Maerkedahl RB, Svenningsen SL: **A quorum-sensing-induced bacteriophage defense mechanism**. *mBio* 2013, **4**:e00362-00312.
14. Tan D, Svenningsen SL, Middelboe M: **Quorum sensing determines the choice of antiphage defense strategy in *Vibrio anguillarum***. *mBio* 2015, **6**:e00627.
15. Høyland-Kroghsbo NM, Paczkowski J, Mukherjee S, Broniewski J, Westra E, Bondy-Denomy J, Bassler BL: **Quorum sensing controls the *Pseudomonas aeruginosa* CRISPR-Cas adaptive immune system**. *Proc Natl Acad Sci USA* 2017, **114**:131-135.
16. Patterson AG, Jackson SA, Taylor C, Evans GB, Salmond GPC, Przybilski R, Staals RHJ, Fineran PC: **Quorum sensing controls adaptive immunity through the regulation of multiple CRISPR-Cas systems**. *Mol Cell* 2016, **64**:1102-1108.
17. Hazan R, Engelberg-Kulka H: ***Escherichia coli mazEF*-mediated cell death as a defense mechanism that inhibits the spread of phage P1**. *Mol Genet Genom* 2004, **272**:227-234.
18. Ding Y, Zhang D, Zhao X, Tan W, Zheng X, Zhang Q, Ji X, Wei Y: **Autoinducer-2-mediated quorum-sensing system resists T4 phage infection in *Escherichia coli***. *J Basic Microbiol* 2021, **61**:1113-1123.
19. Goo E, An JH, Kang Y, Hwang I: **Control of bacterial metabolism by quorum sensing**. *Trends Microbiol* 2015, **23**:567-576.
20. Laganenka L, Sander T, Lagonenko A, Chen Y, Link H, Sourjik V: **Quorum sensing and metabolic state of the host control lysogeny-lysis switch of bacteriophage T1**. *MBio* 2019, **10**:e01884-19.
21. Silpe JE, Bassler BL: **A host-produced quorum-sensing autoinducer controls a phage lysis-lysogeny decision**. *Cell* 2019, **176**:268-280.e213.
22. • Shah M, Taylor VL, Bona D, Tsao Y, Stanley SY, Pimentel-Elardo SM, McCallum M, Bondy-Denomy J, Howell PL, Nodwell JR, *et al.*: **A phage-encoded anti-activator inhibits quorum sensing in *Pseudomonas aeruginosa***. *Mol Cell* 2021, **81**:571-583.e576.
This study provides a compelling example of how phages can disrupt key biological pathways of the host via production of quorum-sensing antiactivator proteins. Aqs1 produced by *Pseudomonas* phage DMS3 was shown to inhibit LasR, the master regulator of quorum sensing, and to block superinfection of phages requiring the pilus for infection.
23. Tyc O, Song C, Dickschat JS, Vos M, Garbeva P: **The ecological role of volatile and soluble secondary metabolites produced by soil bacteria**. *Trends Microbiol* 2017, **25**:280-292.

24. Hardy A, Kever L, Frunzke J: **Antiphage small molecules produced by bacteria — beyond protein-mediated defenses**. *Trends Microbiol* 2023, **31**:92-106.

25. •• Kronheim S, Daniel-Ivad M, Duan Z, Hwang S, Wong AI, Mantel I, Nodwell JR, Maxwell KL: **A chemical defence against phage infection**. *Nature* 2018, **564**:283-286.
Systematic screening of bacterial secondary metabolites and demonstration of the antiphage properties of anthracyclines active against a broad range of phages.

26. Minotti G, Menna P, Salvatorelli E, Cairo G, Gianni L: **Anthracyclines: molecular advances and pharmacologic developments in antitumor activity and cardiotoxicity**. *Pharmacol Rev* 2004, **56**:185-229.

27. •• Kever L, Hardy A, Luthe T, Hünnefeld M, Gätgens C, Milke L, Wiechert J, Wittmann J, Moraru C, Marienhagen J, *et al.*: **Aminoglycoside antibiotics inhibit phage infection by blocking an early step of the infection cycle**. *mBio* 2022, **13**:e0078322.
Demonstration of the antiphage properties of aminoglycoside antibiotics. Using strains resistant to the molecule of interest allowed for the appreciation of the antiphage properties. Acetylation of apramycin abolished its antibacterial properties but retained its ability to block phage infection.

28. Krause KM, Serio AW, Kane TR, Connolly LE: **Aminoglycosides: an overview**. *Cold Spring Harb Perspect Med* (6) 2016, **6**:a027029.

29. Hopwood DA: **How do antibiotic-producing bacteria ensure their self-resistance before antibiotic biosynthesis incapacitates them?** *Mol Microbiol* 2007, **63**:937-940, https://doi.org/10.1101/cshperspect.a027029

30. Tenconi E, Rigali S: **Self-resistance mechanisms to DNA-damaging antitumor antibiotics in actinobacteria**. *Curr Opin Microbiol* 2018, **45**:100-108.

31. Traxler MF, Rozen DE: **Ecological drivers of division of labour in Streptomyces**. *Curr Opin Microbiol* 2022, **67**:102148.

32. Dimitriu T, Kurilovich E, Łapińska U, Severinov K, Pagliara S, Szczelkun MD, Westra ER: **Bacteriostatic antibiotics promote CRISPR-Cas adaptive immunity by enabling increased spacer acquisition**. *Cell Host Microbe* 2022, **30**:31-40.e35.

33. Pons JP, Dimitriu T, Westra ER, van Houte S: **Antibiotics that affect translation can antagonize phage infectivity by interfering with the deployment of counter-defences**. *Proc Natl Acad Sci U S A* (4) 2023, **120**:e2216084120, https://doi.org/10.1073/pnas.221608412

34. • Tzipilevich E, Pollak-Fiyaksel O, Shraiteh B, Ben-Yehuda S: **Bacteria elicit a phage tolerance response subsequent to infection of their neighbors**. *Embo J* 2022, **41**:e109247.
For *Bacillus subtilis,* it was shown that neighboring cells respond to phage infection by D-alanylation of their cell wall-teichoic acids, thereby rendering their peptidoglycan layer resistant to phage attachment enabling active growth and constriction of plaque size.

35. Luthe T, Kever L, Hänsch S, Hardy A, Tschowri N, Weidtkamp-Peters S, Frunzke J: ***Streptomyces* development is involved in the efficient containment of viral infections**. *microLife* 2023, **4**:1-13, https://doi.org/10.1093/femsml/uqad002

36. Wohlfarth JC, Feldmüller M, Schneller A, Kilcher S, Burkolter M, Meile S, Pilhofer M, Schuppler M, Loessner MJ: **L-form conversion in Gram-positive bacteria enables escape from phage infection**. *Nat Microbiol* 2023, **8**:387-399.

37. Ongenae V, Mabrouk AS, Crooijmans M, Rozen D, Briegel A, Claessen D: **Reversible bacteriophage resistance by shedding the bacterial cell wall**. *Open Biol* 2022, **12**:210379.

38. Abe K, Kawano Y, Iwamoto K, Arai K, Maruyama Y, Eichenberger P, Sato T: **Developmentally-regulated excision of the SPβ prophage reconstitutes a gene required for spore envelope maturation in *Bacillus subtilis***. *PLoS Genet* 2014, **10**:e1004636.

39. Toyofuku M, Nomura N, Eberl L: **Types and origins of bacterial membrane vesicles**. *Nat Rev Microbiol* 2019, **17**:13-24.

40. Brown L, Wolf JM, Prados-Rosales R, Casadevall A: **Through the wall: extracellular vesicles in Gram-positive bacteria, mycobacteria and fungi**. *Nat Rev Microbiol* 2015, **13**:620-630.

41. Bayer MH, Costello GP, Bayer ME: **Isolation and partial characterization of membrane vesicles carrying markers of the membrane adhesion sites**. *J Bacteriol* 1982, **149**:758-767.

42. Beerens D, Franch-Arroyo S, Sullivan TJ, Goosmann C, Brinkmann V, Charpentier E: **Survival strategies of *Streptococcus pyogenes* in response to phage infection**. *Viruses* (4) 2021, **13**:612, https://doi.org/10.3390/v13040612

43. Manning AJ, Kuehn MJ: **Contribution of bacterial outer membrane vesicles to innate bacterial defense**. *BMC Microbiol* 2011, **11**:258.

44. Reyes-Robles T, Dillard RS, Cairns LS, Silva-Valenzuela CA, Housman M, Ali A, Wright ER, Camilli A: ***Vibrio cholerae* outer membrane vesicles inhibit bacteriophage infection**. *J Bacteriol* (15) 2018, **200**:e00792-17.

45. Stephan MS, Broeker NK, Saragliadis A, Roos N, Linke D, Barbirz S: **In vitro analysis of O-antigen-specific bacteriophage P22 inactivation by *Salmonella* outer membrane vesicles**. *Front Microbiol* 2020, **11**:510638.

46. Mandal PK, Ballerin G, Nolan LM, Petty NK, Whitchurch CB: **Bacteriophage infection of *Escherichia coli* leads to the formation of membrane vesicles via both explosive cell lysis and membrane blebbing**. *Microbiology* (4) 2021, **167**:001021.

47. Yasuda M, Yamamoto T, Nagakubo T, Morinaga K, Obana N, Nomura N, Toyofuku M: **Phage genes induce quorum sensing signal release through membrane vesicle formation**. *Microbes Environ* (1) 2022, **37**:ME21067.

48. Toyofuku M, Morinaga K, Hashimoto Y, Uhl J, Shimamura H, Inaba H, Schmitt-Kopplin P, Eberl L, Nomura N: **Membrane vesicle-mediated bacterial communication**. *Isme J* 2017, **11**:1504-1509.

49. Dragoš A, Kovács ÁT: **The peculiar functions of the bacterial extracellular matrix**. *Trends Microbiol* 2017, **25**:257-266.

50. Flemming HC, van Hullebusch ED, Neu TR, Nielsen PH, Seviour T, Stoodley P, Wingender J, Wuertz S: **The biofilm matrix: multitasking in a shared space**. *Nat Rev Microbiol* 2023, **21**:70-86.

51. Flemming HC, Wuertz S: **Bacteria and archaea on Earth and their abundance in biofilms**. *Nat Rev Microbiol* 2019, **17**:247-260.

52. Taylor BP, Penington CJ, Weitz JS: **Emergence of increased frequency and severity of multiple infections by viruses due to spatial clustering of hosts**. *Phys Biol* 2017, **13**:066014.

53. Ciofu O, Moser C, Jensen P, Høiby N: **Tolerance and resistance of microbial biofilms**. *Nat Rev Microbiol* 2022, **20**:621-635.

54. Bryan D, El-Shibiny A, Hobbs Z, Porter J, Kutter EM: **Bacteriophage T4 infection of stationary phase *E. coli*: life after log from a phage perspective**. *Front Microbiol* 2016, **7**:1391.

55. Łoś M, Golec P, Łoś JM, Weglewska-Jurkiewicz A, Czyz A, Wegrzyn A, Wegrzyn G, Neubauer P: **Effective inhibition of lytic development of bacteriophages lambda, P1 and T4 by starvation of their host, *Escherichia coli***. *BMC Biotechnol* 2007, **7**:13.

56. Melo LDR, França A, Brandão A, Sillankorva S, Cerca N, Azeredo J: **Assessment of Sep1virus interaction with stationary cultures by transcriptional and flow cytometry studies**. *FEMS Microbiol Ecol* (10) 2018, **94**, https://doi.org/10.1093/femsec/fiy143

57. Tkhilaishvili T, Lombardi L, Klatt AB, Trampuz A, Di Luca M: **Bacteriophage Sb-1 enhances antibiotic activity against biofilm, degrades exopolysaccharide matrix and targets persisters of *Staphylococcus aureus***. *Int J Antimicrob Agents* 2018, **52**:842-853.

58. Abedon ST: **Bacteriophage exploitation of bacterial biofilms: phage preference for less mature targets?** *FEMS Microbiol Lett* (3) 2016, **363**:fnv246.

59. Abedon ST: **Phage "delay" towards enhancing bacterial escape from biofilms: a more comprehensive way of viewing resistance to bacteriophages**. *AIMS Microbiol* 2017, **3**:186-226.

60. Bull JJ, Christensen KA, Scott C, Jack BR, Crandall CJ, Krone SM: **Phage-bacterial dynamics with spatial structure: self**

organization around phage sinks can promote increased cell densities. *Antibiotics* (1) 2018, **7**:8, https://doi.org/10.3390/antibiotics7010008

61. Hewson I, Fuhrman JA: **Viriobenthos production and virioplankton sorptive scavenging by suspended sediment particles in coastal and pelagic waters**. *Micro Ecol* 2003, **46**:337-347.

62. Rabinovitch A, Aviram I, Zaritsky A: **Bacterial debris-an ecological mechanism for coexistence of bacteria and their viruses**. *J Theor Biol* 2003, **224**:377-383.

63. • Simmons EL, Bond MC, Koskella B, Drescher K, Bucci V, Nadell CD: **Biofilm structure promotes coexistence of phage-resistant and phage-susceptible bacteria**. *mSystems* (3) 2020, **5**:e00877-19.
This study combines simulations and *in vivo* work to show how phage-resistant cells can protect clusters of susceptible cells, which promotes the (co)existence of susceptible cells in the presence of phages.

64. Yin J, McCaskill JS: **Replication of viruses in a growing plaque: a reaction-diffusion model**. *Biophys J* 1992, **61**:1540-1549.

65. Simmons M, Drescher K, Nadell CD, Bucci V: **Phage mobility is a core determinant of phage-bacteria coexistence in biofilms**. *Isme J* 2018, **12**:531-543.

66. Briandet R, Lacroix-Gueu P, Renault M, Lecart S, Meylheuc T, Bidnenko E, Steenkeste K, Bellon-Fontaine MN, Fontaine-Aupart MP: **Fluorescence correlation spectroscopy to study diffusion and reaction of bacteriophages inside biofilms**. *Appl Environ Microbiol* 2008, **74**:2135-2143.

67. Doolittle MM, Cooney JJ, Caldwell DE: **Tracing the interaction of bacteriophage with bacterial biofilms using fluorescent and chromogenic probes**. *J Ind Microbiol* 1996, **16**:331-341.

68. Lacroix-Gueu P, Briandet R, Lévêque-Fort S, Bellon-Fontaine MN, Fontaine-Aupart MP: **In situ measurements of viral particles diffusion inside mucoid biofilms**. *C R Biol* 2005, **328**:1065-1072.

69. Melo LDR, Pinto G, Oliveira F, Vilas-Boas D, Almeida C, Sillankorva S, Cerca N, Azeredo J: **The protective effect of *Staphylococcus epidermidis* biofilm matrix against phage predation**. *Viruses* (10) 2020, **12**:1076, https://doi.org/10.3390/v12101076

70. González S, Fernández L, Gutiérrez D, Campelo AB, Rodríguez A, García P: **Analysis of different parameters affecting diffusion, propagation and survival of Staphylophages in bacterial biofilms**. *Front Microbiol* 2018, **9**:2348.

71. Dunsing V, Irmscher T, Barbirz S, Chiantia S: **Purely polysaccharide-based biofilm matrix provides size-selective diffusion barriers for nanoparticles and bacteriophages**. *Biomacromolecules* 2019, **20**:3842-3854.

72. Vidakovic L, Singh PK, Hartmann R, Nadell CD, Drescher K: **Dynamic biofilm architecture confers individual and collective mechanisms of viral protection**. *Nat Microbiol* 2018, **3**:26-31.

73. Chaudhry W, Lee E, Worthy A, Weiss Z, Grabowicz M, Vega N, Levin B: **Mucoidy, a general mechanism for maintaining lytic phage in populations of bacteria**. *FEMS Microbiol Ecol* (10) 2020, **96**:fiaa162.

74. Darch SE, Kragh KN, Abbott EA, Bjarnsholt T, Bull JJ, Whiteley M: **Phage inhibit pathogen dissemination by targeting bacterial migrants in a Chronic Infection Model**. *mBio* (2) 2017, **8**:e00240-17.

75. Pires DP, Melo LDR, Azeredo J: **Understanding the complex phage-host interactions in biofilm communities**. *Annu Rev Virol* 2021, **8**:73-94.

76. Hansen MF, Svenningsen SL, Røder HL, Middelboe M, Burmølle M: **Big impact of the tiny: bacteriophage-bacteria interactions in biofilms**. *Trends Microbiol* 2019, **27**:739-752.

77. Tesson F, Bernheim A: **Synergy and regulation of antiphage systems: toward the existence of a bacterial immune system?** *Curr Opin Microbiol* 2022, **71**:102238.

78. Maguin P, Varble A, Modell JW, Marraffini LA: **Cleavage of viral DNA by restriction endonucleases stimulates the type II CRISPR-Cas immune response**. *Mol Cell* 2022, **82**:907-919.e907.

79. Dal Co A, van Vliet S, Kiviet DJ, Schlegel S, Ackermann M: **Short-range interactions govern the dynamics and functions of microbial communities**. *Nat Ecol Evol* 2020, **4**:366-375.

80. van Gestel J, Bareia T, Tenennbaum B, Dal Co A, Guler P, Aframian N, Grinberg S, D'Souza GG, Erez Z, *et al.*: **Short-range quorum sensing controls horizontal gene transfer at micron scale in bacterial communities**. *Nat Commun* 2021, **12**:2324.

81. Zhang Z, Du C, de Barsy F, Liem M, Liakopoulos A, van Wezel GP, Choi YH, Claessen D, Rozen DE: **Antibiotic production in *Streptomyces* is organized by a division of labor through terminal genomic differentiation**. *Sci Adv* 2020, **6**:eaay5781.

82. Shaer Tamar E, Kishony R: **Multistep diversification in spatiotemporal bacterial-phage coevolution**. *Nat Commun* 2022, **13**:7971.

3.2 *Streptomyces* development is involved in the efficient containment of viral infections

Luthe, T., Kever, L., Hänsch, S., Hardy, A., Tschowri, N., Weidkamp-Peters, S., & Frunzke, J.

Published in *MicroLife*, 2023

Role	Definition
Conceptualization	TL (50%), JF (50%)
Data curation	TL (90%), SH (10%),
Formal analysis	TL (60%), LK (15%), SH (5%), AH (5%), NT (5%), SW-P (5%), JF (5%)
Funding acquisition	JF (100%)
Investigation	TL (75%), LK (10%), SH (10%), AH (5%)
Methodology	TL (55%), LK (10%), SH (10%), AH (5%), NT (5%), SW-P (5%), JF (10%)
Project administration	JF (100%)
Resources	SW-P (25%), JF (75%)
Software	-
Supervision	JF (100%)
Validation	TL (65%), SH (10%), LK (5%), AH (5%), NT (5%), SW-P (5%), JF (5%)
Visualization	TL (90%), JF (10%)
Writing – original draft	TL (90%), JF (10%)
Writing – review and editing	JF (45%), TL (25%), LK (15%), AH (5%), NT (5%), SH (2.5%), SW-P (2.5%),

Overall contribution: 75%

microLife, 2023, **4**, 1–13
DOI: 10.1093/femsml/uqad002
Advance access publication date: 16 January 2023
Research Article

Streptomyces development is involved in the efficient containment of viral infections

Tom Luthe[1], Larissa Kever[1], Sebastian Hänsch[2], Aël Hardy[1], Natalia Tschowri[3], Stefanie Weidtkamp-Peters[2], Julia Frunzke[1,*]

[1]Institute of Bio- and Geosciences, IBG-1: Biotechnology, Forschungszentrum Jülich, 52425 Jülich, Germany
[2]Center for Advanced Imaging, Heinrich Heine Universität Düsseldorf, 40225 Düsseldorf, Germany
[3]Institute of Microbiology, Leibniz Universität Hannover, 30419 Hannover, Germany
***Corresponding author:** Institute of Bio- and Geosciences, IBG-1: Biotecnology, Forschungzentrum Jülich, 52425 Jülich, Germany. Tel: +49 2461 615430; Email: j.frunzke@fz-juelich.de
Editor: Martin Loessner

Abstract

The formation of plaques represents the hallmark of phage infection visualizing the clearance of the bacterial lawn in structured environments. In this study, we have addressed the impact of cellular development on phage infection in *Streptomyces* undergoing a complex developmental life cycle. Analysis of plaque dynamics revealed, after a period of plaque size enlargement, a significant regrowth of transiently phage-resistant *Streptomyces* mycelium into the lysis zone. Analysis of *Streptomyces venezuelae* mutant strains defective at different stages of cellular development indicated that this regrowth was dependent on the onset of the formation of aerial hyphae and spores at the infection interface. Mutants restricted to vegetative growth (Δ*bldN*) featured no significant constriction of plaque area. Fluorescence microscopy further confirmed the emergence of a distinct zone of cells/spores with reduced cell permeability towards propidium iodide staining at the plaque periphery. Mature mycelium was further shown to be significantly less susceptible to phage infection, which is less pronounced in strains defective in cellular development. Transcriptome analysis revealed the repression of cellular development at the early stages of phage infection probably facilitating efficient phage propagation. We further observed an induction of the chloramphenicol biosynthetic gene cluster highlighting phage infection as a trigger of cryptic metabolism in *Streptomyces*. Altogether, our study emphasizes cellular development and the emergence of transient phage resistance as an important layer of *Streptomyces* antiviral immunity.

Keywords: *Streptomyces*, development, bacteriophages, phage defense, sporulation, viral infection

Introduction

Bacteria are abundant in soil environments where spatial movement is limited and microbial density and diversity are higher than in most other habitats (Fierer 2017, Thompson et al. 2017, Rodriguez-R et al. 2018). In need for nutrients and space, while in constant contact with competitors and predators, soil bacteria developed different strategies to promote survival and distribution. Bacteria of the genus *Streptomyces* are members of the large phylum of Actinobacteria thriving in soil habitats (van Bergeijk et al. 2020). *Streptomyces* are well-known for their production of a wide range of clinically and industrially relevant secondary metabolites (Demain 1999, Watve et al. 2001) as well as their complex multicellular development (Flärdh and Buttner 2009, Barka et al. 2016, Chater 2016).

The most abundant predator in almost every environment, including the soil, are bacteriophages (phages) (Williamson et al. 2017). Phages are viruses infecting bacteria and as such pose a constant threat to bacterial populations, playing a major role in microbial evolution and community dynamics (Clokie et al. 2011, Chevallereau et al. 2021). The research on phages infecting members of the Actinobacteria (actinobacteriophages) has seen enormous efforts in isolating, sequencing and characterizing on many associated host genera including 25 *Streptomyces* species. The over 4000 sequenced genomes curated at The Actinobacteriophage Database (phagesdb.org) reveal an immense diversity of actinobacteriophages regarding genome size, morphology, lifestyle, host range and genomic equipment, but display considerable bias towards the species of *Mycobacterium smegmatis* with more than 2000 sequenced phages (Hatfull 2020). Despite this wealth of data, still little is known about phage-bacteria interactions in a host capable of secondary metabolite production and multicellular development.

In contrast to classical unicellular bacteria, *Streptomyces* do not follow the typical binary fission style of reproduction but undergo a complex life cycle starting from single spores developing into a branched vegetative mycelium with connected compartments that is followed by the erection of unbranched aerial hyphae growing into the air under unfavorable conditions (Elliot and Talbot 2004, Flärdh 2010). From aerial hyphae, chains of unigenomic spores are generated and dispersed (Sigle et al. 2015). During progression of the life cycle, a programmed cell death-like mechanism provides resources for the following developmental steps (Miguélez, Hardisson and Manzanal 1999, Manteca, Fernandez and Sanchez 2006). More precisely, coordinated cell death among the old vegetative mycelium precedes the erection of aerial hyphae (Manteca et al. 2007, Tenconi et al. 2018). In order to protect carbon and nitrogen resources from being captured by other soil-living organisms, production of secondary metabolites such as antibiotics is coupled to developmental processes (Rigali et al. 2008). Recent studies revealed that—besides their antibac-

Received: September 20, 2022. **Revised:** December 9, 2022. **Accepted:** January 13, 2023

terial properties—some of these natural products may actually confer protection against a variety of different phages. This was exemplified by DNA-intercalating molecules of the class of anthracyclines as well as for different aminoglycosides produced by *Streptomyces* (Kronheim et al. 2018, Hardy, Kever and Frunzke 2022, Kever et al. 2022). While first studies suggest a diverse repertoire of antiviral molecules produced by these bacteria, the impact of the developmental peculiarities and multicellular lifestyle of *Streptomyces* on phage-host interactions has not been addressed so far.

Streptomyces multicellular development is governed by a complex regulatory network. Part of this network are *bld* and *whi* genes encoding regulators, which control genes involved in key developmental steps. The so-called 'master regulator' BldD controls more than 160 different targets in the *Streptomyces* genome and is itself regulated by c-di-GMP (McCormick and Flärdh 2012, Tschowri et al. 2014, Bush et al. 2015). In the model strain *Streptomyces venezuelae*, BldD inhibits the expression of the sigma factor BldN, which activates *rdlABC* and *chpBCEFGH* genes encoding rodlins and chaplins necessary for building the hydrophobic sheath (Bibb et al. 2012). Together with SapB, the amyloid layer of hydrophobic rodlins and chaplins is necessary for the escape of aerial hyphae from the aqueous environment. Another target repressed by BldD is *whiB*, which, together with WhiA, stops tip growth of aerial hyphae by blocking expression of *filP*. WhiB activates septation, segregation and cell division in the filaments during transformation from aerial mycelium to spore chains by upregulation of *ftsK*, *parAB* and *ftsZ* (Bush et al. 2013, 2016). While WhiB-like proteins are widespread in Actinobacteria, they were recently shown to be common among actinobacteriophages too. Indeed, 24% of analyzed genomes encode *whiB* homologs, making WhiB-like genes the most abundant transcriptional regulators in actinobacteriophages (Sharma et al. 2021). Besides WhiB-like proteins, actinobacteriophages harbor several other genes potentially involved in the manipulation of cellular development, including *parB*, *ftsK*, or *ssgA* (Hardy et al. 2020). Given the genetic equipment of actinobacteriophages and the complex life cycle of their host it is likely that phages have evolved various mechanisms to manipulate development and that cellular development is an integral part of the multicellular antiphage defense strategies employed by *Streptomyces*.

In this study, we investigated the impact of phage infection on *Streptomyces* development using *S. venezuelae* as a model host. We observed that phage infection on solid media triggered the development of aerial hyphae and sporulation at the infection interface of the plaque. Analysis of mutant strains defective at different stages of *Streptomyces* development further confirmed the importance of cellular development for the establishment of phage-resistance phenotypes promoting the containment of viral infections. Global transcriptome analysis further suggested a suppression of cellular development during the early stages of phage infection.

Results

Impact of phage infection on *Streptomyces* development

To investigate *Streptomyces* development during bacteriophage infection, we monitored plaque formation of six phages (Alderaan, SV1, phi A.streptomycini III, P26, Dagobah and Endor1, see Table S1) on the lawn of three different *Streptomyces* species (*S. venezuelae*, *S. griseus*, and *S. coelicolor*, see Table S2) using stereo microscopy (Fig. 1A). While significant differences were observed with regard to the spatiotemporal dynamics of plaque growth and cellular development, phage infection resulted for all six phage-host pairs in an enhanced formation of aerial hyphae at the infection interface. An even more pronounced phenotype was observed when spotting high titers of phages on plates leading to massive cell lysis and enhanced cellular development at the spot interface (Fig. 1B). Scanning electron microscopy of *S. venezuelae* infected with Alderaan confirmed the formation of spores at the plaque interface, whereas the unaffected outskirts of the bacterial lawn showed mainly vegetative mycelium and only few spore chains under the tested conditions (Fig. 1C).

S. venezuelae development promotes the emergence of transient phage resistance

Since *S. venezuelae* is an established model system for studying cellular development, we focused on plaque growth and dynamics of phage Alderaan in the following.

In order to observe the developmental changes during phage infection, we set up a time series experiment and monitored plaque growth of *S. venezuelae* NRRL B-65442 wild type as well as mutants defective at different stages of development using stereo microscopy (Fig. 2). In the case of the wild-type strain, maximal plaque size was observed approximately 42 h post infection (1.78 mm^2 ± 0.51 mm^2). From 42 hours onwards, plaques were shrinking in size (48.3% reduced plaque area (± 7.1%)) suggesting the regrowth of transiently phage resistant mycelium followed by the erection of aerial hyphae (~66 h onwards; Fig. 2, Video S1).

To further assess the impact of cellular development on the containment of phage infection, we analyzed different *S. venezuelae* mutant strains defective at different stages of the development. These development mutants comprised the hypersporulating *S. venezuelae* strain Δ*bldD:: apr* (Tschowri et al. 2014) and strain Δ*bldN:: apr*, which is restricted to vegetative growth (Bibb et al. 2012). Further, we included the sporulation deficient strain Δ*whiB:: apr*, which is still capable of the formation of aerial hyphae, but is blocked in the formation of spores (Bush et al. 2016). On this strain, phage Alderaan formed significantly smaller plaques (0.98 mm^2 ± 0.49 mm^2), likely caused by accelerated formation of aerial hyphae at the plaque interface in comparison to the wild type. However, also strain Δ*whiB* showed significant regrowth into the lysis zone (55.7% ± 11.0%)—at even earlier time points. However, reduction in plaque area was slightly less pronounced (Fig. 2C). Overexpressing *whiB* led to an abolishment of the growing and shrinking and yielded consistently smaller plaques (Fig. S1). Remarkably, strain Δ*bldN*, which is restricted to vegetative growth, featured large, clear plaques (1.43 mm^2 ± 0.34 mm^2) and no significant reduction in plaque area (19.0% ± 11.9%) (Fig. 2C). In contrast, Alderaan formed significantly smaller plaques on the hypersporulating strain Δ*bldD* (maximum 0.97 mm^2 ± 0.24 mm^2). At later time points, plaques became turbid (zones of regrowth), but did not show significant regrowth from the periphery of the plaque into the lysis zone (Fig. 2A). This is in agreement with the reported phenotype of this mutant, which displays an accelerated formation of spores largely bypassing the formation of aerial hyphae (Tschowri et al. 2014). Complementation of *bldD* (strain SVNT11) restored the differentiation surrounding the plaque and the growing and shrinking characteristic comparable to the WT as well as it yielded clear plaques again (Fig. S1).

Based on this comparative analysis of mutants defective at different stages of development, it was tempting to speculate that the emergence of transiently phage-resistant mycelium would al-

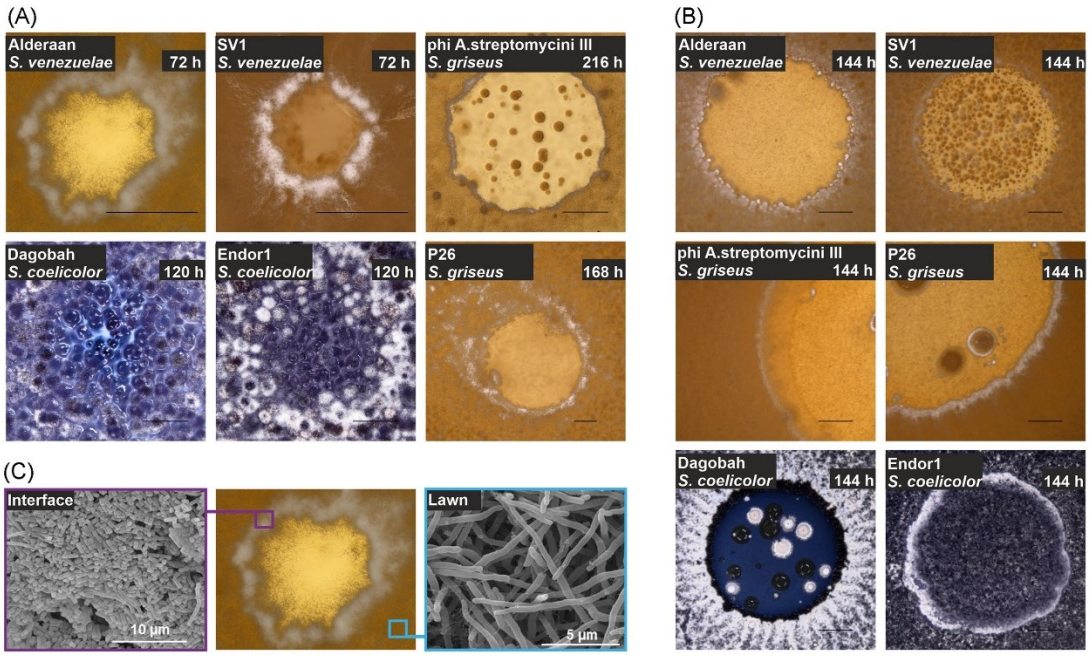

Figure 1. Phage infection leads to enhanced formation of aerial hyphae and spores at the plaque interface. (**A**) Stereo microscopy of representative plaques of the phages Alderaan and SV1 infecting *S. venezuelae*, phi A.streptomycini III and P26 infecting *S. griseus* and Dagobah and Endor1 infecting *S. coelicolor*. Scale bars represent 500 μm. (**B**) Stereo microscopy of spots of the six phage-host pairs. Scale bars represent 2 mm. (**C**) Scanning electron micrographs of samples from *S. venezuelae* infected by Alderaan taken from the plaque interface (purple) or lawn (cyan).

low regrowth into the lysis zone. To examine this premise, we sampled mycelium from the interface at different time points post infection. Infection with phage Alderaan of freshly inoculated cultures confirmed susceptibility to phage infection and is in line with the hypothesis of the formation of transiently phage-resistant mycelium at the infection interface (Fig. S2). Overall, these results indicate a critical role of *Streptomyces* development in containing phage infection and suggest that transition from vegetative mycelium to aerial hyphae (preserved in the wild-type and Δ*whiB* strain) as critical step.

Besides the classical development cycle, *S. venezuelae* can enter another type of growth referred to as the exploration phenotype. Exploration is characterized by the rapid spreading of explorer mycelium across surfaces and is triggered by glucose starvation or in the presence of fungal competitors (Jones et al. 2017). Yet the impact of phage predation on exploratory growth is unknown. Spotting of phage Alderaan onto explorer cells caused a clearance of the region followed by regrowth and enhanced sporulation (Fig. 3A, Video S2). Similarly, explorer cells developed into spores when encountering paper disks soaked with phages (Fig. 3B). This suggests that sporulation is a key strategy to contain phage outbreaks in both the canonical and exploratory lifestyles.

Fluorescent microscopy visualizes developmental patterns emerging upon phage infection

The analysis of plaque formation of phage Alderaan on *S. venezuelae* wild type and different development mutants revealed enhanced formation of aerial hyphae and spores at the plaque interface. To further analyze the spatiotemporal occurrence of developmental patterns post phage infection, we performed staining of single plaques and the surrounding tissue using the fluorescent dyes SYTO9 (green, stains nucleic acids in all cells) and propidium iodide (red, stains nucleic acids in cells with enhanced permeability). This stain is typically referred to as 'live/dead' staining, but it has to be kept in mind that the combination of these two stains allows for the visualization of differences in membrane permeability and membrane potential rather than for a strict discrimination between live and dead cells (Kirchhoff and Cypionka 2017). In the case of *S. venezuelae* wild type infected with Alderaan, a green ring emerged at the plaque interface after 36 h, indicative of differences in cellular development (Fig. 4). This observation is in line with the observed plaque shrinkage linked to the formation of aerial hyphae and spores at the infection interface (Figs. 1 and 2) and is further supported by previous studies showing that *Streptomyces* spores are impermeable to PI staining (Ladwig et al. 2015). This overall distinct pattern was not observed for the hypersporulating strain Δ*bldD* or the vegetatively growing strain Δ*bldN*. However, a faint pattern was also observed for the Δ*whiB* strain after 24 hours showing a higher level of SYTO9 staining at the plaque interface. This fits to the above-described observation that the Δ*whiB* strain featured an accelerated formation of aerial hyphae and a reduction in plaque area over the course of infection (Fig. 2C). Interestingly, *S. venezuelae* Δ*bldD* expressed complementary patches of PI and SYTO9 stained tissue in the lawn, but this pattern formation appeared to be independent of phage infection. Within the lysis zone of the plaque, we observed clusters of SYTO9 stained cells indicating faster regrowth of the hypersporulating Δ*bldD* strain in comparison to the wild

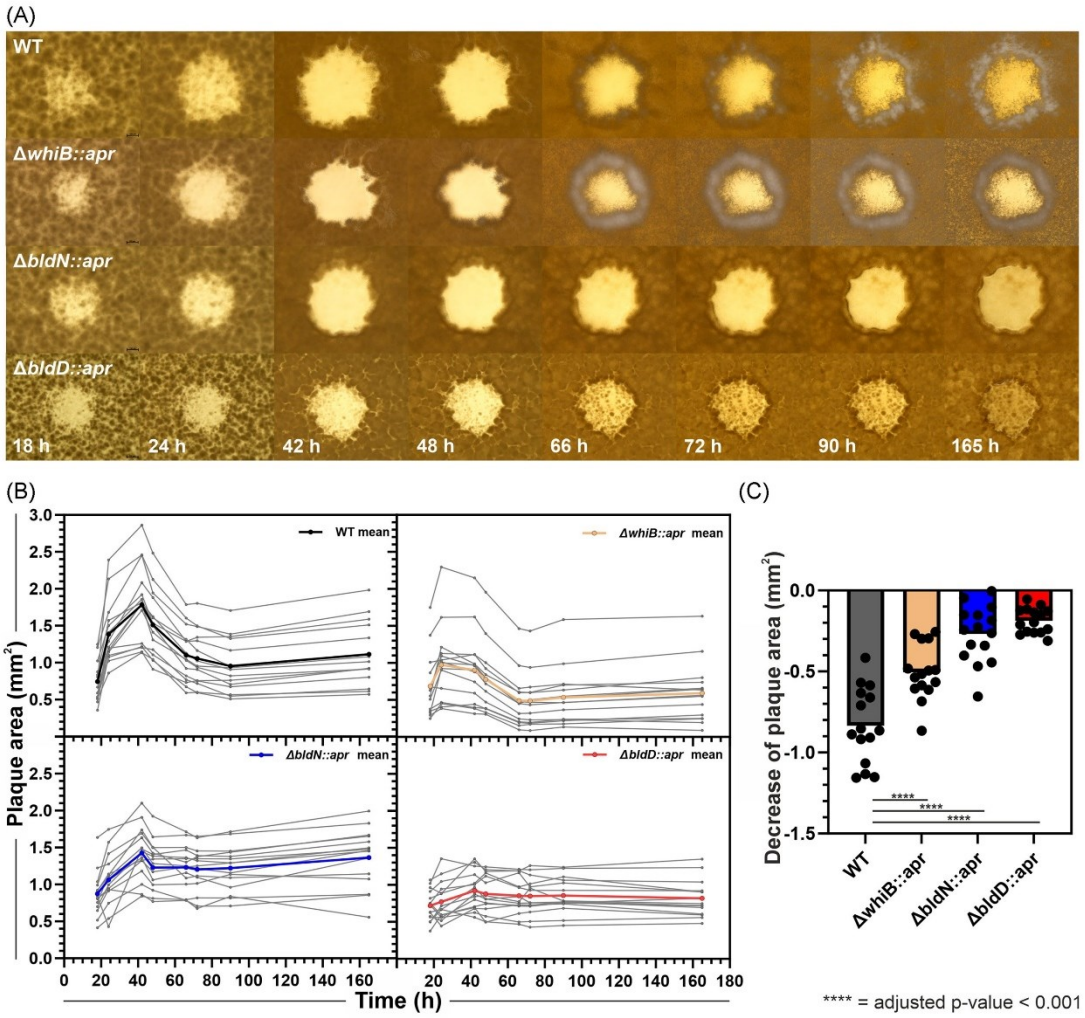

Figure 2. Plaque shrinkage in *S. venezuelae* relies on the formation of aerial hyphae and spores. Imaging and measuring of Alderaan plaques on *S. venezuelae* NRRL B-65442 WT and developmentally impaired strains *S. venezuelae* Δ*bldD*::apr, *S. venezuelae* Δ*bldN*::apr and *S. venezuelae* Δ*whiB*::apr over 165 h. (**A**) Stereo microscope images of a single representative plaque for each strain taken at different time points after infection. (**B**) Plaque area (mm^2) of 15 randomly chosen plaques per strain with calculated means shown in black (*S. venezuelae*), red (Δ*bldD*::apr), blue (Δ*bldN*::apr) and yellow (Δ*whiB*::apr). (**C**) Decrease of plaque area in mm^2 for each strain. Asterisks indicating significant differences (adjusted *P*-value < 0.001). Statistical analysis was performed as one-way ANOVA with Tukey's multiple comparison test in GraphPad Prism.

type, which is in agreement with the formation of turbid plaques (Fig. 2A).

Sporulation fosters the emergence of phage resistance

Analysis of Alderaan plaques revealed faster regrowth of the hypersporulating strain *S. venezuelae* Δ*bldD* within the plaque in comparison to wild-type lawns. Since *S. venezuelae* is able to complete its developmental cycle also in liquid culture, we set to examine whether infection of *S. venezuelae* with phage Alderaan in liquid cultures would follow a similar pattern. Infection at an initial titer of 10^8 PFU/ml resulted in a culture collapse of the wild type and all three developmentally impaired strains compared to uninfected controls (Fig. 5). Over the course of the experiment, pH values stayed constant between 7.0 and 7.5 for all strains, infected and uninfected. Interestingly, the hypersporulating strain Δ*bldD* showed reproducibly faster regrowth after 30–40 h upon phage infection (Fig. 5D). Regrowth was also observed for the wild-type strain in several experiments but at later time points and with a high variability in timing. Reinfection of strains recovered from the Δ*bldD* culture after 70 h (Fig. 5) revealed complete resistance to infection with phage Alderaan on plates (Fig. S3). Measurement of the phage titer over time showed the maximal titer at approximately 8 h post infection. However, regrowth of Δ*bldD* coincided with a significant drop in phage titer (Fig. 5D). Notably, using a lower initial phage titer of 10^7 PFU/ml resulted in an only very minor growth defect of the wild type but also showed faster regrowth of the Δ*bldD* strain in comparison to

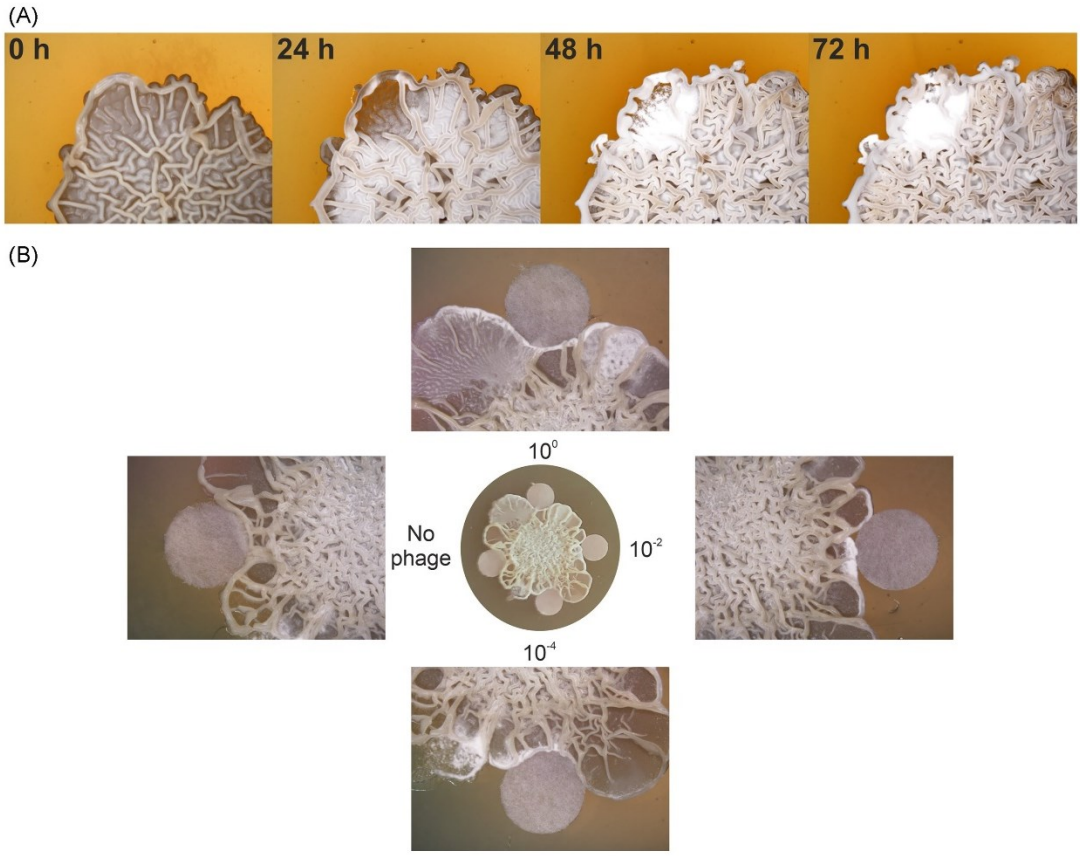

Figure 3. Sporulation of explorer cells in reaction to phage infection. (**A**) Stereo microscopy imaging of *S. venezuelae* explorer cells infected with phage Alderaan (after 6 days of exploration). (**B**) Explorer cells were imaged 3 days after contact with phage-soaked filter disks at indicated titers or soaked with phage buffer as control (no phage).

Δ*bldN* and Δ*whiB* (Fig. S4). These data suggested an overall lower susceptibility of the wild type, in particular evident at low phage titers.

In conclusion, enhanced sporulation seems to favour regrowth following culture collapse in liquid cultures. In accordance with the findings reported above, sporulation appears to be associated with decreased phage susceptibility and supports population expansion under phage challenge in *Streptomyces*.

Mature mycelium is less susceptible to phage infection

Regrowth of the plaque periphery (Fig. 2) and the emergence of aerial hyphae and sporulation at the plaque interface suggested an impact of the developmental stage on phage susceptibility. We further addressed this hypothesis by spotting phage Alderaan on *S. venezuelae* mycelium grown on agar overlay plates (0–24 h; Fig. 6A). Remarkably, all four strains were resistant to infections when grown for 24 h prior to spotting. At this stage, a mature and dense vegetative mycelium seems to significantly reduce phage susceptibility. Interestingly, a similar phenotype was already observed at 8 and 12 h post incubation in the case of *S. venezuelae* wild type and Δ*bldD*, but was delayed for Δ*bldN* and Δ*whiB*. Besides the significant reduction in phage titer, plaque sizes were smaller at later time points, which is probably the result of less susceptible host cells and constrained diffusion of phage particles (Fig. S5). Additionally, phage adsorption to non-growing spores in SM buffer and old mycelium grown for 24 h in liquid culture was impaired when compared to freshly germinating spores in medium (Fig. S6).

These results indicated an important impact of *Streptomyces* development on the emergence of phage-resistant phenotypes. However, quantification of the plaque phage load by qPCR (genome equivalents of Alderaan) and measurement of infectivity (PFU/mm^2) revealed also a significant reduction over time (Fig. 6B). This effect was most pronounced for the *S. venezuelae* wild-type strain showing a significant decrease in plaque load between 42 and 66 h. Taken together, these results emphasize the observed dynamics in plaque growth and shrinkage as a consequence of a reduced plaque load and the development of transiently phage-resistant mycelium.

Phage infection influences expression of developmental genes and biosynthetic gene clusters

To gain further insights into the processes underlying adaptation to phage infection, we performed an RNA-seq analysis of

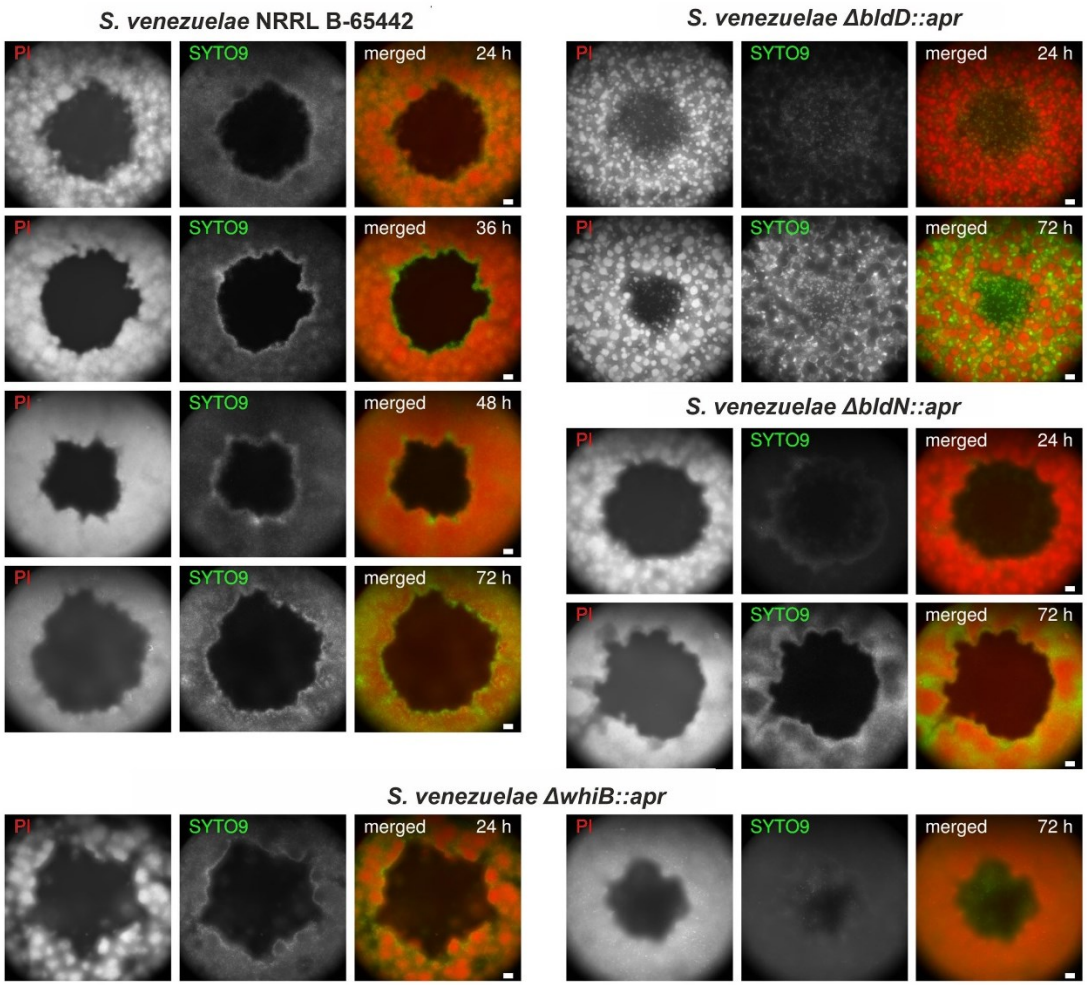

Figure 4. Analysis of Alderaan plaques on *S. venezuelae* indicates distinct developmental pattern formation in response to phage infection. Wide-field fluorescence microscopy of stained plaques and surrounding tissue of *S. venezuelae* wild type (WT) and different development mutants (Δ*bldD*, Δ*bldN* and Δ*whiB*). Representative images of three biological replicates are shown. Cells were stained with propidium iodide (PI, red) and SYTO9 (green). Both channels are shown separately in grey scales and as a merged image. Scale bars represent 100 μm.

infected mycelium from the plaque interface of the *S. venezuelae* wild type harvested 24 and 72 h after infection with Alderaan (Fig. 7A). A comprehensive overview of the obtained data for all *S. venezuelae* and Alderaan genes can be found in Supplementary Table S5. While we observed high levels of Alderaan gene expression at the 24 h time point, infection appeared to be fully contained at 72 h showing almost no detectable expression of Alderaan genes (Fig. 7B). In addition, the integrated prophage Chymera (KU958700.1) ranging from 3114820 to 3149561 bp of the *S. venezuelae* genome shows several differentially expressed genes including for example the site-specific integrase. However, general expression levels are low indicating no complete prophage induction (Fig. S7).

Of the more than 7000 *S. venezuelae* genes, 2483 and 1305 genes were significantly up- or downregulated during phage infection after 24 and 72 h, respectively (FDR *P*-value $\leq$ 0.05; Table S5, Sheet 2 and 3). At 24 h the most upregulated gene during infection of *S. venezuelae* encodes a lysine tRNA ($\log_2$-fold change 7.7). Interestingly, there are 26 additional tRNA genes upregulated at this time ranging from a $\log_2$-fold change of 4.5 to 1.3. This trend abolished at the later 72 h time point when phage infection was fully contained.

At the early stages of infection, several genes involved in *Streptomyces* development showed strong downregulation ($\log_2$-fold change between -1.2 and -5.4), including almost all *whi* genes, *bldM* and *bldO*, *ssgB*, *treZ*, *sigH* and *sigN*, *rdlA* and *rdlC* as well as three of the six *chaplin* genes (*chpBCF*) (Fig. 7C; Table S5, Sheet 4). This repression of genes involved in cellular development coincided with the high expression of phage genes observed at the 24 h time point. After 72 h, when cellular development was visible at the infection interface, *whi* genes were not differentially expressed anymore except for *whiD* and *whiE* genes still showing reduced expression levels. In contrast, several genes involved in the formation of aerial hyphae showed enhanced expression, including

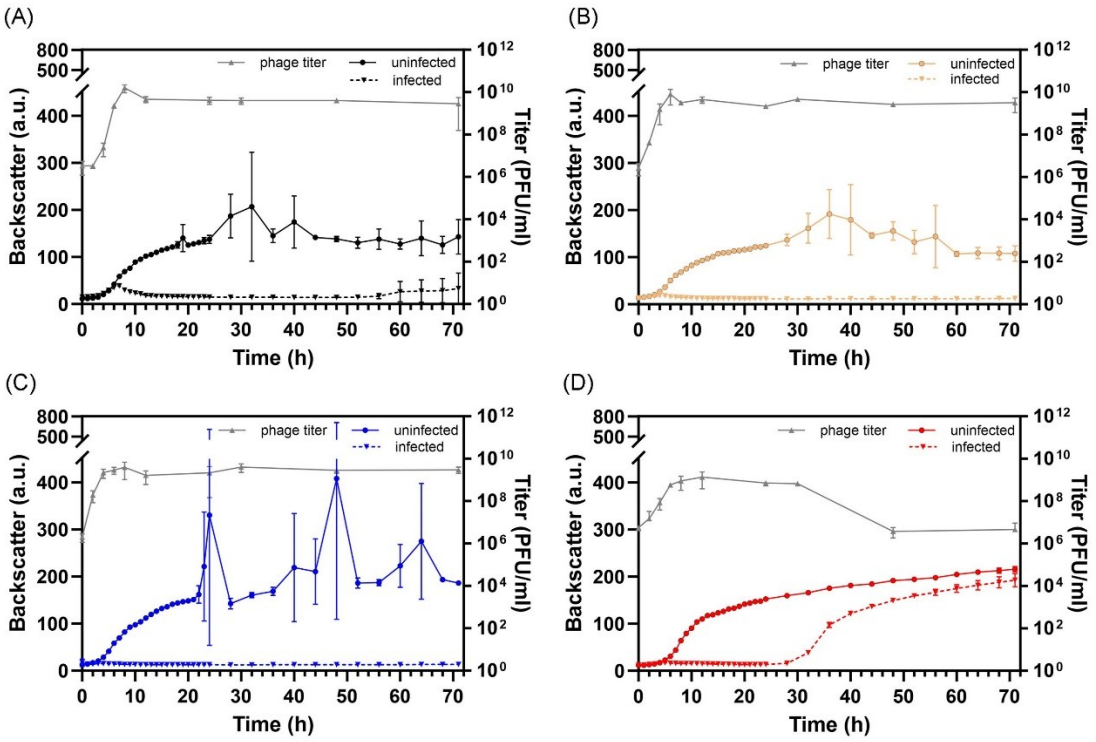

Figure 5. Enhanced sporulation of *S. venezuelae* Δ*bldD* enables the faster regrowth of phage-resistant cells. Infection of *S. venezuelae* WT (**A**) and different development mutants *S. venezuelae* Δ*whiB*::apr (**B**), Δ*bldN*::apr (**C**) and Δ*bldD*::apr (**D**) with Alderaan over 72 h in GYM medium. Strains were cultivated in 48-well microtiter plates (see material and methods) and infection was started with an initial titer of 10^8 PFU/ml (n = 3). Phage titer (PFU/ml, grey line+triangles) was determined by agar overlay assays (n = 3). An additional infection experiment with an initial titer of 10^7 PFU/ml is shown in Fig. S4.

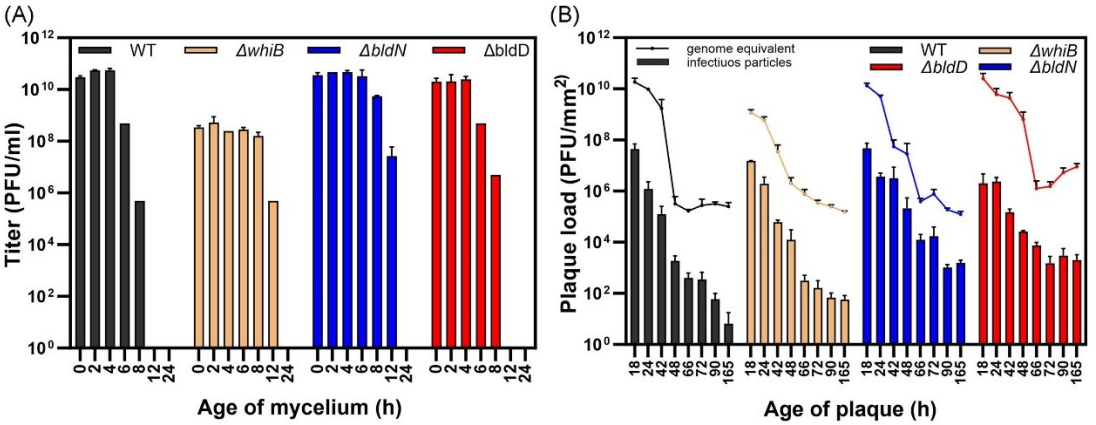

Figure 6. Mature mycelium is less susceptible to phage infection. (**A**) Spotting of phage Alderaan on lawns of *S. venezuelae* strains at different time points after plating (n = 2). (**B**) Determination of plaque load and infectivity of Alderaan particles from plaques as genome equivalents quantified by qPCR (line plot, n = 3) and infectious particles quantified by double agar overlay (bar plot, n = 3) in PFU/mm². See Fig. S5 for details on plaque morphology.

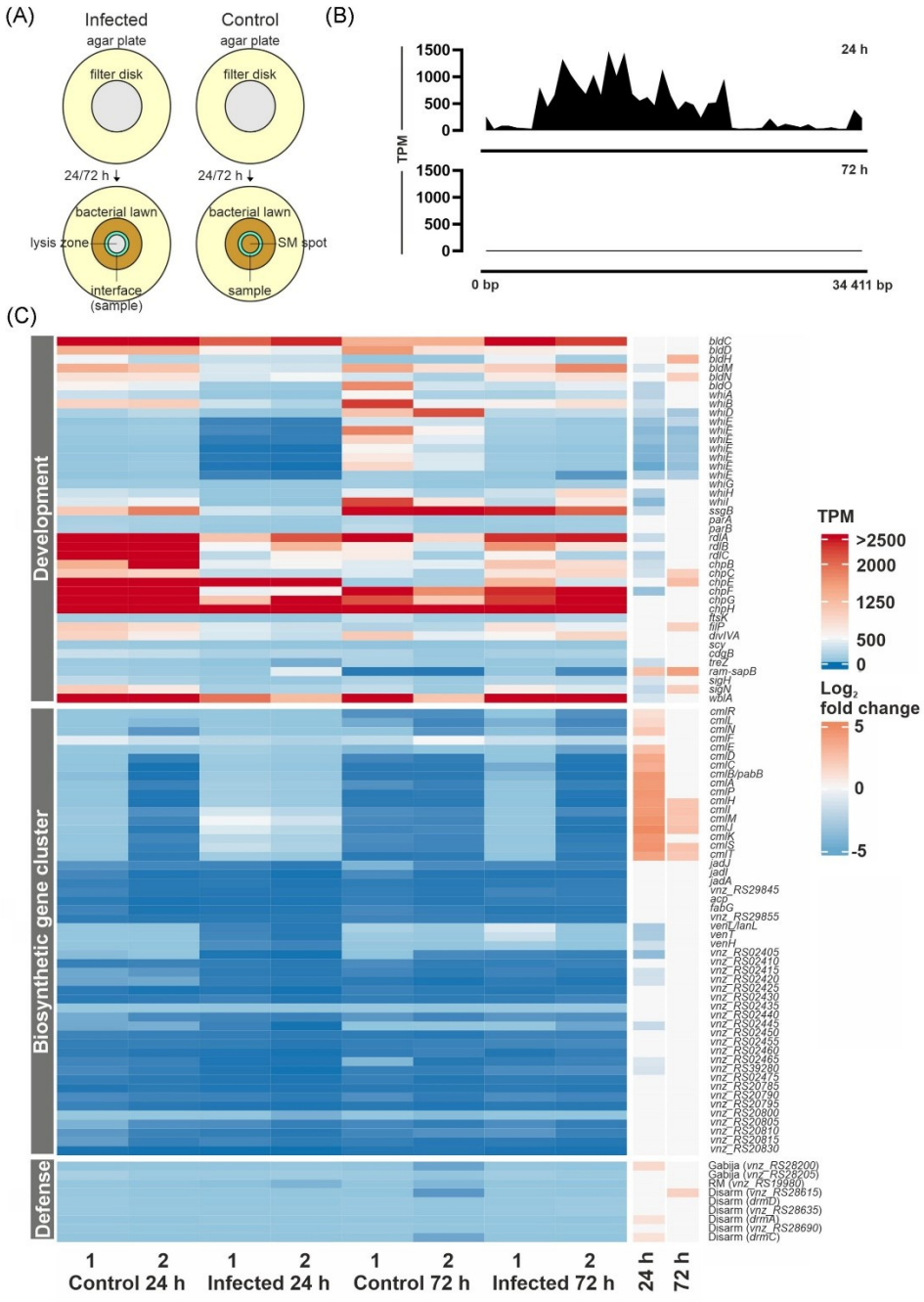

Figure 7. Global transcriptome analysis of *S. venezuelae* cells at the infection interface. (**A**) Sampling strategy of *S. venezuelae* lawns grown on filter disks and infected with Alderaan or spotted with SM buffer as control. Turquoise ring represents the sampling zone of cells at the infection interface, between lysis zone (grey) and bacterial lawn (brown). (**B**) Alderaan gene expression in transcripts per million (TPM) detected at different time points. (**C**) Heat map of selected genes involved in development, biosynthetic gene clusters and phage defense. Shown are expression levels in TPM ranging from 0 TPM (dark blue) to >2500 TPM (dark red) and data for two independent biological replicates ('control' or 'infected', 24 or 72 h). The $\log_2$ fold change calculated for infected vs control at the given time point is shown on the right, color-coded according to the legend ranging from blue (-5) to red (5). Empty boxes represent samples where differential gene expression was not significant (FDR *P*-value > 0.05).

sapB, *bldH*, *bldN*, *filP* and *sigN*. As targets of BldN, *chpC*, and *chpE* also featured increased expression at the infection interface after 72 h (Fig. 7C; Table S5, Sheet 4). These results provide important insights into the modulation of *Streptomyces* development during phage infection and suggest the repression of developmental processes during the early phase of infection. After 72 h, the containment of infection (no Alderaan transcripts), coincided with the enhanced expression of several genes involved in the formation of spore-bearing aerial hyphae.

Besides developmental processes affected by phage infection, genes from three of the five biosynthetic gene clusters in *S. venezuelae* featured differential expression during ongoing infection (24 h; Table S5, Sheet 5). Most importantly, 16 out of 17 genes from the chloramphenicol cluster are strongly upregulated during infection with Alderaan (Fig. 7C). Conversely, all three genes of the venezuelin gene cluster and six of 15 genes belonging to a cluster encoding five different compounds are downregulated (Table S5, Sheet 5). Jadomycin and gaburedin biosynthetic gene clusters are not influenced under the tested conditions. When testing for an effect of chloramphenicol on phage infection, Alderaan showed no decreased phage titer in the presence of different concentrations of the antibiotic (Fig. S8).

For detection of potential defense genes, DefenseFinder (https://defense-finder.mdmparis-lab.com/) (Abby et al. 2014, Tesson et al. 2022) and PADLOC (https://padloc.otago.ac.nz/padloc/) (Payne et al. 2021) were used to screen the *S. venezuelae* genome (NZ_CP018074) yielding a total of 19 genes belonging to eight different types of defense systems (Table S5, Sheet 6). Four of those genes belonging to three systems were detected by both tools (Fig. 7C). While all defense genes mostly have expression values in the low and middle two-digit range, except for *vnz_RS11150* encoding a dGTPase detected by PADLOC there is no system significantly and consistently up- or downregulated upon phage infection.

Discussion

In this study, we demonstrated the important impact of cellular development on the emergence of transient phage resistance as part of the antiviral strategies employed by *Streptomyces*. Analysis of plaque formation—as the hallmark of phage infection—displayed that after a period of steep growth in plaque area, transiently phage-resistant mycelium reconquered the lysis zone. This process was dependent on the onset of cellular development, in particular the formation of aerial hyphae, as illustrated by the analysis of mutants defective at different stages of development.

The last few years have witnessed an unprecedented expansion in our knowledge on bacterial immune systems with the discovery of many new systems, some of which are conserved from bacteria to humans (Tal and Sorek 2022, Wein and Sorek 2022). Besides the innate and adaptive immune systems acting at the cellular level, multicellular antiviral strategies including the secretion of antiviral molecules, release of membrane vesicles and biofilm structure represent an emerging scheme in antiviral defense of bacteria (Kronheim et al. 2018, Bond et al. 2021, Hardy, Kever and Frunzke 2022, Kever et al. 2022). In this study, we showed that *S. venezuelae* is able to reconquer the lysis zone upon the late stages of phage infection. This development of aerial hyphae and spores at the plaque interface was, in fact, observed for a variety of different phages infecting *Streptomyces* species (Fig. 1). Mutational analysis revealed that the characteristic growth and constriction of the plaque is most pronounced in the *S. venezuelae* wild-type strain capable of full development. Interestingly, the observed phenotype is reminiscent of the plaque dynamics observed for phages SPP1 and Phi29 infecting *Bacillus subtilis*. There, the phenomenon of plaque constriction was attributed to a response modulated by the ECF sigma factor SigX leading to alterations of the modification of wall teichoic acids thereby interfering with phage attachment (Tzipilevich et al. 2022).

Further studies point towards the underappreciated prevalence of mechanisms involved in the generation of transient phage resistance. Those include the modification of capsule components in *Klebsiella* (Hesse et al. 2020), the O-antigen length in *Salmonella* (Cota et al. 2015), or the shedding of cell wall components, which was recently shown to render *Streptomyces*, *E. coli*, and *B. subtilis* transiently resistant to phage infection in osmoprotective environments (Fabijan et al. 2021, Ongenae, Briegel and Claessen 2021, Ongenae et al. 2022).

These studies add an additional layer of complexity to the general assumption that plaque growth is mainly constrained by the entry of bacterial cells into the stationary phase (Abedon and Yin 2009). When defining size and kinetics of a plaque, diffusivity, burst size, adsorption rate, and latent period are important phage-related parameters to consider (Abedon and Yin 2009, Gallet, Kannoly and Wang 2011, Abedon 2018). As shown in our study, Alderaan infecting *S. venezuelae* formed significantly smaller plaques on older mycelium probably due to reduced diffusivity in dense mycelial structures.

Differentiation from vegetative mycelium to aerial hyphae and spores also comes with changes in the cell surface including the formation of a hydrophobic rodlet structure (Claessen et al. 2004, Yang et al. 2017) as well as compositional changes and thickening of the spore envelope (Bradley and Ritzi 1968, Sexton and Tocheva 2020) thus influencing phage adsorption as shown here. This is underlined by the ability of fungal mycelium to retain phages and reduce the PFU as well as mass yields correlating with hydrophobicity (Ghanem et al. 2019). Studies on phage-host interactions in *E. coli* biofilms also conclude that reduced diffusivity and cell surface protection are key strategies in spatially constrained environments, although these phages can remain infectious and act as an additional layer of protection against incoming competitors (Vidakovic et al. 2018, Bond et al. 2021). In addition, spores being by definition metabolically inactive, productive phage infection can only occur upon germination as it was for example shown for endospores of *B. subtilis* where infection and lysis halted during the spore phase (Gabiatti et al. 2018).

Following a typical parasitic behavior, phages also manipulate cellular development to promote their own distribution through spores, as it was observed for example with the *B. subtilis* prophage SPβ regulating sporulation (Abe et al. 2014). This is further supported by the ubiquitous distribution of phage-encoded sporulation-specific sigma factors with a proposed role in altering bacterial dormancy (Schwartz, Lehmkuhl and Lennon 2022). In this study, transcriptome analysis revealed the repression of *S. venezuelae* developmental genes in the early stages of active Alderaan infection suggesting phage-driven measures enhancing propagation. While sporulation-specific sigma factors are ubiquitously found in Firmicutes, WhiB-like transcriptional regulators are prevalent in the genomes of actinobacteriophages including phage Alderaan (Sharma et al. 2021). WhiB-like regulators have been shown by various studies to play diverse roles in controlling cellular development, oxidative stress response, production of secondary metabolites and cell division (Bush 2018). It is therefore tempting to assume that phages infecting bacteria undergoing cellular development are equipped with diverse measures to

modulate development promoting phage propagation and distribution.

Recent studies revealed that secondary metabolites of the class of anthracyclines and aminoglycoside antibiotics, produced by *Streptomyces*, provide protection against phage infection (Kronheim et al. 2018, Hardy, Kever and Frunzke 2022, Kever et al. 2022). Besides first phenomenological evidence for the phage-triggered induction of actinorhodin production (Hardy et al. 2020), the effect of phage infection on the activation of biosynthetic gene clusters has not yet been investigated. In our study, transcriptome analysis revealed an induction of the chloramphenicol gene cluster upon Alderaan infection. A direct antiphage effect of chloramphenicol was not observed under the tested lab conditions. However, interaction in natural microbial communities are multi-layered and the production of antibiotics affecting translation might suppress immune adaptation of host populations (Chevallereau et al. 2020). In this context, a recent study provides evidence for a role of antibiotics inhibiting protein synthesis in the prevention of phage amplification by interfering with the production of counter-defences, such as the synthesis of anti-CRISPR proteins (Pons et al. 2022).

In conclusion, our study emphasizes the importance of cellular development for the emergence of transient phage resistance during multicellular development of *Streptomyces*. These results suggest that phage infection in multicellular bacterial assemblies is sensed and triggers the establishment of a resistance response—here the formation of aerial hyphae and spores—with an important role for the containment of infections. It remains subject of further investigations, whether this transient resistance might accelerate the acquisition of genetic resistance towards phage infection, as described for phenotypic tolerance to antibiotics facilitating the evolution of resistance (Liu et al. 2020).

Material and methods

Bacteria, phages and growth conditions

Tables S1 and S2 list all bacteriophages and bacterial strains used in this study, respectively. For liquid cultivation of wild type strains, spore stocks were used for inoculation whereas developmental mutant strains were inoculated from mycelial stocks. Cultivation was performed in GYM medium (per liter: 4 g glucose, 4 g yeast extract, 10 g malt extract, pH = 7.3) at 30°C and 170 rpm. *S. coelicolor* was cultivated in YEME medium (per liter: 3 g yeast extract, 3 g malt extract, 5 g peptone, 10 g glucose, 340 g sucrose). For growth of mutant strains in the absence of phages, apramycin was added to precultures at a concentration of 10 μg/ml. For solid growth medium, GYM agar was used for all strains and experiments (GYM medium plus 2 g $CaCO_3$ per liter, 1.5% agar). Triggering exploration phenotypes was achieved by using YP agar (per liter: 10 g yeast extract, 20 g peptone, 1.5% agar) supplemented with 10 mM $MgCl_2$ and 10 mM $CaCl_2$ to support phage amplification. *Escherichia coli* strains DH5α and ET12567/pUZ8002 were cultivated in LB medium supplemented with the respective antibiotics during cloning.

Plasmid construction and cloning

Details concerning plasmids and oligonucleotides used for constructing plasmids pIJ10257_*whiB*$_{Sven}$ and pSVNT-3 are listed in Tables S3 and S4, respectively. PCR amplification and restriction digestion were performed as described in standard protocols (Sambrook and Russel 2001). Plasmid construction was done using Gibson assembly (Gibson 2011). Synthesis of oligonucleotides and sequencing were performed by Eurofins Genomics (Ebersberg, Germany). Transfer of plasmids into *Streptomyces spp.* was done using conjugation through the *E. coli* ET12567/pUZ8002 strain (MacNeil et al. 1992).

Phage infection on solid media

Double agar overlays were performed using GYM soft agar without $CaCO_3$ and only 0.4% agar for the top layer. Quantification of infectious phage particles was performed by spotting 2 μl of phage dilutions in SM buffer (0.1 M NaCl, 8 mM $MgSO_4$, 50 mM Tris-HCl, pH 7.5) onto a double agar overlay inoculated with the respective *Streptomyces* species at an initial OD_{450} of 0.4 from overnight cultures or directly mixing 100 μl of the phage solution into the inoculated soft agar before plating.

For re-infecting experiments, mycelium was harvested after different time points from plaque interface. Triplicates from individual plaques per strain at each time point were picked using a sterile loop and incubated for 24 h at 30°C and 900 rpm in 1 ml of fresh medium. About 250 μl of these cultures were used for a double agar overlay and spotting of phage dilutions.

Testing of phage susceptibility to chloramphenicol was performed as described previously (Kever et al. 2022). In this case, GYM agar for bottom and top layers were supplemented with 0, 10, 50, 100, or 200 μg/ml chloramphenicol when used for spotting of Alderaan dilutions.

Infection in liquid cultures

Infection of liquid cultures was performed in the BioLector microcultivation system (Beckman Coulter, US) (Kensy et al. 2009). Overnight cultures were adjusted to an OD_{450} of 0.15 and centrifuged for 5 min at 5000 x *g*, the supernatant was discarded and the pellet resuspended in 1/10 of the initial volume. Phages were added to a final titer of 10^8 PFU/ml and SM buffer was used for uninfected controls. After 10 minutes of incubation at room temperature, free phages were removed by centrifugation for 5 min at 5000 × *g* and discarding the supernatant. The pellet was resuspended in the initial volume of GYM medium. For cultivation, biological triplicates were incubated at 30°C and 1200 rpm in FlowerPlates (Beckman Coulter, US). The backscattered light intensity was measured in 15 minutes intervals with a wavelength of 620 nm (gain of 25). For determination of phage titer over the course of infection, supernatants were sampled at indicated time points and subsequently spotted on double agar overlays as described above.

Imaging and measuring of plaques

Stereo microscopy was performed using the SMZ-18 stereomicroscope (Nikon, Japan) equipped with a P2-SHR Plan Apo 1x N.A. objective (Nikon, Japan), a P2-DBL LED plain base (Nikon, Japan) and a DS-Fi3 digital microscope camera (Nikon, Japan). The H301-MINI temperature-controlled chamber (Okolab, Italy) and UNO-STAGE-TOP-INCUBATOR (Okolab, Italy) were used for incubation at 30°C during live-imaging. Image and video processing and measuring of plaque sizes was done using the NIS-Elements AR v.5.30.03 (Nikon, Japan).

Electron microscopy

To visualize the mycelial differentiation at the infection interface in comparison to the uninfected lawn, double agar overlays were conducted as described in 'Phage infection on solid media'. After 72 h post infection, agar plates were overlaid with 4 ml B2 buffer (87 mM $Na_2HPO_4 \times 2H_2O$, 13 mM NaH_2PO_4 x H_2O, pH 7.4) contain-

ing 3% glutaraldehyde and incubated for 1 h at RT, before storing at 4°C until imaging. Microscopic analysis was conducted in the facility for electron microscopy (EME, institute for pathology) at the Universitätsklinikum Aachen (Germany).

Fluorescence microscopy of plaques

After infection on solid medium three single plaques were randomly selected for each strain and time point and were cut out of the agar as small blocks. Neutral buffered formalin 10% (v/v) in 1x PBS (137 mM NaCl, 2.7 mM KCl, 10 mM Na_2HPO_4, 2 mM K_2HPO_4) was used for fixation of the plaques by incubation for 12–18 h. Afterwards plaques were washed three times in 1x PBS and stored at 4°C until microscopy. Live-dead staining was performed directly before imaging with 5 µl 1:2 dilution of the staining mix containing propidium iodide and SYTO9 (LIVE/DEAD™ *Bac*Light™ Bacterial Viability Kit, Invitrogen) placed directly onto the plaque and incubated for 5 min at room temperature in the dark.

Epifluorescence microscopy was applied at an inverted Nikon Eclipse Ti microscope system (Nikon instruments, Japan) equipped with a Nikon S Fluor 10x DIC N1 dry objective lens and a Hammamatsu Orca Flash 4.0 (Hammamatsu Photonics, Japan). Stained samples were imaged face down and half submerged in water in a 35 mm glass Bottom µ-Dish (Ibidi, Germany). To measure the SYTO™ compound of the BacLight™ stain, a Nikon GFPHQ Filterset (Ex 470/40 DM 495LP Em 525/50) was utilized with 30 ms exposure time and a Nikon INTENSILIGHT C-HGFIE as light source, while for the corresponding propidium iodide signal a Nikon TXRed HYQ filterset (Ex 560/55 DM 595LP Em 645/75) was used with 7 ms exposure time. Z-Stacks of the full sample were acquired for all channels at a step size of 1 µm. Subsequently, maximum intensity projections were generated within a local omero image database installation, which was used to generate figures of microscopic measurements as well.

Plaque load determination

Quantification of phage particles per plaque over time was performed using qPCR and determination of PFU/mm^2 using double agar ovelay assay as described above. Infection was done as described in 'Phage infection on solid media' on GYM agar. For each time point, three plaques were imaged and measured as described in 'Imaging of plaques' and cut out as small agar blocks. The plaques were submerged in SM buffer for 2 h at 500 rpm and room temperature before centrifugation for 20 min at 8000 x g. The supernatant was stored at 4°C until further use. For qPCR, 1 µl of the supernatant was mixed with 10 µl 2x Universal qPCR Master Mix (New England Biolabs, USA) and 1 µl of each primer targeting the minor tail gene (Alderaan_HQ601_00028_fw: CTCGGCTATCCGATCATCC; Alderaan_HQ601_00028_rev: TTGG TTGCGGTTGATGGAC; final conc. 0.5 µM) in a final volume of 20 µl with dd. H_2O. Reactions were conducted in the qTower 2.2 (Analytik Jena, Germany) in duplicates with phage lysate dilutions as standards. The resulting concentrations were used to calculate the plaque load as genome equivalents in PFU/mm^2 using the initial volume of SM buffer and the measured plaque size.

Quantification of plaque load as infectious particles in PFU/mm^2 was performed as described in 'Phage infection on solid medium' on *S. venezuelae* NRRL B-65442 with the herein supernatant as input phage solution.

Transcriptome analysis

For transcriptomic analyses of *S. venezuelae* NRRL B-65442, 1 ml of an overnight culture adjusted to an OD_{450} of 2 was transferred onto a nylon membrane filter (0.45 µm pore size, diameter 47 mm, Cytiva, USA) placed on a GYM agar plate. After air-drying, 10 µl Alderaan phage stock (10^{10} PFU/ml) or SM buffer as control were spotted in the middle of the filter. Incubation was performed at 30°C for 24 h or 72 h. Mycelial material from the edge of formed spots was scraped from the filter and ground up under liquid nitrogen. RNA purification was done using the Monarch Total RNA Miniprep Kit (New England Biolabs, USA). Depletion of rRNA, library preparation and sequencing were conducted by GENEWIZ (Germany).

Analysis of sequencing results was performed using CLC genomics workbench v.20 (Qiagen, Germany). First, quality control of the reads was conducted and subsequent trimming for adapter sequences and low-quality reads (0.05) as well as ambiguous nucleotides was performed. As references, *S. venezuelae* NRRL B-65442 (NZ_CP018074.1) and Alderaan (MT711975.1) genomes were used for read mapping. Transcripts per million (TPM) were calculated with the 'RNA-seq Analysis' tool of CLC genomics workbench (mismatch cost 2; insertion cost 3; deletion cost 3; length fraction 0.9; similarity fraction 0.9; strand specificity both; maximum number of hits for a read 10). Determination of differentially expressed genes was done using the 'Differential Expression in Two Groups' tool in CLC combining duplicates for comparing infected and uninfected samples at 24 and 72 h separately with an FDR *P*-value of ≤ 0.05. A heatmap presenting the TPM annotated with differential expression values was constructed in R using the ComplexHeatmap package (Gu, Eils and Schlesner 2016).

Author contributions

Conceptualization: TL, JF | Data curation: TL, SH | Formal analysis: all | Funding acquisition: JF | Investigation: TL, LK, SH, AH | Methodology: all | Project administration: JF | Resources: SW-P, JF | Supervision: JF | Validation: all | Visualization: TL, JF | Writing—original draft: TL, JF | Writing—review and editing: all

Funding

We thank the European Research Council (ERC Starting Grant 757563) and the Deutsche Forschungsgemeinschaft (SPP 2330, project 464434020) for financial support. Research in Natalia Tschowri's lab is funded by the ERC Starting Grant (101039556) and the DFG Priority Programme SPP 1879 (TS 325/2–2) and SPP 2389 (TS 325/4–1). We would like to acknowledge the Center for Advanced Imaging (CAi) at Heinrich-Heine-University Düsseldorf for support and for providing access to the Nikon Eclipse Ti system as well as Eva Miriam Buhl at the facility for electron microscopy, Universitätsklinikum Aaachen. For phages P26 and phi A.streptomycini III we thank Johannes Wittmann at the German Collection of Microorganisms and Cell Cultures (DSMZ, Braunschweig).

Supplementary data

Supplementary data are available at *FEMSML* online.

Conflict of interest statement. The authors declare no conflict of interest.

Data availability

The RNA-sequencing data discussed in this publication have been deposited in NCBI's Gene Expression Omnibus (Edgar, Domrachev and Lash 2002) under the accession number GSE213718.

References

Abby SS, Néron B, Ménager H *et al.* MacSyFinder: a program to mine genomes for molecular systems with an application to CRISPR-cas systems. *PLoS One* 2014;**9**:e110726.

Abe K, Kawano Y, Iwamoto K *et al.* Developmentally-regulated excision of the spβ prophage reconstitutes a gene required for spore envelope maturation in *Bacillus subtilis*. *PLos Genet* 2014;**10**:e1004636.

Abedon ST. Detection of bacteriophages: phage plaques. In: Harper David R., Abedon STand BBH and MML(ed), *Bacteriophages: Biology, Technology, Therapy*. Cham: Springer International Publishing, 2018,1–32.

Abedon ST, Yin J. Bacteriophage plaques: theory and analysis. *Methods Mol Biol*. 2009;**501**. United States, 161–74.

Barka EA, Vatsa P, Sanchez L *et al.* Taxonomy, physiology, and natural products of actinobacteria. *Microbiol Mol Biol Rev* 2016;**80**:1–43.

van Bergeijk DA, Terlouw BR, Medema MH *et al.* Ecology and genomics of actinobacteria: new concepts for natural product discovery. *Nat Rev Microbiol* 2020;**18**:546–58.

Bibb MJ, Domonkos A, Chandra G *et al.* Expression of the chaplin and rodlin hydrophobic sheath proteins in *Streptomyces venezuelae* is controlled by σ(BldN) and a cognate anti-sigma factor, RsbN. *Mol Microbiol* 2012;**84**:1033–49.

Bond MC, Vidakovic L, Singh PK *et al.* Matrix-trapped viruses can prevent invasion of bacterial biofilms by colonizing cells. *Elife* 2021;**10**, doi: 10.7554/eLife.65355.

Bradley SG, Ritzi D. Composition and ultrastructure of *Streptomyces venezuelae*. *J Bacteriol* 1968;**95**:2358–64.

Bush MJ. The actinobacterial WhiB-like (Wbl) family of transcription factors. *Mol Microbiol* 2018;**110**:663–76.

Bush MJ, Bibb MJ, Chandra G *et al.* Genes required for aerial growth, cell division, and chromosome segregation are targets of WhiA before sporulation in *Streptomyces venezuelae*. *MBio* 2013;**4**:e00684–13.

Bush MJ, Chandra G, Bibb MJ *et al.* Genome-wide chromatin immunoprecipitation sequencing analysis shows that WhiB is a transcription factor that cocontrols its regulon with WhiA to initiate developmental cell division in Streptomyces. *MBio* 2016;**7**:e00523–16.

Bush MJ, Tschowri N, Schlimpert S *et al.* c-di-GMP signalling and the regulation of developmental transitions in Streptomycetes. *Nat Rev Microbiol* 2015;**13**:749–60.

Chater KF. Recent advances in understanding Streptomyces. *F1000Research* 2016;**5**:2795.

Chevallereau A, Meaden S, Fradet O *et al.* Exploitation of the cooperative behaviors of anti-CRISPR phages. *Cell Host & Microbe* 2020;**27**:189–198.e6.

Chevallereau A, Pons BJ, van Houte S *et al.* Interactions between bacterial and phage communities in natural environments. *Nat Rev Microbiol* 2022;**20**:49–62, doi: 10.1038/s41579-021-00602-y.

Claessen D, Stokroos I, Deelstra HJ *et al.* The formation of the rodlet layer of Streptomycetes is the result of the interplay between rodlins and chaplins. *Mol Microbiol* 2004;**53**:433–43.

Clokie MR, Millard AD, Letarov A V *et al.* Phages in nature. *Bacteriophage* 2011;**1**:31–45.

Cota I, Sánchez-Romero MA, Hernández SB *et al.* Epigenetic control of Salmonella enterica O-antigen chain length: a trade-off between virulence and bacteriophage resistance. *PLos Genet* 2015;**11**:e1005667.

Demain AL. Pharmaceutically active secondary metabolites of microorganisms. *Appl Microbiol Biotechnol* 1999;**52**:455–63.

Edgar R, Domrachev M, Lash AE. Gene Expression Omnibus: NCBI gene expression and hybridization array data repository. *Nucleic Acids Res* 2002;**30**:207–10.

Elliot MA, Talbot NJ. Building filaments in the air: aerial morphogenesis in bacteria and fungi. *Curr Opin Microbiol* 2004;**7**:594–601.

Fabijan AP, Kamruzzaman M, Martinez-Martin D *et al.* L-form switching confers antibiotic, phage and stress tolerance in pathogenic *Escherichia coli*. *Biorxiv* 2021, doi: 10.1101/2021.06.21.449206. bioRxiv

Fierer N. Embracing the unknown: disentangling the complexities of the soil microbiome. *Nat Rev Microbiol* 2017;**15**:579–90.

Flärdh K. Cell polarity and the control of apical growth in Streptomyces. *Curr Opin Microbiol* 2010;**13**:758–65.

Flärdh K, Buttner MJ. Streptomyces morphogenetics: dissecting differentiation in a filamentous bacterium. *Nat Rev Microbiol* 2009;**7**:36–49.

Gabiatti N, Yu P, Mathieu J *et al.* Bacterial endospores as phage genome carriers and protective shells. *Appl Environ Microbiol* 2018;**84**, doi: 10.1128/AEM.01186-18.

Gallet R, Kannoly S, Wang I-N. Effects of bacteriophage traits on plaque formation. *BMC Microbiol* 2011;**11**:181.

Ghanem N, Stanley CE, Harms H *et al.* Mycelial effects on phage retention during transport in a microfluidic platform. *Environ Sci Technol* 2019;**53**:11755–63.

Gibson DG. Enzymatic assembly of overlapping DNA fragments. *Methods Enzymol* 2011;**498**:349–61.

Gu Z, Eils R, Schlesner M. Complex heatmaps reveal patterns and correlations in multidimensional genomic data. *Bioinformatics* 2016;**32**:2847–9.

Hardy A, Kever L, Frunzke J. Antiphage small molecules produced by bacteria – beyond protein-mediated defenses. *Trends Microbiol* **31**:92–106, 2023, doi: 10.1016/j.tim.2022.08.001.

Hardy A, Sharma V, Kever L *et al.* Genome sequence and characterization of five bacteriophages infecting *Streptomyces coelicolor* and *Streptomyces venezuelae*: Alderaan, Coruscant, Dagobah, Endor1 and Endor2. *Viruses* 2020;**12**:1065.

Hatfull GF. Actinobacteriophages: genomics, dynamics, and applications. *Ann Rev Virol* 2020;**7**:37–61.

Hesse S, Rajaure M, Wall E *et al.* Phage resistance in multidrug-resistant *Klebsiella pneumoniae* ST258 evolves via diverse mutations that culminate in impaired adsorption. *MBio* 2020;**11**, doi: 10.1128/mBio.02530-19.

Jones SE, Ho L, Rees CA *et al.* Streptomyces exploration is triggered by fungal interactions and volatile signals. *Elife* 2017;**6**, doi: 10.7554/eLife.21738.

Kensy F, Zang E, Faulhammer C *et al.* Validation of a high-throughput fermentation system based on online monitoring of biomass and fluorescence in continuously shaken microtiter plates. *Microb Cell Fact* 2009;**8**:31.

Kever L, Hardy A, Luthe T *et al.* Aminoglycoside antibiotics inhibit phage infection by blocking an early step of the infection cycle. *MBio* 2022;**13**:e0078322.

Kirchhoff C, Cypionka H. Propidium ion enters viable cells with high membrane potential during live-dead staining. *J Microbiol Methods* 2017;**142**:79–82.

Kronheim S, Daniel-Ivad M, Duan Z *et al.* A chemical defence against phage infection. *Nature* 2018;**564**:283–6.

Ladwig N, Franz-Wachtel M, Hezel F *et al.* Control of morphological differentiation of *Streptomyces coelicolor* A3(2) by phosphorylation of MreC and PBP2. *PLoS One* 2015;**10**:e0125425.

Liu J, Gefen O, Ronin I *et al.* Effect of tolerance on the evolution of antibiotic resistance under drug combinations. *Science* 2020;**367**:200–4.

MacNeil DJ, Gewain KM, Ruby CL *et al.* Analysis of *Streptomyces avermitilis* genes required for Avermectin biosynthesis utilizing a novel integration vector. *Gene* 1992;**111**:61–68.

Manteca A, Claessen D, Lopez-Iglesias C *et al.* Aerial hyphae in surface cultures of *Streptomyces lividans* and *Streptomyces coelicolor* originate from viable segments surviving an early programmed cell death event. *FEMS Microbiol Lett* 2007;**274**: 118–25.

Manteca A, Fernandez M, Sanchez J. Cytological and biochemical evidence for an early cell dismantling event in surface cultures of *Streptomyces antibioticus*. *Res Microbiol* 2006;**157**:143–52.

McCormick JR, Flärdh K. Signals and regulators that govern Streptomyces development. *FEMS Microbiol Rev* 2012;**36**:206–31.

Miguélez EM, Hardisson C, Manzanal MB. Hyphal death during colony development in *Streptomyces antibioticus*: morphological evidence for the existence of a process of cell deletion in a multicellular prokaryote. *J Cell Biol* 1999;**145**:515–25.

Ongenae V, Briegel A, Claessen D. Cell wall deficiency as an escape mechanism from phage infection. *Open Biology* 2021;**11**: 210199.

Ongenae V, Mabrouk AS, Crooijmans M *et al.* Reversible bacteriophage resistance by shedding the bacterial cell wall. *Open Biology* 2022;**12**:210379.

Payne LJ, Todeschini TC, Wu Y *et al.* Identification and classification of antiviral defence systems in bacteria and archaea with PADLOC reveals new system types. *Nucleic Acids Res* 2021;**49**: 10868–78.

Pons BJ, Dimitriu T, Westra ER *et al.* Antibiotics that affect translation can antagonize phage infectivity by interfering with the deployment of counter-defences. *Biorxiv* 2022, doi: 10.1101/2022.09.07.506948. bioRxiv

Rigali S, Titgemeyer F, Barends S *et al.* Feast or famine: the global regulator DasR links nutrient stress to antibiotic production by Streptomyces. *EMBO Rep* 2008;**9**:670–5.

Rodriguez-R LM, Gunturu S, Tiedje JM *et al.*Nonpareil 3: fast estimation of metagenomic coverage and sequence diversity. *Msystems* 2018;**3**, doi: 10.1128/mSystems.00039-18.

Sambrook J, Russel D. *Molecular Cloning: a laboratory Manual*. 3rd ed. *Cold Spring Harbor*. Cold Spring Harbor, New York: Cold Spring Harbor Laboratory Press, 2001.

Schwartz DA, Lehmkuhl BK, Lennon JT. Phage-encoded Sigma factors alter bacterial dormancy. *Msphere* 2022;**7**:e0029722.

Sexton DL, Tocheva EI. Ultrastructure of exospore formation in streptomyces revealed by cryo-electron tomography. *Front Microbiol* 2020;**11**:581135.

Sharma V, Hardy A, Luthe T *et al.* Phylogenetic distribution of WhiB- and Lsr2-type regulators in actinobacteriophage genomes. *Microbiol Spectr* 2021;**9**:e0072721.

Sigle S, Ladwig N, Wohlleben W *et al.* Synthesis of the spore envelope in the developmental life cycle of *Streptomyces coelicolor*. *Int J Med Microbiol* 2015;**305**:183–9.

Tal N, Sorek R. SnapShot: bacterial immunity. *Cell* 2022;**185**:578–578.e1. e1.

Tenconi E, Traxler MF, Hoebreck C *et al.* Production of prodiginines is part of a programmed cell death process in Streptomyces coelicolor. *Front Microbiol* 2018;**9**:1742.

Tesson F, Hervé A, Mordret E *et al.* Systematic and quantitative view of the antiviral arsenal of prokaryotes. *Nat Commun* 2022;**13**:2561.

Thompson LR, Sanders JG, McDonald D *et al.* A communal catalogue reveals Earth's multiscale microbial diversity. *Nature* 2017;**551**:457–63.

Tschowri N, Schumacher MA, Schlimpert S *et al.* Tetrameric c-di-GMP mediates effective transcription factor dimerization to control Streptomyces development. *Cell* 2014;**158**:1136–47.

Tzipilevich E, Pollak-Fiyaksel O, Shraiteh B *et al.* Bacteria elicit a phage tolerance response subsequent to infection of their neighbors. *EMBO J* 2022;**41**:e109247.

Vidakovic L, Singh PK, Hartmann R *et al.* Dynamic biofilm architecture confers individual and collective mechanisms of viral protection. *Nature Microbiology* 2018;**3**:26–31.

Watve MG, Tickoo R, Jog MM *et al.* How many antibiotics are produced by the genus Streptomyces? *Arch Microbiol* 2001;**176**:386–90.

Wein T, Sorek R. Bacterial origins of human cell-autonomous innate immune mechanisms. *Nat Rev Immunol* 2022;**22**:629–38, doi: 10.1038/s41577-022-00705-4.

Williamson KE, Fuhrmann JJ, Wommack KE *et al.* Viruses in soil ecosystems: an unknown quantity within an unexplored territory. *Ann Rev Virol* 2017;**4**:201–19.

Yang W, Willemse J, Sawyer EB *et al.* The propensity of the bacterial rodlin protein RdlB to form amyloid fibrils determines its function in *Streptomyces coelicolor*. *Sci Rep* 2017;**7**:42867.

3.3 Phylogenetic distribution of WhiB- and Lsr2-Type Regulators in Actinobacteriophage Genomes

Sharma, V., Hardy, A., **Luthe, T.,** & Frunzke, J.

Published in *Microbiology Spectrum*, 2021

Role	Definition
Conceptualization	VS (50%), JF (50%)
Data curation	VS (100%)
Formal analysis	VS (75%), TL (25%)
Funding acquisition	JF (100%)
Investigation	VS (80%), TL (15%), AH (5%)
Methodology	VS (80%), TL (10%), AH (5%), JF (5%)
Project administration	VS (50%), JF (50%)
Resources	-
Software	VS (75%), TL (25%)
Supervision	JF (100%)
Validation	VS (90%), TL (10%)
Visualization	VS (70%), TL (30%)
Writing – original draft	VS (65%), JF (15%), AH (10%), TL (10%)
Writing – review and editing	JF (40%), AH (40%), VS (10%), TL (10%)

Overall contribution: 15%

AMERICAN SOCIETY FOR MICROBIOLOGY | Microbiology Spectrum

RESEARCH ARTICLE

Phylogenetic Distribution of WhiB- and Lsr2-Type Regulators in Actinobacteriophage Genomes

Vikas Sharma,[a] Aël Hardy,[a] Tom Luthe,[a] Julia Frunzke[a]

[a]Institute of Bio- and Geosciences (IBG-1) Biotechnology, Forschungszentrum Jülich, Jülich, Germany

ABSTRACT Viruses that infect different actinobacterial host species are known as actinobacteriophages. They are composed of highly divergent and mosaic genomes due to frequent gene exchange between their bacterial hosts and related viral species. This is also reflected by the adaptive incorporation of host transcription factors (TFs) into phage regulatory networks. Previous studies discovered Lsr2-type and WhiB-type regulators encoded by actinobacteriophage genomes. However, limited information is available about their distribution, evolution, and impact on host species. In this study, we computationally screened the distribution of known bacterial and phage TFs inside 2951 complete actinobacteriophage genomes and identified 13 different TF domains. Among those, WhiB, Lsr2, MerR, and Cro/CI-like proteins were widespread and found in more than 10% of the analyzed actinobacteriophage genomes. Neighboring genomic context analysis of the *whiB* and *lsr2* loci showed group-specific conservation of gene synteny and potential involvement of these genes in diverse regulatory functions. Both genes were significantly enriched in temperate phages, and the Lsr2-encoding genomes featured an overall lower GC content. Phylogenetic analysis of WhiB and Lsr2 proteins showed the grouping of phage sequences within bacterial clades, suggesting gene acquisition by phages from their bacterial host species or by multiple, independent acquisition events. Overall, our study reports the global distribution of actinobacteriophage regulatory proteins and sheds light on their origin and evolution.

IMPORTANCE Actinobacteriophages are viruses that infect bacterial species of the diverse phylum of Actinobacteria. Phages engage in a close relationship with their bacterial host. This is also reflected by the adoption of genetic material from their host and its incorporation into phage regulatory circuits. In this study, we systematically searched the genomes of actinobacteriophages for the presence of transcription factor domains. We show that proteins belonging to the regulator families of WhiB and Lsr2 belong to the most abundant regulatory proteins encoded by actinobacteriophages. Further phylogenetic analysis shed light on their origin and evolution. Altogether, this study provides an important basis for further experimental investigation of their role in the coordination of the phage life cycle and their interaction with the host regulatory network in this important bacterial phylum.

KEYWORDS actinobacteriophages, transcriptional regulators, comparative analysis, phylogeny, WhiB, Lsr2, Actinobacteria, bacteriophages, phylogenetic analysis

Actinobacteriophages are viruses that infect hosts of the bacterial phylum Actinobacteria (1). This phylum includes a variety of Gram-positive bacteria that are of high medical, ecological, and biotechnological relevance. It covers important human pathogens from the genera of *Mycobacteria, Corynebacteria,* and *Streptomyces* as prominent inhabitants of the soil and antibiotic producers in addition to the nonpathogenic bacterium *Corynebacterium glutamicum*, which is one of the most important organisms in the biotechnology platform (2).

Editor Alison Sinclair, University of Sussex

Ad Hoc Peer Reviewer Simon White, University of Connecticut

Address correspondence to Vikas Sharma, v.sharma@fz-juelich.de, or Julia Frunzke, j.frunzke@fz-juelich.de.

Received 21 August 2021
Accepted 27 October 2021
Published 24 November 2021

The continuous effort of research- and education-oriented programs such as the 'Phage Hunters Integrating Research and Education' (PHIRE) and 'Science Education Alliance-Phage Hunters Advancing Genomics and Evolutionary Sciences' (SEA-PHAGES) has contributed to the discovery and sequencing of a variety of actinobacteriophage-infecting species of different actinobacterial genera (3, 4). As of the spring 2021, the actinobacteriophage database (https://phagesdb.org) comprised of more than 18,000 isolated phages and more than 3500 complete genome sequences. While >2000 mycobacteriophages that are listed in the database were predominantly isolated using the host *Mycobacterium smegmatis* mc^2155, the phages of *Gordonia*, *Arthrobacter*, *Microbacterium*, *Actinoplanes*, *Propionibacterium*, *Rhodococcus*, *Tsukamurella*, *Tetrasphaera*, *Corynebacterium*, *Brevibacterium*, *Rothia*, and *Streptomyces* were isolated on different strains and species (1, 3, 5).

This wealth of information unraveled the substantial genomic diversity of phages that infect Actinobacteria. Genomes of these phages include a significant amount of viral 'dark matter', with more than 70% of their genes encoding proteins of unknown function (1, 6, 7). Moreover, all isolated actinobacteriophages possess a linear, double-stranded DNA genome that ranges in size from 14 to 194 kbp and belong to the viral families of *Siphoviridae*, *Myoviridae*, and *Podoviridae* (1, 4, 8). Only a few examples of nontailed *Tectiviridae* phages that feature lipid-containing virions have been described (9). Actinobacteriophage genomes comprise a highly mosaic genome architecture, which is probably the result of nonhomologous recombination events rather than sequence-directed processes. These processes are likely facilitated by systems that catalyze nonhomologous end joining (NHEJ) or may also involve Ku-like proteins, which have been found in several phages (10). Investigation of the gene exchange rate between these phages revealed a high gene content flux within temperate phages compared to virulent phages (8).

The relationship between these phages was established based on overall pairwise nucleotide sequence similarity and shared gene content, which divides actinobacteriophage genomes into more than two dozen distinct clusters and over 100 subclusters. A cluster comprises a group of phages that shares at least 35% of genes with at least one other member of the cluster. Phages without close relatives are assigned as singletons (11, 12). A similar phylogenetic pattern was observed by using genome-wide, shared protein family (Pfam) domains content-based clustering. The resulting analysis also delineated clades in close agreement with already defined clusters and proposed an alternative approach to classifying actinobacteriophage genomes (5). However, these data are markedly affected by sampling bias (e.g., with more than 1800 phages infecting *M. smegmatis*) and the true picture likely represents a continuum of diversity.

Actinobacteriophages can be grouped into one of two different lifestyles. Obligatory lytic phages use their host as a 'virion production factory', which typically leads to cell lysis and death of the host cell. In contrast, temperate phages follow one of two life cycle paths following infection of the host cell. They will either follow the lytic path to replicate and produce new viral particles, or they will follow the lysogenic path and establish a long-term association with their host cell as a prophage by efficiently silencing the expression of lytic genes (13). Stressful environmental conditions may trigger the induction of the prophage, which results in the entry into the lytic cycle. An intricate genetic switch encoded by the phage system accomplishes this decision. *Escherichia coli* phage lambda represents the canonical example of developmental decision making (14). Here, the lysis-lysogeny decision is defined by the CI and Cro regulators in a bistable genetic switch. While regulators of the Cro/CI family are ubiquitous in actinobacteriophages, the overall regulatory equipment largely differs from that of the extensively studied phages that infect Proteobacteria.

Recent studies described the importance of the role of the Lsr2-like protein CgpS for maintaining the lysogenic state of the large prophage CGP3 of *C. glutamicum* (15). Lsr2-like proteins are highly conserved among members of the phylum of Actinobacteria in which they are involved in the control of horizontally-acquired ('xenogeneic') genomic regions, including virulence gene clusters, cryptic prophages, and cryptic metabolism (15–18). The

Lsr2-like protein CgpS was the first phage-encoded xenogeneic silencer protein to be described and was found to bind AT-rich regions within the CGP3 island in which it tightly silences phage gene expression (19). Lsr2-like proteins were later found in additional phage genomes, but a comprehensive analysis is currently missing (20).

A further class of regulatory proteins that are exclusively found in Actinobacteria are the WhiB-like proteins. Sequencing of a multitude of actinobacterial genomes revealed the prevalence of these regulators within this phylum, where they carry out important functions like virulence, morphological differentiation, stress response, and antibiotic resistance (21, 22). WhiB-like proteins were also described in phages infecting *Mycobacteria* species. WhiB of phage TM4 was shown to inhibit the expression of the host *whiB2* gene resulting in morphological changes upon expression (23). WhiB of phage Tweety was suggested to be targeted by prophage-mediated defense mechanisms (24). Yet, the functions of WhiB-like proteins in the phage life cycle remain largely enigmatic.

The adoption of prevalent actinobacterial regulators by actinobacteriophages illustrates the intricate link between the phages and their host and raises questions about their evolution and impact on the phage life cycle. In this study, we systematically analyzed the genomes of actinobacteriophages with respect to their regulatory equipment. This approach revealed proteins of the WhiB family as the most abundant regulators of actinobacteriophages, followed by members of the Cro/CI, MerR, and the Lsr2-like family. Comprehensive analyses that focus on WhiB- and Lsr2-like genes showed cluster-specific distributions and conserved gene synteny. Further phylogenetic analyses suggested multiple independent gene acquisition events by actinobacteriophages from the respective host species.

RESULTS AND DISCUSSION

Distribution of bacterial transcription factor domains in actinobacteriophages. To explore the distribution of bacterial and phage transcription factors (TFs) in actinobacteriophages, we initially performed a genome-wide search of conserved protein domains obtained from 2951 complete phage genomes (Table S1) in the NCBI Conserved Domain Database (CDD) using RPS-BLAST (25). A search with known bacterial and phage transcription factor domains obtained from the P2TF (26), Pfam (27), and Phamerator databases (28) revealed 36 different major TF domains that were present in at least 10 or more of the 1702 actinobacteriophage genomes (Table S2). Twenty-eight out of the thirty-six identified domains are completely or partially overlapping within the corresponding genome coordinates but belong to different source databases (Pfam, Clusters of Orthologous Genes [COG], Simple Modular Architecture Research Tool [Smart], and The Institute for Genomic Research [TIGR]). Consequently, these identical domains were collapsed, and the list of actinobacteriophage-encoded TF domains was reduced to 13 unique TF domains whose distributions ranged from 0.4% to 23% within the analyzed genomes (Fig. 1 and Table S2). Interestingly, the WhiB, Cro/CI-type, MerR, and Lsr2 domains were the most abundant and present in more than 10% of the analyzed phage genomes. However, instead of cluster bias, these identified domains were prevalent in different groups of phages. Moreover, their distribution appears to not be lifestyle specific because these domains are encoded by temperate and virulent phages.

Next, we investigated the co-occurrence of different TF domains to understand if they are functionally linked or involved in the same regulatory circuit. The most striking result of this analysis was a negative correlation between the Cro/CI and Lsr2 domains, suggesting that phage genomes rarely share these two types of repressors (Fig. S1).

Distribution of *whiB* and *lsr2* genes in actinobacteriophage clusters. We focused our analysis on WhiB and Lsr2 regulators, which showed a negative correlation with the well-known Cro/CI-like proteins and were among the most abundant regulators found in actinobacteriophages (Fig. 1). To understand their evolutionary histories, an unrooted phylogenetic tree was constructed based on genome-wide k-mer frequency profiles clustering using 2951 complete actinobacteriophage genomes. The resulting phylogenetic tree delineated the phages into multiple distinct clusters or groups (Fig. 2) that showed high

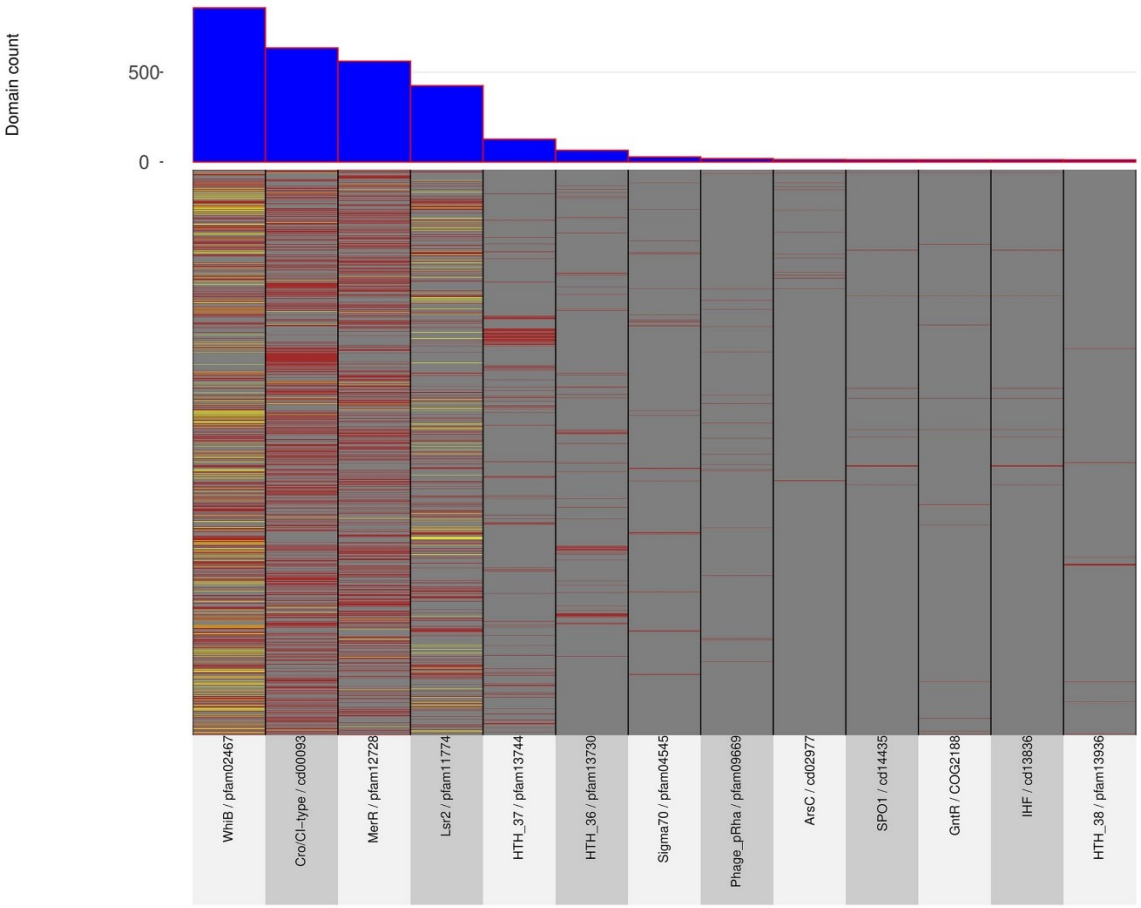

FIG 1 Distribution of 13 transcription factor domains across 1702 actinobacteriophage genomes. The heatmap indicates the domain count (1 = red; 2 = yellow) per phage genome. The bar plot above the heatmap presents the overall domain abundance based on the total count of Pfam domains across the genomes.

congruence with the allocated clusters obtained from the PhagesDB database (https://phagesdb.org) (4). The phylogenetic mapping of the WhiB and Lsr2 protein domains on the actinobacteriophage tree revealed a nonrandom distribution across the known phage clusters. Except for a few clusters, individual proteins mostly showed a clade-specific distribution pattern, indicating that there was no biological link between the two proteins, which was in line with our correlation analysis (Fig. S1). Additionally, the phage genomes that encode more than one copy of the protein domains also fall within unique and specific clusters, suggesting multiple, independent gene transfer events following a common origin and evolution from group-specific ancestral viruses. Besides that, the level of conservation between the WhiB- and Lsr2-encoding phages were calculated using a pairwise genome comparison. The resulting analyses, according to the known clusters, reflected the conservation level. As expected, phages belonging to the singleton cluster showed a high variation in comparison to other clusters, suggesting the involvement of genes in diverse functions (Fig. S2). In contrast, a high conservation – as observed for most clusters – suggests that these regulators are playing critical roles in the life cycles of that particular group of phages.

WhiB-type proteins represent the most abundant regulators in actinobacteriophages. Remarkably, our analysis revealed that WhiB-type proteins were the most abundant regulator class in actinobacteriophages followed by the Cro/CI-type

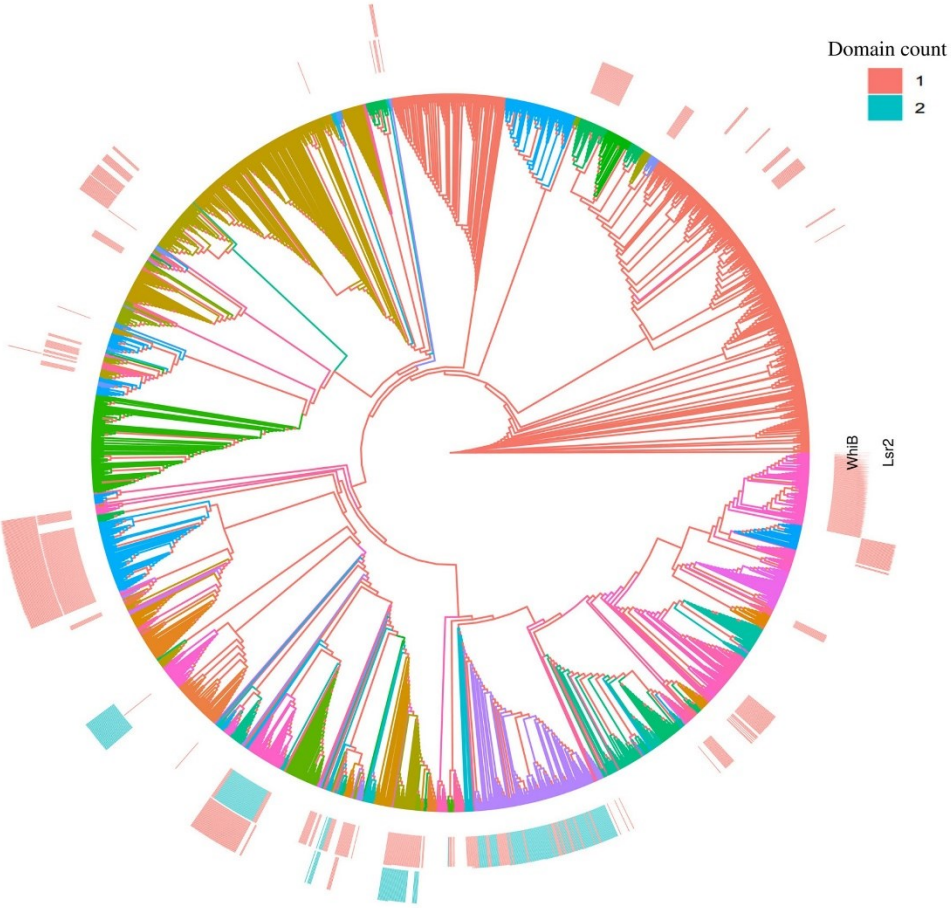

FIG 2 Lsr2 and WhiB are nonrandomly distributed among actinobacteriophage genomes. The k-mer clustering-based phylogenetic tree is based on complete nucleotide sequences from 2951 actinobacteriophage genomes. Sequences are color-coded according to already assigned clusters information obtained from PhagesDB (4). The concentric heatmaps represent the Pfam domain counts (1 = green; 2 = red) of WhiB (inner ring) and Lsr2 (outer ring) of the corresponding genomes.

regulators and MerR- and Lsr2-like proteins. To provide insight into their potential role in the phage life cycle, further investigations were focused on phage-encoded WhiB- and Lsr2-like proteins. A systematic tBLASTn similarity search was conducted to detect all sequence homologs among the 2951 actinobacteriophage genomes using the query protein sequence library of the *whiB* and *lsr2* genes separately and a custom-designed pipeline. The resulting similarity searches revealed the presence of *whiB* and *lsr2* genes in 24% (711/2951) and 11% (354/2951) of the total analyzed actinobacteriophage genomes, respectively. Compared to the protein domain-based analysis, the BLAST-based similarity searches retained a few more sequence homologs of both genes (Table S2), which was probably due to parameter and methodological differences between the two approaches.

Overall, we identified more than >800 putative *whiB* genomic loci within 8 out of 13 different host genera (*Arthrobacter*, *Corynebacterium*, *Gordonia*, *Microbacterium*, *Mycobacterium*, *Propionibacterium*, *Rhodococcus*, and *Streptomyces*, Fig. 3A). *Tsukamurella* phages (1 *whiB* gene found in 2 phage genomes) were not included in the analysis due to the small dataset. *Mycobacterium* stands among the largest group of WhiB-encoding phages (with 492

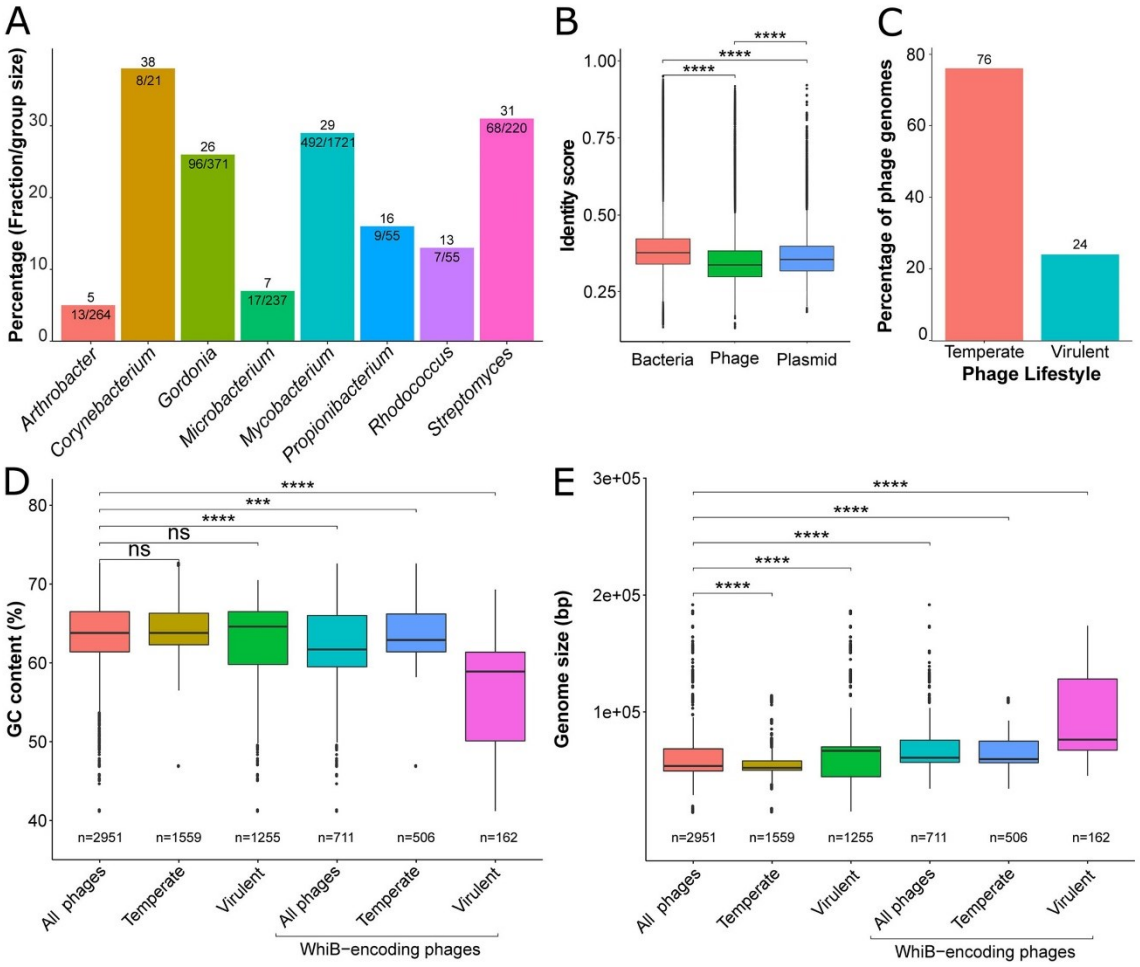

FIG 3 WhiB-type proteins represent the most abundant regulators in actinobacteriophages. (A) Bar plot representing the actual count and proportion of WhiB-encoding phages according to host genus. (B) Global pairwise identity between WhiB amino acid sequences encoded by phage, bacterial, and plasmid phage genomes. (C) Distribution of WhiB-encoding phages is displayed according to phage lifestyle (temperate and virulent actinobacteriophages). (D) Box plot presenting the GC content of actinobacteriophages depending on their lifestyle and the presence of a *whiB* locus. (E) Box plot presenting the genome size of actinobacteriophages depending on their lifestyle and the presence of a *whiB* locus. Level of significance is indicated based on the *P value* (ns, not significant; ***, $P < 0.001$; ****, $P < 0.0001$).

representatives), but this is also a result of the high number of *Mycobacterium* phage genomes (>1700) in the actinobacteriophage database (4). The normalized percentage of WhiB-encoding genomes obtained by considering the overall group size of the corresponding host genus showed, on average, a higher frequency within *Corynebacterium* phages (38%, 8/21) compared to other identified host genera (Fig. 3A). While most of the phage genomes carry only one copy of the *whiB* gene, 182 phages that infect members of the genera *Mycobacterium*, *Propionibacterium*, and *Gordonia* encode two homologs (Fig. S3). Moreover, the distribution of WhiB-encoding phages showed multiple clusters with 100% presence of representative members according to assigned clusters. This observation indicated that closely related phages tend to have a higher chance of harboring such genes (Fig. S4). Calculation of protein pairwise identities revealed a rather low sequence identity of 25 to 48% (Fig. S5), suggesting different functions in the phage circuitry. Moreover, a comparison of the global pairwise identity of WhiB proteins from phages, bacteria, and plasmids

displayed a high variability of phage-encoded proteins, suggesting further functional adaptation (Fig. 3B).

Overall, we observed a higher abundance of *whiB* genes in temperate phages compared to virulent phages (Fig. 3C). Phage genomes encoding this gene but without lifestyle information were not included in this analysis. The comparative analysis with respect to GC content and genome size showed, on average, a lower GC content but an increased overall genome size for *whiB*-encoding temperate and virulent phages (Fig. 3D and E).

Lsr2-like proteins are enriched in genomes of temperate phages featuring a lower GC content. Lsr2-like genes were detected in 11% (354/2951) of the total analyzed phage genomes and are distributed over 430 putative loci. Phages encoding Lsr2-like proteins belong to five different host genera, including *Mycobacterium*, *Gordonia*, *Streptomyces*, *Arthrobacter*, and *Microbacterium* (Fig. 4A). Overall, *lsr2* genes were found to be the most abundant in the genomes of phages that infect *Streptomyces*, with approximately 35% of *Streptomyces* phages encoding Lsr2 homologs (20). Phages encoding more than one copy of a *lsr2* gene were found in all host genera except *Microbacterium* (76/354 phage genomes; Fig. S6). In comparison to WhiB, Lsr2-encoding phages also showed a similar distribution pattern according to the known clusters. More than 50% of these clusters showed a 100% presence of phage representative members, suggesting high relatedness between the genomes (Fig. S7). The determination of protein pairwise identities between copies encoded in the same genome revealed significant variation. Interestingly, *Arthrobacter* and *Streptomyces* phage Lsr2 protein copies shared 100% of sequence identity, which is because the corresponding genes are located within the direct terminal repeats (DTR) of these phage genomes (29) (Fig. S8). In contrast, *Mycobacterium* and *Gordonia* sequences share less than 40% of identity between protein copies, suggesting independent gene transfer events and presumably expression of proteins with different functions. Similar to WhiB, phage-encoded Lsr2-like proteins featured the lowest pairwise identity compared to the bacterial- or plasmid-encoded Lsr2 proteins (Fig. 4B).

Analysis of the distribution of Lsr2-encoding phages according to their lifestyle (normalized to group size) showed a three times higher abundancy in temperate phages (Fig. 4C). In agreement with previous studies (20), further analysis revealed a lower GC content on average and a bigger genome size for Lsr2-encoding phages (Fig. 4D and E).

Neighboring genomic context analyses. To gain insight into the potential function and origin of phage-encoded WhiB and Lsr2-like proteins, we analyzed the neighboring genomic context in actinobacteriophage genomes, reasoning that gene families enriched in the vicinity of *whiB* and *lsr2* may illuminate their function. For this purpose, we extracted the 5 kb upstream and downstream regions around the *whiB* and *lsr2* genomic loci in actinobacteriophage genomes. These 10 kb regions were centered on either *lsr2* or *whiB* and are referred to as 'extended genomic loci'. All extended genomic loci were then functionally annotated using an automated pipeline (Prokka v. 1.11 [30]) combined with different custom databases (see the Materials and Methods). Overall, this analysis showed a highly syntenic, but cluster-specific, organization of neighboring genes (Fig. 5A to C and Table S3 and S4) (4).

For *whiB* extended genomic loci, domains found in more than 50% of the sequences for each cluster are listed in Table S4. According to our analyses, the most abundant domains are DUF732 (37.9%) and PHA02446 (29.7%) which are associated with uncharacterized or hypothetical proteins as well as HTH_7 (26.3%), SSB (25.2%), and Phage_integrase (19.8%) domains.

In the following, we focused on representative members of the clusters EK, K, and T for visualization of genomic synteny at the *whiB* extended genomic loci (Fig. 5A to C). Phages in the cluster EK infect *Microbacterium foliorum* and share domains associated with DNA replication in the 10 kb region surrounding *whiB* (Fig. 5A), including genes encoding a primase/polymerase (64.3% of the sequences in this cluster), DNA primases (85.7%), DNA helicases (50%), and DNA polymerase I (100%) as well as a Cas4 family exonuclease (100%) and NrdH-like glutaredoxin (37.5%).

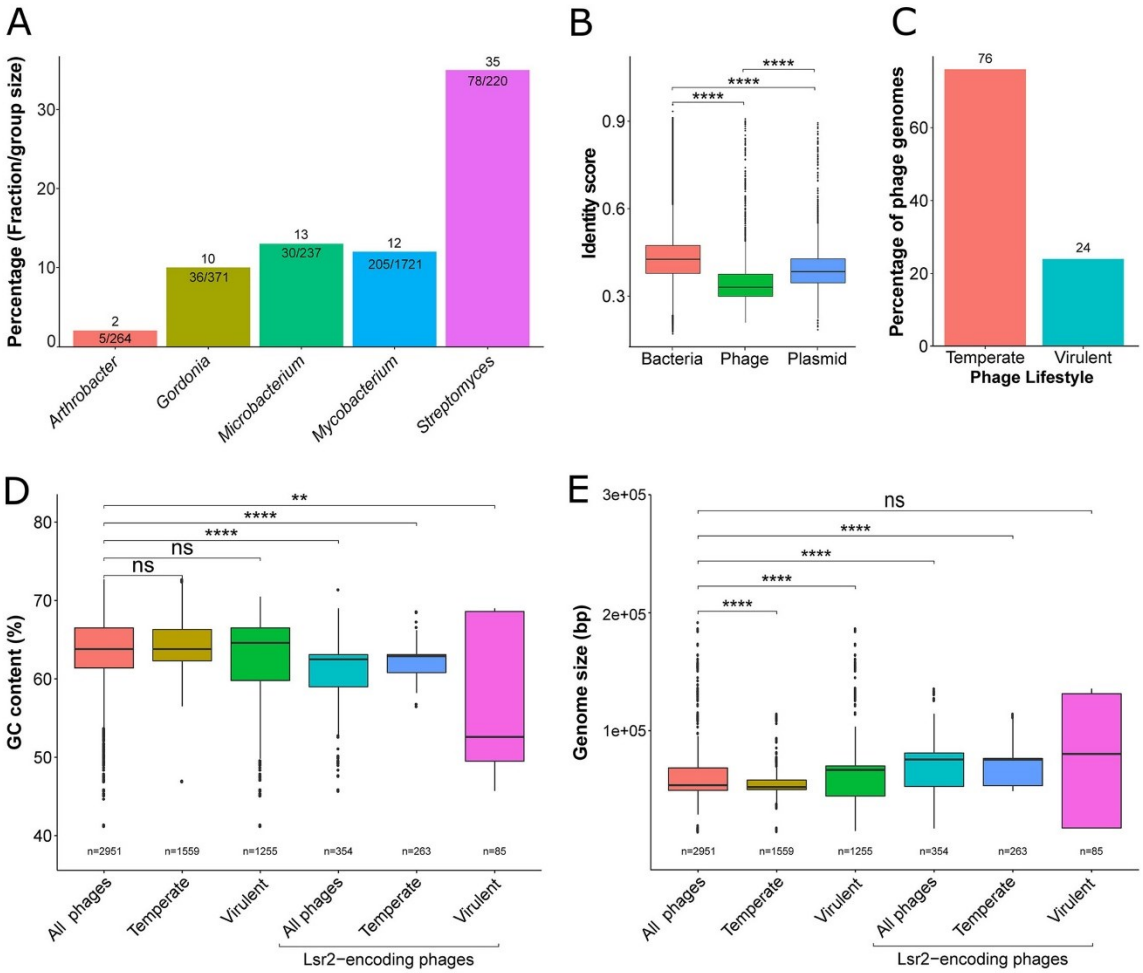

FIG 4 Lsr2-like proteins are enriched in genomes of temperate phages featuring a lower GC content. (A) Bar plot represents the actual count and proportion of Lsr2-encoding phages according to host genus. (B) Global pairwise identity between Lsr2 amino acid sequences encoded by phage, bacterial, and plasmid phage genomes. (C) Distribution proportion of Lsr2-encoding phages is displayed according to phage lifestyle (temperate and virulent actinophages). (D) Box plot presenting the GC content of actinobacteriophages depending on their lifestyle and the presence of a *lsr2* locus. (E) Box plot presenting the genome size of actinobacteriophages depending on their lifestyle and the presence of a *lsr2* locus. Level of significance is indicated based on the *P value* (ns, not significant; **, $P < 0.01$; ****, $P < 0.0001$).

Based on the *whiB* extended genomic loci context found in the cluster T phages, we hypothesized a role of WhiB in lysis-lysogeny decision making (Fig. 5C). Domains found in the ~10 kb region surrounding *whiB* in those sequences were Phage_integrase (100% of the sequences), HTH_17 representing excisionases (100%), and DUF3799, which is associated with exonucleases (100%), as well as the COG1476 (100%) and HTH_3 (85.7%) domains associated with Cro/CI family transcriptional regulators. However, many genes in the direct vicinity of *whiB* code for hypothetical proteins (Fig. 5A and C). Therefore, deducing the function based on this analysis is difficult and requires further experiments to elucidate the role of phage-encoded WhiB proteins in the phage life cycle.

Phages in cluster K (96 sequences encoding *whiB*) infect *Mycobacterium smegmatis* (Fig. 5B). Here, an RNase_T domain associated with exonucleases, such as the ε subunit of DNA polymerase III, were present in 100% of the sequences in this cluster. Other

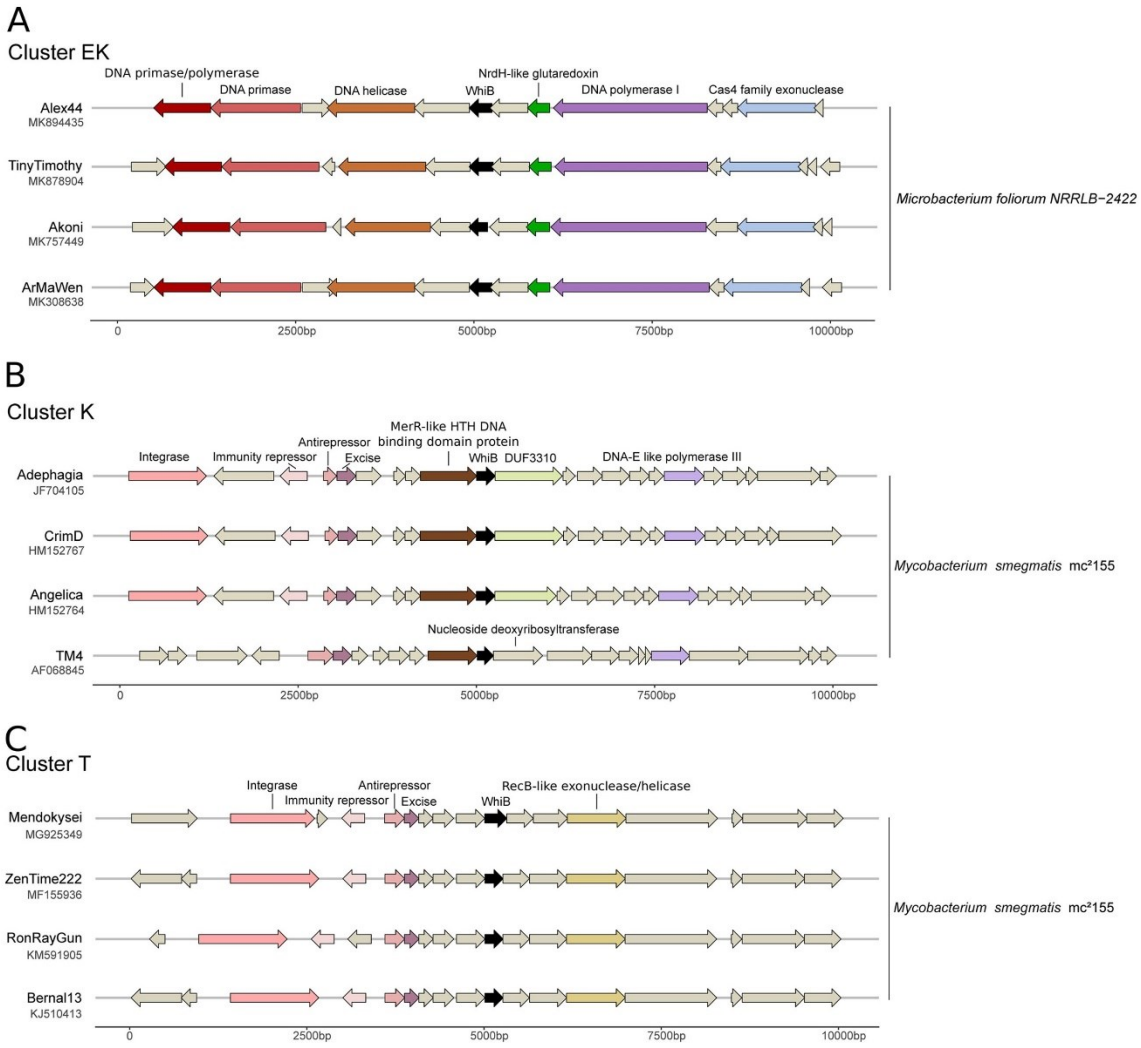

FIG 5 Syntenic genomic organization of the *whiB* loci in clusters EK, K, and T phages. (A to C) Gene synteny plot showing the 5 kb regions flanking *whiB* across phage genomes of the clusters EK (A), K (B), and T (C) following the cluster assignment determined by phagesDB (4).

abundant domains include Phage_integrase (95.8%) and HTH_17 (84.4%), which is associated with DNA-binding of excisionases. One member of this cluster, TM4 (AF068845) is the only WhiB-encoding bacteriophage investigated for the biological function of WhiB during infection. Rybniker et al. (23) reported $WhiB_{TM4}$ as a dominant, negative regulator that inhibited the gene expression of the host *whiB2* gene. Furthermore, a TM4-resistant phenotype that inhibited secondary infections was observed, pointing toward a function of WhiB in a potential superinfection exclusion mechanism (23). However, synteny of the neighboring genes in the TM4 phage was slightly different from most of the other cluster K sequences because it, for example, lacks the Phage_integrase domain in this region. A recent study focusing on prophage-mediated viral defense suggested that the WhiB of temperate phage Tweety (cluster F) was targeted by the heterotypic prophage-mediated defense. Phages lacking the intact protein (by single base substitutions resulting in stop codons) were able to escape the defense mechanism and successfully lyse *M. smegmatis* lysogens (24).

Next, we investigated the gene synteny and GC content within the *lsr2* phage extended genomic loci (Fig. 6 and Table S5 and S6). Similar to *whiB*, we counted all domains detected in the extended genomic loci of *lsr2* and indicated their relative abundance in the different clusters (Table S5 and S6). When we looked for shared domains across different phage clusters, it seemed that the proteins involved in lysogeny (integrase domains: Phage_int_SAM_4, resolvase, and Phage_integrase; immunity repressor: HTH_3; antirepressor domain: HTH_17) and nucleotide metabolism and modification (glutaredoxin domains: Glutaredoxin and Glutaredoxin-like_protein_NrdH; DNA-sulfur modification-associated protein DndB domain) were enriched in the areas surrounding Lsr2. However, it is worth noting that there are marked differences between clusters, and no domain was found in all clusters.

Further, we looked in more detail at the genomic organization of *lsr2* extended genomic loci in members of selected clusters: clusters A, BD, and J (Fig. 6). Interestingly, in cluster A, Lsr2 was found between a module of structural proteins (minor tail proteins) and an operon encoding homologs of the ParA and ParB proteins (Fig. 6A). ParA and ParB are proteins involved in the partitioning of plasmids and bacterial chromosomes during cell division. Additionally, mycobacteriophages of cluster A that lack an integrase were shown to use the *parABS* system to promote maintenance of their DNA as extrachromosally replicating entities (31, 32).

In cluster BD, Lsr2 is found upstream of the integrase and is close to a ribonucleotide reductase and a thymidylate synthase, suggesting a role of Lsr2 in lysogeny and/or nucleotide biosynthesis (Fig. 6B).

Members of cluster J have two copies of *lsr2* (Fig. 6C). The first copy is close to the gene encoding a glutaredoxin homolog and a putative pyrophosphorylase, further highlighting the potential connection of Lsr2 with nucleotide biosynthesis. Intriguingly, the second copy of Lsr2 consists of a fusion of the Ku protein with the C-terminal, DNA-binding domain of Lsr2. More precisely, the first 250 amino acids of this fusion protein are highly homologous with the Ku protein of *Mycobacterium smegmatis*, but the last 30 amino acids show relatively high identity with Lsr2, including the 'AT-hook' RGR motif (16). Ku binds to DNA double-strand break ends and is required for the nonhomologous end joining (NHEJ) pathway of DNA repair in all branches of cellular life (33). Interestingly, two of such Ku-Lsr2 fusion proteins encoded in members of the J cluster phages (Omega and Corndog) were shown to enable circularization of the incoming phage genomes (10), but the presence of the Lsr2 domain was not recognized nor was its contribution investigated.

Previous reports emphasized the preferential binding of Lsr2-like proteins to AT-rich genomic regions in bacterial genomes (15–17). More precisely, the preferential binding was to regions that featured a distinct drop in GC profile close to the transcription start site (19). Inspection of GC profiles in phage genomes at the *lsr2* genomic loci revealed a distinct drop in GC content in the *lsr2* upstream region in members of clusters A, BD, and J, suggesting autoregulation of Lsr2 in these phages (Fig. 6 and Fig. S9). In cluster A phages, an additional drop was observed upstream of the *parAB* operon, which probably corresponds to the *ori* region of these phages. As mentioned above, the *parABS* system is used by cluster A temperate phages that lack an integration cassette to promote their maintenance as extrachromosomal prophages (31). The *ori* region upstream of the *parAB* operon was found to be required for prophage stability. The localization of *lsr2* in this genomic context as well as the distinct drop in GC content upstream of *lsr2* and in the *ori* region could hint towards a role for Lsr2-like proteins in prophage maintenance in cluster A phages. Involvement in the maintenance of lysogeny was previously described for the Lsr2-like xenogeneic silencing protein CgpS in *C. glutamicum* (15, 19). Here, interference with CgpS binding resulted in prophage induction and, consequently, to cell death.

Remarkably, in *Streptomyces* phages belonging to the BE cluster, the *lsr2* genes are located within the direct terminal repeat regions. The direct terminal repeats of BE cluster phages (10 to 12 kbp) are the longest found in actinobacteriophages to date

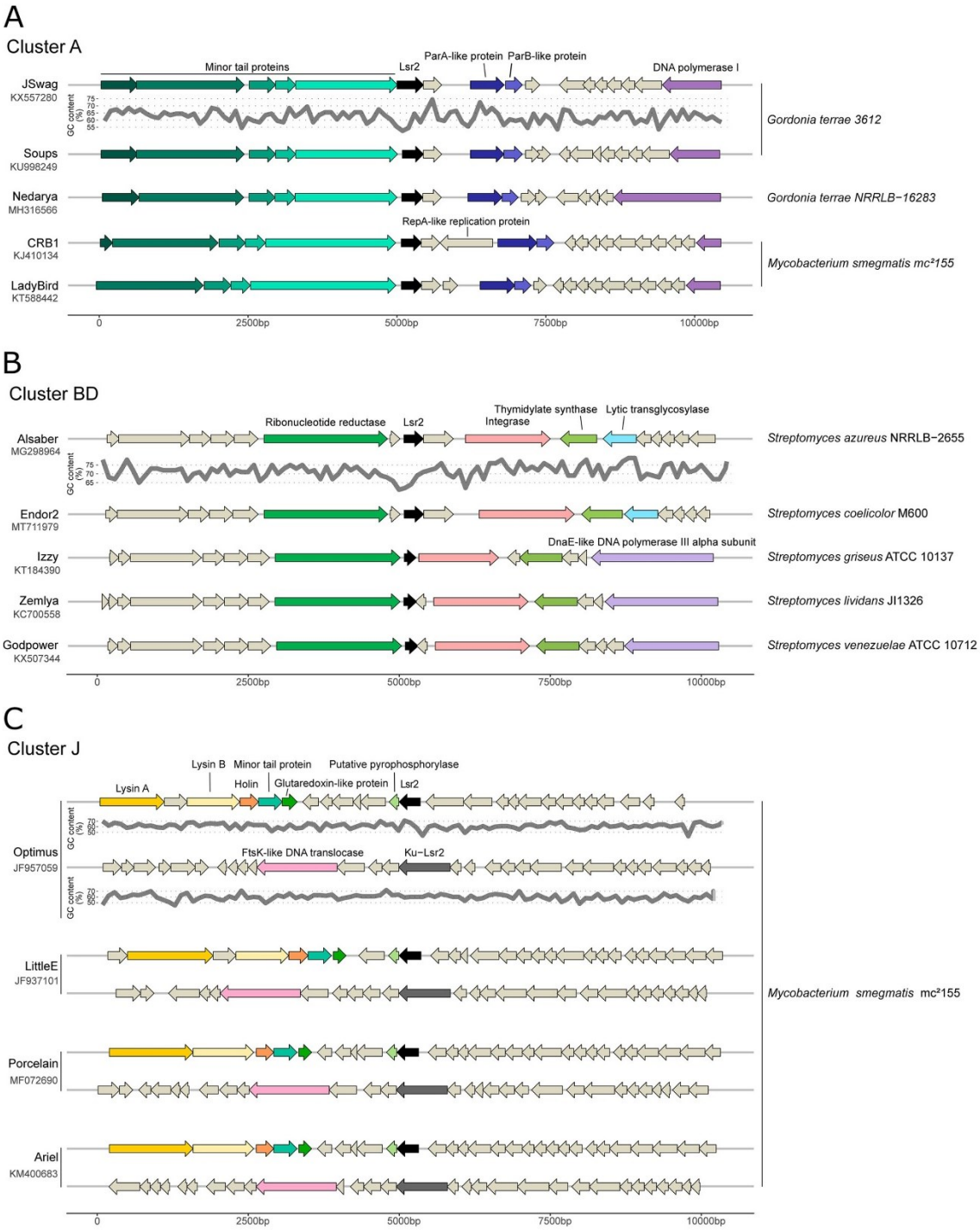

FIG 6 Syntenic genomic organization of the lsr2 loci in cluster A, BD, and J phages. (A to C) Gene synteny plot showing the 5 kb regions flanking *lsr2* across randomly selected representative phage genomes of cluster A (A), BD (B), and J (C) following the cluster assignment determined by phagesDB (4). GC content is displayed below the gene synteny plot for the one representative genome per cluster.

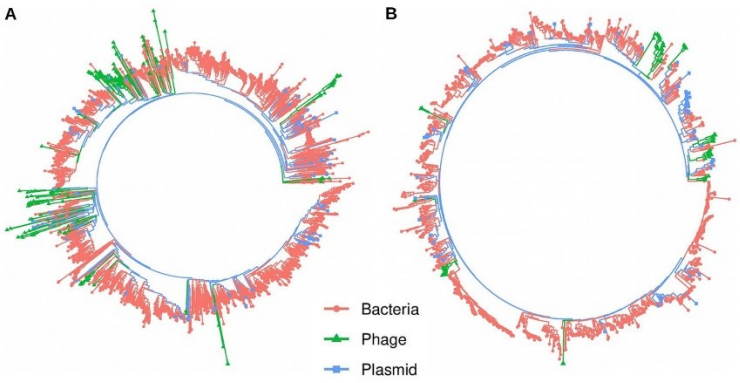

FIG 7 Phylogenetic analysis revealed complex evolutionary histories of the phage-encoded Lsr2 and WhiB homologs. (A) Unrooted maximum likelihood phylogenetic tree constructed using > 2300 WhiB protein sequences obtained from phage (green), bacteria (red), and plasmid (blue) genomes. Sequences are color-coded based on source groups (bacteria, phage, and plasmid). (B) Unrooted maximum likelihood phylogenetic tree constructed using >950 Lsr2 protein sequences obtained from phage, bacteria, and plasmid genomes.

(29). The genome alignment and GC content comparison of the *lsr2* extended genomic loci from *Streptomyces* phage Coruscant against phage Mildred21 (Fig. S10) showed a significantly higher GC content of the direct repeat region (54.4%) compared to the rest of the genome (47.0%). This finding suggests a block transfer of this ~12 kb region from a phage or bacteria that possessed a distinctively GC-rich genome. However, this large genomic region does not map to any phage or host genome, suggesting acquisition from a bacterial host that has not yet been sequenced.

Phylogenetic analysis reveals complex evolutionary histories of phage-encoded Lsr2 and WhiB homologs. The phylogenetic relationship was established using the identified WhiB and Lsr2 protein sequences from actinobacteriophages, plasmids, and bacterial genomes. Instead of using all identified homologs, we separately clustered the protein sequences from bacteria, phage, and plasmid genomes at the 90% amino acid identity threshold using UCLUST (34). The longest sequence was selected as a representative from each resulting cluster and used for further analyses.

The WhiB and Lsr2 maximum likelihood, unrooted phylogenetic tree that was constructed with the high quality protein sequence alignment showed a complex evolutionary history. In the WhiB phylogeny, most phage-encoded sequences form a paraphyletic group and fall within bacterial clades, suggesting viruses acquired genes from their host or that this occurred from independent gene transfers from different sources (Fig. 7A). Zooming into the WhiB subclades showed different evolutionary patterns. One subclade showed gene transfer by *Streptomyces* phages from their host bacteria (Fig. S11). Another subclade displayed gene transfer events within *Mycobacterium* phages (viruses acquired genes from their host; Fig. S12). Here, one bacterial sequence (*NZ_CP034072_1_3673830* to *NZ_CP034072_1_3675228*) deeply clustered within temperate *Mycobacterium* phages. Further inspection revealed that this bacteria-encoded *whiB* gene is located within a prophage region, as determined using the PHASTER online webserver (data not shown) (35). Overall, phage encoded WhiB proteins formed clusters according to the phage lifestyle (Fig. S11 and S12).

Similarly, Lsr2 phylogenetic analysis also showed the paraphyletic grouping of phage sequences within bacterial branches, suggesting acquisition of this gene from their hosts or due to multiple independent acquisition events (Fig. 7B). Zooming in on the phylogenetic groups revealed diverse patterns. One subclade showed gene acquisition in temperate *Streptomyces* and *Gordonia* phages from their host (Fig. S13 and S14). Another subclade showed gene transfer events between unrelated phages (*Mycobacterium* phages to *Gordonia* phages; Fig. S15). However, it is important to

mention that retracing the history of gene transfer events is sometimes impossible, especially between unrelated phages. Moreover, multiple bacterial sequences also form paraphyletic clades for both gene-based phylogenies, reflecting gene exchanges between diverse bacterial species. Overall, *whiB* and *lsr2* gene-based phylogenies revealed complex evolutionary histories. The scattering of the actinobacteriophage sequences on both trees may suggest multiple independent acquisitions of genes by phages from their hosts and related viruses, in accordance with previous reports (20, 36) (Fig. 7A and B).

WhiB- and Lsr2-like proteins are widespread in actinobacteria. Therefore, it is no surprise that phages have taken advantage of their properties. Our analysis revealed that WhiB proteins exist in more than 23% of the sequenced actinobacteriophage genomes, which is similar to the widespread Cro/CI family of phage regulators that have been identified in approximately 20% of the genomes. Previous studies revealed an interplay with the host-encoded WhiB proteins (23), and it is likely that their phage-encoded counterparts may manipulate the network of their host and have an important influence on central processes of their host, such as cellular development, antibiotic production, and/or resistance (21).

Lsr2-like proteins have already been described as xenogeneic silencers that repress the expression of 'foreign', AT-rich DNA elements in host genomes (16, 17, 20, 37). Because foreign DNA in the form of viruses is one of the most primordial threats in the evolution of life, the role of Lsr2-like proteins in the control of the phage gene expression is probably ancient. This hypothesis is also supported by the high variability in amino acid sequence and high conservation of secondary structure of Lsr2 proteins (15). Considering the genomic synteny of *lsr2* in phage genomes as well as the results of previous studies, we postulate a role of phage-encoded Lsr2-like proteins in maintaining the lysogenic state of the prophage. However, expression of a different xenogeneic silencer has also been demonstrated to strongly interfere with the formation of the oligomeric nucleoprotein complex required for silencing and may, therefore, also represent a strategy of virulent phages to defend against silencing upon infection of the host (20). An interesting example is provided by the H-NST protein, a truncated H-NS variant lacking the DNA-binding domain, which was shown to antagonize H-NS in enteropathogenic and uropathogenic *E. coli* (38).

For a comprehensive understanding, experimental approaches are needed to decipher the likely diverse roles of WhiB and Lsr2 proteins in the control of the phage life cycle and their interplay with host regulatory networks. Considering the unique regulatory equipment of actinobacteriophages, future studies will not only deliver fundamental new insights into their regulation but also the minimalist elegance of phage regulatory circuits provides constant inspiration for the fields of synthetic biology and metabolic engineering.

MATERIALS AND METHODS

Data collection. The list of 3396 complete actinobacteriophage available genomes was retrieved on 14 May 2020 from PhagesDB (4). The 2946/3396 complete actinobacteriophage genomes with valid NCBI accession numbers were downloaded with the list information using a NCBI-genome-download python script (https://github.com/kblin/ncbi-genome-download) from the NCBI file transfer protocol (FTP) site. Additionally, five recently sequenced *Streptomyces* phages (accession numbers: MT711976, MT711977, MT711975, MT711978, and MT711979) (5) were included for the current analysis. In total, the 2951 actinobacteriophage genomes that were used in the current study were included in the supplementary information (Table S1). The 2381 complete actinobacterial genomes and plasmid sequences were downloaded from the NCBI FTP site.

Identification of regulatory gene domains within actinobacteriophage genomes. Genome-wide distributions of conserved protein domains were determined using the nucleotide sequences of 2951 actinobacteriophages genomes as a query against CDD database using RPS-BLAST version (BLAST 2.2.31+) with an E-value of 0.001 (25). The list of putative transcription factors or regulatory gene information was extracted in tabular format from the three different databases (P2TF [26], Pfam [27], and Phamerator [28]). The regulatory protein domain unique IDs were mapped and filtered from the genome-wide predicted protein domains across the actinobacteriophage genomes using a custom-designed R script. Filtered domains were manually curated for the valid transcription factors based on published literature (Table S2). Lastly, only the domains encoded by more than 10 phage genomes were

included for further analysis to represent the most abundant and widely distributed domains. The density and correlation analysis of identified transcription factors protein domains that were identified inside the actinobacteriophage genomes was displayed using the R packages Superheat (39) and corrplot v. 0.84 (40).

Whole-genome phylogeny. We used an alignment-free approach based on a machine learning perspective to estimate the phylogenetic tree with the 2951 actinobacteriophage genomes using an R script (https://bioinformaticshome.com/bioinformatics_tutorials/R/phylogeny_estimation.html). Initially, the script looks for k-mer frequency profiles within the different phage genomes. Pairwise comparisons were then performed to calculate the distance between k-mer pairs using the Jensen-Shannon divergence measure (41). Finally, a phylogenetic tree was obtained after the clustering of the output distance matrix using the neighbor-joining algorithm. The phylogenetic tree visualization and mapping of *whiB* and *lsr2* domains were displayed using the R package ggtree v. 2.0.1 (42).

WhiB and Lsr2 sequence detection pipeline. The complete WhiB and Lsr2 sequence homologs were collected independently using a custom design pipeline following a similar approach used in previous studies (43, 44). The TBLASTN searches (45) were conducted using a known set of WhiB and Lsr2 protein sequence libraries as the query against the targeted 2951 actinobacteriophage complete nucleotide sequences with an E-value of 10^{-5}. The identified overlapping genomic loci hits were merged using SAMtools v. 1.7 (46). To ensure the complete gene sequence length, the *whiB* and *lsr2* genomic loci hits were extended by 500 bp and 5 kbp upstream and downstream, respectively. The extended loci were then translated into proteins using the Emboss translate program. The predicted proteins were compared against the WhiB and Lsr2 sequence libraries using BLASTp (45) with and E-value of 10^{-5} to exclude false positives from the analysis. The proteins with the best BLAST hits against the WhiB and Lsr2 proteins were retained and used for further analysis. Besides screening the phage genomes, the same steps of the pipeline were used to identify the WhiB and Lsr2 sequence homologs inside the 2381 complete host actinobacterial genomes and their plasmid sequences.

Sequence alignment and phylogenetic analysis of WhiB and Lsr2 proteins. Complete WhiB and Lsr2 protein homologous sequences were collected from phage, bacteria, and plasmid genomes using the custom-designed pipeline. To avoid identical sequences in the analysis, the identified protein sequences for both genes in each source organism (phage, bacteria, and plasmid genomes) were separately clustered at 90% identity using UCLUST (34). The longest sequence was then selected from each resulting cluster as a representative for the sequence alignment. The protein sequences were aligned using the MAFFT v. 7 online server with default parameters (47). The output of multiple sequence alignments was manually curated and checked for the best fit evolutionary model using ProtTest v. 3.4.2 (48). The maximum likelihood-like phylogeny for each gene was constructed separately with the identified optimal model using FastTree v. 2.1.10 (49). The phylogenetic tree was visualized using the R package ggtree v. 2.0.1 (42).

Neighboring genomic context analysis. The 5 kb flanking regions extended upstream and downstream around the *whiB* and *lsr2* genomic loci hits were extracted in FASTA format using the previously mentioned homologous detection pipeline. These regions were annotated using the Prokka 1.11 pipeline (30) with the help of multiple databases with different databases (CDD, Conserved Domain Database (30); pVOGs, Prokaryotic Virus Orthologous Groups (50); NCBI viral proteins). The annotated extended regions for both genes were used for gene synteny visualization using the R package Gggenes v. 0.4.0 (https://github.com/wilkox/gggenes). The quantitative gene domain distribution within the annotated extended regions was calculated using a custom R script. The GC content across the *lsr2* extended region was calculated according to a 100 bp window using a Perl script. The GC plot was obtained using ggplot2 v. 3.2.1 in R (51).

Comparative analyses of WhiB and Lsr2-like proteins. Comparative analyses the distribution, lifestyle, GC content, and genome size variation of phages containing *whiB* and *lsr2*-like genes were conducted in R using different packages (ggplot2 v. 3.2.1 [51], rstatix v. 0.6.0, gplots v. 3.0.1.2, tidyverse v. 1.3.0, and ggpubr v. 0.4.0). The pairwise identity scores between the WhiB and Lsr2 protein sequences obtained from the bacterial, phage, and plasmid genomes were calculated with MAFFT v. 7.310 (47) using the sequence demarcation tool (SDT) in Python (52). The output of the pairwise identity scores were displayed using the R package ggplot2 v. 3.2.1 (51). Statistically significant differences between the groups were determined based on pairwise Wilcoxon tests using R package rstatix v. 0.6.0.

Data availability. The complete sequences of phage genomes used in the current study are available on the PhagesDB website (4). The identified phage encoded WhiB and Lsr2 sequences, phylogenetic trees, and R scripts used for the data analysis are available on a Github repository (https://github.com/sharmavikas3529/Actinophage-regulators-data.git).

SUPPLEMENTAL MATERIAL

Supplemental material is available online only.

SUPPLEMENTAL FILE 1, PDF file, 1.4 MB.

SUPPLEMENTAL FILE 2, XLSX file, 0.3 MB.

ACKNOWLEDGMENTS

We thank the students and faculty members of the SEA-PHAGES program for their contributions to phage discovery and genomics and the SEA-PHAGES program for permission to use the unpublished data compiled at https://phagesdb.org. We especially

thank Graham Hatfull for his expert comments and suggestions. We thank the European Research Council (ERC Starting Grant, grant number 757563) for financial support.

We declare no conflicts of interest.

REFERENCES

1. Hatfull GF. 2020. Actinobacteriophages: genomics, dynamics, and applications. Annu Rev Virol 7:37–61. https://doi.org/10.1146/annurev-virology-122019-070009.
2. Barka EA, Vatsa P, Sanchez L, Gaveau-Vaillant N, Jacquard C, Meier-Kolthoff JP, Klenk H-P, Clément C, Ouhdouch Y, van Wezel GP. 2016. Taxonomy, physiology, and natural products of Actinobacteria. Microbiol Mol Biol Rev 80:1–43. https://doi.org/10.1128/MMBR.00019-15.
3. Hanauer DI, Graham MJ, Betancur L, Bobrownicki A, Cresawn SG, Garlena RA, Jacobs-Sera D, Kaufmann N, Pope WH, Russell DA, Jacobs WR, Sivanathan V, Asai DJ, Hatfull GF, SEA-PHAGES. 2017. An inclusive research education community (iREC): impact of the SEA-PHAGES program on research outcomes and student learning. Proc Natl Acad Sci U S A 114:13531–13536. https://doi.org/10.1073/pnas.1718188115.
4. Russell DA, Hatfull GF. 2017. PhagesDB: the actinobacteriophage database. Bioinformatics 33:784–786. https://doi.org/10.1093/bioinformatics/btw711.
5. Hardy A, Sharma V, Kever L, Frunzke J. 2020. Genome sequence and characterization of five bacteriophages infecting Streptomyces coelicolor and Streptomyces venezuelae: Alderaan, Coruscant, Dagobah, Endor1 and Endor2. Viruses 12:1065. https://doi.org/10.3390/v12101065.
6. Hatfull GF. 2018. Mycobacteriophages. Microbiol Spectr 6:76–78. https://doi.org/10.1128/microbiolspec.GPP3-0026-2018.
7. Hatfull GF. 2015. Dark matter of the biosphere: the amazing world of bacteriophage diversity. J Virol 89:8107–8110. https://doi.org/10.1128/JVI.01340-15.
8. Mavrich TN, Hatfull GF. 2017. Bacteriophage evolution differs by host, lifestyle and genome. Nat Microbiol 2:1–9. https://doi.org/10.1038/nmicrobiol.2017.112.
9. Caruso SM, DeCarvalho TN, Huynh A, Morcos G, Kuo N, Parsa S, Erill I. 2019. A novel genus of Actinobacterial tectiviridae. Viruses 11:1134. https://doi.org/10.3390/v11121134.
10. Pitcher RS, Brissett NC, Doherty AJ. 2007. Nonhomologous end-joining in bacteria: a microbial perspective. Annu Rev Microbiol 61:259–282. https://doi.org/10.1146/annurev.micro.61.080706.093354.
11. Pope WH, Mavrich TN, Garlena RA, Guerrero-Bustamante CA, Jacobs-Sera D, Montgomery MT, Russell DA, Warner MH, Hatfull GF, Science Education Alliance-Phage Hunters Advancing Genomics and Evolutionary Science (SEA-PHAGES), Hatfull GF. 2017. Bacteriophages of Gordonia spp. Display a spectrum of diversity and genetic relationships. mBio 8:e01069-17. https://doi.org/10.1128/mBio.01069-17.
12. Pope WH, Bowman CA, Russell DA, Jacobs-Sera D, Asai DJ, Cresawn SG, Jacobs WR, Hendrix RW, Lawrence JG, Hatfull GF, Mycobacterial Genetics Course. 2015. Whole genome comparison of a large collection of mycobacteriophages reveals a continuum of phage genetic diversity. Elife 4:e06416. https://doi.org/10.7554/eLife.06416.
13. Ptashne M. 2004. A genetic switch: phage lambda revisited. 3rd ed Cold Spring Harbor Laboratory Press. Cold Spring Harbor NY.
14. Oppenheim AB, Kobiler O, Stavans J, Court DL, Adhya S. 2005. Switches in bacteriophage lambda development. Annu Rev Genet 39:409–429. https://doi.org/10.1146/annurev.genet.39.073003.113656.
15. Pfeifer E, Hünnefeld M, Popa O, Polen T, Kohlheyer D, Baumgart M, Frunzke J. 2016. Silencing of cryptic prophages in Corynebacterium glutamicum. Nucleic Acids Res 44:10117–10131. https://doi.org/10.1093/nar/gkw692.
16. Gordon BRG, Li Y, Wang L, Sintsova A, van Bakel H, Tian S, Navarre WW, Xia B, Liu J. 2010. Lsr2 is a nucleoid-associated protein that targets AT-rich sequences and virulence genes in Mycobacterium tuberculosis. Proc Natl Acad Sci U S A 107:5154–5159. https://doi.org/10.1073/pnas.0913551107.
17. Gehrke EJ, Zhang X, Pimentel-Elardo SM, Johnson AR, Rees CA, Jones SE, Hindra Gehrke SS, Turvey S, Boursalie S, Hill JE, Carlson EE, Nodwell JR, Elliot MA. 2019. Silencing cryptic specialized metabolism in Streptomyces by the nucleoid-associated protein Lsr2. Elife 8:e47691. https://doi.org/10.7554/eLife.47691.
18. Will WR, Navarre WW, Fang FC. 2015. Integrated circuits: how transcriptional silencing and counter-silencing facilitate bacterial evolution. Curr Opin Microbiol 23:8–13. https://doi.org/10.1016/j.mib.2014.10.005.
19. Wiechert J, Filipchyk A, Hünnefeld M, Gätgens C, Brehm J, Heermann R, Frunzke J. 2020. Deciphering the rules underlying xenogeneic silencing and counter-silencing of lsr2-like proteins using cgps of Corynebacterium glutamicum as a model. mBio 11:e02273-19. https://doi.org/10.1128/mBio.02273-19.
20. Pfeifer E, Hünnefeld M, Popa O, Frunzke J. 2019. Impact of xenogeneic silencing on phage–host interactions. J Mol Biol 431:4670–4683. https://doi.org/10.1016/j.jmb.2019.02.011.
21. Bush MJ. 2018. The actinobacterial WhiB-like (Wbl) family of transcription factors. Mol Microbiol 110:663–676. https://doi.org/10.1111/mmi.14117.
22. Jakimowicz P, Cheesman MR, Bishai WR, Chater KF, Thomson AJ, Buttner MJ. 2005. Evidence that the Streptomyces developmental protein WhiD, a member of the WhiB family, binds a [4Fe-4S] cluster. J Biol Chem 280:8309–8315. https://doi.org/10.1074/jbc.M412622200.
23. Rybniker J, Nowag A, Van Gumpel E, Nissen N, Robinson N, Plum G, Hartmann P. 2010. Insights into the function of the WhiB-like protein of mycobacteriophage TM4 – a transcriptional inhibitor of WhiB2. Mol Microbiol 77:642–657. https://doi.org/10.1111/j.1365-2958.2010.07235.x.
24. Dedrick RM, Jacobs-Sera D, Bustamante CAG, Garlena RA, Mavrich TN, Pope WH, Reyes JCC, Russell DA, Adair T, Alvey R, Bonilla JA, Bricker JS, Brown BR, Byrnes D, Cresawn SG, Davis WB, Dickson LA, Edgington NP, Findley AM, Golebiewska U, Grose JH, Hayes CF, Hughes LE, Hutchison KW, Isern S, Johnson AA, Kenna MA, Klyczek KK, Mageeney CM, Michael SF, Molloy SD, Montgomery MT, Neitzel J, Page ST, Pizzorno MC, Poxleitner MK, Rinehart CA, Robinson CJ, Rubin MR, Teyim JN, Vazquez E, Ware VC, Washington J, Hatfull GF. 2017. Prophage-mediated defence against viral attack and viral counter-defence. Nat Microbiol 2:16251. https://doi.org/10.1038/nmicrobiol.2016.251.
25. Marchler-Bauer A, Derbyshire MK, Gonzales NR, Lu S, Chitsaz F, Geer LY, Geer RC, He J, Gwadz M, Hurwitz DI, Lanczycki CJ, Lu F, Marchler GH, Song JS, Thanki N, Wang Z, Yamashita RA, Zhang D, Zheng C, Bryant SH. 2015. CDD: NCBI's conserved domain database. Nucleic Acids Res 43:D222–D226. https://doi.org/10.1093/nar/gku1221.
26. Ortet P, De Luca G, Whitworth DE, Barakat M. 2012. P2TF: a comprehensive resource for analysis of prokaryotic transcription factors. BMC Genomics 13:628–628. https://doi.org/10.1186/1471-2164-13-628.
27. Mistry J, Chuguransky S, Williams L, Qureshi M, Salazar GA, Sonnhammer ELL, Tosatto SCE, Paladin L, Raj S, Richardson LJ, Finn RD, Bateman A. 2021. Pfam: the protein families database in 2021. Nucleic Acids Res 49:D412–D419. https://doi.org/10.1093/nar/gkaa913.
28. Cresawn SG, Bogel M, Day N, Jacobs-Sera D, Hendrix RW, Hatfull GF. 2011. Phamerator: a bioinformatic tool for comparative bacteriophage genomics. BMC Bioinformatics 12:395–315. https://doi.org/10.1186/1471-2105-12-395.
29. Hughes LE, Shaffer CD, Ware VC, Aguayo I, Aziz RM, Bhuiyan S, Bindert IS, Calovich-Benne CK, Chapman J, Donegan-Quick R, Farooq A, Garcia C, Graham LH, Green BY, Kenna MA, Kneeream ER, Laing CE, Mageeney CM, Meridew SN, Mikolon AR, Morgan RE, Nayek S, Olugbade ID, Pike KC, Schlegel LE, Shishido TC, Suresh T, Suri N, Hafer KW, Garlena RA, Russell DA, Cresawn SG, Pope WH, Jacobs-Sera D, Hatfull GF. 2018. Eight genome sequences of cluster BE1 phages that infect Streptomyces species. Genome Announc 6:e01146-17. https://doi.org/10.1128/genomeA.01146-17.
30. Seemann T. 2014. Prokka: rapid prokaryotic genome annotation. Bioinformatics 30:2068–2069. https://doi.org/10.1093/bioinformatics/btu153.
31. Wetzel KS, Aull HG, Zack KM, Garlena RA, Hatfull GF. 2020. Protein-Mediated and RNA-based origins of replication of extrachromosomal mycobacterial prophages. mBio 11:e00385-20. https://doi.org/10.1128/mBio.00385-20.
32. Dedrick RM, Mavrich TN, Ng WL, Reyes JCC, Olm MR, Rush RE, Jacobs-Sera D, Russell DA, Hatfull GF. 2016. Function, expression, specificity, diversity and incompatibility of actinobacteriophage parABS systems. Mol Microbiol 101:625–644. https://doi.org/10.1111/mmi.13414.
33. Fell VL, Schild-Poulter C. 2015. The Ku heterodimer: function in DNA repair and beyond. Mutat Res Rev Mutat Res 763:15–29. https://doi.org/10.1016/j.mrrev.2014.06.002.
34. Edgar RC. 2010. Search and clustering orders of magnitude faster than BLAST. Bioinformatics 26:2460–2461. https://doi.org/10.1093/bioinformatics/btq461.

35. Arndt D, Grant JR, Marcu A, Sajed T, Pon A, Liang Y, Wishart DS. 2016. PHASTER: a better, faster version of the PHAST phage search tool. Nucleic Acids Res 44:W16–W21. https://doi.org/10.1093/nar/gkw387.
36. Piña-Iturbe A, Suazo ID, Hoppe-Elsholz G, Ulloa-Allendes D, González PA, Kalergis AM, Bueno SM. 2020. Horizontally Acquired Homologs of Xenogeneic Silencers: modulators of Gene Expression Encoded by Plasmids, Phages and Genomic Islands. Genes (Basel) 11:142. https://doi.org/10.3390/genes11020142.
37. Duan B, Ding P, Navarre WW, Liu J, Xia B. 2021. Xenogeneic Silencing and Bacterial Genome Evolution: mechanisms for DNA Recognition Imply Multifaceted Roles of Xenogeneic Silencers. Mol Biol Evol 38:4135–4148. https://doi.org/10.1093/molbev/msab136.
38. Williamson HS, Free A. 2005. A truncated H-NS-like protein from enteropathogenic Escherichia coli acts as an H-NS antagonist. Mol Microbiol 55:808–827. https://doi.org/10.1111/j.1365-2958.2004.04421.x.
39. Barter RL, Yu B. 2018. Superheat: an R Package for Creating Beautiful and Extendable Heatmaps for Visualizing Complex Data. J Comput Graph Stat 27:910–922. https://doi.org/10.1080/10618600.2018.1473780.
40. Wei T, Simko V, Levy M, Xie Y, Jin Y, Zemla J. 2017. R package "corrplot": Visualization of a Correlation Matrix. https://cran.r-project.org/web/packages/corrplot/corrplot.pdf.
41. Sims GE, Jun S-R, Wu GA, Kim S-H. 2009. Alignment-free genome comparison with feature frequency profiles (FFP) and optimal resolutions. Proc Natl Acad Sci USA 106:2677–2682. https://doi.org/10.1073/pnas.0813249106.
42. Yu G, Smith DK, Zhu H, Guan Y, Lam TT-Y. 2017. ggtree: an r package for visualization and annotation of phylogenetic trees with their covariates and other associated data. Methods Ecol Evol 8:28–36. https://doi.org/10.1111/2041-210X.12628.
43. Diop SI, Geering ADW, Alfama-Depauw F, Loaec M, Teycheney P-Y, Maumus F. 2018. Tracheophyte genomes keep track of the deep evolution of the Caulimoviridae. Sci Rep 8:1–9. https://doi.org/10.1038/s41598-017-16399-x.
44. Sharma V, Lefeuvre P, Roumagnac P, Filloux D, Teycheney P-Y, Martin DP, Maumus F. 2020. Large-scale survey reveals pervasiveness and potential function of endogenous geminiviral sequences in plants. Virus Evol 6:71. https://doi.org/10.1093/ve/veaa071.
45. Altschul SF, Gish W, Miller W, Myers EW, Lipman DJ. 1990. Basic local alignment search tool. J Mol Biol 215:403–410. https://doi.org/10.1016/S0022-2836(05)80360-2.
46. Li H, Handsaker B, Wysoker A, Fennell T, Ruan J, Homer N, Marth G, Abecasis G, Durbin R, Subgroup 1000 Genome Project Data Processing. 2009. The sequence alignment/map format and SAMtools. Bioinformatics 25:2078–2079. https://doi.org/10.1093/bioinformatics/btp352.
47. Katoh K, Standley DM. 2014. MAFFT: iterative refinement and additional methods. Methods Mol Biol 1079:131–146. https://doi.org/10.1007/978-1-62703-646-7_8.
48. Darriba D, Taboada GL, Doallo R, Posada D. 2010. ProtTest-HPC: Fast Selection of Best-Fit Models of Protein Evolution. *In*: Guarracino M.R. et al. (eds) Euro-Par 2010 Parallel Processing Workshops. Euro-Par 2010. Lecture Notes in Computer Science. 6586 Springer, Berlin, Heidelberg.
49. Price MN, Dehal PS, Arkin AP. 2010. FastTree 2 – approximately maximum-likelihood trees for large alignments. PLoS One 5:e9490. https://doi.org/10.1371/journal.pone.0009490.
50. Grazziotin AL, Koonin EV, Kristensen DM. 2017. Prokaryotic virus orthologous groups (pVOGs): a resource for comparative genomics and protein family annotation. Nucleic Acids Res 45:D491–D498. https://doi.org/10.1093/nar/gkw975.
51. Ginestet C. 2011. ggplot2: elegant graphics for data analysis. J R Stat Soc Ser A-Statistics Soc 174:245–246. https://doi.org/10.1111/j.1467-985X.2010.00676_9.x.
52. Muhire BM, Varsani A, Martin DP. 2014. SDT: a virus classification tool based on pairwise sequence alignment and identity calculation. PLoS One 9:e108277. https://doi.org/10.1371/journal.pone.0108277.

3.4 Investigation on *Streptomyces* Phage-encoded WhiB-like Transcriptional Regulators

Luthe, T., & Frunzke, J.

To be submitted

Role	Definition
Conceptualization	TL (70%), JF (30%)
Data curation	TL (100%)
Formal analysis	TL (100%)
Funding acquisition	JF (100%)
Investigation	TL (100%)
Methodology	TL (80%), JF (20%)
Project administration	TL (50%), JF (50%)
Resources	-
Software	TL (100%)
Supervision	JF (70%), TL (30%)
Validation	TL (75%), JF (25%)
Visualization	TL (100%)
Writing – original draft	TL (80%), JF (20%)
Writing – review and editing	TL (50%), JF (50%)

Overall contribution: 80%

Investigation on *Streptomyces* Phage-encoded WhiB-like Transcriptional Regulators

Tom Luthe and Julia Frunzke*

Institute of Bio- and Geosciences, IBG-1: Biotechnology, Forschungszentrum Jülich, 52425 Jülich, Germany

*Corresponding author:

Julia Frunzke; Email: j.frunzke@fz-juelich.de ; Phone: +49 2461 615430

Abstract

Streptomyces bacteria are special regarding their key traits of filamentous growth undergoing a complex multicellular development and the ability to produce diverse secondary metabolites. Both features are involved in shaping phage-host interactions in this genus and bacteriophages are likely having the potential to interfere with their hosts' regulatory networks by harboring a unique repertoire of transcriptional regulators. This study addressed the relevance of phage-encoded proteins related to host development. Here we analyzed 337 complete and annotated genomes of phages infecting different *Streptomyces* species for the presence of genes encoding host development-associated proteins and found members of the WhiB, FtsK, ParB, ParA and SsgA families to be encoded in a total of one-third of the genomes. Phages encoding any of these proteins overall tend to being virulent with larger genome size and lower GC content compared to phages not encoding these proteins. With WhiB-like proteins being the most abundant transcriptional regulator found, phylogenetic analysis of these proteins revealed high diversity while resembling known actinobacteriophage clusters. Expression of phage *whiB* genes in *Streptomyces venezuelae* confirmed a significant impact on cellular development, but was not able to complement the sporulation phenotype of a Δ*whiB* strain. By using RT-qPCR and RNA-sequencing we were able to confirm early expression of phage *whiB* genes during native infection. Altogether, these results suggest a distinct function of the phage-encoded WhiB-like proteins, which likely interfere with host development processes to improve phage propagation.

Keywords: *Streptomyces*, development, transcription regulation, WhiB, bacteriophage, viral infection

Introduction

The actinobacterial genus *Streptomyces* comprises high GC species widely distributed in predominantly soil environments. These Gram-positive microorganisms are renowned for their ability to produce a plethora of specialized metabolites such as bioactive compounds like antibiotics, anti-tumor and anti-fungal molecules as well as other biotechnologically relevant substances (Alam et al., 2022; Demain, 1999). Furthermore, *Streptomyces* represent a model for the study of cellular development and emergent multicellular properties. Multicellular differentiation during their lifecycle starts by germinating from single spores developing into a branched vegetative mycelium and transforming into unbranched spore-bearing aerial hyphae (Bush et al., 2015; Chater, 2016; Flärdh & McCormick, 2017).

Multicellular development and metabolite production are closely linked in *Streptomyces* being coordinated by underlying regulatory networks sharing key regulatory proteins (Barka et al., 2016;

den Hengst et al., 2010). Especially the Actinobacteria specific [4Fe-4S] cluster carrying WhiB-like (Wbl) transcription factors are of importance to both transition from aerial hyphae to spores (WhiB, WhiD) as well as antibiotic production and resistance (WblA, WblC) among other, yet unknown functions (Bush, 2018). Structure and function of the founding member WhiB in the context of development in *Streptomyces* are under constant investigation revealing a unique mechanism of transcription activation requiring WhiB and WhiA interaction on the DNA in order to recruit the RNA polymerase initiation complex to their shared regulon including for example *ftsZ*, *ftsW*, *ftsK*, *sepH*, *sepX*, *parA*, *parB* and *whiG* (Bush et al., 2013, 2016; Lilic et al., 2023).

Given the intricate developmental processes expressed by *Streptomyces*, it is likely that these processes also influence the interactions of these bacteria with their viruses. While bacteriophages (phages), viruses which infect bacteria, have been known for over a century, previous research primarily focused on unicellular bacteria, typically involving model organisms or pathogens. However, recent studies on bacteriophages infecting a broader range of bacterial hosts, including Actinobacteria like *Streptomyces*, have begun to illuminate previously unexplored terrain. This emerging research sheds light on phage-host interactions in multicellular bacteria, offering promising implications for biotechnology, ecology and medicine (Georjon et al., 2023; Hatfull, 2020; Kever et al., 2022; Luthe et al., 2023; Ongenae et al., 2022; Sharma et al., 2021).

Close interactions between bacteriophages and their hosts are already known and investigated extensively for some model organisms. This also includes the sporulating Firmicutes bacterium *Bacillus subtilis* where phages are thought to regulate sporulation for example by encoding sporulation-specific sigma factors (Schwartz et al., 2022). In actinobacteriophages, it was shown that WhiB-like proteins represent the most abundant transcriptional regulators found in 24% of all analyzed genomes (Sharma et al., 2021). Additionally, some actinobacteriophages are described that harbor other genes encoding for proteins relevant to cell division and sporulation such as FtsK, ParB and SsgA (Hardy et al., 2020). As the WhiB family is essential in the life cycle of *Streptomyces* together with our previous study, highlighting *Streptomyces* development as an important factor for successful phage infection (Luthe et al., 2023), it is intriguing to further investigate the role of phage-encoded WhiB-like proteins. This demands for a more focused analysis of the genetic equipment and impact of phages on multicellular development in bacteriophages infecting specifically *Streptomyces*.

Here we analyzed 337 complete and annotated genomes of phages infecting different *Streptomyces* species for the presence of genes encoding for host development-associated proteins. We compared phages on the foundation of their genetic equipment and used phylogenetic analysis to investigate the diversity of WhiB-like proteins. Phenotypic characterization revealed that phage-encoded WhiB-like proteins have not the same function as the canonical host WhiB but induce morphological changes impacting phage propagation. RT-qPCR during infection established *whiB* as an early gene of moderate expression.

Results

Abundance of development-associated genes in *Streptomyces* phages

The prevalence of WhiB-like regulators in actinobacteriophages strongly underscores that phages adapted to the intricate bacterial lifestyles, suggesting a propensity to interfere with their host's biological processes. In this study, we searched overall 57 gene products known to be involved in *Streptomyces* development in 337 complete and annotated genomes of bacteriophages infecting specifically *Streptomyces.* This led to the discovery of 35.9% (121/337) of phages encoding at least one of these proteins (Figure 1, Table S2). Namely, we found WhiB family (109), FtsK-like (67), ParB-like (47), ParA-like (2) and SsgA family (1) proteins present in this set of phages. Phages harboring any kind of development-associated gene belong to only 9 of the 20 known actinobacteriophage cluster including the singletons. Interestingly, specific combinations of genes encoding these proteins are associated with distinct clusters. Solely phages of cluster BE encode the combination of WhiB-like, FtsK-like and ParB-like proteins (44). Similarly, the combination of WhiB-like and FtsK-like proteins (13) is mainly encoded by cluster BG phages. Harboring only an *ftsK*-like gene (9) is restricted to phages belonging to cluster BM as well as BQ and WhiB family regulators alone (51) is encoded by phages from cluster BC, BF, BH, BK and singletons. SsgA was found as the only development-associated protein of singleton phage Dagobah. Interestingly, all phages harbor only one copy of their respective genes except for singleton phage mu1/6 which has two genes encoding WhiB-like proteins.

In general, 216 bacteriophages encode none of the development-associated proteins (64.1%), 61 encode only one (18.1%), for 15 phages we found two proteins (4.4%) and 45 of them encode three proteins (13.4%) (Figure 2A). That being said, there are interesting patterns when looking for the lifestyle of phages harboring specific genetic equipment (Figure 2B). In total, these 337 phages exhibit an even distribution of 47.7% predicted/described as temperate (161) and 49.0% as virulent (165) with additional 3.0% unknown (10) and 0.3% phage-plasmid (1). But phages encoding none of the development associated proteins tend to be temperate (69.0%, 149/216) whereas phages encoding at least one developmental protein are most likely virulent (86.0%, 104/121). This ratio only increases when looking for example at phages encoding WhiB-like proteins with 89.9% being virulent (98/109), 92.3% (12/13) of the WhiB and FtsK combination and 100% of the WhiB, FtsK and ParB combination (44/44) being virulent phages. Similar differences can be observed for genome size (Figure 2C) and GC content (Figure 2D). The total set of phages comprises genomes ranging from 14,787 bp to 200,048 bp (mean=69,672 bp) and GC contents between 46.9% and 72.7% (mean=61.83%). Although the maximum range of size and GC content is not really affected by the presence of genes encoding development-associated proteins, these phages overall have significantly larger genomes (mean=105,369 bp) and lower GC content (mean=57.1%) compared to all phages and the none-encoding ones (size mean=49,675 bp, GC mean=64.8%).

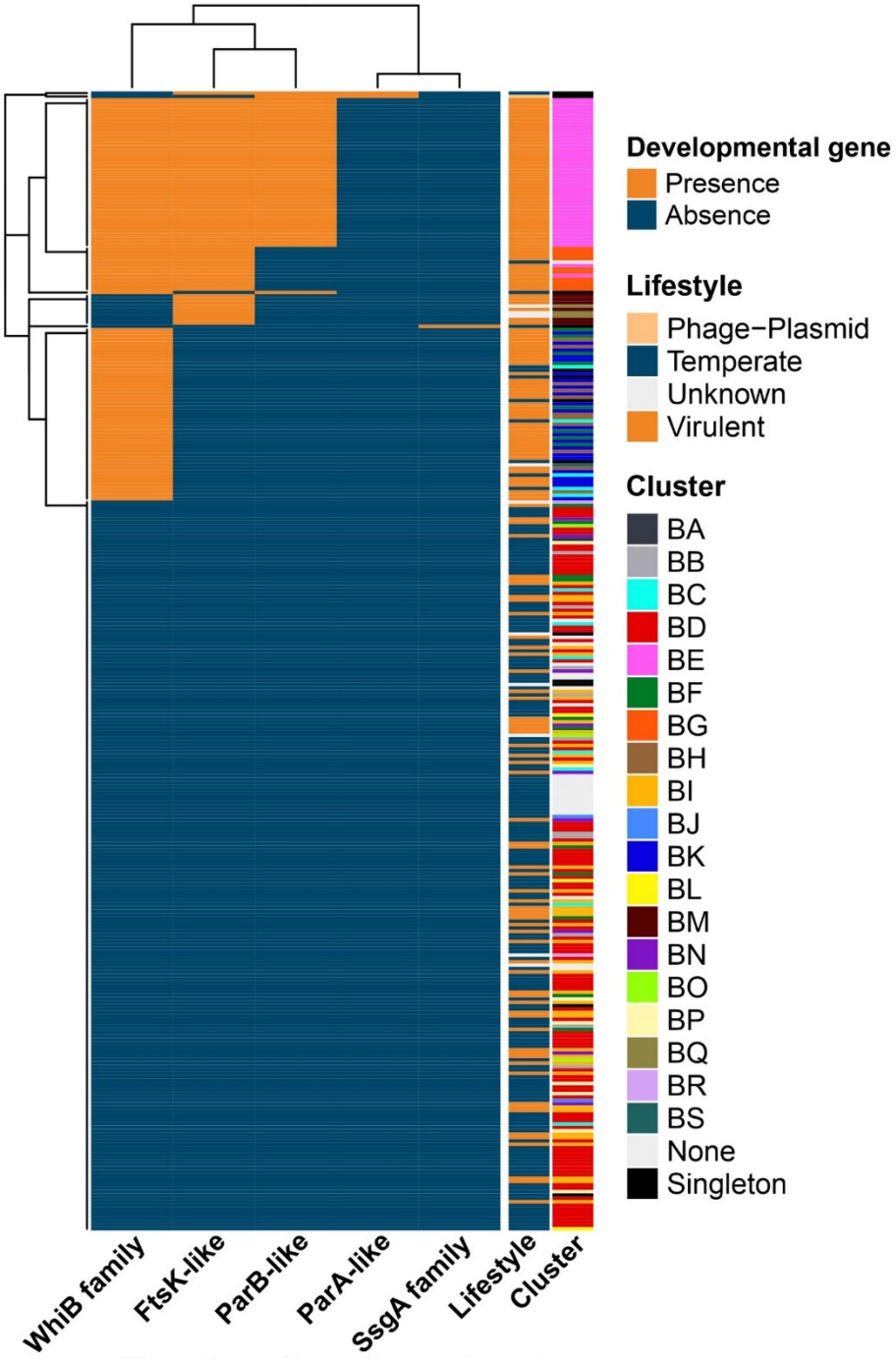

Figure 1: Matrix of 337 actinobacteriophage genomes investigated for the presence of genes encoding for proteins involved in the development of their host *Streptomyces*. Presence (orange) or absence (blue) of genes encoding for one of the five found protein families is indicated for each phage (row). Annotation of the predicted/described lifestyle and actinobacteriophage cluster of each phage is given as color-coded.

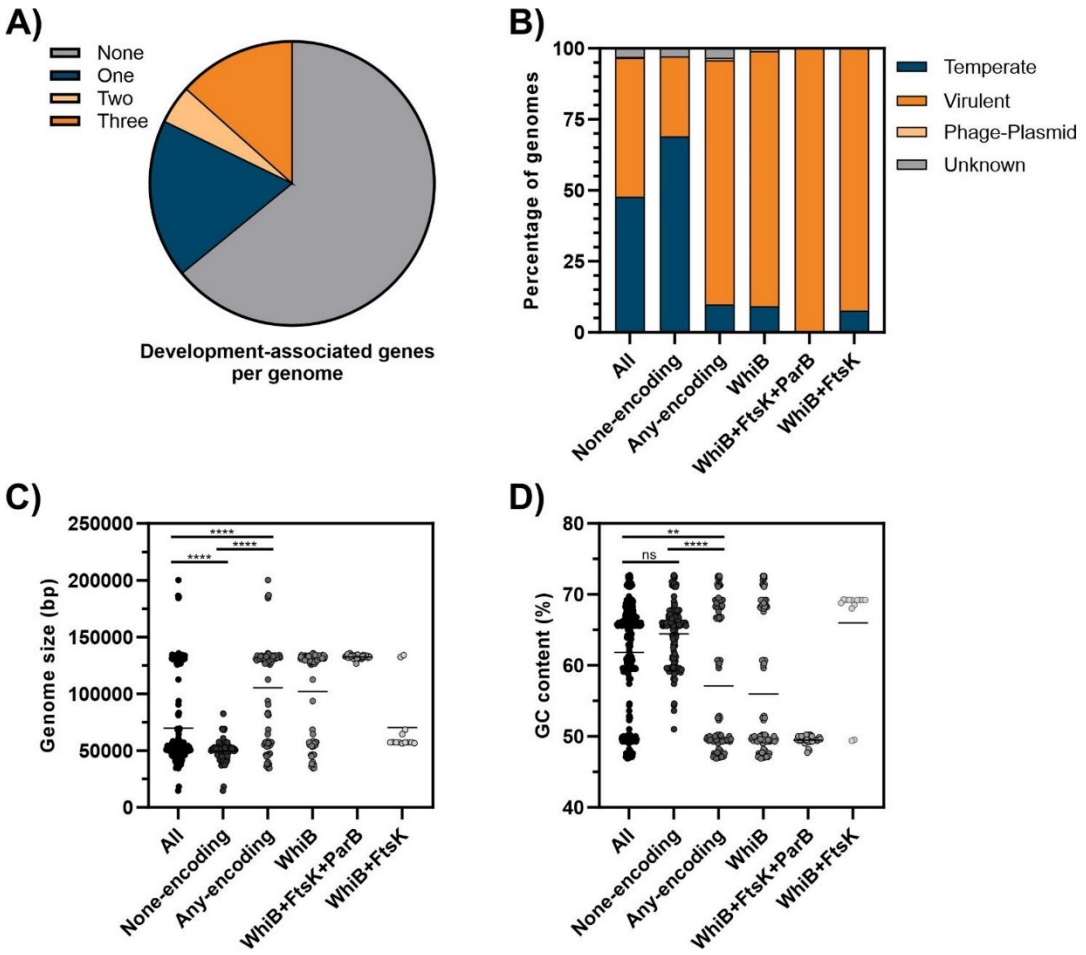

Figure 2: Bacteriophage genome analysis reveals differences between phages encoding development-associated genes and non-encoding phages. A) Percentage of bacteriophage genomes encoding none (grey), one (blue), two (light orange) or three (orange) development-associated proteins. **B)** Percentage of phage genomes belonging to the temperate (blue), virulent (orange), phage-plasmid (light orange) or unknown (grey) lifestyle according to their respective genetic equipment. **C)** Genome size (bp) of the different groups of phages encoding development-associated proteins. **D)** GC content (%) of the different groups of phages encoding development-associated proteins. **C)** and **D)** Bars represent the mean of groups. The Kruskal-Wallis test was used in GraphPad Prism to test for significant difference between groups: ns = not significant, ** = $p < 0.01$, **** = $p < 0.0001$. All n=337, None-encoding n=216, Any-encoding n=121, WhiB n=109, WhiB+FtsK+ParB n= 44, WhiB+FtsK n=13.

Phage-encoded WhiB in phages infecting *Streptomyces*

Since WhiB-like proteins were identified as the most frequently found development-associated protein in *Streptomyces* infecting phages, further analysis was focused on representatives of this family. Amino acid sequences of all 110 WhiB proteins from 109 phage genomes were aligned with 14 WhiB-like family proteins from the model species *Streptomyces venezuelae* NRRL B-65442. Phage-encoded WhiB-like proteins range in size between 55 aa and 250 aa, while WhiB-like sequences from *S. venezuelae* have sizes from 82 aa to 227 aa. Except for phages Jay2Jay and

BRock, all four invariant cysteines are conserved among sequences. Interestingly, these two phages encode the shortest WhiB-like proteins, with Jay2Jay (55 aa) missing the first and BRock (82 aa) the second cysteine residue potentially failing to form the Fe-S cluster. The conserved middle region of a subset of 39 phage- and host encoded WhiB-like representative sequences is compared in Figure 3. The known five residue motif (G[V/I]WGG) of the host WhiB-like proteins can be found in phage sequences as well but is slightly modified in some cases swapping for example the tryptophan with arginine in 13 cases. In eight of these sequences, this is accompanied by an exchange of the first glycine with threonine. 15 other phages use threonine instead of valine or isoleucine.

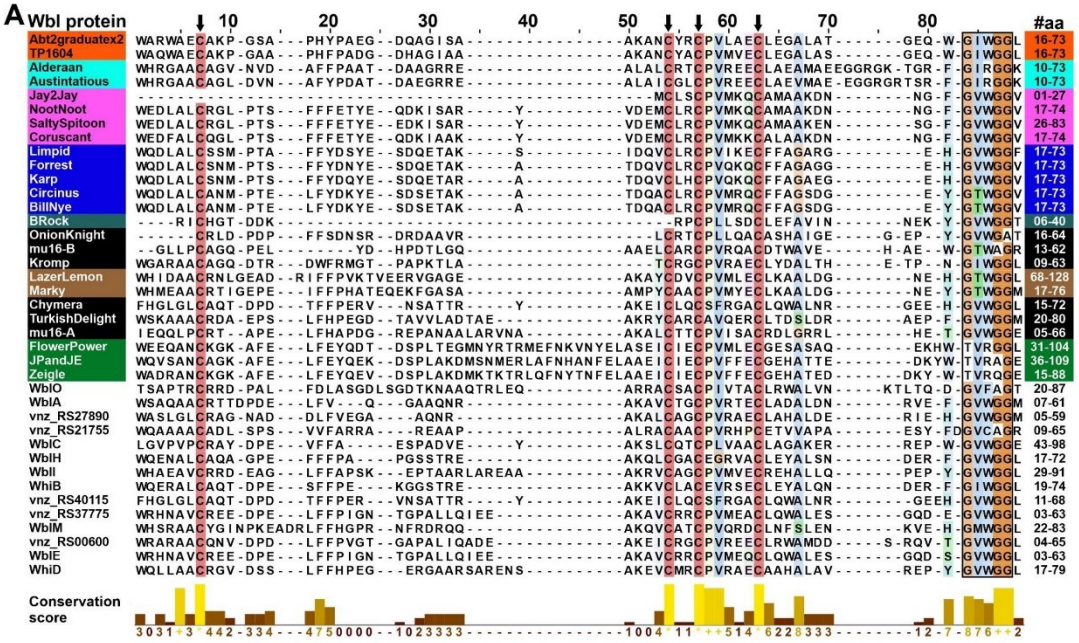

Figure 3: Multiple sequence alignment of WhiB-like transcriptional regulators. Shown are the conserved middle regions of a representative subset of 39 host- and phage-encoded WhiB-like transcriptional regulators. The full sequences of all 124 proteins were aligned using MUSCLE algorithm in MEGAX and arranged in Jalview. Labels of phage-encoded Wbl proteins are highlighted according to their actinobacteriophage cluster in red (BG), turquoise (BC), pink (BE), blue (BK), petrol (BS), brown (BH), green (BF) and black (singleton). *S. venezuelae* sequence labels are white. The alignment shows the four conserved cysteines (black arrows) and the (G[V/I]GG) motif (box). For each position the conservation score is given based on physico-chemical properties calculated according to the AMAS method for all 124 Wbl proteins (Livingstone & Barton, 1993).

Phylogenetic analysis of the phage-encoded WhiB-like proteins highlights the great diversity between these proteins but resembles the known actinobacteriophage cluster (Figure SA). Known isolation hosts are only rarely fitting to specific clusters in our analysis. Focusing on a smaller set of WhiB family proteins, only WhiB-like sequences from phages infecting *S. venezuelae* (Alderaan, PapayaSalad, Austintatious, Bioscum, Ididsumtinwong, Coruscant and Chymera) were aligned with the host sequences and a phylogenetic tree was drawn in order to infer possibly similar functions

from clustering (Figure 4). Supporting bootstrap values are high (0.99) for grouping of WhiB-like from Alderaan, PapayaSalad, Austintatious, Bioscum and Ididsumtinwong. But the formation of a sister group with host-encoded WblM is not very well supported (0.30). Additionally, the function of WblM is not yet known. Coruscant appears to be placed randomly next to this supported only by a bootstrap of 0.10. Most interesting, the WhiB-like protein encoded by Chymera (and the host version of this prophage-encoded Wbl proteins, vnz_RS40115) formed a sister group (0.54) to host-encoded WhiB and WblH.

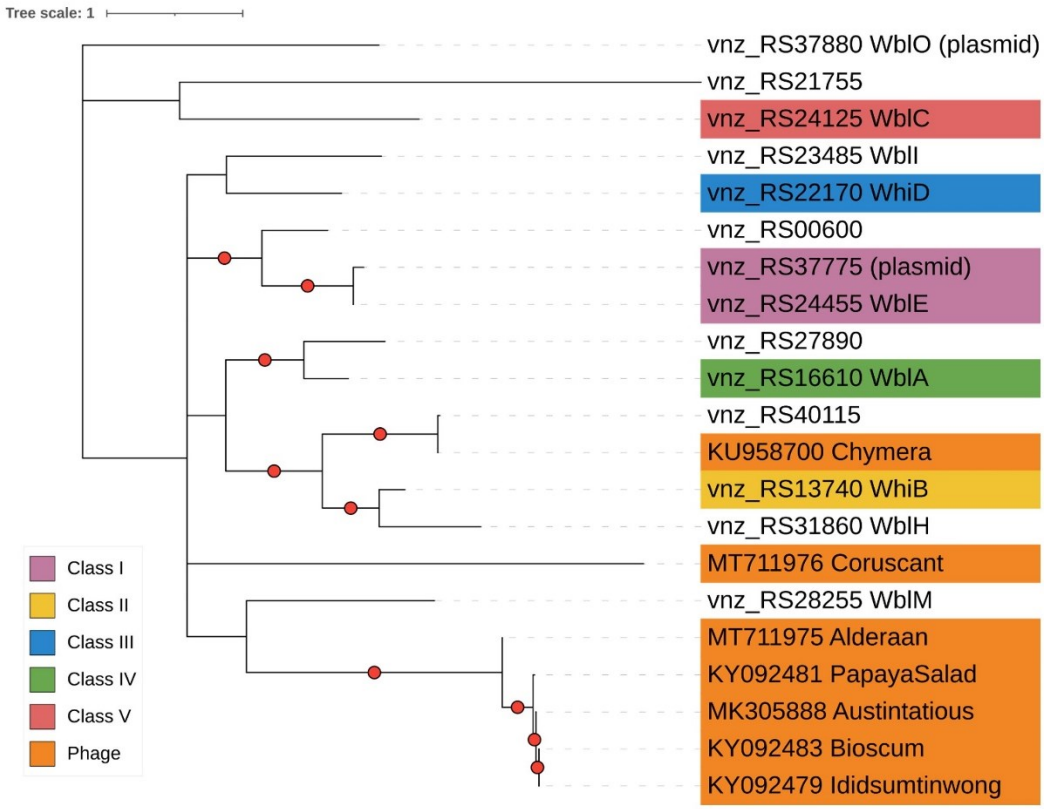

Figure 4: Phylogenetic tree of WhiB-like proteins from *S. venezuelae* and phages infecting *S. venezuelae*. Protein sequences were aligned in MEGA X using MUSCLE and phylogenetic analysis was performed using the WAG+G+I+F as best fit model. iTol was used for visualization of the tree. Bootstrap values from 500 replicates over 50% are marked by a red dot. Labels are color-coded according to the five classes of paralogues and the origin of sequence.

Phage-encoded WhiB-like regulators affect host morphology plaque size

In order to get insights into possible functions of phage-encoded WhiB-like proteins we used a Δ*whiB* strain of *S. venezuelae*, unable to sporulate (Bush et al., 2016). The ability to sporulate again and form the green spore pigment, can be restored by complementing this strain with host *whiB*

expressed under the native promoter on a plasmid (Figure 5A). The same approach expressing *whiB* from phages Alderaan, Coruscant and Chymera failed to restore this function and by that separating *S. venezuelae* WhiB function from these three phage-encoded proteins representing the known *S. venezuelae* phage WhiB-like diversity. Moreover, expressing phage *whiB* constitutively in the wild-type background during growth in fact revealed significant morphological differences after 24 h (Figure 5B). Compared to *S. venezuelae* WT, strains expressing *whiB* from Alderaan and Coruscant show longer mycelial structures with less branches and significantly less spores. In contrast, expression of *whiB* from Chymera appeared to be similar to an overexpression of host *whiB*, heavily sporulating after 24 hours of cultivation. This is a first prove of differences in function between phage-encoded WhiB-like proteins. It is important to note, that all strains expressing phage *whiB* are able to sporulate eventually. Although phage titer of Alderaan and Coruscant were the same on strains expressing different *whiB* (Figure 5C), plaque sizes tend to be smaller when expressing additional *whiB* from Chymera and *S. venezuelae* for infection with Alderaan and bigger when expressing *whiB* from Alderaan for infection with Coruscant (Figure 5D, E).

Phage-encoded WhiB is expressed during infection

To gain insights into the involvement of WhiB-like proteins during the phages life cycle, expression of the *whiB* genes from virulent phages Alderaan and Coruscant were monitored during infection using RT-qPCR and compared to the respective *minor tail* gene (Figure 6A). Expression of $whiB_{Alderaan}$ already started 5 minutes after infection, rising up to almost $\log_2$ relative expression of 6 at 120 minutes after infection. This is earlier than the *minor tail* gene with its earliest detected increase in expression 40 minutes after infection. Expression of $whiB_{Coruscant}$ started later and is slower with the first increase measured 20 minutes after infection reaching a $\log_2$ relative expression of approximately 4 at the end of the experiment.

Using RNA-sequencing to investigate the complete expression patterns of Alderaan during infection of *S. venezuelae* showed three main expression patterns (Figure 6B). Genes 1-8 and 38-50 are expressed early already after 5 minutes featuring increasing expression until 90 minutes after infection. This also includes *whiB* (gene 44) and a gene encoding a Cro-like transcriptional regulator, which showed the strongest expression at the early time points 5, 20 and 40 minutes after infection. Genes 9-32 are expressed late between 40 and 90 minutes after infection, comprising most of the morphological as well as lysis genes. Interestingly genes 33-37 are only weakly expressed at 90 minutes but not earlier. Here most genes encode for hypothetical proteins of unknown function. In the direct neighborhood of $whiB_{Alderaan}$ there are two hypothetical proteins, one DNA single strand annealing protein and a helix-turn-helix domain containing protein. Overall, the expression of *whiB* was weakest in comparison to the genes in close vicinity. These results characterize $Alderaan_{whiB}$ as an early gene of moderate expression during liquid infection of *S. venezuelae*.

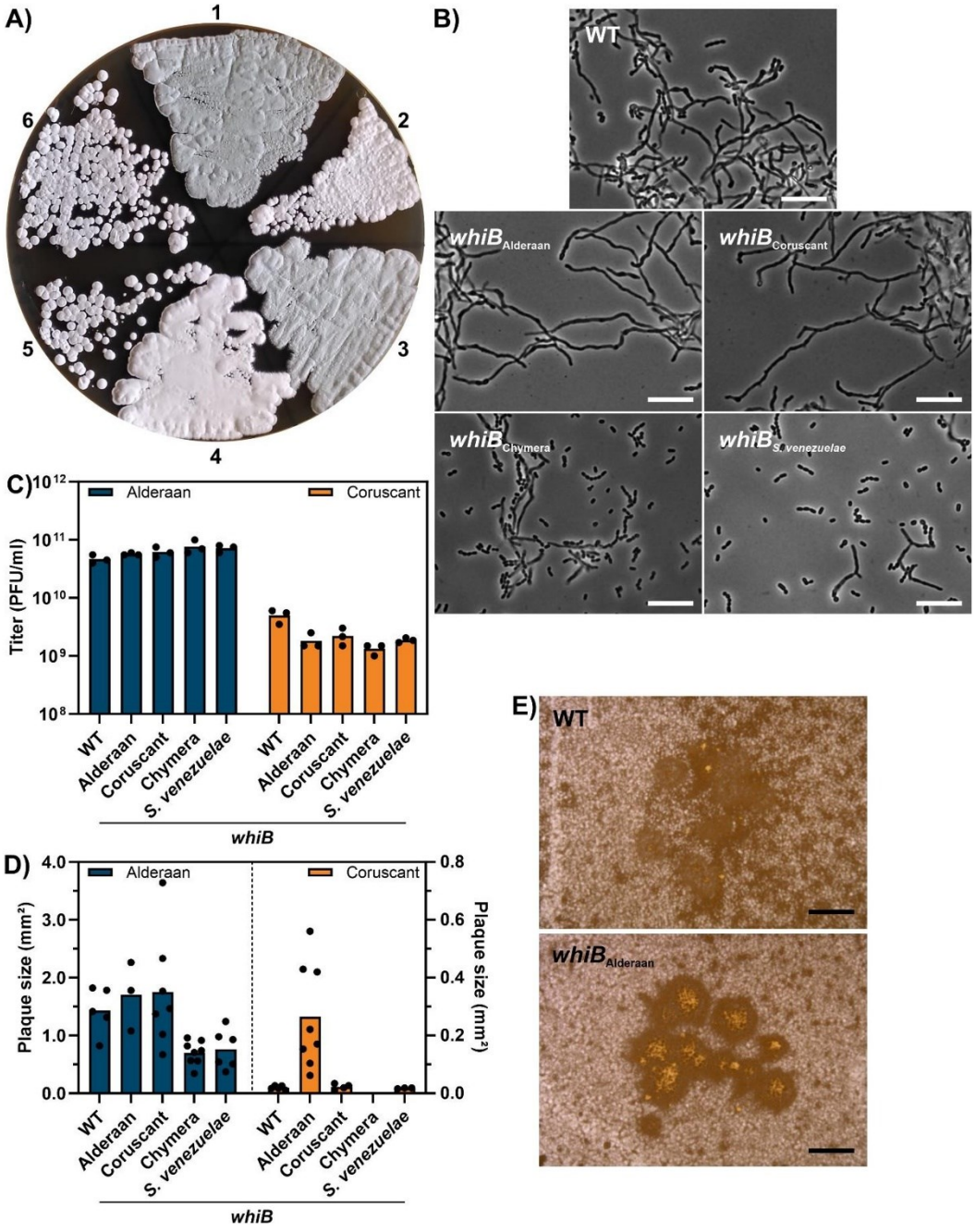

Figure 5: Phenotypic effects of phage-encoded WhiB in *S. venezuelae*. A) Comparison of the formation of the green spore pigment of the *S. venezuelae* WT (1) with the Δ*whiB* strain (2) and complementations with *whiB* from *S. venezuelae* (3), Alderaan (4), Coruscant (5) and Chymera (6) under the native host *whiB* promoter after 2 days on MYM agar. **B)** *S. venezuelae* WT and wild-type strains constitutively expressing *whiB* from Alderaan, Coruscant, Chymera and *S. venezuelae* grown for 24 h in GYM medium examined under the microscope show morphological differences. Scale bars represent 10 µm. **C)** Titer of Alderaan and Coruscant on strains expressing *whiB* are comparable to the ones of the WT. **D)** Plaque sizes of Alderaan and Coruscant on strains expressing *whiB* differ on some strains compared to the WT. **E)** Stereo microscope images of plaques formed by Coruscant infecting *S. venezuelae* WT and the strain expressing *whiB* from Alderaan. Scale bars represent 2 mm.

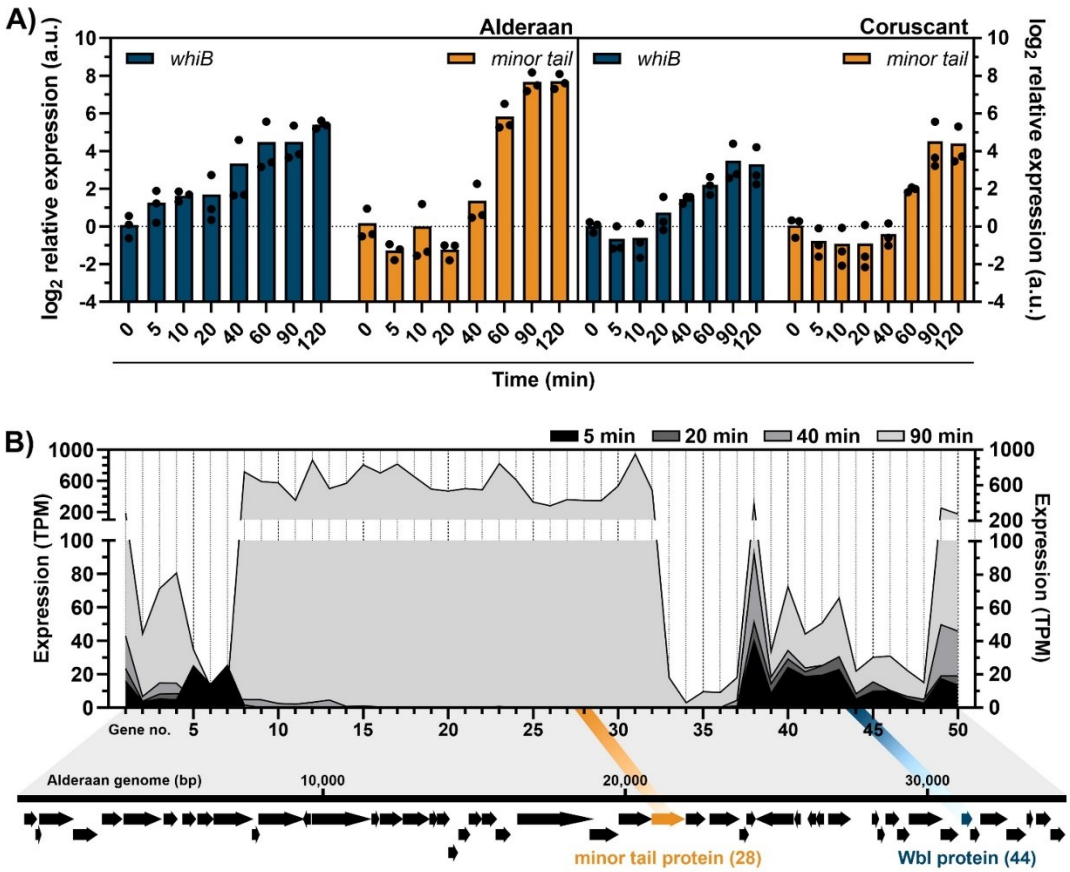

Figure 6: Gene expression of Alderaan and Coruscant during infection of *S. venezuelae*. A) log_2 relative expression from RT-qPCR of *whiB* and *minor tail* from Alderaan as well as *whiB* and *minor tail* of Coruscant. **B)** Expression of the complete Alderaan genome in transcripts per million (TPM) from RNA-sequencing at 5, 20, 40 and 90 minutes after infection.

Discussion

In this study, we found five proteins involved in host development to be encoded in varying combinations in over one third of bacteriophages infecting *Streptomyces*. Especially the Actinobacteria specific WhiB-like family of transcriptional regulators is common among these phages. Using a larger set of *Streptomyces* phages searching for WhiB-encoding genes we were able to find all phages identified in a previous study (Sharma et al., 2021), additionally adding new ones but confirming the same ratio of phages harboring Wbl protein encoding genes. Except for one phage encoding an SsgA family protein, we did not find any other unique proteins involved in multicellular development of *Streptomyces*. As proteins belonging to FtsK, ParB and ParA families are in general important during cell division in all prokaryotes, DNA partitioning of plasmids and also known to be encoded by diverse bacteriophages infecting unicellular bacteria (Dedrick et al., 2016; Iyer et al., 2004), they cannot be considered distinct developmental genes although being involved

especially in sporulation of *Streptomyces*. But it is worth noting, that exactly these respective genes in *Streptomyces* are under transcriptional control of the canonical host WhiB (Bush et al., 2016). Taken into account that there were no other key regulators or developmental proteins of *Streptomyces* found to be encoded in these phages, it seems unlikely that they are in general heavily interfering with their host development except for using WhiB-like proteins. The striking association of encoding WhiB-like proteins with being virulent clearly rules out a function in lysis-lysogeny decision making as it is for example described for the Cro/CI transcriptional regulators from phage λ (Oppenheim et al., 2005).

Presence of the [4Fe-4S] cluster coordinated by four conserved cysteine residues was shown to be essential for protein-protein interactions with sigma factors in *S. venezuelae* as well as *Mycobacterium tuberculosis* (Burian et al., 2013; Lilic et al., 2023; Stewart et al., 2020). Most investigated phages in this study also contain all four cysteine residues with the last three of them always having the exact same spacing. Therefore, formation of the [4Fe-4S] cluster is likely to be conserved in the phage proteins as well. This was already proven to be relevant for the correct functioning of the phage-encoded WhiB of mycobacterial phage TM4 (Rybniker et al., 2010). Furthermore, the previously described (G[V/I]WGG) motif close to the last cysteine, facing the cluster is hypothesized to play an additional role in interaction (Soliveri et al., 2000). As this motif and the three preceding residues were shown to determine specificity in terms of sigma factor binding (Burian et al., 2013; Bush, 2018; Casonato et al., 2012), the observed changes in phage homologues probably modulate the affinity towards different sigma factors or other interaction partners.

Phage-encoded WhiB-like proteins are highly diverse and grouping is in accordance with known actinobacteriophage clusters but seems to be mostly independent of the known isolation hosts. This probably is a result of incomplete host range data for all phages and can additionally be attributed to the fact that the different WhiB-like paralogues from different *Streptomyces* species are clustering together forming functional classes (Bush, 2018). This leads to the hypothesis that phage WhiB-like diversity is greater compared to that of host WhiB-like proteins and suggests that distinct functions may have emerged in phages.

Although the phylogeny suggests closest similarity between WhiB and WblH from *Streptomyces* with the prophage encoded WhiB-like of Chymera, in our assays the function of WhiB and Chymera encoded WhiB-like regulators are not the same even when regulated under the same promoter. Nevertheless, expressed constitutively in addition to the regulated host WhiB, both *Streptomyces* WhiB and Chymera WhiB are similar in terms of faster sporulation compared to the wild-type strain. Comparably to what was observed for Alderaan infection of the hypersporulating strain Δ*bldD*, WhiB-induced sporulation also interferes with phage propagation resulting in smaller plaque sizes (Luthe et al., 2023). Although initial susceptibility was not affected, similar to the WhiB-like protein from mycobacteriophage TM4, production of phage-encoded WhiB-like proteins has consequences for the success of other phages. This aligns with the overall notion of phage-phage competition often

seen in temperate phages (Ko & Hatfull, 2018; Owen et al., 2021; Rybniker et al., 2010). On the other hand, expression of *whiB* from Alderaan improves infection with Coruscant resulting in larger plaque sizes. Most importantly, although morphological changes are similar, this distinguishes Alderaan from Coruscant encoded WhiB-like protein function as the one from Coruscant has no such improving effect on Alderaan infection.

In order to shed light on how these transcriptional regulators are contributing to phage infection, future work has to establish methods for in-depth functional investigations. Studies of transcription regulation in *Streptomyces*, including the WhiB-like family, so far used chromatin immunoprecipitation sequencing and pull down assays in order to elucidate the regulon and interaction partners of WhiB (Bush et al., 2013, 2016; Lilic et al., 2023). These techniques are essential next steps in order to understand the full impact of phage-encoded WhiB on infection. Attempts in deleting *whiB* genes from the phage genomes of Alderaan and Coruscant by using rebooting (Kilcher et al., 2018) and bacteriophage recombineering (Marinelli et al., 2008) so far were not successful. But comparing bacteriophage infection directly in presence and absence of *whiB* would be groundbreaking for further evaluation of its function and importance.

Material and Methods

Identifying developmental genes in bacteriophages

337 phages with complete and annotated genomes on NCBI GenBank associated with *Streptomyces* were collected (Table S1, Sheet 1) and used in a custom R script applying ape 5.6-2 (Paradis & Schliep, 2019) to search the annotation (both standard and RefSeq) with a list of 57 gene product names generally involved in the development of *Streptomyces* (Table S1, Sheet 2). Additional information about all phages was added to the combined findings from The Actinobacteriophage Database (phagesdb.org) and manual curation (Table S2). For visualization, a presence absence matrix was constructed using the ComplexHeatmap package in R (Gu et al., 2016).

Phylogenetic analysis of phage-encoded WhiB-like proteins

110 identified phage-encoded WhiB family proteins and 14 WhiB family proteins from *S. venezuelae* (or a subset of that) were analyzed in MEGA X (Kumar et al., 2018) by generating multiple sequence alignments of the amino acid sequences using MUSCLE (Edgar, 2004) and constructing a maximum-likelihood phylogenetic tree applying the WAG+G+I+F algorithm (Whelan & Goldman, 2001) with 500 bootstrap replicates. Visualization of the tree was done with iTOL (Letunic & Bork, 2021). Visualization of the multiple sequence alignment was performed using Jalview (Waterhouse et al., 2009).

Bacteria, phages and growth conditions

Table S3 lists information about the used bacteriophages Alderaan and Coruscant and Table S4 lists all bacterial strains used in this study. For standard liquid cultivation, strains were inoculated from spore stocks in GYM medium (per liter: 4 g glucose, 4 g yeast extract, 10 g malt extract, pH = 7.3) at 30 °C and 170 rpm. For growth of strains other than WT, indicated antibiotics were used at 10 µg/ml concentration. For solid growth, if not stated differently, GYM agar was used (GYM medium plus 2 g $CaCO_3$ per liter, 1.5% agar). During cloning, *Escherichia coli* strains DH5α and

ET12567/pUZ8002 were cultivated in LB medium supplemented with the respective antibiotics. The complementation assay, 10 µl spore stocks (for Δ*whiB* mycelial stock) were streaked on MYM agar (per liter: 4 g maltose, 4 g yeast extract, 10 g malt extract, 1.5% agar, 50% tap water, pH = 7.3) supplemented with 2 ml trace element solution per liter (Kieser et al., 2000) and incubated for 2 days at 30 °C.

Plasmid construction and cloning

PCR amplification and restriction digestion were performed as described in standard protocols (Sambrook & Russel, 2001). Gibson assembly was used for plasmid construction (Gibson, 2011). Synthesis of oligonucleotides and sequencing were performed by Eurofins Genomics (Ebersberg, Germany) and transfer of plasmids into *Streptomyces* spp. was done using conjugation through *E. coli* ET12567/pUZ8002 (MacNeil et al., 1992). All plasmids and oligonucleotides used can be found in Table S5 and S6.

Phage infection on solid media

Double agar overlays were performed using GYM soft agar without $CaCO_3$ and only 0.4% agar for the top layer. Spotting of 2 µl phage dilutions in SM buffer (0.1 M NaCl, 8 mM MgSO4, 50 mM Tris-HCl, pH = 7.5) onto double agar overlay incubated with the respective *S. venezuelae* strain at an initial OD_{450} = 0.4 from overnight cultures was used to quantify infectious phage particles. For imaging and measuring of plaques, 100 µl of a given phage dilution was mixed directly with the inoculated soft agar before plating. Stereomicroscope SMZ-18 (Nikon, Japan) was used as described previously (Luthe et al., 2023).

Microscopy

For microscopy, the Axio Imager M2 (Zeiss, Germany) was used. Liquid samples were spotted on 1% (w/v) agarose pads placed on microscope slides. Images were taken in brightfield with 1000x magnification using immersion oil. Processing of the images was done using the AxioVision software (Zeiss, Germany).

RT-qPCR and Transcriptome analysis

Infection for RT-qPCR (biological triplicates) and RNA-sequencing (biological duplicates) were performed identically in liquid cultures. GYM medium (50% tap water) was inoculated to an OD_{450} = 0.4 with overnight cultures of *S. venezuelae* NRRL B-65442. Overnight cultures were centrifuged 5 min at 4000 xg and 10 °C, the supernatant was discarded and the pellet resuspended in the needed volume of medium. Infection was performed with $1*10^9$ PFU/ml of the respective phage and incubated for 10 min at RT. For uninfected controls, the same volume of SM buffer was added instead of phages. In order to wash away unbound phage particles, the cultures were centrifuged 3 times for 3 min at 4000 xg and 10 °C. Incubation was at 30 °C and 120 rpm. Sampling for RT-qPCR was done at 0, 5, 10, 20, 40, 60, 90 and 120 minutes, for RNA-seq at 5, 20, 40 and 90 minutes after infection by centrifuging 3 min at 4000 xg and 4 °C, discarding the supernatant and freezing the pellets in liquid nitrogen. Pellets were stored at -80 °C until proceeded with RNA isolation using the Monarch Total RNA Miniprep Kit (New England Biolabs, USA).

Reference gene candidates for RT-qPCR were validated by PCR and RefFinder (Xie et al., 2023) on the basis of suitable genes previously found in *S. coelicolor* (Li et al., 2015) and used in *S. venezuelae* (Kever et al., 2022). Oligonucleotides used are listed in Table S6. RT-qPCR was performed using Luna Universal One-Step RT-qPCR Kit (New England Biolabs, USA). Relative expression was calculated for each gene of interest by using the geometric mean of multiple internal control genes (Vandesompele et al., 2002).

For RNA-seq analysis, depletion of rRNA, library preparation and sequencing were conducted by GENEWIZ (Germany). Analysis of sequencing results was performed using CLC genomics workbench v.20 (Qiagen, Germany) as described previously (Luthe et al., 2023). Briefly, trimming of adapter sequences, ambiguous nucleotides and low-quality reads (0.05) was performed after initial

quality control. Genome sequences of *S. venezuelae* (NZ_CP018074.1), its plasmid (NZ_CP018075.1) and Alderaan (MT711975.1) were used for mapping (costs for mismatch = 2, insertion = 3, deletion = 3, length fraction = 0.9, similarity fraction = 0.9, strand specificity both, max number of hits per read 10).

Acknowledgements

We thank the European Research Council (ERC Starting Grant 757563) and the Deutsche Forschungsgemeinschaft (SPP 2330, project 464434020) for financial support.

References

Alam, K., Mazumder, A., Sikdar, S., Zhao, Y.-M., Hao, J., Song, C., Wang, Y., Sarkar, R., Islam, S., Zhang, Y., & Li, A. (2022). *Streptomyces*: The biofactory of secondary metabolites. *Frontiers in Microbiology*, *13*, 968053. https://doi.org/10.3389/fmicb.2022.968053

Barka, E. A., Vatsa, P., Sanchez, L., Gaveau-Vaillant, N., Jacquard, C., Meier-Kolthoff, J. P., Klenk, H.-P., Clément, C., Ouhdouch, Y., & van Wezel, G. P. (2016). Taxonomy, Physiology, and Natural Products of Actinobacteria. *Microbiology and Molecular Biology Reviews : MMBR*, *80*(1), 1–43. https://doi.org/10.1128/MMBR.00019-15

Burian, J., Yim, G., Hsing, M., Axerio-Cilies, P., Cherkasov, A., Spiegelman, G. B., & Thompson, C. J. (2013). The mycobacterial antibiotic resistance determinant WhiB7 acts as a transcriptional activator by binding the primary sigma factor SigA (RpoV). *Nucleic Acids Research*, *41*(22), 10062–10076. https://doi.org/10.1093/nar/gkt751

Bush, M. J. (2018). The actinobacterial WhiB-like (Wbl) family of transcription factors. *Molecular Microbiology*, *110*(5), 663–676. https://doi.org/10.1111/mmi.14117

Bush, M. J., Bibb, M. J., Chandra, G., Findlay, K. C., & Buttner, M. J. (2013). Genes required for aerial growth, cell division, and chromosome segregation are targets of WhiA before sporulation in *Streptomyces venezuelae*. *MBio*, *4*(5), e00684-13. https://doi.org/10.1128/mBio.00684-13

Bush, M. J., Chandra, G., Bibb, M. J., Findlay, K. C., & Buttner, M. J. (2016). Genome-Wide Chromatin Immunoprecipitation Sequencing Analysis Shows that WhiB Is a Transcription Factor That Cocontrols Its Regulon with WhiA To Initiate Developmental Cell Division in *Streptomyces*. *MBio*, *7*(2), e00523-16. https://doi.org/10.1128/mBio.00523-16

Bush, M. J., Tschowri, N., Schlimpert, S., Flärdh, K., & Buttner, M. J. (2015). c-di-GMP signalling and the regulation of developmental transitions in streptomycetes. *Nature Reviews. Microbiology*, *13*(12), 749–760. https://doi.org/10.1038/nrmicro3546

Casonato, S., Cervantes Sánchez, A., Haruki, H., Rengifo González, M., Provvedi, R., Dainese, E., Jaouen, T., Gola, S., Bini, E., Vicente, M., Johnsson, K., Ghisotti, D., Palù, G., Hernández-Pando, R., & Manganelli, R. (2012). WhiB5, a transcriptional regulator that contributes to *Mycobacterium tuberculosis* virulence and reactivation. *Infection and Immunity*, *80*(9), 3132–3144. https://doi.org/10.1128/IAI.06328-11

Chater, K. F. (2016). Recent advances in understanding *Streptomyces*. *F1000Research*, *5*, 2795. https://doi.org/10.12688/f1000research.9534.1

Dedrick, R. M., Mavrich, T. N., Ng, W. L., Cervantes Reyes, J. C., Olm, M. R., Rush, R. E., Jacobs-Sera, D., Russell, D. A., & Hatfull, G. F. (2016). Function, expression, specificity, diversity and incompatibility of actinobacteriophage *parABS* systems. *Molecular Microbiology*, *101*(4), 625–644. https://doi.org/10.1111/mmi.13414

Demain, A. L. (1999). Pharmaceutically active secondary metabolites of microorganisms. *Applied Microbiology and Biotechnology*, *52*(4), 455–463. https://doi.org/10.1007/s002530051546

den Hengst, C. D., Tran, N. T., Bibb, M. J., Chandra, G., Leskiw, B. K., & Buttner, M. J. (2010). Genes essential for morphological development and antibiotic production in *Streptomyces coelicolor* are targets of BldD during vegetative growth. *Molecular Microbiology*, *78*(2), 361–

379. https://doi.org/10.1111/j.1365-2958.2010.07338.x
Edgar, R. C. (2004). MUSCLE: multiple sequence alignment with high accuracy and high throughput. *Nucleic Acids Research*, *32*(5), 1792–1797. https://doi.org/10.1093/nar/gkh340
Flärdh, K., & McCormick, J. R. (2017). The *Streptomyces* O-B one connection: a force within layered repression of a key developmental decision. *Molecular Microbiology*, *104*(5), 695–699. https://doi.org/10.1111/mmi.13688
Georjon, H., Tesson, F., Shomar, H., & Bernheim, A. (2023). Genomic characterization of the antiviral arsenal of Actinobacteria. *Microbiology (Reading, England)*, *169*(8). https://doi.org/10.1099/mic.0.001374
Gibson, D. G. (2011). Enzymatic assembly of overlapping DNA fragments. *Methods in Enzymology*, *498*, 349–361. https://doi.org/10.1016/B978-0-12-385120-8.00015-2
Gu, Z., Eils, R., & Schlesner, M. (2016). Complex heatmaps reveal patterns and correlations in multidimensional genomic data. *Bioinformatics (Oxford, England)*, *32*(18), 2847–2849. https://doi.org/10.1093/bioinformatics/btw313
Hardy, A., Sharma, V., Kever, L., & Frunzke, J. (2020). Genome Sequence and Characterization of Five Bacteriophages Infecting *Streptomyces coelicolor* and *Streptomyces venezuelae*: Alderaan, Coruscant, Dagobah, Endor1 and Endor2. *Viruses*, *12*(10), 1065. https://doi.org/10.3390/v12101065
Hatfull, G. F. (2020). Actinobacteriophages: Genomics, Dynamics, and Applications. *Annual Review of Virology*, *7*(1), 37–61. https://doi.org/10.1146/annurev-virology-122019-070009
Iyer, L. M., Makarova, K. S., Koonin, E. V, & Aravind, L. (2004). Comparative genomics of the FtsK-HerA superfamily of pumping ATPases: implications for the origins of chromosome segregation, cell division and viral capsid packaging. *Nucleic Acids Research*, *32*(17), 5260–5279. https://doi.org/10.1093/nar/gkh828
Kever, L., Hardy, A., Luthe, T., Hünnefeld, M., Gätgens, C., Milke, L., Wiechert, J., Wittmann, J., Moraru, C., Marienhagen, J., & Frunzke, J. (2022). Aminoglycoside Antibiotics Inhibit Phage Infection by Blocking an Early Step of the Infection Cycle. *MBio*, e0078322. https://doi.org/10.1128/mbio.00783-22
Kieser, T., Bibb, M., Chater, K., Butter, M., Hopwood, D., Bittner, M., & Buttner, M. (2000). *Practical Streptomyces Genetics: A Laboratory Manual*. John Innes Foundation.
Kilcher, S., Studer, P., Muessner, C., Klumpp, J., Loessner, M. J., & Adhya, S. (2018). Cross-genus rebooting of custom-made, synthetic bacteriophage genomes in L-form bacteria. *Proceedings of the National Academy of Sciences of the United States of America*, *115*(3), 567–572. https://doi.org/10.1073/pnas.1714658115
Ko, C.-C., & Hatfull, G. F. (2018). Mycobacteriophage Fruitloop *gp52* inactivates Wag31 (DivIVA) to prevent heterotypic superinfection. *Molecular Microbiology*, *108*(4), 443–460. https://doi.org/https://doi.org/10.1111/mmi.13946
Kumar, S., Stecher, G., Li, M., Knyaz, C., & Tamura, K. (2018). MEGA X: Molecular Evolutionary Genetics Analysis across Computing Platforms. *Molecular Biology and Evolution*, *35*(6), 1547–1549. https://doi.org/10.1093/molbev/msy096
Letunic, I., & Bork, P. (2021). Interactive Tree Of Life (iTOL) v5: an online tool for phylogenetic tree display and annotation. *Nucleic Acids Research*, *49*(W1), W293–W296. https://doi.org/10.1093/nar/gkab301
Li, S., Wang, W., Li, X., Fan, K., & Yang, K. (2015). Genome-wide identification and characterization of reference genes with different transcript abundances for *Streptomyces coelicolor*. *Scientific Reports*, *5*(1), 15840. https://doi.org/10.1038/srep15840
Lilic, M., Holmes, N. A., Bush, M. J., Marti, A. K., Widdick, D. A., Findlay, K. C., Choi, Y. J., Froom, R., Koh, S., Buttner, M. J., & Campbell, E. A. (2023). Structural basis of dual activation of cell division by the actinobacterial transcription factors WhiA and WhiB. *Proceedings of the National Academy of Sciences*, *120*(11). https://doi.org/10.1073/pnas.2220785120
Livingstone, C. D., & Barton, G. J. (1993). Protein sequence alignments: a strategy for the hierarchical analysis of residue conservation. *Bioinformatics*, *9*(6), 745–756. https://doi.org/10.1093/bioinformatics/9.6.745
Luthe, T., Kever, L., Hänsch, S., Hardy, A., Tschowri, N., Weidtkamp-Peters, S., & Frunzke, J. (2023). *Streptomyces* development is involved in the efficient containment of viral infections. *MicroLife*. https://doi.org/10.1093/femsml/uqad002
MacNeil, D. J., Gewain, K. M., Ruby, C. L., Dezeny, G., Gibbons, P. H., & MacNeil, T. (1992).

Analysis of *Streptomyces avermitilis* genes required for avermectin biosynthesis utilizing a novel integration vector. *Gene*, *111*(1), 61–68. https://doi.org/10.1016/0378-1119(92)90603-m

Marinelli, L. J., Piuri, M., Swigonová, Z., Balachandran, A., Oldfield, L. M., van Kessel, J. C., & Hatfull, G. F. (2008). BRED: a simple and powerful tool for constructing mutant and recombinant bacteriophage genomes. *PloS One*, *3*(12), e3957. https://doi.org/10.1371/journal.pone.0003957

Ongenae, V., Mabrouk, A. S., Crooijmans, M., Rozen, D., Briegel, A., & Claessen, D. (2022). Reversible bacteriophage resistance by shedding the bacterial cell wall. *Open Biology*, *12*(6), 210379. https://doi.org/10.1098/rsob.210379

Oppenheim, A. B., Kobiler, O., Stavans, J., Court, D. L., & Adhya, S. (2005). Switches in bacteriophage lambda development. *Annual Review of Genetics*, *39*, 409–429. https://doi.org/10.1146/annurev.genet.39.073003.113656

Owen, S. V, Wenner, N., Dulberger, C. L., Rodwell, E. V, Bowers-Barnard, A., Quinones-Olvera, N., Rigden, D. J., Rubin, E. J., Garner, E. C., Baym, M., & Hinton, J. C. D. (2021). Prophages encode phage-defense systems with cognate self-immunity. *Cell Host & Microbe*, *29*(11), 1620-1633.e8. https://doi.org/10.1016/j.chom.2021.09.002

Paradis, E., & Schliep, K. (2019). ape 5.0: an environment for modern phylogenetics and evolutionary analyses in R. *Bioinformatics*, *35*(3), 526–528. https://doi.org/10.1093/bioinformatics/bty633

Rybniker, J., Nowag, A., van Gumpel, E., Nissen, N., Robinson, N., Plum, G., & Hartmann, P. (2010). Insights into the function of the WhiB-like protein of mycobacteriophage TM4--a transcriptional inhibitor of WhiB2. *Molecular Microbiology*, *77*(3), 642–657. https://doi.org/10.1111/j.1365-2958.2010.07235.x

Sambrook, J., & Russel, D. (2001). *Molecular cloning: a laboratory manual* (3rd ed). Cold Spring Harbor Laboratory Press.

Schwartz, D. A., Lehmkuhl, B. K., & Lennon, J. T. (2022). Phage-Encoded Sigma Factors Alter Bacterial Dormancy. *MSphere*, e0029722. https://doi.org/10.1128/msphere.00297-22

Sharma, V., Hardy, A., Luthe, T., & Frunzke, J. (2021). Phylogenetic Distribution of WhiB- and Lsr2-Type Regulators in Actinobacteriophage Genomes. *Microbiology Spectrum*, *9*(3), e0072721. https://doi.org/10.1128/Spectrum.00727-21

Soliveri, J. A., Gomez, J., Bishai, W. R., & Chater, K. F. (2000). Multiple paralogous genes related to the *Streptomyces coelicolor* developmental regulatory gene whiB are present in *Streptomyces* and other actinomycetes. *Microbiology (Reading, England)*, *146 (Pt 2*, 333–343. https://doi.org/10.1099/00221287-146-2-333

Stewart, M. Y. Y., Bush, M. J., Crack, J. C., Buttner, M. J., & Le Brun, N. E. (2020). Interaction of the *Streptomyces* Wbl protein WhiD with the principal sigma factor σ(HrdB) depends on the WhiD [4Fe-4S] cluster. *The Journal of Biological Chemistry*, *295*(28), 9752–9765. https://doi.org/10.1074/jbc.RA120.012708

Vandesompele, J., De Preter, K., Pattyn, F., Poppe, B., Van Roy, N., De Paepe, A., & Speleman, F. (2002). Accurate normalization of real-time quantitative RT-PCR data by geometric averaging of multiple internal control genes. *Genome Biology*, *3*(7), research0034.1. https://doi.org/10.1186/gb-2002-3-7-research0034

Waterhouse, A. M., Procter, J. B., Martin, D. M. A., Clamp, M., & Barton, G. J. (2009). Jalview Version 2—a multiple sequence alignment editor and analysis workbench. *Bioinformatics*, *25*(9), 1189–1191. https://doi.org/10.1093/bioinformatics/btp033

Whelan, S., & Goldman, N. (2001). A General Empirical Model of Protein Evolution Derived from Multiple Protein Families Using a Maximum-Likelihood Approach. *Molecular Biology and Evolution*, *18*(5), 691–699. https://doi.org/10.1093/oxfordjournals.molbev.a003851

Xie, F., Wang, J., & Zhang, B. (2023). RefFinder: a web-based tool for comprehensively analyzing and identifying reference genes. *Functional & Integrative Genomics*, *23*(2), 125. https://doi.org/10.1007/s10142-023-01055-7

4. Appendix

In addition to the data provided in this section, supplementary information can be found online.

For chapter 4.1 “Supplementary material to 3.2 *Streptomyces* development is involved in the efficient containment of viral infections”, additional supplementary video S1 and S2 can be found under PMID 37223739 and https://doi.org/10.1093/femsml/uqad002. Table S5 is stored on Sciebo https://fz-juelich.sciebo.de/s/Gh8v3SJmSQfIBOh. RNA-seq raw data can be found under GEO accession GSE213718.

For chapter 4.2 “Supplementary material to 3.3 Phylogenetic distribution of WhiB- and Lsr2-Type Regulators in Actinobacteriophage Genomes”, additional supplementary tables S1, S2, S3, S4, S5 and S6 can be found under PMID 34817283 and https://doi.org/10.1128/Spectrum.00727-21.

4.1 Supplementary material to 3.2 *Streptomyces* development is involved in the efficient containment of viral infections

Supplementary Information to

Streptomyces development is involved in the efficient containment of viral infections

Tom Luthe[1], Larissa Kever[1], Sebastian Hänsch[2], Aël Hardy[1], Natalia Tschowri[3] Stefanie Weidtkamp-Peters[2], Julia Frunzke[1*]

[1]Institute of Bio- and Geosciences, IBG-1: Biotechnology, Forschungszentrum Jülich, 52425 Jülich, Germany

[2]Center for Advanced Imaging, Heinrich Heine Universität Düsseldorf, 40225 Düsseldorf, Germany

[3]Institute of Microbiology, Leibniz Universität Hannover, 30419 Hannover, Germany

*Corresponding author:

Julia Frunzke; Email: j.frunzke@fz-juelich.de, Phone: +49 2461 615430

Tables

Supplementary Table S1: Phages used in this study.

Supplementary Table S2: Bacterial strains used in this study.

Supplementary Table S3: Plasmids used in this study.

Supplementary Table S4: Oligonucleotides used in this study.

Supplementary Table S5: RNA-Sequencing Data (separate file). For transcriptome analysis of Alderaan infected mycelium from *S. venezuelae*, plaque interface samples were taken as described in Figure 7A and subsequently processed and analyzed as described in the material and methods section. Here we present a complete overview of the expression of Alderaan and *S.venezuelae* genes as transcripts per million from two replicates for each time point under infected and uninfected control conditions (Sheet 1). Additionally, we show the significantly ($p \leq 0.05$) differentially expressed genes as log2 fold changes at 24 h (Sheet 2) as well as 72 h (Sheet 3) after infection and from that filter developmental genes (Sheet 4), biosynthetic gene clusters (Sheet 5) and defense genes (Sheet 6).

Figures

Supplementary Figure S1: Plaque development on the *whiB* overexpressing strain and the *bldD* complementation SVNT11.

Supplementary Figure S2: Re-infection of mycelium from plaque interfaces.

Supplementary Figure S3: Plaque count of Alderaan on regrown *ΔbldD* mycelium from liquid infections.

Supplementary Figure S4: Liquid infection of *S. venezuelae* strains with Alderaan.

Supplementary Figure S5: Plaques of Alderaan on aged mycelium of *S. venezuelae*.

Supplementary Figure S6: Adsorption of phage Alderaan to *S. venezuelae*.

Supplementary Figure S7: Expression of the Chymera genome during infection of *S. venezuelae*.

Supplementary Figure S8: Plaque formation of Alderaan in presence of chloramphenicol.

Videos

Supplementary Video S1: Dynamics of plaque growth and constriction of *S. venezuelae* infected with phage Alderaan (separate file). A double agar overlay of phage Alderaan on *S. venezuelae* was performed on GYM agar and incubated for 18 h at 30 °C before live-imaging a single plaque for additional 72 h every hour under the stereomicroscope.

Supplementary Video S2: Infection of *S. venezuelae* explorer cells by phage Alderaan (separate file). *S. venezuelae* was grown for 6 days at 30 °C on YP agar supplemented with 10 mM $MgCl_2$ and 10 mM $CaCl_2$ before 4 µl of a 10^9 PFU/ml Alderaan solution were spotted on one edge of exploring cells. Live-images were taken under the stereomicroscope every 30 min for 65 h.

Tables

Supplementary Table S1: Phages used in this study.

Phage	Host organism	Taxonomy	Cluster (phagesdb.org)	Lifestyle	Reference
Alderaan	*S. venezuelae* NRRL B-65442	*Austintatiousvirus*	BC	Temperate[1,2] / Virulent[3,4]	(Hardy *et al.* 2020)
SV1	*S. venezuelae* NRRL B-65442	*Picardvirus*	BC	Temperate[1] / Virulent[3,5]	(Stuttard 1979)
phi A.streptomycini III	*S. griseus* DSM 40236	*Woodruffvirus*	BG	Virulent[1,3,4]	DSM 49153
P26	*S. griseus* DSM 40236	*Woodruffvirus*	BG	Virulent[1,3,4]	DSM 49026
Dagobah	*S. coelicolor* M145	Viruses	Singleton	Temperate[2,3,5]	(Hardy *et al.* 2020)
Endor1	*S. coelicolor* M145	*Camvirus*	BD	Temperate[1,2,3,5]	(Hardy *et al.* 2020)

[1]according to cluster; [2]according to PhageAl; [3]according to plaque morphology; [4]according to absence of integrase and lysogens; [5]according to literature

Supplementary Table S2: Bacterial strains used in this study.

Strain	Genotype	Reference
***Streptomyces venezuelae* NRRL B-65442**	Wild-type strain	(Gomez-Escribano *et al.* 2021)
S. venezuelae* Δ*bldD::apr	Δ*bldD::apr*	(Tschowri *et al.* 2014)
S. venezuelae* Δ*bldN::apr	Δ*bldN::apr*	(Bibb *et al.* 2012)
S. venezuelae* Δ*whiB::apr	Δ*whiB::apr*	(Bush *et al.* 2016)
***S. griseus* DSM 40236**	Wild-type strain	(Liu *et al.* 2005)
***S. coelicolor* M145**	*S. coelicolor* A3(2) lacking plasmids SCP1 and SCP2	(Kieser *et al.* 2000)
***S. venezuelae whiB*$_{Sven}$ OE**	*S. venezuelae* NRRL B-65442 carrying plasmid pIJ10257_*whiB*$_{Sven}$	This study
***S. venezuelae* Δ*bldD::apr* / pMS82-*bldD* (SVNT11)**	*S. venezuelae* Δ*bldD*::apr carrying plasmid pSVNT-3	This study
***Escherichia coli* DH5α**	*supE44 ΔlacU169 (f80lacZDM15) hsdR17 recA1 endA1 gyrA96 thi-1 relA1*	Invitrogen
***Escherichia coli* ET12567/pUZ8002**	*dam-13::Tn9 dcm-6 hsdMhsdR*, carrying plasmid pUZ8002	(MacNeil *et al.* 1992)

Supplementary Table S3: Plasmids used in this study.

Plasmid	Characteristics					Reference	
pIJ10257	Hyg^R; constitutive ermE* promoter; ΦBT1 phage integration site					(Hong *et al.* 2005)	
pMS82	Hyg^R; ΦBT1 phage integration site					(Gregory, Till and Smith 2003)	
Plasmid	**Characteristics**	**Template**	**Primer**	**Vector**	**Restriction enzymes**	**Sequencing primer**	**Ref.**
pIJ10257_*whiB*$_{Sven}$ OE	*whiB* vnz_RS13740 of *S. venezuelae*	*S. venezuelae* NRRL B-65442	1 + 2	pIJ10257	HindIII; NdeI	3 + 4	This study
pSVNT-3	*bldD* vnz_RS05310 with 534 bp upstream and 404 bp downstream of the ORF	*S. venezuelae* NRRL B-65442	5 + 6	pMS82	HindIII; KpnI	7 + 8	This study

Supplementary Table S4: Oligonucleotides used in this study.

Number	Name	Sequence
1	Sven_whiB_pIJ10257_fwd	AGAACAGGAGGCCCCATATGATGACCGAGTTGTTCCAGGA
2	Sven_whiB_pIJ10257_rev	AGAACCTAGGATCCAAGCTTTCAGACGGCGGCCTT
3	pIJ10257_seq_fw	TGGCACCGCGATGCTGTTGT
4	pIJ10257_seq_rev	TCAGCGAGCTGAAGAAAGAC
5	bldD_HindIII_pMS82_long_fw	GTCAAGCTTGATCTCGGTGCGGCCGATG
6	bldD_KpnI_pMS82_long_rev	CCTGGGTACCGAGCTCATCGCGACCTACG
7	pMS82-seq-fw	GATGTCATCAGCGGTGGAGT
8	pMS82-seq-rev	CTGATGTGCTCAGTATCAC

Figures

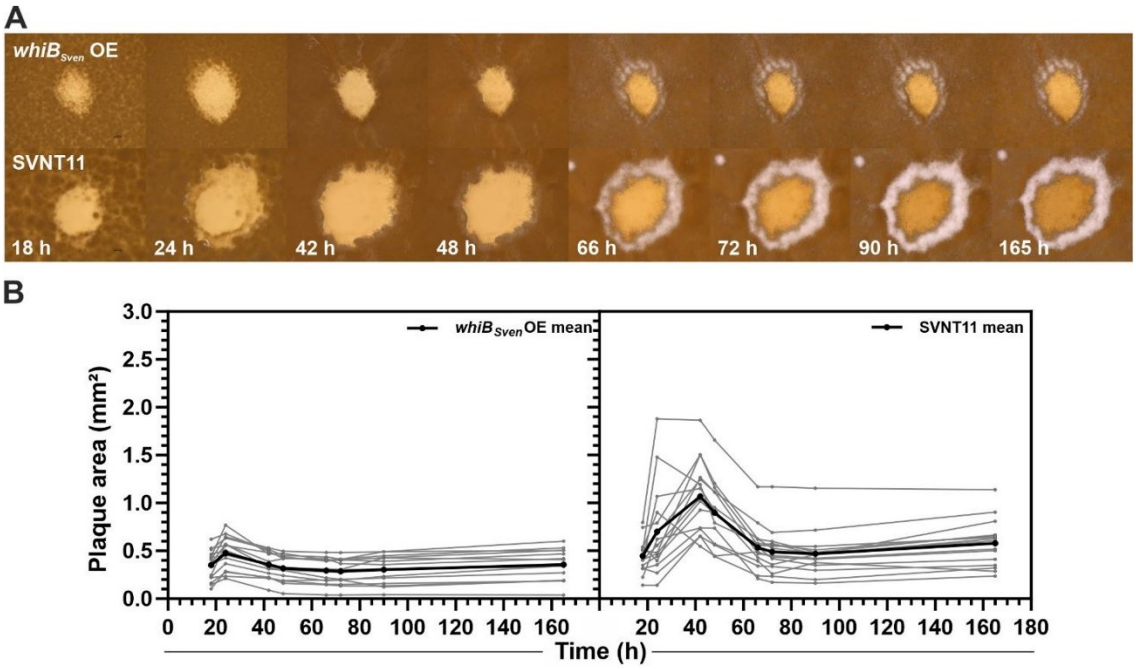

Supplementary Figure S1: Plaque development on the *whiB* overexpressing strain and the *bldD* complementation SVNT11. (A) Stereo microscope images of a single representative plaque for each strain taken at different time points after infection. **(B)** Plaque area (mm^2) of 15 randomly chosen plaques per strain with calculated means.

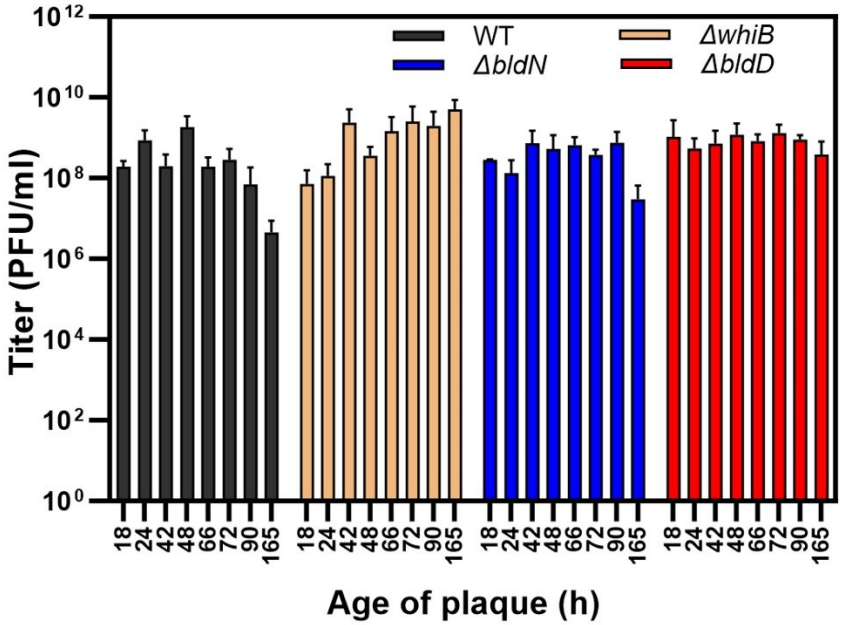

Supplementary Figure S2: Re-infection of mycelium from plaque interfaces. Samples were taken from plaque interfaces of differently aged plaques (n=3 for each strain and time point) and cultivated for 24 h in fresh medium before being used for double agar overlay assays.

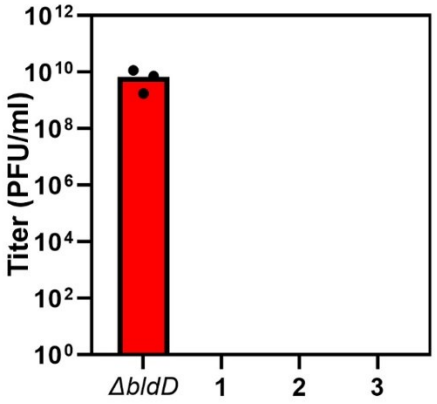

Supplementary Figure S3: Plaque count of Alderaan on *ΔbldD* mycelium regrown from liquid infections. Alderaan titer on *S. venezuelae* Δ*bldD::apr* (Δ*bldD*) and on the three regrown cultures during liquid infection harvested after 70 h (1, 2, 3). Spotting was performed in triplicates.

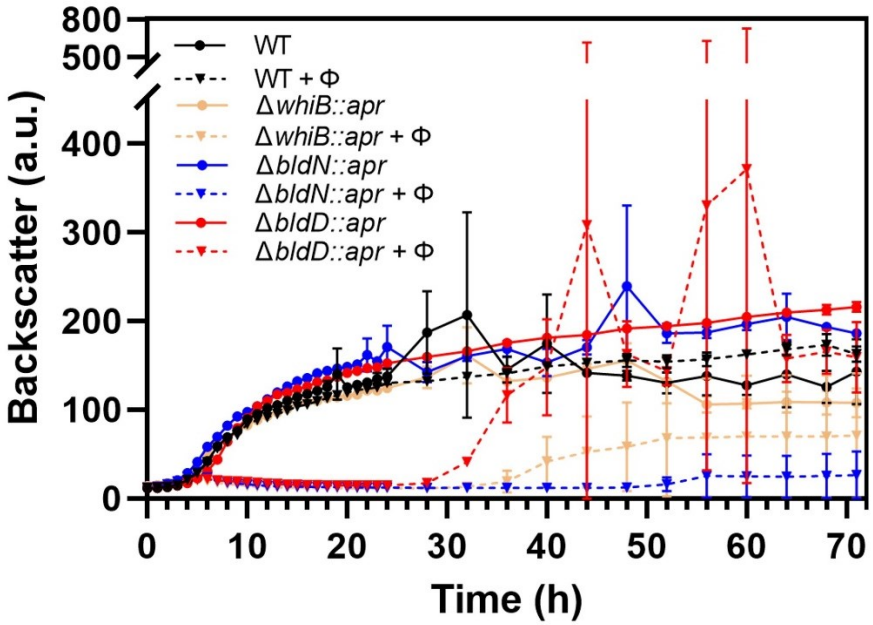

Supplementary Figure S4: Liquid infection of *S. venezuelae* wild type, Δ*whiB*, Δ*bldN* and Δ*bldD* with Alderaan. Infection was performed and growth was measured in the BioLector microcultivation system with an initial titer of 10^7 PFU/ml (n=3).

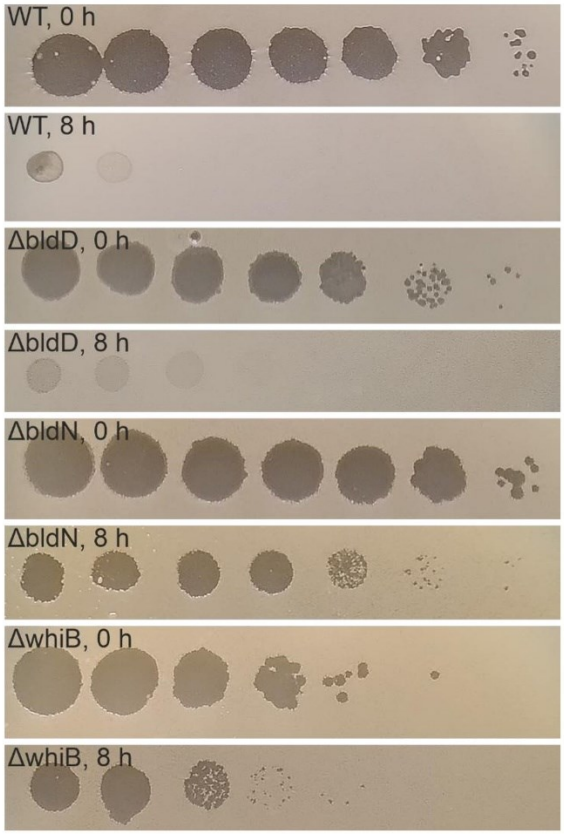

Supplementary Figure S5: Plaques of Alderaan on aged mycelium of *S. venezuelae*. Shown are representative plaques; further details are provided in Figure 6A.

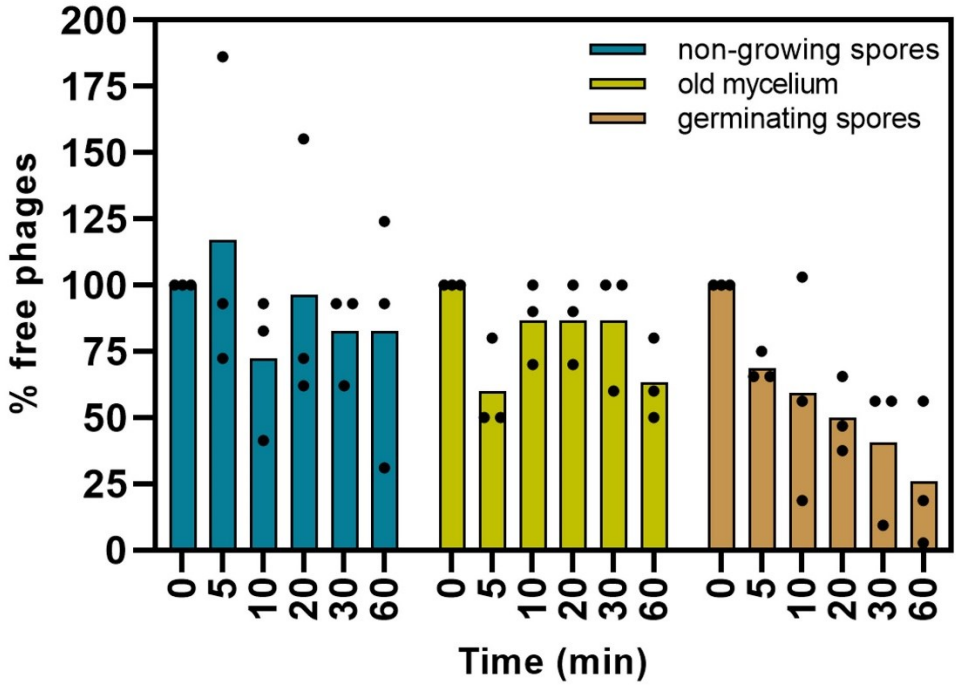

Supplementary Figure S6: Adsorption of phage Alderaan to *S. venezuelae*. 10^7 PFU/ml of phage Alderaan were added to different developmental stages of *S. venezuelae* liquid cultures. Spores were inoculated in SM buffer (turquois, non-growing) and GYM medium (brown, germinating) at a final concentration of 10^8 spores/ml (= OD_{450} of 0.15) and incubated for 4 h at 30 °C and 170 rpm. A mycelial stock from an overnight culture was used to inoculate GYM medium at a final OD_{450} of 0.15 and was grown for 24 h (yellow, old mycelium). Samples were taken at the indicated time points, centrifuged and supernatants were spotted to determine phage titers of biological triplicates and plot the percentage of free phages.

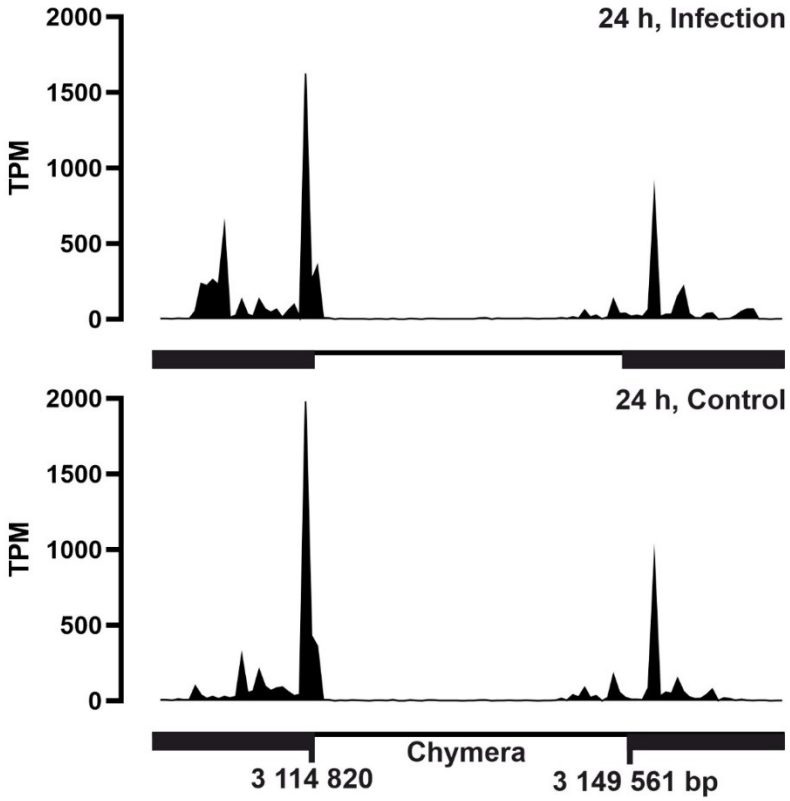

Supplementary Figure S7: Expression of the Chymera genome during infection of *S. venezuelae*. RNA-seq analysis of biological duplicates. Expression in transcripts per million (TPM) taken at 24 h from infected and uninfected (control) samples.

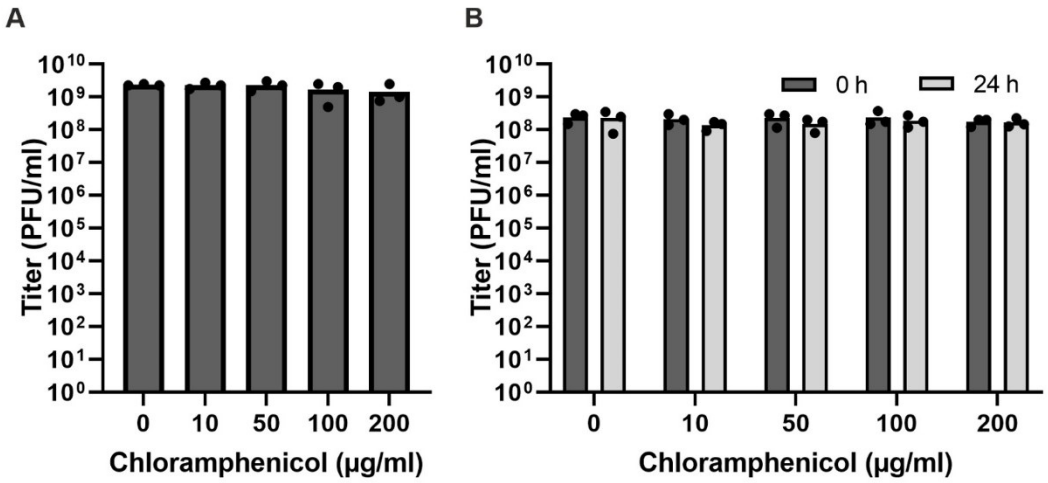

Supplementary Figure S8: Plaque formation of Alderaan in presence of chloramphenicol. The titer in PFU/ml was measured with Alderaan infecting *S. venezuelae* WT. **(A)** Different chloramphenicol concentrations were added to the bottom as well as the top agar. **(B)** Chloramphenicol was added to phage-containing SM buffer and incubated for 0 or 24 h at 30 °C and 900 rpm before spotting.

References

Bibb MJ, Domonkos A, Chandra G *et al.* Expression of the chaplin and rodlin hydrophobic sheath proteins in Streptomyces venezuelae is controlled by σ(BldN) and a cognate anti-sigma factor, RsbN. *Mol Microbiol* 2012;**84**:1033–49.

Bush MJ, Chandra G, Bibb MJ *et al.* Genome-Wide Chromatin Immunoprecipitation Sequencing Analysis Shows that WhiB Is a Transcription Factor That Cocontrols Its Regulon with WhiA To Initiate Developmental Cell Division in Streptomyces. *MBio* 2016;**7**:e00523-16.

Gomez-Escribano JP, Holmes NA, Schlimpert S *et al.* Streptomyces venezuelae NRRL B-65442: genome sequence of a model strain used to study morphological differentiation in filamentous actinobacteria. *J Ind Microbiol Biotechnol* 2021, DOI: 10.1093/jimb/kuab035.

Gregory MA, Till R, Smith MCM. Integration site for Streptomyces phage phiBT1 and development of site-specific integrating vectors. *J Bacteriol* 2003;**185**:5320–3.

Hardy A, Sharma V, Kever L *et al.* Genome Sequence and Characterization of Five Bacteriophages Infecting Streptomyces coelicolor and Streptomyces venezuelae: Alderaan, Coruscant, Dagobah, Endor1 and Endor2. *Viruses* 2020;**12**:1065.

Hong H-J, Hutchings MI, Hill LM *et al.* The Role of the Novel Fem Protein VanK in Vancomycin Resistance in Streptomyces coelicolor. *J Biol Chem* 2005;**280**:13055–61.

Kieser T, Bibb M, Chater K *et al. Practical Streptomyces Genetics: A Laboratory Manual*. Norwich: John Innes Foundation, 2000.

Liu Z, Shi Y, Zhang Y *et al.* Classification of Streptomyces griseus (Krainsky 1914) Waksman and Henrici 1948 and related species and the transfer of “Microstreptospora cinerea” to the genus Streptomyces as Streptomyces yanii sp. nov. *Int J Syst Evol Microbiol* 2005;**55**:1605–10.

MacNeil DJ, Gewain KM, Ruby CL *et al.* Analysis of Streptomyces avermitilis genes required for avermectin biosynthesis utilizing a novel integration vector. *Gene* 1992;**111**:61–8.

Stuttard C. Transduction of auxotrophic markers in a chloramphenicol-producing strain of Streptomyces. *J Gen Microbiol* 1979;**110**:479–82.

Tschowri N, Schumacher MA, Schlimpert S *et al.* Tetrameric c-di-GMP mediates effective transcription factor dimerization to control Streptomyces development. *Cell* 2014;**158**:1136–47.

Additional supplementary video S1 and S2 can be found under PMID 37223739 and https://doi.org/10.1093/femsml/uqad002. Table S5 is stored on Sciebo https://fz-juelich.sciebo.de/s/Gh8v3SJmSQfIBOh. RNA-seq raw data can be found under GEO accession GSE213718.

4.2 Supplementary material to 3.3 Phylogenetic distribution of WhiB- and Lsr2-Type Regulators in Actinobacteriophage Genomes

Supplementary Material

Title: Phylogenetic distribution of WhiB- and Lsr2-type regulators in actinobacteriophage genomes

Vikas Sharma[1*], Aël Hardy[1], Tom Luthe[1], and Julia Frunzke[1*]

[1]Institute of Bio- und Geosciences, IBG-1: Biotechnology, Forschungszentrum Jülich, 52425 Jülich, Germany

*Corresponding authors:

Vikas Sharma; Email: v.sharma@fz-juelich.de; Phone: +49 2461 612544

Julia Frunzke; Email: j.frunzke@fz-juelich.de; Phone: +49 2461 615430

Content:

Legends of supplementary tables

Supplementary Figures

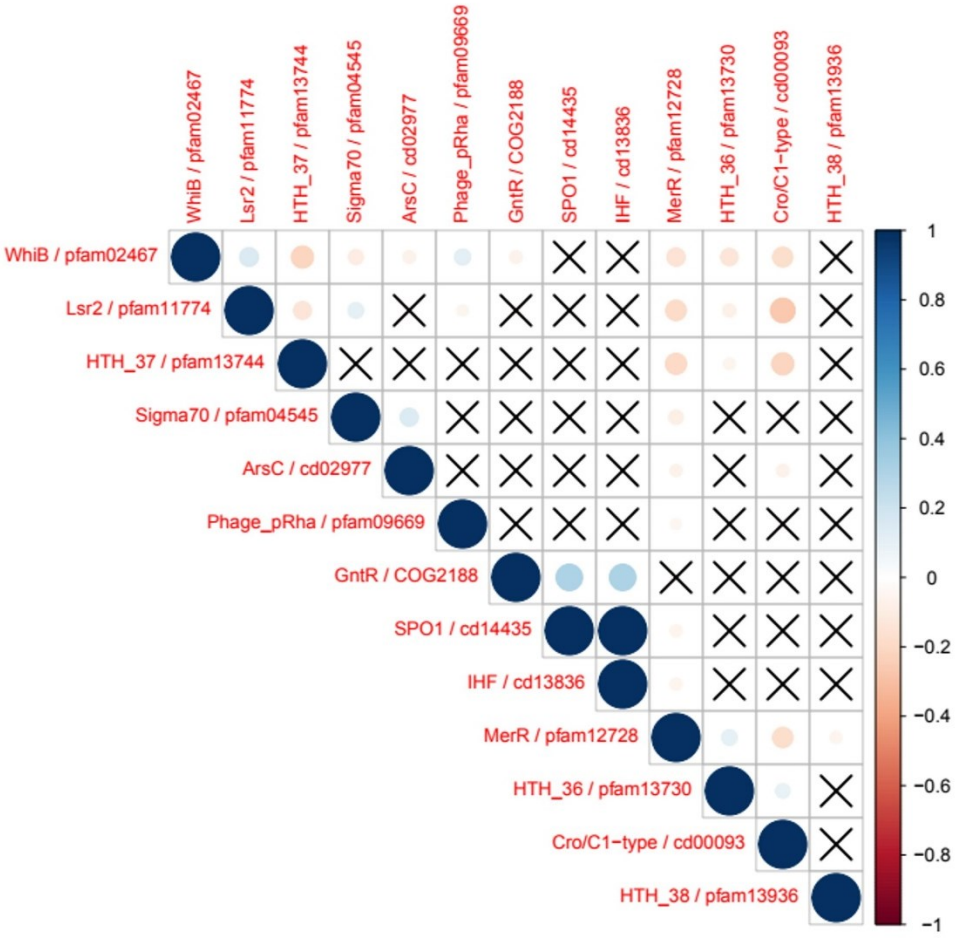

Fig. S1: Correlation heatmap matrix of the thirteen identified regulatory protein domains within actinobacteriophages. Circle color (Dark red: high negative correlation, Dark blue: high positive correlation) and the size indicate the correlation significance. Insignificant coefficients between the variables are denoted with the cross marks "X." Interestingly, this analysis revealed a negative correlation between Cro/CI and Lsr2 domains, suggesting that phage genomes rarely share these two different type of repressors.

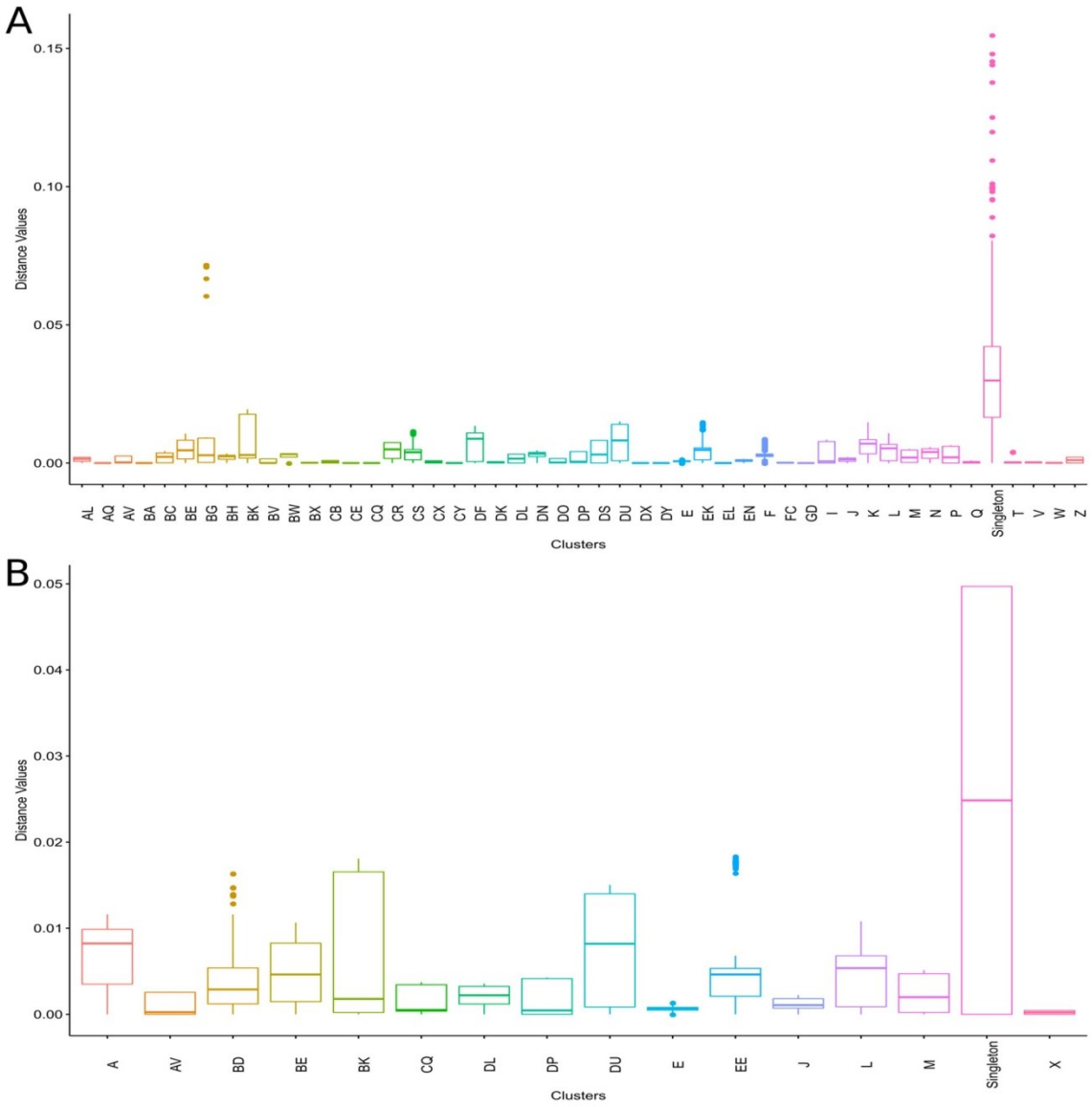

Fig. S2: Pairwise distance between different actinobacteriophage clusters calculated using Jensen-Shannon divergence method (1). A. Boxplot representation shows the pairwise distance between WhiB-encoding phages. B. Boxplot representation shows the pairwise distance between Lsr2-encoding phages.

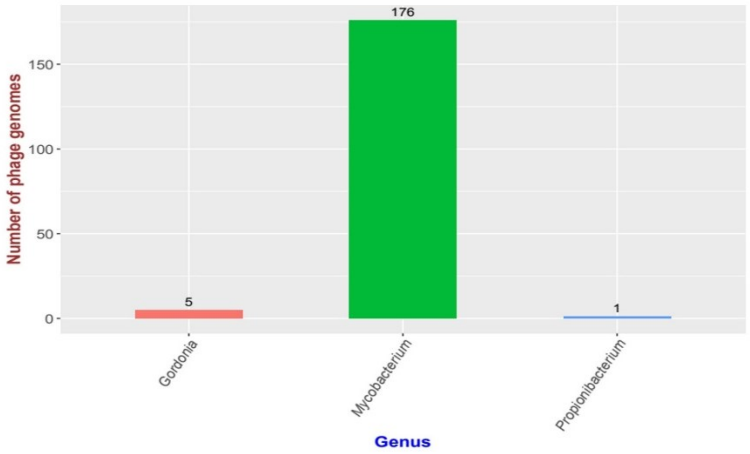

Fig.S3: Bar-plot displaying the distribution of actinobacteriophage genomes that encode two copies of *whiB* genes according to their host genus.

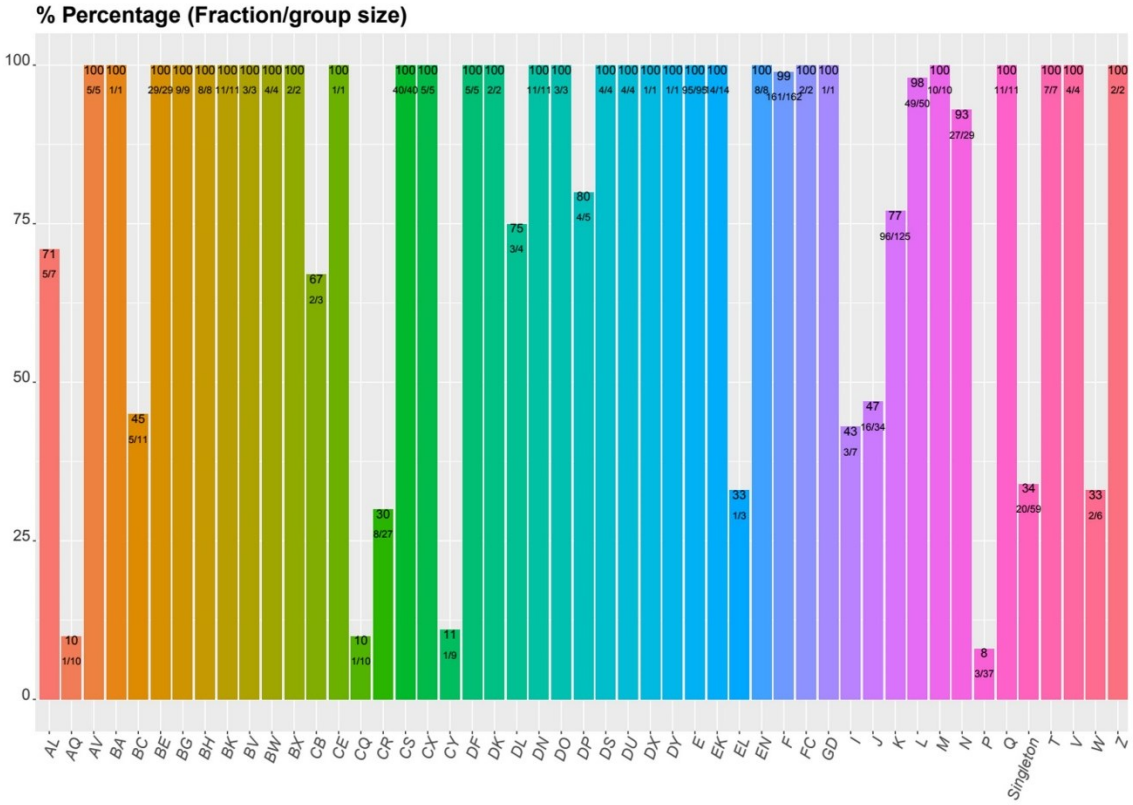

Fig. S4: Bar-plot representing the actual count and proportion of WhiB-encoding phages according to the known clusters.

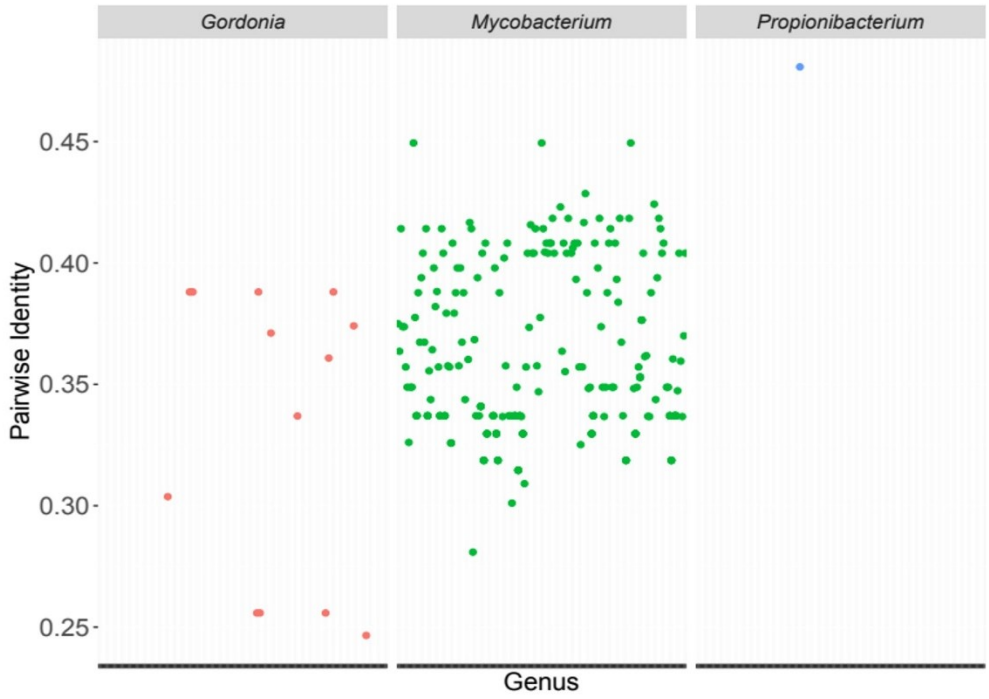

Fig.S5: Dot-plot represents the global protein pairwise sequence identity between phage-encoded *whiB* gene copies per genome according to their host genus.

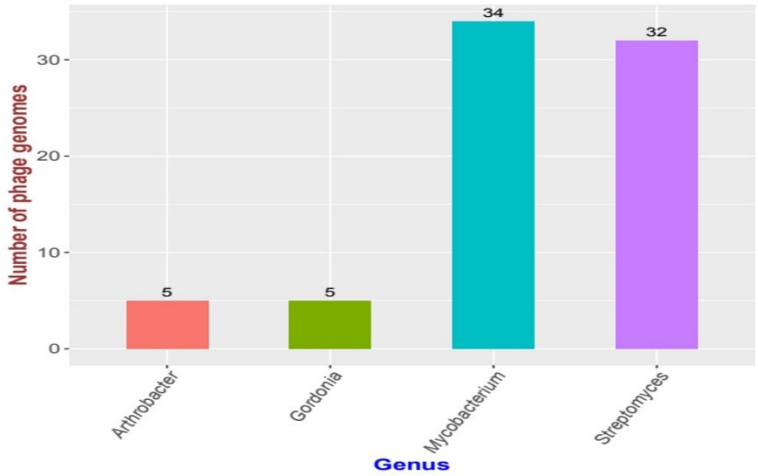

Fig. S6: Bar-plot displays the distribution of actinobacteriophage genomes that encode two copies of *lsr2* genes according to their host genus.

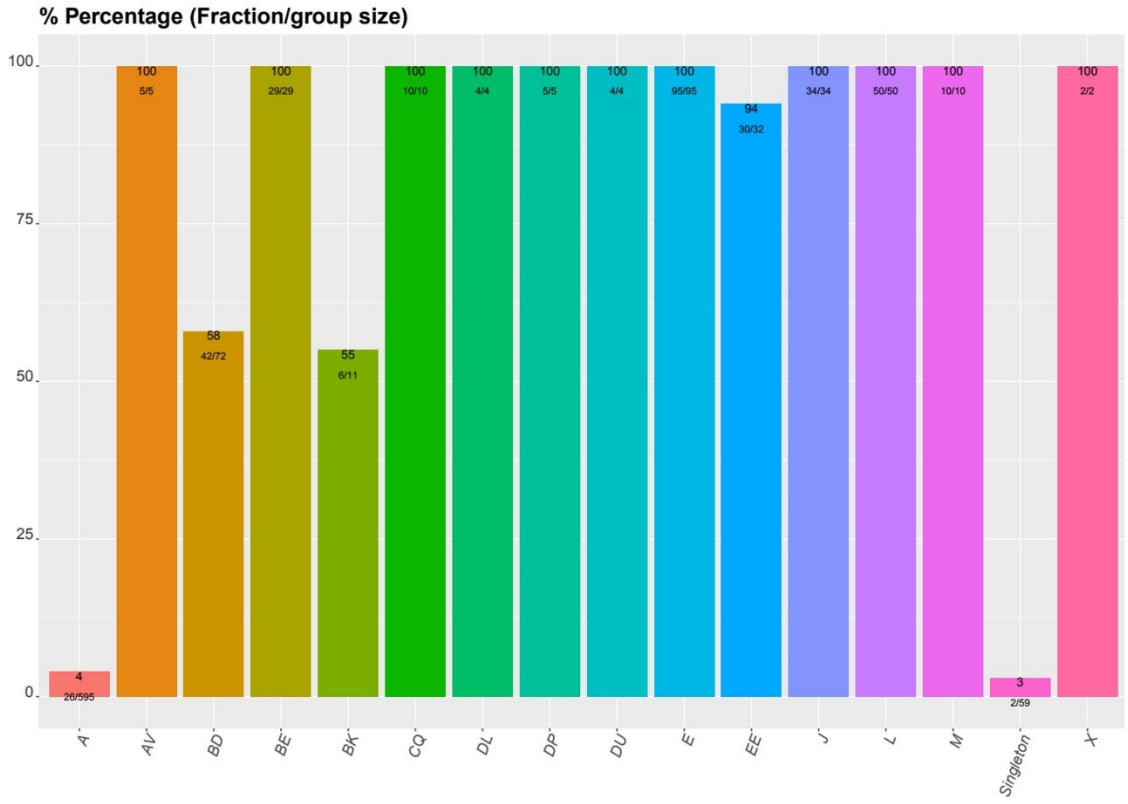

Fig. S7: Bar-plot representing the actual count and proportion of Lsr2-encoding phages according to the known clusters.

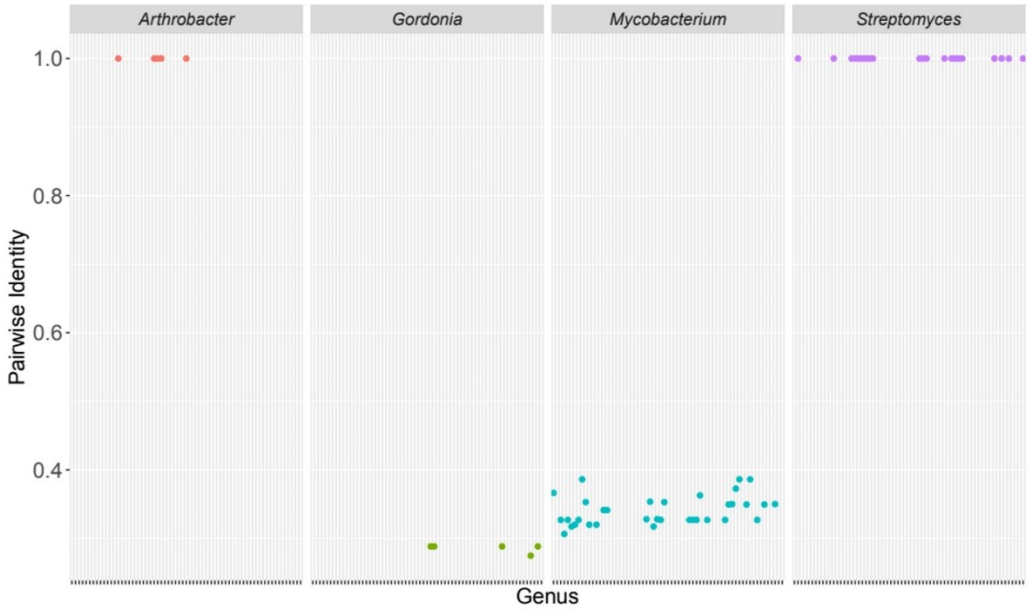

Fig.S8: Dot-plot represents the global protein pairwise sequence identity between phage-encoded *lsr2* gene copies per genome according to their host genus. Please note, in the case of *Athrobacter* and *Streptomyces*, the *lsr2* gene copies are found in the direct repeat regions of the phages, sharing 100% of sequence identity.

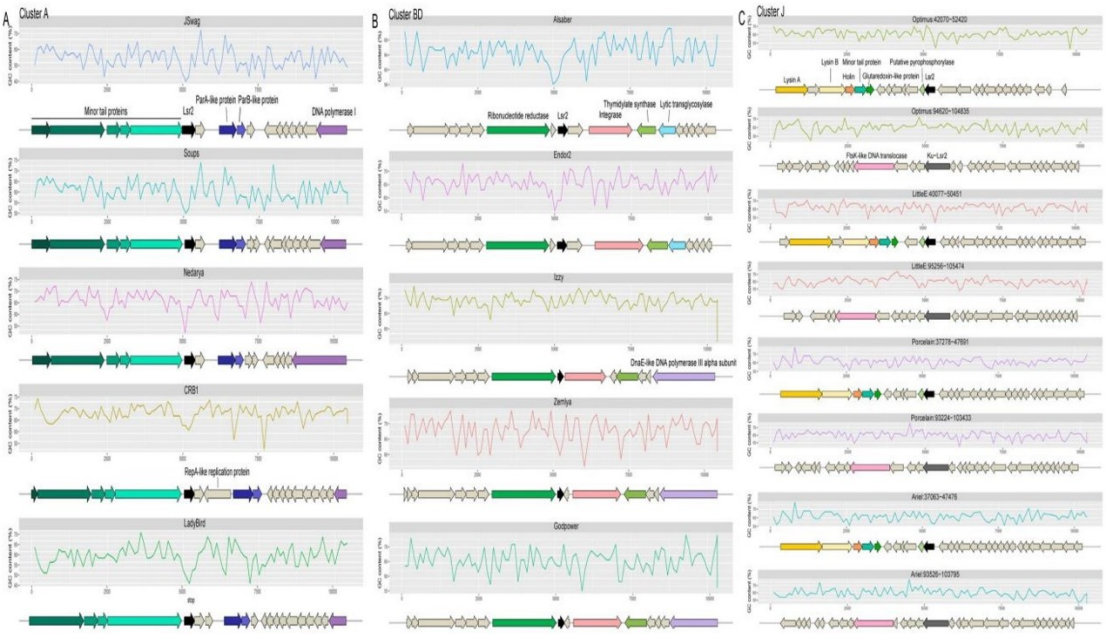

Fig. S9.A-C: Gene synteny plot showing the 5 kb regions flanking *lsr2* across randomly selected representative phage genomes of cluster A, BD and J, following the cluster assignment determined by phagesDB (2). GC content is displayed above the gene synteny plot for all genomes.

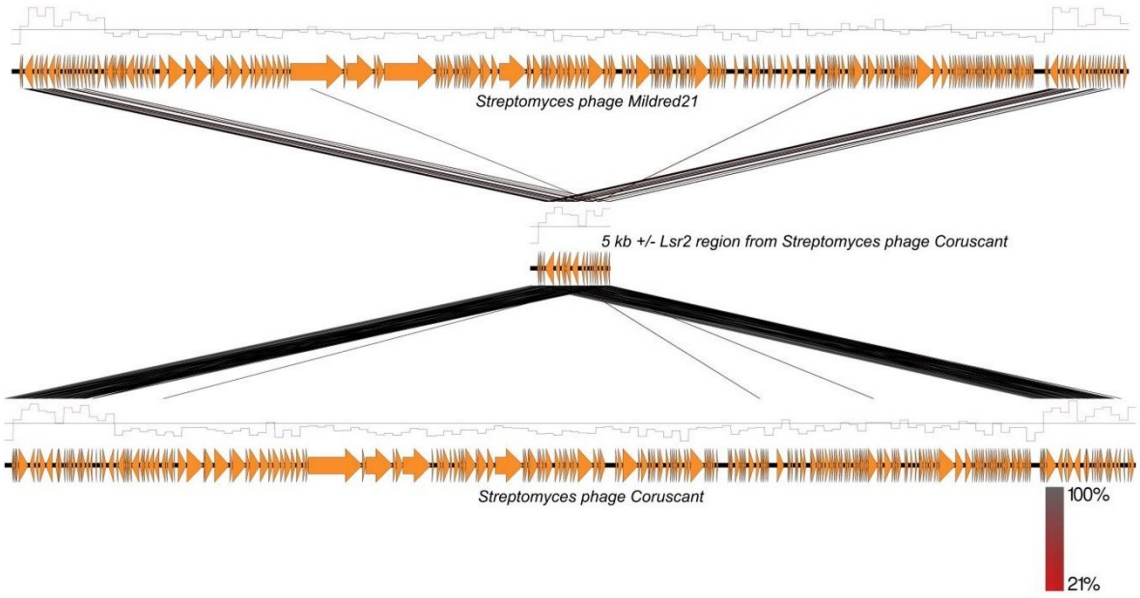

Fig. S10: Lsr2 homologs encoded by *Streptomyces* phages of the BE cluster are located in GC-rich, long direct terminal repeats. Genome comparison of two *Streptomyces* phages (Mildred21 & Coruscant) against the 10-kb region centered around Lsr2, visualized using Easyfig v 2.2.2 software (3). Gray shades show conserved regions with a high level of sequence identity, as calculated based on tBLASTx (4). Arrows indicate open reading frames (ORFs), and GC content is indicated on top of the genomes.

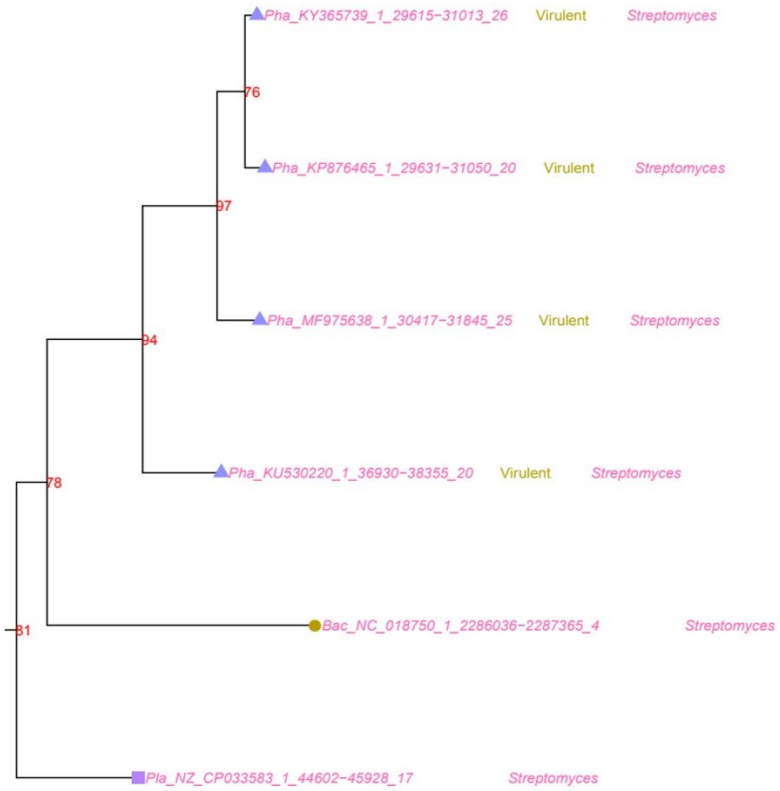

Fig. S11: WhiB phylogenetic subclade suggesting the acquisition of *whiB* by virulent *Streptomyces* phages from their host species. Tree tips shape indicate sequence source (bacteria: circle, phage: triangle, and plasmid: square). Sequences are color-coded according to the host genus. Phage lifestyle and genus information are shown on the right. Confidence values displayed on the nodes were estimated based on SH test using FastTree (5).

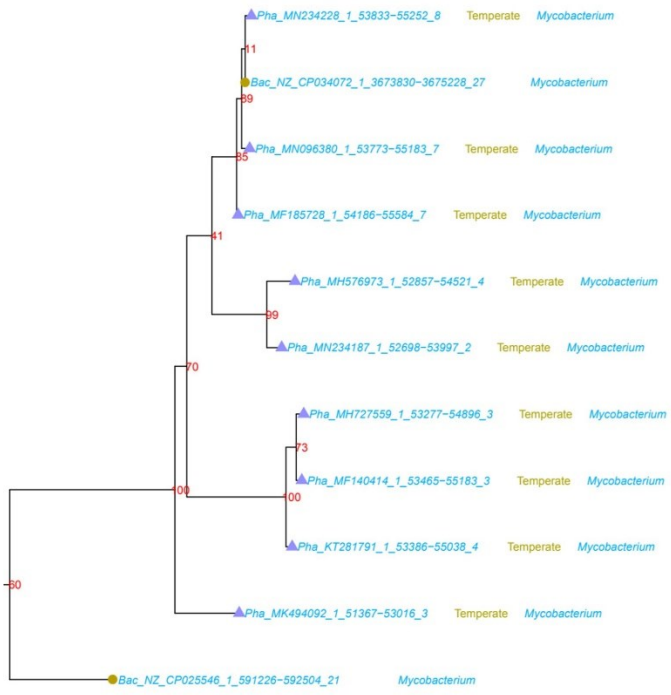

Fig. S12: WhiB phylogeny subclade suggesting the acquisition of *whiB* by temperate *Mycobacterium* phages from their host species. Tree tips shape indicate sequence source (bacteria: circle, and phage: triangle). Sequences are color-coded according to the host genus. Phage lifestyle and genus information are shown on the right. Confidence values displayed on the nodes were estimated based on SH test using FastTree (5).

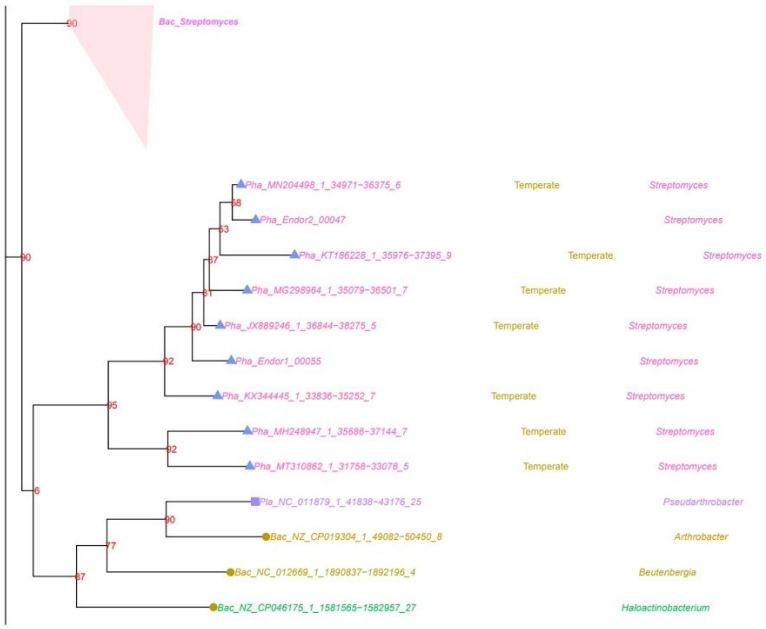

Fig. S13: Lsr2 phylogeny subclade suggesting the acquisition of *lsr2* by temperate *Streptomyces* phages from their hosts. Tree tips shape indicate sequence source (bacteria: circle, phage: triangle, and plasmid: square). Sequences are color-coded according to the phage lifestyle and host genus. Phage lifestyle and genus information are shown on the right. Confidence values displayed on the nodes were estimated based on SH test using FastTree (5).

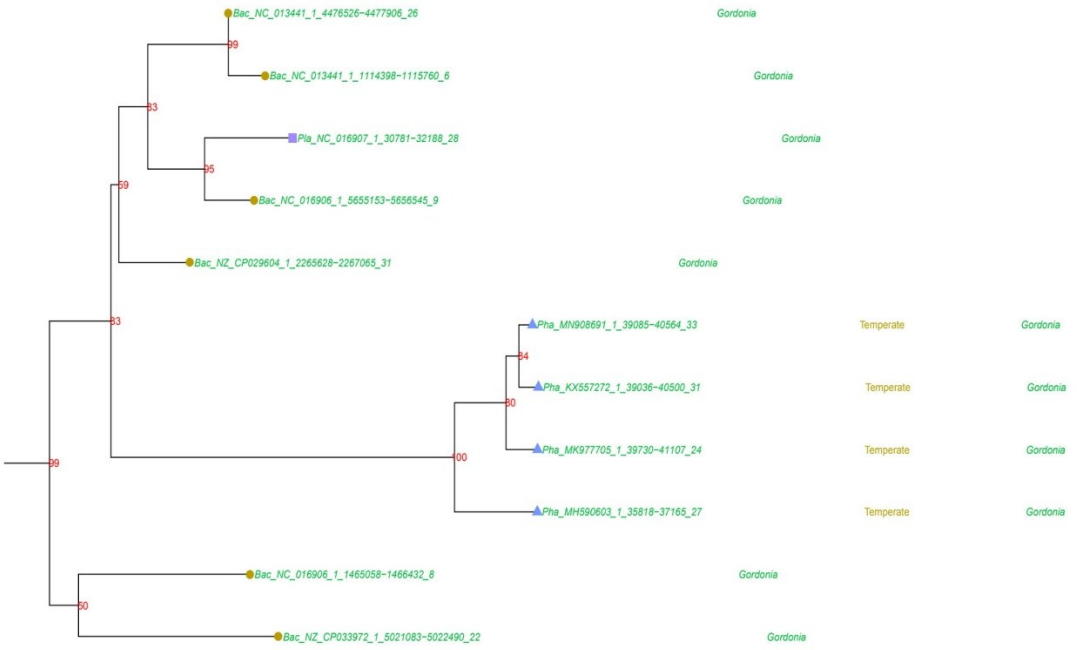

Fig. S14: Lsr2 phylogeny subclade suggesting the acquisition of *lsr2* by temperate *Gordonia* phages from their host species. Tree tips shape indicate sequence source (bacteria: circle, phage: triangle, and plasmid: square). Sequences are color-coded according to the host genus. Phage lifestyle and genus information are shown on the right. Confidence values displayed on the nodes were estimated based on SH test using FastTree (5).

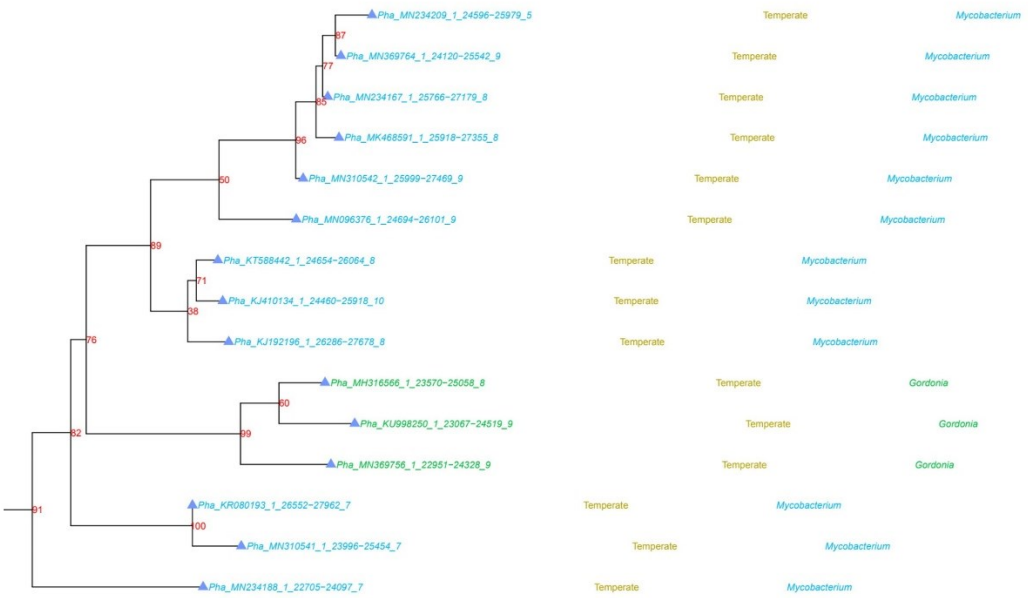

Fig.15: Lsr2 phylogeny subclade suggesting a transfer of *lsr2* from temperate *Gordonia* phages to *Mycobacterium* phages. Tree tips shape indicate sequence source (bacteria: circle, phage: triangle, and plasmid: square). Sequences are color-coded according to the host genus. Phage lifestyle and genus information are shown on the right. Confidence values displayed on the nodes were estimated based on SH test using FastTree (5).

Legends of supplementary tables

Table S1: The 2951 actinobacteriophage genomes used in the current study with corresponding information such as genome size, lifestyle, GC content, assigned clusters, etc (downloaded from phagesdb.org).

Table S2; Sheet1: Identified thirteen regulatory protein domains distribution across actinobacteriophage genomes. Merged overlapping domains are highlighted in bold.

Table S2; Sheet2: List of identified ninety-four manually curated regulatory protein domains; distribution across actinobacteriophage genomes.

Table S3: List of genes and their quantitative distribution within 5 kb flanking *whiB* genomic loci regions identified within the actinobacteriophage genomes according to assigned clusters.

Table S4: Summary of the gene domains within 5 kb flanking *whiB* genomic loci regions identified within the actinobacteriophage genomes according to assigned clusters.

Table S5: List of gene domains and their quantitative distribution within 5 kb flanking *lsr2* genomic loci regions identified within the actinobacteriophage genomes according to assigned clusters.

Table S6: Summary of the gene domains within 5 kb flanking *lsr2* genomic loci regions identified within the actinobacteriophage genomes according to assigned clusters.

REFERENCES

1. Sims GE, Jun S-R, Wu GA, Kim S-H. 2009. Alignment-free genome comparison with feature frequency profiles (FFP) and optimal resolutions. Proc Natl Acad Sci 106:2677–2682.
2. Russell DA, Hatfull GF. 2017. PhagesDB: the actinobacteriophage database. Bioinformatics 33:784–786.
3. Sullivan MJ, Petty NK, Beatson SA. 2011. Easyfig: a genome comparison visualizer. Bioinformatics 27:1009–1010.
4. Altschul SF, Gish W, Miller W, Myers EW, Lipman DJ. 1990. Basic local alignment search tool. J Mol Biol 215:403–410.
5. Price MN, Dehal PS, Arkin AP. 2010. FastTree 2 – Approximately Maximum-Likelihood Trees for Large Alignments. PLoS One 5:e9490.

Additional supplementary tables S1, S2, S3, S4, S5 and S6 can be found under PMID 34817283 and https://doi.org/10.1128/Spectrum.00727-21

4.3 Supplementary material to 3.4 Investigation on *Streptomyces* Phage-encoded WhiB-like Transcriptional Regulators

Supplementary Information to

Investigation on Streptomyces Phage-encoded WhiB-like Transcriptional Regulators

Tom Luthe and Julia Frunzke

Institute of Bio- and Geosciences, IBG-1: Biotechnology, Forschungszentrum Jülich, 52425 Jülich, Germany

Corresponding author

Julia Frunzke; Email j.frunzke@fz-juelich.de, Phone: +49 2461 615430

Tables

Supplementary Table S1 (separate file): Phage genome accession numbers and list of development-associated gene products.

Supplementary Table S2 (separate file): Presence and absence of developmental gene products with phage annotation.

Supplementary Table S3: Phages used in this study.

Supplementary Table S4: Bacterial strains used in this study.

Supplementary Table S5: Plasmids used in this study.

Supplementary Table S6: Oligonucleotides used in this study.

Figures

Supplementary Figure S1: Phylogenetic tree of 110 WhiB-like protein sequences from 109 actinobacteriophages infecting *Streptomyces*.

Tables

Supplementary Table S3: Phages used in this study.

Phage	Host organism	Taxonomy	Cluster (phagesdb.org)	Lifestyle	Reference
Alderaan	*S. venezuelae* NRRL B-65442	*Austintatiousvirus*	BC	Virulent	(Hardy et al., 2020)
Coruscant	*S. venezuelae* NRRL B-65442	*Boydwoodruffvirinae*	BE	Virulent	(Hardy et al., 2020)

Supplementary Table S4: Bacterial strains used in this study.

Strain	Genotype	Reference
***Streptomyces venezuelae* NRRL B-65442**	Wild-type strain	(Gomez-Escribano et al., 2021)
S. venezuelae* Δ*whiB	Δ*whiB::apr*	(Bush et al., 2016)
***S. venezuelae* Comp1**	Δ*whiB::apr*, pIJ-Comp1	This study
***S. venezuelae* Comp2**	Δ*whiB::apr*, pIJ-Comp2	This study
***S. venezuelae* Comp3**	Δ*whiB::apr*, pIJ-Comp3	This study
***S. venezuelae* Comp5**	Δ*whiB::apr*, pIJ-Comp5	This study
***S. venezuelae whiB*$_{Alderaan}$**	pIJ10257-*whiB*$_{Alderaan}$	This study
***S. venezuelae whiB*$_{Coruscant}$**	pIJ10257-*whiB*$_{Coruscant}$	This study
***S. venezuelae whiB*$_{Chymera}$**	pIJ10257-*whiB*$_{Chymera}$	This study
***S. venezuelae whiB*$_{Sven}$**	pIJ10257-*whiB*$_{Sven}$	This study
***Escherichia coli* DH5α**	*supE44 ΔlacU169 (f80lacZDM15) hsdR17 recA1 endA1 gyrA96 thi-1 relA1*	Invitrogen
***Escherichia coli* ET12567/pUZ8002**	*dam-13::Tn9 dcm-6 hsdMhsdR,* carrying plasmid pUZ8002	(MacNeil et al., 1992)

Supplementary Table S5: Plasmids used in this study.

Plasmid	Characteristics	Template	Primer	Vector	Restriction enzymes	Seq primer	Ref.
pIJ10257	Hyg^R; constitutive ermE* promoter; ΦBT1 phage integration site	-	-	-	-	-	(Hong et al., 2005)
pIJ-Comp1	pIJ101-terminator sequence in front of *whiB*$_{Sven}$ promoter controlling *whiB*$_{Sven}$ (*vnz_RS13740*)	S. venezuelae NRRL B-65442 and pIJ101 terminator sequence	5+6+7+8	pIJ10257	HindIII; KpnI	2+4	This study

pIJ-Comp2	pIJ101-terminator sequence in front of *whiB*$_{Sven}$ promoter controlling *whiB*$_{Alderaan}$	Alderaan, S. venezuelae NRRL B-65442 and pIJ101 terminator sequence	5+6+7+9+10+11	pIJ10257	HindIII; KpnI	2+4	This study
pIJ-Comp3	pIJ101-terminator sequence in front of *whiB*$_{Sven}$ promoter controlling *whiB*$_{Coruscant}$	Coruscant, S. venezuelae NRRL B-65442 and pIJ101 terminator sequence	5+6+7+12+13+14	pIJ10257	HindIII; KpnI	2+4	This study
pIJ-Comp5	pIJ101-terminator sequence in front of *whiB*$_{Sven}$ promoter controlling *whiB*$_{Chymera}$ (*vnz_RS14115*)	S. venezuelae NRRL B-65442 and pIJ101 terminator sequence	5+6+7+15+16+17	pIJ10257	HindIII; KpnI	2+4	This study
pIJ10257-*whiB*$_{Alderaan}$	*whiB*$_{Alderaan}$	Alderaan	18+11	pIJ10257	HindIII; NdeI	3+4	This study
pIJ10257-*whiB*$_{Coruscant}$	*whiB*$_{Coruscant}$	Coruscant	19+14	pIJ10257	HindIII; NdeI	3+4	This study
pIJ10257-*whiB*$_{Chymera}$	*whiB*$_{Chymera}$	S. venezuelae NRRL B-65442	20+17	pIJ10257	HindIII; NdeI	3+4	This study
pIJ10257-*whiB*$_{Sven}$	*whiB*$_{Sven}$ (*vnz_RS13740*)	S. venezuelae NRRL B-65442	21+8	pIJ10257	HindIII; NdeI	3+4	This study

Supplementary Table S6: Oligonucleotides used in this study.

Number	Name	Sequence	Usage
1	pIJ101-terminator	CCCGGGCGTGGGCCAAGGCGGAGGCCGAGAAGGGC TCCGGAAGCTAGATCAAAAATCGGCTTCCTCGCGCGC GCACGCGAGGGCCCCCTCCTGGAAACCGTCGCAACCT TGCAACTTCGCAGGTCAGACCCGGTTGCGGGGGGTC AACCGGGGTGCAACGGCTCAACCGGGTGGGCAACCC CCGGAAACCACGTCGTCTGGACGTGAAGAGCCCCGT CGGGCGGTGCCTGACGGGGCTTCTCAATGGGCGAGT GATCAGTCCCGGTGGACGCGCCAGCGGCCCGCCGGA GCGACGGACTCC	cloning
2	Seq1_fwd	GTATCACCGCCAGTGGTATT	
3	Seq2_fwd	TGGCACCGCGATGCTGTTGT	
4	Seq3_rev	TCAGCGAGCTGAAGAAAGAC	
5	Term_KpnI_fwd	GAAAAACGCTCACTGGTACCCCCGGGCGTGGGCCA	
6	Term_rev	GGAGTCCGTCGCTCCGGCG	
7	P13740_fwd_term	CCGCCGGAGCGACGGACTCCGGGTGGGGTGGTTCC TCAGCA	
8	Sven-whiB_HindIII_rev	AGAACCTAGGATCCAAGCTTTCAGACGGCGGCCTT	
9	P13740_rev_Ald-whiB	CAGAACAGACGAGGGGCGCACATGAACCTCCACAC GCTCAA	
10	Ald-whiB_fwd_P13740	AGAACAGACGAGGGGCGCACATGAACCTCCACACG CTCAACCC	
11	Ald-whiB_HindIII_rev	AGAACCTAGGATCCAAGCTTTCACGCGGCGGCCTC	
12	P13740_rev_Coru-whiB	TGCTCAAGGATTCTTGACACGTGCGCCCCTCGTCTG TTCT	
13	Coru-whiB_fwd_P13740	AGAACAGACGAGGGGCGCACGTGTCAAGAATCCTTG AGC	
14	Coru-whiB_HindIII_rev	AGAACCTAGGATCCAAGCTTTCATTCACTGAGTCTTA CCT	

15	P13740_rev_Chy-whiB	GTGCTCAAGGGCATGGGCATGTGCGCCCCTCGTCTGTTCTG	
16	Chy-whiB_fwd_P13740	AGAACAGACGAGGGGCGCACATGCCCATGCCCTTGAGCAC	
17	Chy-whiB_HindIII_rev	TCATGAGAACCTAGGATCCAAGCTTTCACGCCGTACGGGCG	
18	Ald-whiB_NdeI_fwd	AGAACAGGAGGCCCCATATGATGAACCTCCACACGCTCAACCCCAGTTGG	
19	Coru-whiB_NdeI_fwd	AGAACAGGAGGCCCCATATGGTGTCAAGAATCCTTGAGCA	
20	Chy-whiB_NdeI_fwd	CGTCTAGAACAGGAGGCCCCATATGATGCCCATGCCCTTGAGCAC	
21	Sven-whiB_Nde_fwd	AGAACAGGAGGCCCCATATGATGACCGAGTTGTTCCAGGA	
22	qPCR_Sv-RG_05590_fwd	TGGTTCGACCTCCAGTGC	qPCR Ref both
23	qPCR_Sv-RG_05590_rev	CTTGTGCTTCGCGAGCG	qPCR Ref both
24	qPCR_Sv-RG_19670_fwd	CGTGGCCATGCTCAGC	qPCR Ref Ald
25	qPCR_Sv-RG_19670_rev	CGGGTGAAGATCTCCACCTC	qPCR Ref Ald
26	qPCR_Sv-RG_25045_fwd	CAAGGCCCCCGCCTT	qPCR Ref Coru
27	qPCR_Sv-RG_25045_rev	AGACACCGTCGTGCAGCTTG	qPCR Ref Coru
28	q_Ald-tail_fwd	CTCGGCTATCCGATCATCC	qPCR Ald
29	q_Ald-tail_rev	TTGGTTGCGGTTGATGGAC	
30	q_Ald-whiB_fwd	ATGAACCTCCACACGCTCAAC	
31	q_Ald-whiB_rev	TCGCGGCCGGGAAGAA	
32	q_Coru-tail_fwd	TGCTAAGCCACGGTTGATGAG	qPCR Coru

33	q_Coru-tail_rev	AAGCTCTCGCCACGAGACA	
34	q_Coru-whiB_fwd	CCTGAGGAGGTTAAGTGGGAAG	
35	q_Coru-whiB_rev	GCCACCCCAAACACCAAAG	

Figures

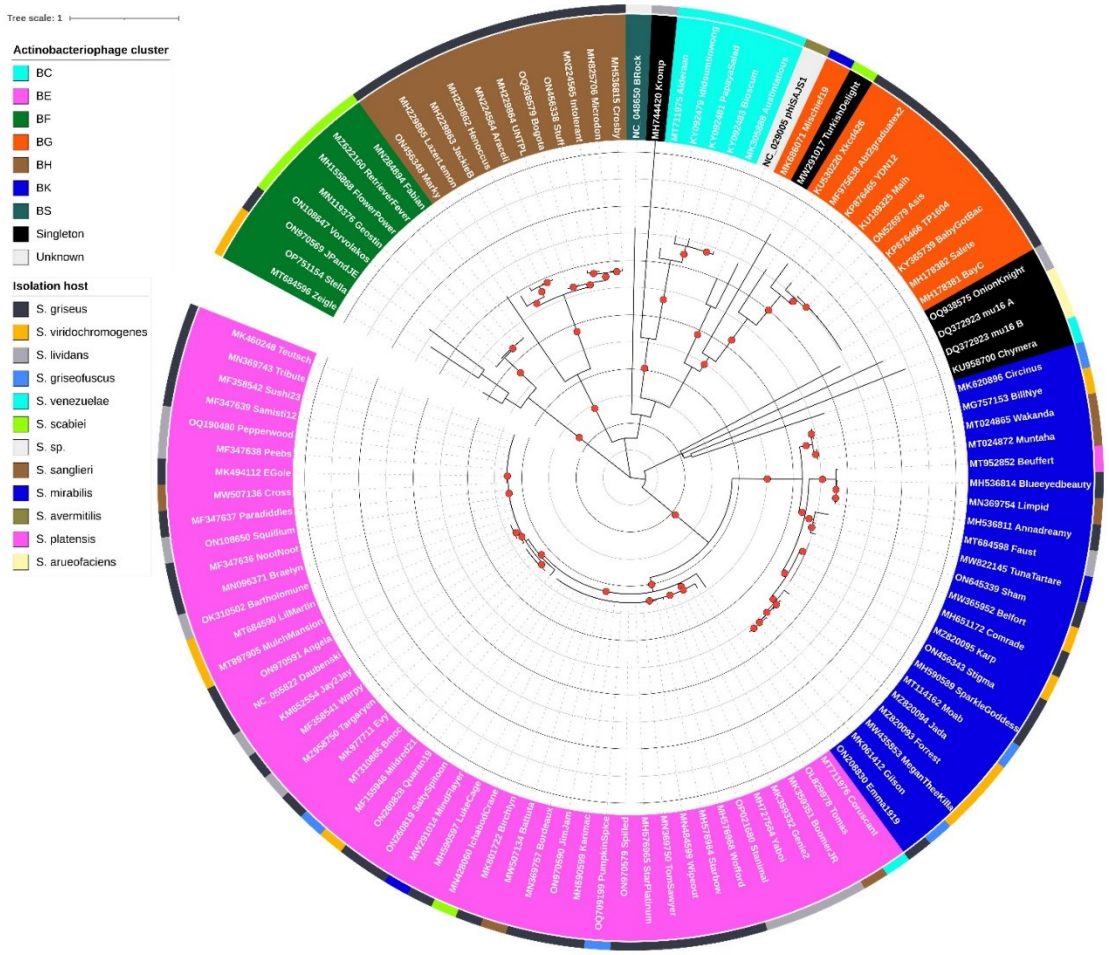

Supplementary Figure S1: Phylogenetic tree of 110 WhiB-like protein sequences from 109 actinobacteriophages infecting *Streptomyces*. Protein sequences were aligned in MEGA X using MUSCLE and phylogenetic analysis was performed using the WAG+G+I+F as best fit model. iTol was used for visualization of the tree. Bootstrap values from 500 replicates over 50% are marked by a red dot. Labels are color-coded according to the actinobacteriophage cluster and outer annotation is color-coded according to the known isolation host.

References

Bush, M. J., Chandra, G., Bibb, M. J., Findlay, K. C., & Buttner, M. J. (2016). Genome-Wide Chromatin Immunoprecipitation Sequencing Analysis Shows that WhiB Is a Transcription Factor That Cocontrols Its Regulon with WhiA To Initiate Developmental Cell Division in Streptomyces. *MBio*, *7*(2), e00523-16. https://doi.org/10.1128/mBio.00523-16

Gomez-Escribano, J. P., Holmes, N. A., Schlimpert, S., Bibb, M. J., Chandra, G., Wilkinson, B., Buttner, M. J., & Bibb, M. J. (2021). Streptomyces venezuelae NRRL B-65442: genome sequence of a model strain used to study morphological differentiation in filamentous actinobacteria. *Journal of Industrial Microbiology & Biotechnology*. https://doi.org/10.1093/jimb/kuab035

Hardy, A., Sharma, V., Kever, L., & Frunzke, J. (2020). Genome Sequence and Characterization of Five Bacteriophages Infecting Streptomyces coelicolor and Streptomyces venezuelae: Alderaan, Coruscant, Dagobah, Endor1 and Endor2. *Viruses*, *12*(10), 1065. https://doi.org/10.3390/v12101065

Hong, H.-J., Hutchings, M. I., Hill, L. M., & Buttner, M. J. (2005). The Role of the Novel Fem Protein VanK in Vancomycin Resistance in Streptomyces coelicolor. *Journal of Biological Chemistry*, *280*(13), 13055–13061. https://doi.org/https://doi.org/10.1074/jbc.M413801200

MacNeil, D. J., Gewain, K. M., Ruby, C. L., Dezeny, G., Gibbons, P. H., & MacNeil, T. (1992). Analysis of Streptomyces avermitilis genes required for avermectin biosynthesis utilizing a novel integration vector. *Gene*, *111*(1), 61–68. https://doi.org/10.1016/0378-1119(92)90603-m

Supplementary Table S1 Sheet 1: Phage genome accession numbers.

Name	Accession
Aaronocolus	KT124227
Aaronocolus	NC_042051
AbbeyMikolon	MG593800
AbbeyMikolon	NC_047904
Abt2graduatex2	MF975638
Alsaber	MG298964
Alsaber	NC_054677
Alvy	MN234208
Alvy	NC_054669
Amela	KT186228
Amela	NC_028904
Amethyst	MF766044
Amethyst	NC_054664
Andris	OP751147
Angela	ON970591
Animus	MN234192
Annadreamy	MH536811
Annadreamy	NC_048719
Annihilus	ON081336
Araceli	MN224564
Asis	ON526979
Asten	MK433276
Attoomi	MG593801
Attoomi	NC_047905
Austintatious	MK305888
Austintatious	NC_048153
AxeJC	ON392164
AxeJC	NC_073485
BabyGotBac	KY365739
BartholomewSD	MK460245
Bartholomune	OK310502
Battuta	MW507134
BayC	MH178381
BeardedLady	MF541403
Belfort	MW365952
Beuffert	MT952852
BillNye	MG757153
BillNye	NC_042105
Bilo	MZ820086
Bing	MG757154
Bing	NC_042106
Bioscum	KY092483
Birchlyn	MK801722
Blueeyedbeauty	MH536814
Blueeyedbeauty	NC_048720
Bmoc	MT310865
Bmoc	NC_055842
Bogota	OQ938579

BoomerJR	MK359351
Bordeaux	MN369757
Bovely	MK433270
Bowden	MK392363
Braelyn	MN096371
Braelyn	NC_055813
Brataylor	KX507345
BRock	KX925554
BRock	NC_048650
BroPlease	ON526970
BryanRecycles	MF541404
Caelum	MK524524
Caelum	NC_054666
Caliburn	KT152029
Caliburn	NC_028892
Celeste	MF541405
Celia	MN062705
Celia	NC_054655
CherryBlossom	MN204495
Chucky	MZ648032
Chymera	KU958700
Chymera	NC_073457
Circinus	MK620896
ClubPenguin	MT310852
Comrade	MH651172
Comrade	NC_048728
CricKo	MT310854
Crosby	MH536815
Cross	MW507136
Cumberbatch	MT451982
Cumberbatch	NC_073488
Danzina	KT124228
Danzina	NC_041860
Darolandstone	MH825699
Darolandstone	NC_048072
Dattran	MF541406
Daubenski	MN444876
Daubenski	NC_055822
Daudau	MF766045
Daudau	NC_054668
Diane	MF766046
Diane	NC_054663
Doxi13	ON970617
DrGrey	MF467948
DrGrey	NC_042016
Dryad	MT498037
Dubu	MK937595
Dubu	NC_070828
Dwayne	MW365953
Eastland	ON392165

Eastland	NC_073490
Eddasa	MH171096
EGole	MK494112
EGole	NC_055791
EhyElimayoE	MW291021
Ejemplo	ON526985
Eklok	MT521991
Eklok	NC_073484
phiELB20	JX262376
phiELB20	NC_041849
Emma1919	ON208830
Esketit	MK967386
Esperer	MF541407
Euratis	MK450426
Evy	MK977711
Evy	NC_055809
Fabian	MN284894
Faust	MT684598
Faust	NC_070783
FidgetOrca	MN586056
FlowerPower	MH155868
FlowerPower	NC_048706
Forrest	MZ820093
Forthebois	MK620900
Forthebois	NC_055059
Frankenweenie	OQ921725
FrodoSwaggins	MN586054
Galactica	MT316461
Genie2	MK359332
Geostin	MN119376
Gibson	MK305891
Gilgamesh	MN234216
Gilgamesh	NC_073461
Gilson	MK061412
Gilson	NC_048742
GirlPower	MN204492
Goby	MH171097
Goby	NC_054680
Godpower	KX507344
GreenWeasel	ON526974
Haizum	MH590601
Hank144	MH669004
Hank144	NC_054661
HaugeAnator	MG663582
Heather	MK686069
Henoccus	MH229862
HFrancette	ON456341
HFrancette	NC_073487
Hippo	MW365951
Hiyaa	MK279841

Hiyaa	NC_048139
Hoshi	MN204500
HotFries	MH155869
Hydra	KT124229
Hydra	NC_042052
Ibantik	MH155870
Ibantik	NC_073462
IceWarrior	MK433259
IchabodCrane	MN428060
Ididsumtinwong	KY092479
Ididsumtinwong	NC_047792
Ignacio	MT451980
Ignacio	NC_073483
Immanuel3	MG518520
Immanuel3	NC_048686
Indigenous	MW055905
Indigo	MK433271
Intolerant	MN224565
Issmi	MT310863
Issmi	NC_054667
Izzy	KT184390
Izzy	NC_028976
JackieB	MH229863
Jada	MZ820094
Janus	MK392366
Janus	NC_054660
Jash	MF541408
Jay2Jay	KM652554
Jay2Jay	NC_029098
Jaylociraptor	MN204494
JimJam	ON970590
JPandJE	ON970569
JustBecause	MH744418
Kardashian	MN204496
Karimac	MH590599
Karimac	NC_048724
Karp	MZ820095
Katalie	MZ820088
Keanu	MT723933
Kela	MT310898
KimJongPhill	MW822144
KimJongPhill	NC_070830
Kradal	MK620894
Kromp	MH744420
Lannister	KT184391
Lannister	NC_028827
LazerLemon	MH229865
Legacy	ON208832
Leviticus	MN096375
LibertyBell	MH669006

Lika	KC700556
Lika	NC_021298
Lilbooboo	MK450431
Lilbooboo	NC_048155
LilMartin	MT684590
Limpid	MN369754
Lizz	MZ648036
Lorelei	KX507343
Lorelei	NC_054681
LukeCage	MH590597
LukeCage	NC_048723
Madamato	MK433269
Maih	KU189325
Maneekul	MH171095
Manuel	MG518519
Manuel	NC_048685
Marky	ON456348
Maya	MT684589
MeganTheeKilla	MW435853
Meibysrarus	MN204497
Microdon	MH825706
Miek	OQ938581
Mildred21	MF155946
Mildred21	NC_042008
MindFlayer	MW291014
Mischief19	MK686071
Moab	MT114162
Mojorita	KY092482
Moozy	MH155872
mu1/6	DQ372923
mu1/6	NC_007967
MulchMansion	MT897905
Muntaha	MT024872
Muntaha	NC_070786
Nabi	MH171094
Namo	MK433260
Nanodon	KX344445
Nanodon	NC_031078
Nerdos	MK433278
Nesbitt	MH001457
Nishikigoi	MK392364
NootNoot	MF347636
NootNoot	NC_042009
Olicious	MK112550
Oliynyk	MF541409
OlympicHelado	KX670789
Omar	MG593802
Omar	NC_054662
OnionKnight	OQ938575
Ozzie	MF541410

OzzyJ	MG757163
Pablito	OK412919
Pablito	NC_070968
Paedore	MH001460
Paedore	NC_054671
PapayaSalad	KY092481
PapayaSalad	NC_047793
Paradiddles	MF347637
Paradiddles	NC_042010
Peebs	MF347638
Peebs	NC_042011
Pepperwood	OQ190480
Percastrophe	MG663583
PherryCruz	MK686070
Phettuccine	MN586009
phiBT1	AJ550940
phiBT1	NC_004664
phi-C31	AJ006589
phi-C31	NC_001978
phiCAM	JX889246
phiCAM	NC_041856
phiHau3	JX182369
phiHau3	NC_018836
phiSASD1	GQ379227
phiSASD1	NC_014229
PHTowN	MT498053
Picard	KY092480
Picard	NC_047794
Piccadilly	OL455886
Piccadilly	NC_073489
Popy	MK433268
PumpkinSpice	OQ709199
ZL12	GQ919031
ZL12	NC_013420
Quaran19	ON260828
R4	JX182370
R4	NC_019414
Rainydai	MH155877
Raleigh	KY092484
Raleigh	NC_047795
Rana	MH171093
RavenPuff	MH155878
RedBear	MZ648039
RemusLoopin	MK686068
RetrieverFever	MZ622160
RickRoss	OP434453
Rima	KX670790
Rima	NC_041889
Romero	MG663584
Rooney	MZ648033

RosaAsantewaa	MK686072
RosePharie	OP021678
Rowa	MG593803
Rowa	NC_047906
Rusticus	MN096381
Saftant	MN204498
Saftant	NC_054675
Salete	MH178382
SaltySpitoon	ON260819
Samisti12	MF347639
Samisti12	NC_042012
SarahRose	MZ820092
Satis	MH576962
Scap1	MF975637
Scap1	NC_042042
Sebastisaurus	MK450433
SendItCS	MH155880
ShakeNBake	MT897908
Sham	ON645339
Shawty	MK433266
Snorlax	OL742563
SoJo	OQ938586
Soshi	MN204504
South40	MZ820091
SparkleGoddess	MH590589
Spectropatronm	MF467949
Spilled	ON970579
SqueakyClean	MF766047
Squillium	ON108650
Stanimal	OP021680
Starbow	MH576964
StarPlatinum	MH576965
StarPlatinum	NC_048721
Stella	OP751154
Stigma	ON456343
Stuff	ON456338
Success	OP751148
Success	NC_073472
Sujidade	KC700557
Sujidade	NC_021304
SunsetPointe	OL455891
Sushi23	MF358542
SV1	JX182371
SV1	NC_018848
TagePhighter	OP820462
TaidaOne	MW712736
Targaryen	MZ958750
Tefunt	MF766048
Tefunt	NC_054665
Teutsch	MK460248

TG1	JX182372
TG1	NC_018853
Thestral	MH651190
Thestral	NC_054670
Thiqqums	MT657340
TieDye	MT684600
TinaBelcher	MK392365
ToastyFinz	KY676784
Toma	MH171098
Tomas	OL829978
Tomas	NC_070781
TomSawyer	MN369750
TonyStarch	ON108646
ToriToki	MG663585
TP1604	KP876466
TP1604	NC_028818
Treat	OL455897
Tribute	MN369743
Triste	MZ648040
Triumph	OQ190479
TrvxScott	MH669016
TuanPN	MN096373
TunaTartare	MW822145
TunaTartare	NC_070784
TurkishDelight	MW291017
TurkishDelight	NC_073473
Unstoppable	OL455894
UNTPL	MH229864
Urza	MN234189
Vash	MK450421
Vash	NC_048154
Verse	KT186229
VieEnRose	ON526983
Vondra	MT451981
Vondra	NC_073486
Vorvolakos	ON108647
VWB	AY320035
VWB	NC_005345
Wakanda	MT024865
Wakanda	NC_070785
Warpy	MF358541
Wentworth	MH019216
Werner	MW435856
Werner	NC_054679
Whatever	MN284899
WheeHeim	MK305890
WheeHeim	NC_055060
Wipeout	MN484599
Wofford	MH576968
Wofford	NC_048722

WRightOn	MG515223
WRightOn	NC_048684
Xkcd426	KU530220
Yaboi	MH727564
Yaboi	NC_048730
Yara	MH019215
Yasdnil	MN096379
Yasdnil	NC_054678
YDN12	KP876465
YDN12	NC_028974
Yosif	MH248947
Yosif	NC_054656
Zeigle	MT684596
Zemlya	KC700558
Zemlya	NC_021339
ZooBear	MG663586
Zuko	MN204493
Zuko	NC_070829
Salutena	MT708548
Salutena	NC_054657
Shaeky	MT701595
Joe	KX815338
Joe	NC_054674
Sitrop	MT701598
Sitrop	NC_054676
Mulchroom	OQ784832
phiSAJS1	KT989433
phiSAJS1	NC_029005
SF3	KT221034
SF3	NC_028952
SF1	KT221033
SF1	NC_028807
SscP1EGY	MW145539
Shady	MT701596
phiScoe54	OQ672750
phiScoe55	OQ672751
phiScoe56	OQ672752
phiScoe45	OQ672749
phiScoe44	OQ672748
phiScoe3	OQ672747
phiScoe25	OQ672746
phiScoe23	OQ672745
phiScoe2	OQ672744
phiScoe15	OQ672743
phiScoe10	OQ672742
phiScoe1	OQ672741
Coruscant	MT711976
Coruscant	NC_070782
Endor2	MT711979
Endor2	NC_054673

Endor1	MT711978
Endor1	NC_054672
Alderaan	MT711975
Dagobah	MT711977
Spernnie	MT701594
Spernnie	NC_054659
Sentinel	MT701597
Sentinel	NC_054658
Sycamore	MT701593
phiRKBJ001	MT936332
JXY1	MN994275
JXY1	NC_048854

Supplementary Table S1 Sheet 2: List of development-associated gene products.

Name
bldA
bldC
bldD
bldG
bldH
bldM
bldN
bldO
whiA
whiB
whiD
whiE
whiG
whiH
whiI
whiJ
ssgA
ssgB
parA
parB
sapB
rdlA
rdlB
rdlC
chpB
chpC
chpE
chpF
chpG
chpH
adpA
ftsZ
ftsK
dpsA
filP
divIVA
scy
cdgB
treZ
ramR
ramC
ramS
ramA
ramB
sigA
sigH
sigN
wblA
wblI
wblC
wblE
wblM
wblH
wblO
sepH
sepX
mtrA

Supplementary Table S2: Presence and absence of developmental gene products with phage annotation.

Accession	Name	WhiB.family	FtsK.like	ParB.like	ParA.like	SsgA.family	Cluster	Host	Lifestyle	Size (bp)	GC (%)	Morphotype
KT124227	Aaronocolus	0	0	0	0	0	BD	S. griseus	Temperate	49562	66.2	Unknown
MG593800	AbbeyMikolon	0	0	0	0	0	BL	S. lividans	Temperate	42551	66.8	SIPHO
MF975638	Abt2graduatex2	1	1	0	0	0	BG	S. griseus	Virulent	57385	69.2	SIPHO
MT711975	Alderaan	1	0	0	0	0	BC	S. venezuelae	Virulent	34411	72	SIPHO
MG298964	Alsaber	0	0	0	0	0	BD	S. azureus	Temperate	48803	65.9	SIPHO
MN234208	Alvy	0	0	0	0	0	BD	S. platensis	Temperate	53011	67.5	SIPHO
KT186228	Amela	0	0	0	0	0	BD	S. venezuelae	Temperate	49452	65.6	SIPHO
MF766044	Amethyst	0	0	0	0	0	BD	S. xanthochromogenes	Temperate	49372	67.2	SIPHO
OP751147	Andris	0	0	0	0	0	BD	S. lividans	Temperate	50588	67.2	SIPHO
ON970591	Angela	1	1	1	0	0	BE	S. griseus	Virulent	133582	49.4	SIPHO
MN234192	Animus	0	0	0	0	0	BD	S. griseus	Temperate	50793	67	SIPHO
MH536811	Annadreamy	1	0	0	0	0	BK	S. griseus	Virulent	125726	47.6	Unknown
ON081336	Annihilus	0	0	0	0	0	BI	S. scabiei	Virulent	43562	61.2	SIPHO
MN224564	Araceli	1	0	0	0	0	BH	S. griseus	Virulent	55045	68.2	PODO
ON526979	Asis	1	1	0	0	0	BG	S. griseus	Virulent	57239	69.2	Unknown
MK433276	Asten	0	0	0	0	0	BD	S. griseus	Temperate	51571	65.7	SIPHO
MG593801	Attoomi	0	0	0	0	0	Singleton	S. azureus	Temperate	41872	69.7	Unknown
MK305888	Austintatious	1	0	0	0	0	BC	S. venezuelae	Temperate	36213	72.6	Unknown
ON392164	AxeJC	0	0	0	0	0	BP	S. sanglieri	Temperate	37765	71.4	SIPHO
KY365739	BabyGotBac	1	1	0	0	0	BG	S. griseus	Virulent	57165	69.2	SIPHO
MK460245	BartholomewSD	0	0	0	0	0	BD	S. platensis	Temperate	52131	67.6	SIPHO
OK310502	Bartholomune	1	1	1	0	0	BE	S. lividans	Virulent	131879	50.2	SIPHO
MW507134	Battuta	1	1	1	0	0	BE	S. sanglieri	Virulent	130734	49.5	SIPHO
MH178381	BayC	1	1	0	0	0	BG	S. griseus	Virulent	57243	69.2	SIPHO
MF541403	BeardedLady	0	0	0	0	0	BD	S. xanthochromogenes	Temperate	49941	66.2	SIPHO
MW365952	Belfort	1	0	0	0	0	BK	S. viridochromogenes	Virulent	128959	47	SIPHO
MT952852	Beuffert	1	0	0	0	0	BK	S. platensis	Virulent	129935	47.7	Unknown
MG757153	BillNye	1	0	0	0	0	BK	S. viridochromogenes	Virulent	127084	52.8	SIPHO
MZ820086	Bilo	0	0	0	0	0	BI	S. lividans	Virulent	43835	60.6	SIPHO
MG757154	Bing	0	0	0	0	0	BI	S. lividans	Virulent	56341	59.4	SIPHO
KY092483	Bioscum	1	0	0	0	0	BC	S. venezuelae	Temperate	37830	72.3	Unknown
MK801722	Birchlyn	1	1	1	0	0	BE	S. griseus	Virulent	126524	49.2	SIPHO
MH536814	Blueeyedbeauty	1	0	0	0	0	BK	S. griseus	Virulent	130473	47.9	SIPHO
MT310865	Bmoc	1	1	1	0	0	BE	S. griseofuscus	Virulent	132885	49.6	SIPHO
OQ938579	Bogota	1	0	0	0	0	BH	S. griseus	Virulent	54184	68.3	Unknown
MK359351	BoomerJR	1	1	1	0	0	BE	S. lividans	Virulent	131220	49.2	SIPHO
MN369757	Bordeaux	1	1	1	0	0	BE	S. griseus	Virulent	131317	49.5	SIPHO
MK433270	Bovely	0	0	0	0	0	BD	S. griseus	Temperate	49576	66.2	SIPHO
MK392363	Bowden	0	0	0	0	0	BD	S. xanthochromogenes	Temperate	52603	67.7	SIPHO
MN096371	Braelyn	1	1	1	0	0	BE	S. griseus	Virulent	131234	50.1	SIPHO
KX507345	Brataylor	0	0	0	0	0	BD	S. venezuelae	Temperate	51067	65.7	Unknown
NC_048650	BRock	1	0	0	0	0	BS	S. sp.	Unknown	112523	52.3	MYO
ON526970	BroPlease	0	0	0	0	0	BD	S. griseus	Temperate	50645	67.8	Unknown
MF541404	BryanRecycles	0	0	0	0	0	BD	S. griseus	Temperate	50066	65.9	SIPHO
MK524524	Caelum	0	0	0	0	0	BD	S. lividans	Temperate	50374	67	Unknown
KT152029	Caliburn	0	0	0	0	0	BD	S. griseus	Temperate	49949	66.2	SIPHO
MF541405	Celeste	0	0	0	0	0	BD	S. xanthochromogenes	Temperate	50536	65.8	SIPHO
MN062705	Celia	0	0	0	0	0	BD	S. xanthochromogenes	Temperate	50493	68.6	SIPHO
MN204495	CherryBlossom	0	0	0	0	0	BI	S. griseus	Virulent	55563	59.6	SIPHO
MZ648032	Chucky	0	0	0	0	0	BD	S. lividans	Temperate	51594	65.7	SIPHO
KU958700	Chymera	1	0	0	0	0	Singleton	S. venezuelae	Temperate	34742	71.4	SIPHO
MK620896	Circinus	1	0	0	0	0	BK	S. griseofuscus	Virulent	126383	52.9	SIPHO
MT310852	ClubPenguin	0	0	0	0	0	BI	S. mirabilis	Virulent	56205	59	SIPHO
MH651172	Comrade	1	0	0	0	0	BK	S. griseus	Virulent	129015	47.1	SIPHO
MT711976	Coruscant	1	1	1	0	0	BE	S. venezuelae	Virulent	133697	48	SIPHO
MT310854	CricKo	0	0	0	0	0	BI	S. scabiei	Virulent	57623	58.1	SIPHO
MH536815	Crosby	1	0	0	0	0	BH	S. griseus	Virulent	54036	68.3	SIPHO
MW507136	Cross	1	1	1	0	0	BE	S. sanglieri	Virulent	132807	50.1	SIPHO
MT451982	Cumberbatch	0	0	0	0	0	BP	S. sanglieri	Temperate	37566	71.3	SIPHO
MT711977	Dagobah	0	0	0	0	1	Singleton	S. coelicolor	Temperate	47301	69	SIPHO
KT124228	Danzina	0	0	0	0	0	BD	S. venezuelae	Temperate	50773	65.7	Unknown
MH825699	Darolandstone	0	0	0	0	0	BC	S. platensis	Temperate	40725	72.3	SIPHO
MF541406	Dattran	0	0	0	0	0	BD	S. venezuelae	Temperate	50976	65.8	SIPHO
NC_055822	Daubenski	1	1	1	0	0	BE	S. griseus	Virulent	133090	49.4	SIPHO
MF766045	Daudau	0	0	0	0	0	BD	S. xanthochromogenes	Temperate	50602	67.1	SIPHO
MF766046	Diane	0	0	0	0	0	BD	S. xanthochromogenes	Temperate	50483	66.7	SIPHO
ON970617	Doxi13	0	0	0	0	0	BI	S. scabiei	Virulent	43696	60.9	SIPHO
MF467948	DrGrey	0	0	0	0	0	BI	S. griseus	Virulent	56076	59.5	SIPHO
MT498037	Dryad	0	0	0	0	0	BN	S. viridochromogenes	Virulent	68994	63.8	SIPHO
MK937595	Dubu	0	0	0	0	0	BJ	S. platensis	Temperate	39535	68.7	Unknown
MW365953	Dwayne	0	0	0	0	0	BD	S. lividans	Temperate	51582	65.7	SIPHO
ON392165	Eastland	0	0	0	0	0	BP	S. sanglieri	Temperate	37536	71.2	SIPHO
MH171096	Eddasa	0	0	0	0	0	BD	S. griseus	Temperate	50605	65.9	SIPHO
MK494112	EGole	1	1	1	0	0	BE	S. griseus	Virulent	135653	49.9	SIPHO
MW291021	EhyElimayoE	0	1	0	0	0	BM	S. lividans	Virulent	186386	66.7	SIPHO
ON526985	Ejemplo	0	0	0	0	0	BD	S. griseus	Temperate	51517	65.7	Unknown

MT521991	Eklok	0	0	0	0	0	BP	S. sanglieri	Temperate	37409	71.2	SIPHO
ON208830	Emma1919	1	0	0	0	0	BK	S. griseus	Virulent	128076	47.4	SIPHO
MT711978	Endor1	0	0	0	0	0	BD	S. coelicolor	Temperate	49395	66	SIPHO
MT711979	Endor2	0	0	0	0	0	BD	S. coelicolor	Temperate	48829	65	SIPHO
MK967386	Esketit	0	0	0	0	0	BI	S. griseus	Virulent	54664	59.5	SIPHO
MF541407	Esperer	0	0	0	0	0	BD	S. xanthochromogenes	Temperate	49908	66.2	SIPHO
MK450426	Euratis	0	0	0	0	0	BB	S. griseus	Temperate	41403	62.9	SIPHO
MK977711	Evy	1	1	1	0	0	BE	S. griseus	Virulent	132977	49.6	SIPHO
MN284894	Fabian	1	0	0	0	0	BF	S. scabiei	Virulent	46505	60.7	PODO
MT684598	Faust	1	0	0	0	0	BK	S. lividans	Virulent	130666	47.2	SIPHO
MN586056	FidgetOrca	0	0	0	0	0	BI	S. griseus	Virulent	56115	59.5	Unknown
MH155868	FlowerPower	1	0	0	0	0	BF	S. scabiei	Virulent	46133	60.7	PODO
MZ820093	Forrest	1	0	0	0	0	BK	S. viridochromogenes	Virulent	128513	47.1	SIPHO
MK620900	Forthebois	0	0	0	0	0	BO	S. scabiei	Temperate	18251	53.6	TECTI
OQ921725	Frankenweenie	0	1	0	0	0	BM	S. scabiei	Virulent	200048	66.5	SIPHO
MN586054	FrodoSwaggins	0	0	0	0	0	BI	S. griseus	Virulent	56472	59.4	Unknown
MT316461	Galactica	0	1	0	0	0	BQ	S. mirabilis	Unknown	81216	66.9	SIPHO
MK359332	Genie2	1	1	1	0	0	BE	S. lividans	Virulent	131333	49.3	SIPHO
MN119376	Geostin	1	0	0	0	0	BF	S. scabiei	Virulent	46175	60.7	PODO
MK305891	Gibson	0	0	0	0	0	BN	S. griseus	Virulent	69439	64.4	SIPHO
MN234216	Gilgamesh	0	1	1	1	0	Singleton	S. lividans	Temperate	129136	71.3	SIPHO
MK061412	Gilson	1	0	0	0	0	BK	S. griseofuscus	Virulent	128338	47.4	SIPHO
MN204492	GirlPower	0	0	0	0	0	BI	S. griseus	Virulent	55521	59.1	SIPHO
MH171097	Goby	0	0	0	0	0	BD	S. toxytricini	Temperate	51393	65.8	SIPHO
KX507344	Godpower	0	0	0	0	0	BD	S. venezuelae	Temperate	50701	65.7	Unknown
ON526974	GreenWeasel	0	0	0	0	0	BD	S. griseus	Temperate	50778	67.7	Unknown
MH590601	Haizum	0	0	0	0	0	BD	S. xanthochromogenes	Temperate	50660	66.8	SIPHO
MH669004	Hank144	0	0	0	0	0	BD	S. platensis	Temperate	50547	66.3	SIPHO
MG663582	HaugeAnator	0	0	0	0	0	BF	S. griseus	Virulent	46135	59.6	PODO
MK686069	Heather	0	0	0	0	0	BB	S. mirabilis	Temperate	41238	62.8	SIPHO
MH229862	Henoccus	1	0	0	0	0	BH	S. griseus	Virulent	55137	68.2	SIPHO
ON456341	HFrancette	0	0	0	0	0	BP	S. sanglieri	Temperate	38234	71.2	SIPHO
MW365951	Hippo	0	0	0	0	0	BD	S. lividans	Temperate	51566	65.6	PODO
NC_048139	Hiyaa	0	1	0	0	0	BQ	S. lividans	Unknown	83219	66.7	SIPHO
MN204500	Hoshi	0	0	0	0	0	BI	S. griseus	Virulent	55728	59.5	Unknown
MH155869	HotFries	0	0	0	0	0	BI	S. scabiei	Virulent	43699	60.9	SIPHO
KT124229	Hydra	0	0	0	0	0	BD	S. griseus	Temperate	50727	66.2	SIPHO
MH155870	Ibantik	0	0	0	0	0	Singleton	S. lividans	Temperate	56362	57.4	Unknown
MK433259	IceWarrior	0	0	0	0	0	BI	S. platensis	Virulent	55532	59.5	SIPHO

MN428060	IchabodCrane	1	1	1	0	0	BE	S. scabiei	Virulent	130730	49.4	SIPHO
KY092479	Ididsumtinwong	1	0	0	0	0	BC	S. venezuelae	Temperate	37817	72.4	SIPHO
MT451980	Ignacio	0	0	0	0	0	BP	S. sanglieri	Temperate	38137	71.1	SIPHO
MG518520	Immanuel3	0	0	0	0	0	BF	S. griseus	Virulent	46094	59.6	PODO
MW055905	Indigenous	0	0	0	0	0	BI	S. griseus	Virulent	56119	59.5	SIPHO
MK433271	Indigo	0	0	0	0	0	BD	S. griseus	Temperate	49558	66.2	SIPHO
MN224565	Intolerant	1	0	0	0	0	BH	S. griseus	Virulent	53909	68.4	Unknown
MT310863	Issmi	0	0	0	0	0	BD	S. griseofuscus	Temperate	50643	67.6	SIPHO
KT184390	Izzy	0	0	0	0	0	BD	S. griseus	Temperate	50113	65.9	SIPHO
MH229863	JackieB	1	0	0	0	0	BH	S. griseus	Virulent	54912	68.2	SIPHO
MZ820094	Jada	1	0	0	0	0	BK	S. viridochromogenes	Virulent	127753	47.1	SIPHO
MK392366	Janus	0	0	0	0	0	BD	S. xanthochromogenes	Temperate	50632	67	SIPHO
MF541408	Jash	0	0	0	0	0	BD	S. griseus	Temperate	50066	65.9	SIPHO
KM652554	Jay2Jay	1	1	1	0	0	BE	S. lividans	Virulent	133531	49.5	SIPHO
MN204494	Jaylociraptor	0	0	0	0	0	BI	S. griseus	Virulent	55699	59.5	Unknown
ON970590	JimJam	1	1	1	0	0	BE	S. griseus	Virulent	134078	49.3	SIPHO
KX815338	Joe	0	0	0	0	0	None	S. coelicolor	Temperate	48941	65	SIPHO
ON970569	JPandJE	1	0	0	0	0	BF	S. griseus	Virulent	46427	59.6	PODO
MH744418	JustBecause	0	1	0	0	0	BM	S. lividans	Virulent	184281	66.6	Unknown
MN994275	JXY1	0	0	0	0	0	None	S. sp.	Unknown	45385	60	Unknown
MN204496	Kardashian	0	0	0	0	0	BI	S. griseofuscus	Virulent	55961	59.8	SIPHO
MH590599	Karimac	1	1	1	0	0	BE	S. griseus	Virulent	131909	49.4	SIPHO
MZ820095	Karp	1	0	0	0	0	BK	S. viridochromogenes	Virulent	130557	47	SIPHO
MZ820088	Katalie	0	0	0	0	0	BD	S. lividans	Temperate	51271	65.6	SIPHO
MT723933	Keanu	0	1	0	0	0	BQ	S. lividans	Unknown	82100	66.8	SIPHO
MT310898	Kela	0	1	0	0	0	BM	S. scabiei	Virulent	185323	66.6	SIPHO
MW822144	KimJongPhill	0	0	0	0	0	BR	S. mirabilis	Unknown	82521	64	SIPHO
MK620894	Kradal	0	1	0	0	0	BM	S. griseofuscus	Virulent	186383	66.7	SIPHO
MH744420	Kromp	1	0	0	0	0	Singleton	S. lividans	Temperate	58268	71.4	SIPHO
KT184391	Lannister	0	0	0	0	0	BD	S. venezuelae	Temperate	50165	65.7	Unknown
MH229865	LazerLemon	1	0	0	0	0	BH	S. griseus	Virulent	54798	68.1	SIPHO
ON208832	Legacy	0	0	0	0	0	BD	S. griseus	Temperate	49941	66.2	SIPHO
MN096375	Leviticus	0	0	0	0	0	BD	S. griseus	Temperate	50095	66.2	SIPHO
MH669006	LibertyBell	0	0	0	0	0	BI	S. virginiae	Virulent	52733	59.1	SIPHO
KC700556	Lika	0	0	0	0	0	BD	S. lividans	Temperate	51252	65.8	SIPHO
MK450431	Lilbooboo	0	0	0	0	0	BB	S. griseus	Temperate	41267	62.7	SIPHO
MT684590	LilMartin	1	1	0	0	0	BE	S. viridochromogenes	Virulent	132470	49.5	SIPHO
MN369754	Limpid	1	0	0	0	0	BK	S. sanglieri	Virulent	131038	47.6	SIPHO
MZ648036	Lizz	0	0	0	0	0	BN	S. viridochromogenes	Virulent	69287	64.2	SIPHO

KX507343	Lorelei	0	0	0	0	0	BD	S. griseus	Temperate	50558	65.8	SIPHO
MH590597	LukeCage	1	1	1	0	0	BE	S. griseus	Virulent	133195	49	SIPHO
MK433269	Madamato	0	0	0	0	0	BI	S. griseus	Virulent	55349	59.6	SIPHO
KU189325	Maih	1	1	0	0	0	BG	S. griseus	Virulent	57256	69.3	Unknown
MH171095	Maneekul	0	0	0	0	0	BD	S. xanthochromogenes	Temperate	51612	65.7	SIPHO
MG518519	Manuel	0	0	0	0	0	BF	S. lividans	Virulent	45177	60.1	PODO
ON456348	Marky	1	0	0	0	0	BH	S. griseus	Virulent	54732	67.6	Unknown
MT684589	Maya	0	0	0	0	0	BI	S. indigocolor	Virulent	55713	59.5	Unknown
MW435853	MeganTheeKilla	1	0	0	0	0	BK	S. viridochromogenes	Virulent	128152	47.4	SIPHO
MN204497	Meibysrarus	0	0	0	0	0	BI	S. griseus	Virulent	55097	59.5	SIPHO
MH825706	Microdon	1	0	0	0	0	BH	S. griseus	Virulent	53356	68.6	SIPHO
OQ938581	Miek	0	0	0	0	0	BI	S. scabiei	Virulent	56005	58.2	SIPHO
MF155946	Mildred21	1	1	1	0	0	BE	S. viridochromogenes	Virulent	131976	49.5	SIPHO
MW291014	MindFlayer	1	1	1	0	0	BE	S. mirabilis	Virulent	130258	49.5	SIPHO
MK686071	Mischief19	1	1	0	0	0	BG	S. mirabilis	Virulent	68430	68.5	SIPHO
MT114162	Moab	1	0	0	0	0	BK	S. griseofuscus	Virulent	129370	47.2	SIPHO
KY092482	Mojorita	0	0	0	0	0	BC	S. venezuelae	Temperate	38496	72.5	Unknown
MH155872	Moozy	0	0	0	0	0	BI	S. scabiei	Virulent	43545	61.2	SIPHO
DQ372923	mu1/6	1	0	0	0	0	Singleton	S. aureofaciens	Temperate	38194	71.2	SIPHO
MT897905	MulchMansion	1	1	0	0	0	BE	S. viridochromogenes	Virulent	134105	49.4	Unknown
OQ784832	Mulchroom	0	0	0	0	0	None	S. viridochromogenes	Temperate	14787	51	SIPHO
MT024872	Muntaha	1	0	0	0	0	BK	S. sanglieri	Virulent	127551	52.6	Unknown
MH171094	Nabi	0	0	0	0	0	BD	S. griseus	Temperate	51127	65.8	SIPHO
MK433260	Namo	0	0	0	0	0	BI	S. griseus	Virulent	56168	59.6	Unknown
KX344445	Nanodon	0	0	0	0	0	BD	S. griseus	Temperate	50082	65.7	SIPHO
MK433278	Nerdos	0	0	0	0	0	BD	S. griseus	Temperate	49557	66.2	SIPHO
MH001457	Nesbitt	0	0	0	0	0	BL	S. lividans	Temperate	42446	66.8	SIPHO
MK392364	Nishikigoi	0	0	0	0	0	BD	S. xanthochromogenes	Temperate	50660	66.8	SIPHO
MF347636	NootNoot	1	1	1	0	0	BE	S. griseus	Virulent	131086	50.2	SIPHO
MK112550	Olicious	0	0	0	0	0	BF	S. griseus	Virulent	46139	59.7	PODO
MF541409	Oliynyk	0	0	0	0	0	BD	S. xanthochromogenes	Temperate	49976	65.9	SIPHO
KX670789	OlympicHelado	0	0	0	0	0	BI	S. griseus	Virulent	56189	59.5	SIPHO
MG593802	Omar	0	0	0	0	0	BD	S. azureus	Temperate	49299	67.3	SIPHO
OQ938575	OnionKnight	1	0	0	0	0	Singleton	S. lividans	Temperate	39921	71.1	SIPHO
MF541410	Ozzie	0	0	0	0	0	BD	S. xanthochromogenes	Temperate	49961	66.2	SIPHO
MG757163	OzzyJ	0	0	0	0	0	BD	S. lividans	Temperate	51464	65.7	SIPHO
OK412919	Pablito	0	0	0	0	0	BD	S. lividans	Temperate	49492	66.4	SIPHO
MH001460	Paedore	0	0	0	0	0	BD	S. lividans	Temperate	52743	67	Unknown
KY092481	PapayaSalad	1	0	0	0	0	BC	S. venezuelae	Temperate	38411	72.6	SIPHO

MF347637	Paradiddles	1	1	1	0	0	BE	S. griseus	Virulent	133486	49.5	SIPHO
MF347638	Peebs	1	1	1	0	0	BE	S. lividans	Virulent	133047	50.1	SIPHO
OQ190480	Pepperwood	1	1	1	0	0	BE	S. lividans	Virulent	133012	50.1	SIPHO
MG663583	Percastrophe	0	0	0	0	0	BF	S. griseus	Virulent	45999	59.7	PODO
MK686070	PherryCruz	0	0	0	0	0	BI	S. scabiei	Virulent	43736	61	SIPHO
MN586009	Phettuccine	0	0	0	0	0	BD	S. griseofuscus	Temperate	49530	66.2	SIPHO
AJ006589	phi-C31	0	0	0	0	0	BB	S. coelicolor	Temperate	41491	63.6	SIPHO
AJ550940	phiBT1	0	0	0	0	0	BB	S. coelicolor	Temperate	41831	62.8	SIPHO
JX889246	phiCAM	0	0	0	0	0	BD	S. coelicolor	Temperate	50348	65.6	SIPHO
JX262376	phiELB20	0	0	0	0	0	BD	S. lividans	Temperate	51160	67	Unknown
JX182369	phiHau3	0	0	0	0	0	BD	S. coelicolor	Temperate	50255	67.8	Unknown
MT936332	phiRKBJ001	0	0	0	0	0	BN	S. sp.	Virulent	69373	64	SIPHO
NC_029005	phiSAJS1	1	1	0	0	0	None	S. avermitilis	Temperate	56451	68	SIPHO
GQ379227	phiSASD1	0	0	0	0	0	BJ	S. avermitilis	Temperate	37068	66.3	SIPHO
OQ672741	phiScoe1	0	0	0	0	0	None	S. coelicolor	Temperate	51041	67	SIPHO
OQ672742	phiScoe10	0	0	0	0	0	None	S. coelicolor	Temperate	51094	65	SIPHO
OQ672743	phiScoe15	0	0	0	0	0	None	S. coelicolor	Temperate	49356	66	SIPHO
OQ672744	phiScoe2	0	0	0	0	0	None	S. coelicolor	Temperate	49387	66	SIPHO
OQ672745	phiScoe23	0	0	0	0	0	None	S. coelicolor	Temperate	49768	66	SIPHO
OQ672746	phiScoe25	0	0	0	0	0	None	S. coelicolor	Temperate	49465	66	SIPHO
OQ672747	phiScoe3	0	0	0	0	0	None	S. coelicolor	Temperate	48350	66	SIPHO
OQ672748	phiScoe44	0	0	0	0	0	None	S. coelicolor	Temperate	48760	65	SIPHO
OQ672749	phiScoe45	0	0	0	0	0	None	S. coelicolor	Temperate	48816	66	SIPHO
OQ672750	phiScoe54	0	0	0	0	0	None	S. coelicolor	Temperate	48721	66	SIPHO
OQ672751	phiScoe55	0	0	0	0	0	None	S. coelicolor	Temperate	48461	65	SIPHO
OQ672752	phiScoe56	0	0	0	0	0	None	S. coelicolor	Temperate	48427	65	SIPHO
MT498053	PHTowN	0	0	0	0	0	BN	S. viridochromogenes	Virulent	69271	64.3	Unknown
KY092480	Picard	0	0	0	0	0	BC	S. venezuelae	Temperate	39522	72.6	SIPHO
OL455886	Piccadilly	0	0	0	0	0	BP	S. sanglieri	Temperate	37544	71.2	SIPHO
MK433268	Popy	0	0	0	0	0	BI	S. griseus	Virulent	56470	59.4	SIPHO
OQ709199	PumpkinSpice	1	1	1	0	0	BE	S. griseofuscus	Virulent	132480	49.4	SIPHO
ON260828	Quaran19	1	1	1	0	0	BE	S. griseus	Virulent	131761	49.5	SIPHO
JX182370	R4	0	0	0	0	0	BD	S. coelicolor	Temperate	51071	67	SIPHO
MH155877	Rainydai	0	0	0	0	0	BI	S. scabiei	Virulent	57623	58.1	SIPHO
KY092484	Raleigh	0	0	0	0	0	BC	S. griseus	Temperate	40785	71.8	SIPHO
MH171093	Rana	0	0	0	0	0	BD	S. griseus	Temperate	50980	65.8	SIPHO
MH155878	RavenPuff	0	0	0	0	0	BI	S. scabiei	Virulent	43709	60.9	SIPHO
MZ648039	RedBear	0	0	0	0	0	BD	S. lividans	Temperate	51271	65.6	SIPHO
MK686068	RemusLoopin	0	0	0	0	0	BB	S. mirabilis	Temperate	41376	62	SIPHO

MZ622160	RetrieverFever	1	0	0	0	0	BF	S. scabiei	Virulent	46175	60.7	PODO
OP434453	RickRoss	0	0	0	0	0	BO	S. scabiei	Unknown	18373	54.4	TECTI
KX670790	Rima	0	0	0	0	0	BI	S. azureus	Virulent	56168	59.6	SIPHO
MG663584	Romero	0	0	0	0	0	BF	S. griseus	Virulent	46079	59.7	PODO
MZ648033	Rooney	0	0	0	0	0	BN	S. viridochromogenes	Virulent	69514	64.3	SIPHO
MK686072	RosaAsantewaa	0	0	0	0	0	BI	S. mirabilis	Virulent	42730	58.8	SIPHO
OP021678	RosePharie	0	0	0	0	0	BF	S. lividans	Virulent	46026	60.3	PODO
MG593803	Rowa	0	0	0	0	0	BL	S. azureus	Temperate	42890	61.2	SIPHO
MN096381	Rusticus	0	0	0	0	0	BD	S. tricolor	Temperate	50066	65.9	SIPHO
MN204498	Saftant	0	0	0	0	0	BD	S. griseofuscus	Temperate	48883	65.6	SIPHO
MH178382	Salete	1	1	0	0	0	BG	S. griseus	Virulent	57243	69.2	SIPHO
ON260819	SaltySpitoon	1	1	1	0	0	BE	S. griseus	Virulent	130852	49.5	SIPHO
MT708548	Salutena	0	0	0	0	0	None	S. sp.	Temperate	51956	68	SIPHO
MF347639	Samisti12	1	1	1	0	0	BE	S. griseus	Virulent	133710	49.9	SIPHO
MZ820092	SarahRose	0	0	0	0	0	BD	S. lividans	Temperate	51567	65.6	SIPHO
MH576962	Satis	0	1	0	0	0	BM	S. lividans	Virulent	186702	66.7	Unknown
MF975637	Scap1	0	0	0	0	0	BI	S. scabiei	Virulent	43060	60.9	SIPHO
MK450433	Sebastisaurus	0	0	0	0	0	BB	S. xanthochromogenes	Temperate	41609	62.1	Unknown
MH155880	SendItCS	0	0	0	0	0	BI	S. scabiei	Virulent	55993	58.2	SIPHO
MT701597	Sentinel	0	0	0	0	0	None	S. sp.	Temperate	50272	67	SIPHO
KT221033	SF1	0	0	0	0	0	Singleton	S. flavovirens	Unknown	43150	69	SIPHO
KT221034	SF3	0	0	0	0	0	Singleton	S. flavovirens	Temperate	60934	69	SIPHO
MT701596	Shady	0	0	0	0	0	None	S. sp.	Temperate	45128	62	SIPHO
MT701595	Shaeky	0	0	0	0	0	None	S. sp.	Temperate	45617	63	SIPHO
MT897908	ShakeNBake	0	0	0	0	0	BN	S. viridochromogenes	Virulent	69299	64.2	SIPHO
ON645339	Sham	1	0	0	0	0	BK	S. griseus	Virulent	130327	47.1	Unknown
MK433266	Shawty	0	0	0	0	0	BB	S. platensis	Temperate	40733	63.2	SIPHO
MT701598	Sitrop	0	0	0	0	0	None	S. sp.	Temperate	48481	66	SIPHO
OL742563	Snorlax	0	0	0	0	0	BD	S. lividans	Temperate	51592	65.7	SIPHO
OQ938586	SoJo	0	0	0	0	0	BC	S. mirabilis	Temperate	39033	71.5	SIPHO
MN204504	Soshi	0	0	0	0	0	BI	S. griseus	Virulent	56311	59.5	SIPHO
MZ820091	South40	0	0	0	0	0	BD	S. lividans	Temperate	51271	65.6	SIPHO
MH590589	SparkleGoddess	1	0	0	0	0	BK	S. griseus	Virulent	129742	47.1	SIPHO
MF467949	Spectropatronm	0	0	0	0	0	BI	S. griseus	Virulent	55707	59.5	SIPHO
MT701594	Spernnie	0	0	0	0	0	None	S. sp.	Temperate	50834	66	SIPHO
ON970579	Spilled	1	1	1	0	0	BE	S. griseus	Virulent	132667	49.3	SIPHO
MF766047	SqueakyClean	0	0	0	0	0	BD	S. xanthochromogenes	Temperate	50837	67	SIPHO
ON108650	Squillium	1	1	1	0	0	BE	S. lividans	Virulent	132303	50.2	SIPHO
MW145539	SscP1EGY	0	0	0	0	0	None	S. scabiei	Virulent	51751	58	PODO

OP021680	Stanimal	1	1	1	0	0	BE	S. lividans	Virulent	131706	49.3	SIPHO
MH576964	Starbow	1	1	1	0	0	BE	S. griseus	Virulent	131427	49.5	SIPHO
MH576965	StarPlatinum	1	1	1	0	0	BE	S. griseus	Virulent	133886	49.5	SIPHO
OP751154	Stella	1	0	0	0	0	BF	S. viridochromogenes	Virulent	46511	60	PODO
ON456343	Stigma	1	0	0	0	0	BK	S. griseus	Virulent	129455	47.1	Unknown
ON456338	Stuff	1	0	0	0	0	BH	S. griseus	Virulent	54082	68.4	SIPHO
OP751148	Success	0	0	0	0	0	Singleton	S. lividans	Unknown	57163	61.6	SIPHO
KC700557	Sujidade	0	0	0	0	0	BD	S. lividans	Temperate	51552	65.7	SIPHO
OL455891	SunsetPointe	0	0	0	0	0	BD	S. griseus	Temperate	49957	66.3	Unknown
MF358542	Sushi23	1	1	1	0	0	BE	S. griseus	Virulent	133917	50	SIPHO
JX182371	SV1	0	0	0	0	0	BC	S. venezuelae	Temperate	37612	72.7	SIPHO
MT701593	Sycamore	0	0	0	0	0	None	S. sp.	Temperate	44694	63	SIPHO
OP820462	TagePhighter	0	0	0	0	0	BD	S. lividans	Temperate	51469	65.7	SIPHO
MW712736	TaidaOne	0	0	0	0	0	BI	S. griseus	Virulent	56183	59.5	Unknown
MZ958750	Targaryen	1	1	1	0	0	BE	S. lividans	Virulent	134920	49.5	SIPHO
MF766048	Tefunt	0	0	0	0	0	BD	S. xanthochromogenes	Temperate	50574	66.8	SIPHO
MK460248	Teutsch	1	1	1	0	0	BE	S. griseus	Virulent	132885	50	SIPHO
JX182372	TG1	0	0	0	0	0	BB	S. cattleya	Temperate	40474	64.6	Unknown
MH651190	Thestral	0	0	0	0	0	BD	S. xanthochromogenes	Temperate	52628	67.7	SIPHO
MT657340	Thiqqums	0	0	0	0	0	BI	S. scabiei	Virulent	57624	58.1	SIPHO
MT684600	TieDye	0	0	0	0	0	BI	S. griseus	Virulent	55031	59.5	SIPHO
MK392365	TinaBelcher	0	0	0	0	0	BD	S. xanthochromogenes	Temperate	52490	67.7	Unknown
KY676784	ToastyFinz	0	0	0	0	0	BC	S. viridochromogenes	Temperate	39693	72.5	SIPHO
MH171098	Toma	0	0	0	0	0	BD	S. toxytricini	Temperate	51396	65.8	SIPHO
OL829978	Tomas	1	1	1	0	0	BE	S. sanglieri	Virulent	134464	48.2	Unknown
MN369750	TomSawyer	1	1	1	0	0	BE	S. griseus	Virulent	133961	49.3	Unknown
ON108646	TonyStarch	0	0	0	0	0	BI	S. mirabilis	Virulent	55469	59.6	SIPHO
MG663585	ToriToki	0	0	0	0	0	BF	S. griseus	Virulent	46077	59.7	PODO
KP876466	TP1604	1	1	0	0	0	BG	S. griseus	Virulent	57168	69.2	SIPHO
OL455897	Treat	0	0	0	0	0	BF	S. griseus	Virulent	46094	59.6	Unknown
MN369743	Tribute	1	1	1	0	0	BE	S. griseus	Virulent	133471	50	Unknown
MZ648040	Triste	0	0	0	0	0	BD	S. lividans	Temperate	51568	65.7	SIPHO
OQ190479	Triumph	0	0	0	0	0	BD	S. lividans	Temperate	51233	67.2	SIPHO
MH669016	TrvxScott	0	0	0	0	0	BD	S. platensis	Temperate	52600	67.8	SIPHO
MN096373	TuanPN	0	0	0	0	0	BD	S. griseus	Temperate	51517	65.7	SIPHO
MW822145	TunaTartare	1	0	0	0	0	BK	S. mirabilis	Virulent	130929	46.9	SIPHO
MW291017	TurkishDelight	1	0	1	0	0	Singleton	S. scabiei	Temperate	93606	72.6	SIPHO
OL455894	Unstoppable	0	0	0	0	0	BD	S. griseus	Temperate	49556	66.2	Unknown
MH229864	UNTPL	1	0	0	0	0	BH	S. griseus	Virulent	54495	68.3	SIPHO

MN234189	Urza	0	0	0	0	0	BD	S. griseofuscus	Temperate	50448	68.5	SIPHO
MK450421	Vash	0	0	0	0	0	BB	S. griseus	Temperate	41578	62.5	SIPHO
KT186229	Verse	0	0	0	0	0	BD	S. venezuelae	Temperate	49483	65.6	SIPHO
ON526983	VieEnRose	0	0	0	0	0	BD	S. sanglieri	Temperate	50193	68.6	SIPHO
MT451981	Vondra	0	0	0	0	0	BP	S. sanglieri	Temperate	37129	71.2	SIPHO
ON108647	Vorvolakos	1	0	0	0	0	BF	S. scabiei	Virulent	46174	60.7	PODO
AY320035	VWB	0	0	0	0	0	BA	S. venezuelae	Temperate	49220	71.1	SIPHO
MT024865	Wakanda	1	0	0	0	0	BK	S. sanglieri	Virulent	126614	52.6	Unknown
MF358541	Warpy	1	1	1	0	0	BE	S. griseus	Virulent	132996	49.6	SIPHO
MH019216	Wentworth	0	0	0	0	0	BN	S. griseus	Virulent	68260	64.1	Unknown
MW435856	Werner	0	0	0	0	0	BD	S. lividans	Temperate	51566	65.7	SIPHO
MN284899	Whatever	0	0	0	0	0	BD	S. lividans	Temperate	51591	65.7	SIPHO
MK305890	WheeHeim	0	0	0	0	0	BO	S. scabiei	Temperate	18266	54.6	TECTI
MN484599	Wipeout	1	1	1	0	0	BE	S. griseus	Virulent	132935	49.3	Unknown
MH576968	Wofford	1	1	1	0	0	BE	S. griseus	Virulent	133007	47.7	SIPHO
MG515223	WRightOn	0	0	0	0	0	BF	S. viridochromogenes	Virulent	45221	60.3	PODO
KU530220	Xkcd426	1	1	0	0	0	BG	S. griseus	Virulent	64477	68.8	SIPHO
MH727564	Yaboi	1	1	1	0	0	BE	S. lividans	Virulent	131250	49.3	SIPHO
MH019215	Yara	0	0	0	0	0	BN	S. toxytricini	Virulent	68671	63.9	SIPHO
MN096379	Yasdnil	0	0	0	0	0	BD	S. griseus	Temperate	51631	65.7	SIPHO
KP876465	YDN12	1	1	0	0	0	BG	S. griseus	Virulent	56528	69.2	SIPHO
MH248947	Yosif	0	0	0	0	0	BD	S. toxytricini	Temperate	50129	66.1	SIPHO
MT684596	Zeigle	1	0	0	0	0	BF	S. viridochromogenes	Virulent	44859	60.3	SIPHO
KC700558	Zemlya	0	0	0	0	0	BD	S. lividans	Temperate	51077	66.6	Unknown
GQ919031	ZL12	0	0	1	1	0	Singleton	S. sp.	Phage-Plasmid	90435	69.5	SIPHO
MG663586	ZooBear	0	0	0	0	0	BF	S. griseus	Virulent	46135	59.7	PODO
MN204493	Zuko	0	0	0	0	0	BR	S. griseofuscus	Unknown	82302	63.7	SIPHO

Name	Region	Con5 R1	Con5 R2	Con20 R1	Con20 R2	Con40 R1	Con40 R2	Con90 R1	Con90 R2	Inf5 R1	Inf5 R2	Inf20 R1	Inf20 R2	Inf40 R1	Inf40 R2	Inf90 R1	Inf90 R2
HQ601_00001	138..515	0.00	0.00	0.00	0.00	0.00	0.00	0.00	0.00	10.32	21.42	13.31	33.36	47.97	37.51	127.35	244.93
HQ601_00002	512..658	0.00	0.00	0.00	0.00	0.00	0.00	0.00	0.00	0.91	6.36	3.92	3.92	6.15	7.08	23.18	65.08
HQ601_00003	655..1749	0.00	0.00	0.00	0.00	0.00	0.00	0.00	0.00	3.32	7.11	4.64	11.57	14.85	14.49	43.96	98.30
HQ601_00004	1746..2534	0.00	0.00	0.00	0.00	0.00	0.00	0.00	0.00	2.30	7.10	4.52	12.25	13.01	16.16	53.37	107.49
HQ601_00005	2692..3345	0.00	0.00	0.00	0.00	0.00	0.00	0.18	0.00	18.20	31.74	5.13	9.10	3.65	6.96	22.71	46.94
HQ601_00006	3410..4642	0.00	0.00	0.00	0.00	0.00	0.00	0.00	0.00	8.78	18.94	2.42	4.20	2.46	2.74	8.15	17.14
HQ601_00007	4732..5139	0.00	0.00	0.00	0.00	0.00	0.00	0.00	0.00	15.66	34.86	8.35	18.04	3.48	4.78	5.78	14.17
HQ601_00008	5333..5749	0.00	0.00	0.00	0.00	0.00	0.00	0.00	0.00	0.48	2.74	0.13	0.00	2.32	7.80	422.59	1007.61
HQ601_00009	5832..6350	0.00	0.00	0.00	0.00	0.00	0.00	0.22	0.00	0.00	0.00	0.00	0.12	2.61	6.77	316.98	866.99
HQ601_00010	6370..7641	0.00	0.00	0.00	0.00	0.00	0.00	0.00	0.00	0.00	0.00	0.04	0.00	1.52	3.48	320.83	831.69
HQ601_00011	7654..7872	0.00	0.00	0.00	0.00	0.00	0.00	0.00	0.00	0.00	0.00	0.00	0.00	1.77	2.38	194.68	510.59
HQ601_00012	7859..9352	0.00	0.00	0.00	0.00	0.00	0.00	0.00	0.00	0.05	0.00	0.04	0.13	1.81	4.53	496.25	1238.56
HQ601_00013	complement (9361..9537)	0.00	0.00	0.00	0.00	0.00	0.00	0.00	0.00	0.00	0.00	0.00	0.00	1.82	7.35	312.94	690.31
HQ601_00014	9594..11570	0.00	0.00	0.00	0.00	0.00	0.00	0.00	0.00	0.00	0.00	0.03	0.00	0.59	0.92	298.74	837.72
HQ601_00015	11574..11738	0.00	0.00	0.00	0.00	0.00	0.00	0.00	0.00	0.00	0.63	0.00	0.00	0.39	1.58	485.02	1124.66
HQ601_00016	11850..12572	0.00	0.00	0.00	0.00	0.00	0.00	0.00	0.00	0.00	0.00	0.00	0.00	0.45	0.54	415.08	987.10
HQ601_00017	12612..13469	0.00	0.00	0.00	0.00	0.00	0.00	0.00	0.00	0.00	0.12	0.00	0.00	0.45	0.15	457.40	1173.75
HQ601_00018	13489..13719	0.00	0.00	0.00	0.00	0.00	0.00	0.00	0.00	0.00	0.00	0.00	0.00	0.00	0.56	361.19	946.13
HQ601_00019	13723..14121	0.00	0.00	0.00	0.00	0.00	0.00	0.00	0.00	0.00	0.00	0.00	0.00	0.00	0.00	264.07	729.10
HQ601_00020	14118..14438	0.00	0.00	0.00	0.00	0.00	0.00	0.00	0.00	0.00	0.00	0.00	0.00	0.00	0.00	273.53	664.10
HQ601_00021	14435..14785	0.00	0.00	0.00	0.00	0.00	0.00	0.00	0.00	0.00	0.00	0.00	0.00	0.18	0.37	286.49	717.50
HQ601_00022	14778..15191	0.00	0.00	0.00	0.00	0.00	0.00	0.28	0.00	0.00	0.00	0.00	0.00	0.16	0.31	286.16	686.31
HQ601_00023	15204..15674	0.00	0.00	0.00	0.00	0.00	0.00	0.00	0.00	0.00	0.00	0.00	0.00	0.55	0.83	488.59	1153.19
HQ601_00024	15671..16123	0.00	0.00	0.00	0.00	0.00	0.00	0.00	0.00	0.00	0.00	0.00	0.00	0.00	0.00	357.76	865.27
HQ601_00025	16384..18801	0.00	0.00	0.00	0.00	0.00	0.00	0.00	0.00	0.00	0.04	0.00	0.05	0.05	0.81	176.00	482.60
HQ601_00026	18777..19700	0.00	0.00	0.00	0.00	0.00	0.00	0.00	0.00	0.00	0.00	0.00	0.00	0.07	0.00	146.65	412.99
HQ601_00027	19715..20800	0.00	0.00	0.00	0.00	0.00	0.00	0.00	0.00	0.00	0.00	0.00	0.00	0.24	0.60	208.36	509.41
HQ601_00028	20806..21927	0.00	0.00	0.00	0.00	0.00	0.00	0.00	0.00	0.00	0.00	0.00	0.00	0.06	0.23	190.62	508.96
HQ601_00029	21941..22654	0.00	0.00	0.00	0.00	0.00	0.00	0.00	0.00	0.00	0.00	0.00	0.09	0.00	0.55	208.38	484.07
HQ601_00030	22723..23664	0.00	0.00	0.00	0.00	0.00	0.00	0.00	0.00	0.00	0.00	0.00	0.00	0.00	0.14	307.45	761.11
HQ601_00031	23714..23950	0.00	0.00	0.00	0.00	0.00	0.00	0.00	0.00	0.00	0.00	0.00	0.00	0.27	0.00	546.32	1336.39
HQ601_00032	23947..24210	0.00	0.00	0.00	0.00	0.00	0.00	0.00	0.00	0.00	0.00	0.00	0.00	0.00	0.00	275.34	681.40
HQ601_00033	complement (24277..25461)	0.00	0.00	0.00	0.00	0.00	0.00	0.00	0.00	0.11	0.09	0.22	0.05	0.11	0.44	10.84	24.81
HQ601_00034	complement (25470..25679)	0.00	0.00	0.00	0.00	0.00	0.00	0.00	0.00	0.00	0.00	0.00	0.30	0.00	0.00	2.08	3.80
HQ601_00035	complement (25952..26179)	0.00	0.00	0.00	0.00	0.00	0.00	0.00	0.00	0.00	0.00	0.23	0.00	0.00	0.00	3.83	15.30
HQ601_00036	complement (26188..26448)	0.00	0.00	0.00	0.00	0.00	0.00	0.00	0.00	0.00	0.80	0.00	0.25	0.00	0.00	5.36	12.98
HQ601_00037	26622..27353	0.00	0.00	0.00	0.00	0.00	0.00	0.00	0.00	0.37	1.56	0.36	0.61	0.97	7.82	13.01	23.15
HQ601_00038	28059..28271	0.00	0.00	0.00	0.00	0.00	0.00	0.00	0.00	26.52	53.61	30.76	71.21	80.29	103.83	195.24	415.02
HQ601_00039	28268..28453	0.00	0.00	0.00	0.00	0.00	0.00	0.00	0.00	4.70	12.28	8.74	19.96	15.61	20.98	21.61	45.54
HQ601_00040	28518..28904	0.00	0.00	0.00	0.00	0.00	0.00	0.00	0.00	18.07	30.04	18.15	40.02	42.02	26.22	45.15	99.66
HQ601_00041	28901..29278	0.00	0.00	0.00	0.00	0.00	0.00	0.00	0.00	11.38	25.81	13.73	29.12	26.46	20.99	29.58	58.53
HQ601_00042	29275..30333	0.00	0.00	0.00	0.00	0.00	0.00	0.00	0.00	13.78	25.00	14.75	35.48	32.24	18.43	27.31	73.88
HQ601_00043	30330..30959	0.00	0.00	0.00	0.00	0.00	0.00	0.00	0.00	13.87	31.80	21.72	39.11	36.47	18.79	41.60	89.54
HQ601_00044	31026..31325	0.00	0.00	0.00	0.00	0.00	0.00	0.00	0.00	2.69	7.61	4.89	11.73	6.67	9.97	10.48	33.22
HQ601_00045	31322..31546	0.00	0.00	0.00	0.00	0.00	0.00	0.00	0.00	6.57	12.92	9.09	21.62	15.49	10.41	19.03	41.19
HQ601_00046	31622..32494	0.00	0.00	0.00	0.00	0.00	0.00	0.00	0.00	5.78	14.27	7.21	13.49	9.61	5.22	21.92	39.73
HQ601_00047	32491..33171	0.00	0.00	0.00	0.00	0.00	0.00	0.00	0.00	3.16	7.47	5.00	8.65	5.59	2.29	12.83	32.05
HQ601_00048	33168..33356	0.00	0.00	0.00	0.00	0.00	0.00	0.00	0.00	2.13	3.30	2.22	7.79	3.76	3.44	6.93	23.20
HQ601_00049	33482..33943	0.00	0.00	0.00	0.00	0.00	0.00	0.00	0.00	9.61	24.94	9.76	28.26	50.85	48.43	159.42	341.91
HQ601_00050	33943..34404	0.00	0.00	0.00	0.00	0.00	0.00	0.00	0.00	7.28	19.77	12.37	25.49	48.33	43.36	109.68	238.37

Acknowledgements

Zu aller erst möchte ich mich bei Prof. Dr. Julia Frunzke für die Möglichkeit zur Durchführungen meiner Promotion in ihrem Labor bedanken. Während der Arbeit an diesem spannenden Projekt habe ich mich fachlich und persönlich immer unterstützt und wertgeschätzt gefühlt.

Darüber hinaus möchte ich mich bei meinem Mentor Prof. Dr. Nick Wierckx für die Übernahme des Zweitgutachtens bedanken.

Danke an alle Kolleginnen und Kollegen im IBG-1, insbesondere an die jetzigen und ehemaligen Mitglieder der AG Bakterielle Netzwerke und Interaktionen. Ulli, Conni, Doris, Johanna, Aileen, Eva, Max, Aël, Vikas, Janik, Marius, Biel, Bente, Larissa und Sebastian, ihr alle wart essentiell für den Erfolg meiner Promotion. Ob in gemeinsamen Projekten, durch Diskussionen oder durch jedwede Hilfe und Unterstützung im Alltag. Sowohl im Labor, im Büro, auf Konferenz, in der Mittagspause oder nach Feierabend habt ihr dafür gesorgt, dass es mir jeden Tag Spaß gemacht hat und ich es am Ende durchziehen konnte.

Vielen Dank an alle Kooperationspartner im Forschungszentrum, an der HHU und extern. Vor allem möchte ich mich auch bei meinen Studentinnen Frederike und Rebecca bedanken, dessen Betreuung mir viel Spaß bereitet hat und die mir viel Arbeit abgenommen und signifikant zu dieser Dissertation beigetragen haben. Ich hoffe, ihr habt dabei genau so viel gelernt, wie ich.

Natürlich möchte ich mich bei meinen Freunden und meiner Familie bedanken. Danke für all die Fragen, was ich da mache, wann ich fertig bin, wie es läuft und was ich danach vorhabe. Danke, dass ihr manchmal aber auch explizit nicht nachgefragt habt und wir so viel mehr andere Dinge besprochen und getan haben. Ohne euch wäre der ‚Life' Teil in Work-Life Balance deutlich zu kurz gekommen. Besonders dankbar bin ich für dich, Kirsten. Wenn mich jemand in dieser Zeit am meisten verstanden und unterstützt hat, aber auch das meiste aushalten musste, dann du. Und das war, seit der Bachelorzeit, über Jahre und Kilometer, getrennt und gemeinsam, so unglaublich wichtig. Danke!

Zu guter Letzt, noch Dank an Monster, Moe und mich, denn ohne ging es nich'.

Eidesstattliche Erklärung

Hiermit versichere ich an Eides Statt, dass die Dissertation von mir selbständig und ohne unzulässige fremde Hilfe unter Beachtung der „Grundsätze zur Sicherung guter wissenschaftlicher Praxis an der Heinrich-Heine-Universität Düsseldorf“ erstellt worden ist. Die Dissertation wurde in der vorgelegten oder in ähnlicher Form noch bei keiner anderen Institution eingereicht. Ich habe bisher keine erfolglosen Promotionsversuche unternommen.

_____

Tom Luthe